

Radiative forcing of climate: the historical evolution of the radiative forcing concept, the forcing agents and their quantification, and applications

Article

Accepted Version

Ramaswamy, V., Collins, W., Haywood, J., Lean, J., Mahowald, N., Myhre, G., Naik, V., Shine, K. P. ORCID:
<https://orcid.org/0000-0003-2672-9978>, Soden, B., Stenchikov, G. and Storelvmo, T. (2019) Radiative forcing of climate: the historical evolution of the radiative forcing concept, the forcing agents and their quantification, and applications. Meteorological Monographs, 59. 14.1-14.101. ISSN 0065-9401 doi: 10.1175/AMSMONOGRAPHS-D-19-0001.1 Available at <https://centaur.reading.ac.uk/86599/>

It is advisable to refer to the publisher's version if you intend to cite from the work. See [Guidance on citing](#).

To link to this article DOI: <http://dx.doi.org/10.1175/AMSMONOGRAPHS-D-19-0001.1>

Publisher: American Meteorological Society

including copyright law. Copyright and IPR is retained by the creators or other copyright holders. Terms and conditions for use of this material are defined in the [End User Agreement](#).

www.reading.ac.uk/centaur

CentAUR

Central Archive at the University of Reading

Reading's research outputs online

1
2
3
4
5
6
7
8
9
10
11
12
13
14

Radiative Forcing of Climate: The Historical Evolution of the Radiative Forcing Concept, the Forcing Agents and their Quantification, and Applications

15
16
17
18
19
20
21
22
23
24
25

V. Ramaswamy^{1,c}, W. Collins², J. Haywood³, J. Lean⁴,
N. Mahowald⁵, G. Myhre⁶, V. Naik¹, K.P. Shine⁷, B. Soden⁸,
G. Stenchikov⁹, and T. Storelvmo¹⁰

26
27
28
29
30
31

Submitted for publication to the

American Meteorological Society Centenary Monograph

Revised, September 21, 2019



Early Online Release: This preliminary version has been accepted for publication in *Meteorological Monographs*, may be fully cited, and has been assigned DOI 10.1175/AMSMONOGRAPHS-D-19-0001.1. The final typeset copyedited article will replace the EOR at the above DOI when it is published.

32

33 1. NOAA/ Geophysical Fluid Dynamics Laboratory, Princeton University,
34 Princeton, NJ 08540.

35

36 2. Lawrence Berkeley National Laboratory and University of California,
37 Berkeley, CA 94720.

38

39 3. University of Exeter, and United Kingdom Met Office, Exeter, EX4 4QF, UK.

40

41 4. U. S. Naval Research Laboratory, Washington, DC 20375 (Retired).

42

43 5. Department of Earth and Atmospheric Sciences, Cornell University, Ithaca,
44 NY 14853.

45

46 6. CICERO, Pb. 1129 Blindern, 0318, Oslo, Norway.

47

48 7. Department of Meteorology, University of Reading, Reading RG6 6BB, UK.

49

50 8. Rosentiel School of Marine and Atmospheric Science, University of Miami,
51 Miami, FL 33124.

52

53 9. King Abdulla University of Science and Technology, Thuwal, Jeddah 23955-
54 6900, Saudi Arabia.

55

56 10. University of Oslo, Postboks 1022, Blindern 0315, Norway.

57

58 c – Corresponding Author

59

60

Abstract

61 We describe the historical evolution of the conceptualization, formulation, quantification,
62 application and utilization of “radiative forcing (RF, see e.g., IPCC, 1990)” of Earth’s climate.
63

64
65 Basic theories of shortwave and long wave radiation were developed through the 19th and 20th
66 centuries, and established the analytical framework for defining and quantifying the
67 perturbations to the Earth’s radiative energy balance by natural and anthropogenic influences.
68

69 The insight that the Earth’s climate could be radiatively forced by changes in carbon dioxide,
70 first introduced in the 19th century, gained empirical support with sustained observations of the
71 atmospheric concentrations of the gas beginning in 1957. Advances in laboratory and field
72 measurements, theory, instrumentation, computational technology, data and analysis of well-
73 mixed greenhouse gases and the global climate system through the 20th Century enabled the
74 development and formalism of RF; this allowed RF to be related to changes in global-mean
75 surface temperature with the aid of increasingly sophisticated models. This in turn led to RF
76 becoming firmly established as a principal concept in climate science by 1990.
77

78 The linkage with surface temperature has proven to be the most important application of the RF
79 concept, enabling a simple metric to evaluate the relative climate impacts of different agents.
80

81 The late 1970s and 1980s saw accelerated developments in quantification including the first
82 assessment of the effect of the forcing due to doubling of carbon dioxide on climate (the
83 “Charney” report, National Research Council, 1979). The concept was subsequently extended
84 to a wide variety of agents beyond well-mixed greenhouse gases (WMGHGs: carbon dioxide,
85

methane, nitrous oxide, and halocarbons) to short-lived species such as ozone. The WMO (1986) and IPCC (1990) international assessments began the important sequence of periodic evaluations and quantifications of the forcings by natural (solar irradiance changes and stratospheric aerosols resulting from volcanic eruptions) and a growing set of anthropogenic agents (WMGHGs, ozone, aerosols, land surface changes, contrails). From 1990s to the present, knowledge and scientific confidence in the radiative agents acting on the climate system has proliferated. The conceptual basis of RF has also evolved as both our understanding of the way radiative forcing drives climate change, and the diversity of the forcing mechanisms, have grown. This has led to the current situation where “Effective Radiative Forcing (ERF, e.g., IPCC, 2013)” is regarded as the preferred practical definition of radiative forcing in order to better capture the link between forcing and global-mean surface temperature change. The use of ERF, however, comes with its own attendant issues, including challenges in its diagnosis from climate models, its applications to small forcings, and blurring of the distinction between rapid climate adjustments (fast responses) and climate feedbacks; this will necessitate further elaboration of its utility in the future. Global climate model simulations of radiative perturbations by various agents have established how the forcings affect other climate variables besides temperature e.g., precipitation. The forcing-response linkage as simulated by models, including the diversity in the spatial distribution of forcings by the different agents, has provided a practical demonstration of the effectiveness of agents in perturbing the radiative energy balance and causing climate changes.

The significant advances over the past half-century have established, with very high confidence, that the global-mean ERF due to human activity since preindustrial times is positive (the 2013 IPCC assessment gives a best estimate of 2.3 W m^{-2} , with a range from 1.1

110 to 3.3 W m^{-2} ; 90% confidence interval). Further, except in the immediate aftermath of
111 climatically-significant volcanic eruptions, the net anthropogenic forcing dominates over
112 natural radiative forcing mechanisms. Nevertheless, the substantial remaining uncertainty in
113 the net anthropogenic ERF leads to large uncertainties in estimates of climate sensitivity from
114 observations and in predicting future climate impacts. The uncertainty in the ERF arises
115 principally from the incorporation of the rapid climate adjustments in the formulation, the well-
116 recognized difficulties in characterizing the preindustrial state of the atmosphere, and the
117 incomplete knowledge of the interactions of aerosols with clouds. This uncertainty impairs the
118 quantitative evaluation of climate adaptation and mitigation pathways in the future. A grand
119 challenge in Earth System science lies in continuing to sustain the relatively simple essence of
120 the radiative forcing concept in a form similar to that originally devised, and at the same time
121 improving the quantification of the forcing. This, in turn, demands an accurate, yet increasingly
122 complex and comprehensive, accounting of the relevant processes in the climate system.

123
124
125

126 **Section 1**
127
128
129
130 **Radiative influences driving climate change since preindustrial times: Segue to the RF**
131 **Concept**
132
133
134 **1. Introduction**
135
136
137 Interactions of the incoming solar radiation and outgoing longwave radiation with the Earth's
138 surface and atmosphere affect the planetary heat balance and therefore impact the climate
139 system. The growth in fundamental knowledge of physics and chemistry via observational and
140 theoretical developments through the 18th, 19th and 20th centuries became the platform for
141 describing the agents driving Earth's climate change since preindustrial times (1750) and the
142 formulation of the "Radiative Forcing (RF)" (see Section 2) of climate change. The central
143 purpose of this paper is to trace the progression in the RF concept leading to our current
144 knowledge and estimates of the major agents known to perturb climate. Below, we give a
145 perspective into the key milestones marking advances in the knowledge of RF. Subsequent
146 sections of the paper focus on the evolution of: the concept including its formulation; the known
147 major forcing agents; and various applications of the concept. We attempt to capture the
148 historical evolution of the above foci through approximately the mid-2010. Of necessity, given
149 the nature of the paper for the American Meteorological Society Centennial monograph volume
150 and the vast domain of the topic, the principal aim of this manuscript is to describe the evolution
151 as evidenced through the literature, particularly the major international assessment reports. We
152 refer the reader to the richness of the references cited for the in-depth scientific details marking
153 the steps over the past three centuries to the present state-of-the-art.

154 **Section 1.1 Growth of atmospheric radiation transfer (pre-20th C to mid-20th C)**
155
156
157
158 The basic concepts of planetary energy budget and the greenhouse effect were put forward in the
159 early nineteenth century by Fourier (1824), although the term “greenhouse” was not mentioned.
160 Fourier recognized that the atmosphere is opaque to “dark heat” (infrared radiation), but could
161 not identify the factors. Laboratory experiments related to transmission of light by atmospheric
162 gases at different wavelengths were the subject of atmospheric radiation inquiries as far back as
163 the early 19th century. One of the very first laboratory measurements of infrared absorption was
164 reported by Tyndall (1861). Based on a series of carefully designed laboratory experiments,
165 Tyndall discovered that infrared absorption in the atmosphere is largely due to carbon dioxide
166 and water vapour. Tyndall thought that variations in the atmospheric concentrations of CO₂ and
167 water vapour account for “all the mutations of climate which the researches of geologists reveal”
168 (see Anderson et al., 2016). Very soon after that came spectral measurements, prompted by both
169 scientific curiosity and a quest to explain the then known variations in earth’s climate.
170
171 Arrhenius (1896) made the quantitative connection to estimate the surface temperature increase
172 due to increases in CO₂. He relied on surface radiometric observations (Langley, 1884), used or
173 inferred a number of fundamental principles in shortwave and longwave radiation, pointed out
174 the greenhouse effect of water vapor and CO₂, and made simple assumptions concerning
175 exchange of heat between surface and atmosphere to deduce the temperature change (see
176 Ramanathan and Vogelmann, 1997). In the same study, Arrhenius also discussed the solar
177 absorption in the atmosphere. Arrhenius’ systematic investigation and inferences have proven to
178 be pivotal in shaping the modern-day thinking, and computational modeling of the climate effects
179 due to CO₂ radiative forcing.

180
181 Advances in theoretical developments in classical and, later on, in quantum physics, through the
182 19th and early 20th centuries laid the groundwork concerning light (photon) absorption/emission
183 processes and their linkage to the laws of thermodynamics. This led to the enunciation of basic
184 concepts in the 19th century e.g., Kirchhoff's deductions concerning blackbody radiation, and
185 the associated laws by Planck, Wien, Rayleigh-Jeans, Stefan-Boltzmann. These laws, and the
186 physics of thermal absorption and emission by gases and molecules, were applied to the context
187 of the atmosphere, leading to the formalism of atmospheric longwave radiative transfer (see
188 Chapter 2 in Goody and Yung, 1989).

189
190 Discovery and understanding of observed phenomena played a role throughout in the
191 development of methodologies that were to become building blocks for the quantification of
192 perturbations to the shortwave and longwave radiative fluxes. A combination of fundamental
193 theoretical developments, observations, simple calculations, and arguments sowed the advances,
194 for example, Lord Rayleigh's (Hon. J. W. Strutt) treatise on skylight and color (1871) and the
195 electromagnetic scattering of light (1881). Another example is Mie's theory of electromagnetic
196 extinction (1908) which unified the laws of light reflection, refraction, and diffraction following
197 Huygens, Fresnel, Snell, (see van de Hulst, 1957), and inferred the disposition of light at any
198 wavelength when it interacts with homogeneous spherical particles. Advances in the knowledge
199 of gaseous absorption and emission processes through laboratory-based quantification of
200 absorption lines and band absorption by the important greenhouse gases marked the further
201 growth of atmospheric longwave radiative transfer from the late 19th century into the mid-and-
202 late 20th century (see Chapter 3 in Goody and Yung, 1989). Experimental developments, along
203 with advances in conceptual thinking on the heat balance of the planet, began to provide the

204 platform for quantifying the radiation budget e.g., solar irradiance determination by Abbott and
205 Fowle (1908), and an early estimate of the Earth's global-average energy budget by Dines
206 (1917). Dines' effort was a remarkable intellectual attempt given there was very little then by
207 way of observations of the individual components. Figure 1.1 provides a comparison of the
208 values estimated by Dines (1917) compared to one modern analysis (L'Ecuyer et al. 2015). What
209 we term as radiative forcing (RF) of climate change today can be regarded as a result of this early
210 thinking about the surface-atmosphere heat balance.

211
212 Callendar's work in the 1930s-1950s built upon the earlier explorations of Arrhenius and Ekhholm
213 (1901) to relate global temperature to rising CO₂ concentrations. Callendar (1938) compiled
214 measurements of temperatures from the 19th century onwards and correlated these with
215 measurements of atmospheric CO₂ concentrations. He concluded that the global land
216 temperatures had increased and proposed that this increase could be an effect of the increase in
217 CO₂ (Fleming, 1998). Callendar's assessment of the climate sensitivity (defined as surface
218 temperature change for a doubling of CO₂) was around 2 °C (Archer and Rahmstorf, 2010)
219 which is nowadays regarded as being at the lower end of the modern-day computed values (e.g.,
220 IPCC, 2013). His papers in the 1940s and 1950s influenced the study of CO₂-atmosphere-surface
221 interactions vigorously, both on the computational side which introduced simplified radiation
222 expressions (e.g., Plass, 1956; Yamamoto and Sasamori, 1958) and in initiating the organization
223 of research programs to measure CO₂ concentrations in the atmosphere. Plass recognized the
224 importance of CO₂ as a greenhouse gas in 1953 and published a series of papers (e.g., Plass,
225 1956). He calculated that the 15-micron CO₂ absorption causes the temperature to increase by 3.6
226 °C if the atmospheric CO₂ concentration is doubled and decreases by 3.8 °C when it is halved.
227 These early calculations helped guide future works. Modern monitoring of CO₂ concentrations

228 began with Keeling's pioneering measurements of atmospheric CO₂ concentrations, begun in
229 connection with the International Geophysical Year in 1957 (e.g., Keeling, 1960). This soon
230 spurred the modern computations of the effects due to human-influenced CO₂ increases, and
231 initiated investigations into anthropogenic global warming. The historical developments above,
232 plus many others, beginning principally as scientific curiosity questions concerning the Earth's
233 climate, have formed the foundational basis for the contemporary concept of RF and the
234 estimation of the anthropogenic effects on climate.

235
236 A major part of the work related to radiative drivers of climate change came initially on the
237 longwave side, and more particularly with interest growing in the infrared absorption by CO₂ and
238 H₂O. This came about through the works of many scientists (see references in Chapters 3 and 4,
239 Goody and Yung, 1989). Research expansion comprising theoretical and laboratory
240 measurements continued into the late 20th Century (see references in Chapter 5, Goody and
241 Yung, 1989). Importantly, from the 1960s, existing knowledge of spectral properties of gaseous
242 absorbers began to be catalogued on regularly updated databases, notably HITRAN (see
243 references in Chapter 5, Goody and Yung, 1989).

244
245 On the shortwave measurements side, the Astrophysical Observatory of the Smithsonian
246 Institution (APO) made measurements of the solar constant (now more correctly referred to as
247 the "total solar irradiance" as it is established that this is not a constant) at many locations on the
248 Earth's surface from 1902 to 1962 (Hoyt, 1979). While there were interpretations from these
249 observations about change and variations in the Sun's brightness, the broad conclusion was that
250 the data reflected a strong dependency on atmospheric parameters such as stratospheric aerosols
251 from volcanic eruptions, as well as dust and water vapor. Research into shortwave and longwave

252 radiation transfer yielded increasingly accurate treatments of the interactions with atmospheric
253 constituents (Chapters 4-8 in Goody and Yung, 1989; and Chapters 1-4 in Liou, 2002).

254
255

256

257 **1.2 Advent of the RF concept and its evolution (since the 1950s)**

258

259

260 Advances in computational sciences and technology played a major role alongside the growth in
261 basic knowledge. The increases in computational power from 1950s onwards, with facilitation
262 of scalar and later vector calculations, enhanced the framework of “reference” computations
263 (e.g., Fels et al., 1991; Clough et al., 1992). This enabled setting benchmarks for quantifying the
264 radiative forcing by agents. With developments in community-wide radiative model
265 intercomparisons (e.g., Ellingson et al., 1991; Fouquart et al., 1991; Collins et al., 2006), the
266 comparisons against benchmarks established a definitive means to evaluate radiative biases in
267 global weather and climate models, one of the best examples of a “benchmark” and its
268 application in the atmospheric sciences. The advance in high-performance computing since
269 2000 has endowed the benchmark radiative computations with the ability to capture the details
270 of molecular absorption and particulate extinction at unprecedented spectral resolutions in both
271 the solar and longwave spectrum.

272

273

274 Relative to the previous decades, the 1950s also witnessed the beginning of increasingly
275 sophisticated and practical numerical models of the atmosphere and surface that included
276 radiative and then radiative-convective equilibrium solutions. Hergesell’s (1919) work had
277 superseded earlier calculations in describing the radiative equilibrium solutions using a grey-
278 atmosphere approach. Subsequent studies further advanced the field by recognizing the
279 existence of a thermal structure, making more realistic calculations based on newer
280 spectroscopic measurements and observations (e.g., Murgatroyd, 1960; Mastenbrook, 1963;
Telegadas and London, 1954), developing simplified equations (parameterizations) for use in

281 weather and climate models, and exploring how the radiation balance could be perturbed
282 through changes in the important atmospheric constituents e.g., water vapor and carbon dioxide
283 (Kaplan, 1960; Kondratyev and Niilisk, 1960; Manabe and Moller, 1961; Houghton, 1963;
284 Moller, 1963; Manabe and Strickler, 1964). Manabe and Strickler (1964) and Manabe and
285 Wetherald (1967) set up the basis for the more modern-day calculations in the context of one-
286 dimensional models, invoking radiative-convective equilibrium, where the essential heat
287 balance in the atmosphere-surface system involved solar and longwave radiative, and
288 parameterized convective (latent+sensible heat) processes. In this sense, the 1960s efforts went
289 significantly ahead of Arrhenius' pioneering study and other earlier insightful investigations to
290 recognize and calculate the effects of carbon dioxide in maintaining the present-day climate.

291
292 The foundational model calculations of radiative perturbations of the climate system arose from
293 publications beginning in the 1960s. Manabe and Wetherald (1967) demonstrated how changes
294 in radiative constituents (CO_2 , H_2O , O_3) as well as other influences (solar changes, surface
295 albedo changes) could affect atmospheric and surface temperatures. The field of modeling grew
296 rapidly over the 1960s to 1980s period and three-dimensional models of the global climate
297 system came into existence, enabling an understanding of the complete latitude-longitude-
298 altitude effects of increasing CO_2 . The acceleration of modeling studies resulted in an ever-
299 increasing appreciation of CO_2 as a major perturbing agent of the global climate [Manabe and
300 Bryan, 1969; Manabe and Wetherald, 1975; Ramanathan et al., 1979; Manabe and Stouffer,
301 1980; Hansen et al., 1981; Bryan et al., 1988; Washington and Meehl, 1989; Stouffer et al.,
302 1989; Mitchell et al., 1990]. The growth in the number of studies also galvanized CO_2 -climate
303 assessments using the numerical model simulations (e.g., NRC, 1979, now famously referred to
304 as the "Charney" report,). The Charney study was the first institutionally sponsored scientific

305 assessment based on then available studies. The report concluded a RF due to CO₂ doubling of
306 about 4 W m⁻² and estimated the most probable global warming to be near 3°C with a probable
307 error of $\pm 1.5^\circ\text{C}$. This was a landmark report, has influenced the community immensely, and
308 became a trendsetter for climate science assessments. A second assessment followed (NRC,
309 1982, referred to as the “Smagorinsky” report) which essentially reiterated the conclusions of
310 the Charney report.

311

312 The above studies and assessments established a useful basis for a formalized perspective into
313 mathematical linkages between global-mean RF by greenhouse gases and surface temperature
314 changes, with the applicability extending to global climate impacts. The modern definition and
315 equations for RF took root during this period. The conceptual development that has lent
316 powerful significance to characterizing radiative perturbations via “RF” came through in the
317 1970s with the first formal phrasing (Ramanathan, 1975), and got solidified as a concept in the
318 late 1970s and 1980s (e.g., Ramanathan et al., 1979; Dickinson and Cicerone, 1982) especially
319 through the major international assessment reports e.g., WMO (1986, volume III). Eventually,
320 the IPCC scientific assessments, beginning with IPCC (1990), made this a robust terminology.

321

322 This continues through today even though there have been substantial refinements in the past
323 decade (see Section 2). As the RF concept settled into more rigorous formulations in the 1970s
324 and 1980s, a spate of research extended this exercise to other well-mixed greenhouse gas
325 changes such as methane, nitrous oxide and chlorofluorocarbons (Ramanathan, 1975; Wang et
326 al., 1976; Donner and Ramanathan, 1980; Hansen et al., 1981). This became possible as
327 spectroscopic data and knowledge of their atmospheric concentration changes grew. In later

328 years and decades, the list of well-mixed greenhouse gases grew to include a plethora of
329 halocarbons, sulfur hexafluoride etc. (e.g., Fisher et al., 1990; Pincock et al., 1995).

330
331 Although the RF concept was developed to quantify the changes in radiation balance due to
332 well-mixed greenhouse gases and solar irradiance changes, this was extended to short-lived
333 gases, such as ozone, which exhibit strong spatial and temporal variability (Ramanathan et al. in
334 WMO, 1986; Shine et al., 1990; Isaksen et al., 1992). The concept was also applied to an entire
335 category of effects referred to as “indirect” which accounted for changes in atmospheric
336 concentrations of a radiative constituent affected by non-radiative effects such as chemical or
337 microphysical interactions (see Sections 4 and 5). These were first derived for the case of
338 tropospheric and stratospheric ozone changes occurring through chemical reactions in the
339 atmosphere involving anthropogenic precursor species. Indirect effects also were uncovered for
340 aerosol-related radiative effects obtained through their interactions with water and ice clouds
341 (Charlson et al., 1992, Penner et al., 1992; Schimel et al., 1996).

342
343 The impact of emissions of anthropogenic aerosols, or their precursors, on climate had been
344 recognized as early as the 1970s while recognition of their effects on air pollution goes back
345 more than a century (Brimblecombe and Bowler, 1990). The first quantification, however, in
346 the context of preindustrial to present-day emissions came through Charlson et al. (1991). The
347 forcing connected with the anthropogenic aerosol emissions has acquired a more diverse picture
348 now with the complexity associated with the various species (e.g., different types of
349 carbonaceous aerosols), existence of a variety of mixed states (i.e. aerosols consisting of more
350 than one component), and the influence of each species on the formation of water drops and ice
351 crystals (“indirect” forcing referred to above). Additional complexities with aerosols as

352 compared to the well-mixed greenhouse gases arise because of their inhomogeneous space and
353 time distribution. Estimating preindustrial concentrations of important short-lived gases and
354 aerosols and their precursors is difficult, and is a major contributor to uncertainty in their RF
355 (e.g., Tarasick et al. 2019; Carslaw et al. 2017).

356
357 Besides atmospheric constituents, other radiative influences also began to be quantified under
358 the broad concept of “radiative forcing”. These included land-use and land-cover changes due to
359 vegetation changes, primarily in the Northern Hemisphere. The initial considerations were for
360 the changes induced in the albedo of the surfaces due to human activity (Sagan et al., 1979).
361 Later, other physical factors in the context of forced changes such as surface roughness, trace
362 gas and aerosol emissions, water and water-related changes as a consequence of land surface
363 changes were also considered as it was realized that these too affected the planetary heat
364 balance (e.g., IPCC, 2013).

365
366 A relatively recent entry under the anthropogenic RF label includes the attempts to quantify the
367 forcing due to aviation-induced aerosols and contrails, reported as early as beginning of 1970s,
368 and quantitatively assessed beginning with IPCC (1999) (e.g., Fahey et al., 1999). Emissions
369 from various industrial sectors including transportation (aircraft, shipping, road transport) have
370 been comparatively evaluated and assessed (see Unger et al., 2010). While anthropogenic
371 forcings became increasingly better quantified in the 20th Century, so too were the natural
372 agents, such as solar irradiance changes (see Hoyt and Schatten, 1997) and aerosols formed in
373 the stratosphere in the aftermath of explosive or climatically-significant volcanic eruptions
374 (Franklin, 1784, Robock, 2000). The qualitative recognition of the potential climatic effects due
375 to powerful volcanic eruptions (e.g., Toba, Tambora, Krakatoa eruptions), and solar changes,

376 possibly goes more than two centuries back. As an example, solar irradiance changes and the
377 resultant transmission of sunlight through the atmosphere began to be pursued as both questions
378 of scientific curiosity and for potential impacts on surface climate.

379
380
381

382 **1.3 Scope of the paper**

383

384
385 In this paper we trace the evolution of the knowledge base that began with recognizing the
386 importance of changes in atmospheric composition, how they alter the radiative balance of the
387 planet, and the resulting growth in understanding that has enabled quantification of the radiative
388 effects.

389
390 Notably, this began with considerations of the roles of water vapor and carbon dioxide in the
391 longwave spectrum, and the naturally arising solar irradiance changes and particulates from
392 volcanic eruptions in the shortwave spectrum. The early discoveries and theories on the role of
393 radiation in the planet's heat equilibrium state paved the way for defining the
394 forcing of the Earth's climate system, with gradually increasing attention to the range of
395 anthropogenic influences. The forcing used in this context was meant to characterize the agents
396 driving climate change and nominally on a global-average basis, rather than regional or local
397 scales. In describing the evolution of the RF concept and its applications, we follow a strategy of
398 describing the principal advancements over time, with references to a few of the seminal
399 investigations. Included in these are the well-known chapters on radiative forcing appearing in
400 various assessments and reports e.g., IPCC (e.g., 1990, 1996, 2001, 2007, 2013), WMO (e.g.,
401 1986), NRC (e.g., 1979). Our aim is not to summarize from the assessments but instead to
402 document the key elements happening over time that pushed the frontiers to the state-of-the-art
403 in its successive evolutionary stages through to today. We hew fairly strictly to RF only. We do
404 not discuss "climate feedbacks" *per se* which are an integral part of climate response, but that
405 discussion is outside the scope of this paper.

406
407
408
409
410
411
412
413 Figure 1.2 illustrates the radiative forcing quantification in each of the 5 major IPCC WGI

414
415 Assessments to date (1990, 1996, 2001, 2007, and 2013). All the forcings on the illustration
416 represent a measure of the radiative perturbation at the tropopause brought about by the change
417 in that agent relative to its value/state in 1750. As the knowledge has advanced, there
418
419 has been a growth in the number of forcing agents and an evolution in the estimates of the
420 magnitudes of the agents. The increased attention to scientific uncertainties also becomes
421 evident, representing an advance in the measure of the scientific understanding of.
422
423

424 Quantification of the anthropogenic WMGHG and the secular solar forcing began from the 1st
425 IPCC assessment (IPCC, 1990, or “FAR”). While aerosol radiative effects were recognized in
426 FAR, the tropospheric aerosol quantification was reported in an interim IPCC Special Report
427 (IPCC, 1995) which was reaffirmed in the Second Assessment Report (IPCC, 1996 or SAR).
428 RF from ozone changes was recognized in FAR but quantified later. The RF from stratospheric ozone
429 losses due to the halocarbon-catalyzed chemical reactions, and that due to tropospheric ozone increases from
430 anthropogenic precursor emission increases and related chemistry-climate interactions was first quantified in a
431 special IPCC (1992) report followed by IPCC (1995). A special report on aviation-related impacts appeared as
432 IPCC (1999).

433 The Third Assessment Report (IPCC, 2001, or TAR) added a few more agents that were able to
434 be quantified besides updating the estimates of the greenhouse gas and aerosol agents. This
435 occurred in part due to accounting for the increased knowledge about changes in the species
436 concentrations, and to a lesser extent, due to improvements in the treatment of the processes.

437

438

439 The Fourth Assessment Report (IPCC, 2007, or AR4) introduced new methodologies to
440 estimate short-lived gas RF, and

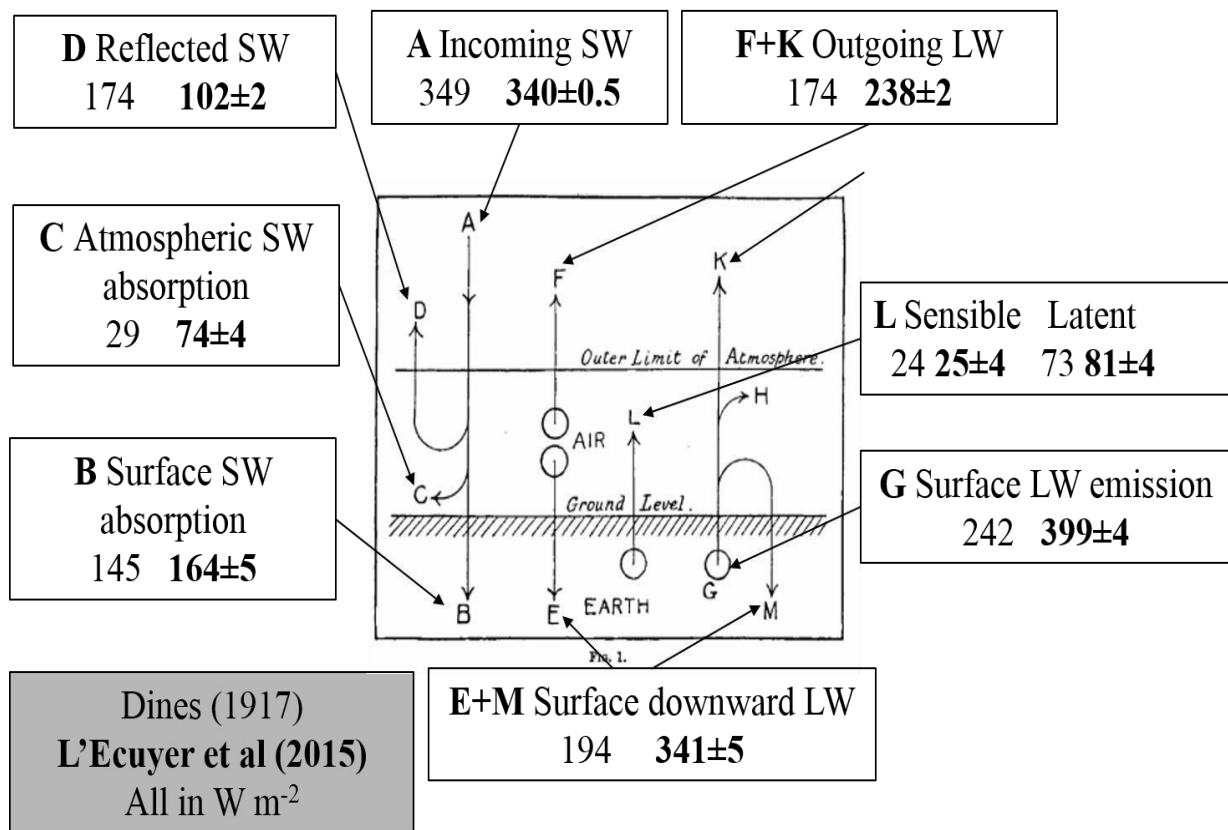
441

442 to express the uncertainty due to tropospheric aerosols which continue to be the principal reason
443 for the large uncertainty in the anthropogenic forcing (Section 10). AR5, the Fifth Assessment
444 Report (IPCC, 2013) introduced a major change in the manner of expressing the radiative
445 forcing by making the transition from radiative forcing (RF) to the effective radiative forcing
446 (ERF). Further details on the progress through the IPCC assessments appear in Section 2. The
447 change in radiative forcing due to CO₂ is due to increase in the concentration between the IPCC
448 assessments, except between SAR and TAR where there was an update in the expression for
449 calculating the radiative forcing. On the other hand, the changes in the short-lived compounds
450 such as ozone and aerosols from one assessment to the other are mainly results of improvements
451 based on observations and modeling representing the knowledge prevailing at the time of the
452 IPCC assessments.

455
456
457 The presentation in this paper aims to capture the principal developments of each forcing and
458 their chief characteristics as they developed over time, and thus does not insist on discussions of
459 all forcing agents to hew to the same format in the discussions. The sections below discuss the
460 major facets of the radiative forcing concept, beginning with its formulation in Section 2.
461
462 Sections 3, 4, 5, 6, 7 address the development of the quantified knowledge, including
463
464 uncertainties, of the anthropogenic forcing agents, in tandem with the
465 developments in the IPCC assessments beginning with the first assessment report in 1990.
466
467 Sections 8 and 9 discuss the natural drivers of climate change.
468
469 The totality of the forcing of the climate system i.e., a synthesis by accounting for all the agents
470 in a scientifically justified manner is examined in Section 10. The role of

472 RF in enabling the development of metrics to allow emissions of different gases to be placed on
 473 an equivalent scale is discussed in Section 11 while the connection of response to the forcing
 474 culled from observations and climate model simulations follows in Section 12. Section 13 traces
 475 the development of the newest ideas in the application of forcing concept viz.,
 476 management of solar and terrestrial radiation in the planet's heat budget based on the RF
 477 discussed in the previous Sections regarding well-mixed greenhouse gases and aerosols. The
 478 concluding section summarizes the major points of the paper's presentation of the development
 479 and utilization and application of radiative forcing, lists the strengths and limitations of the
 480 simple concept, and portrays the unresolved issues and grand challenge related to the viability of
 481 this concept, and the quantification for climate change determination in the future.

482



483
484

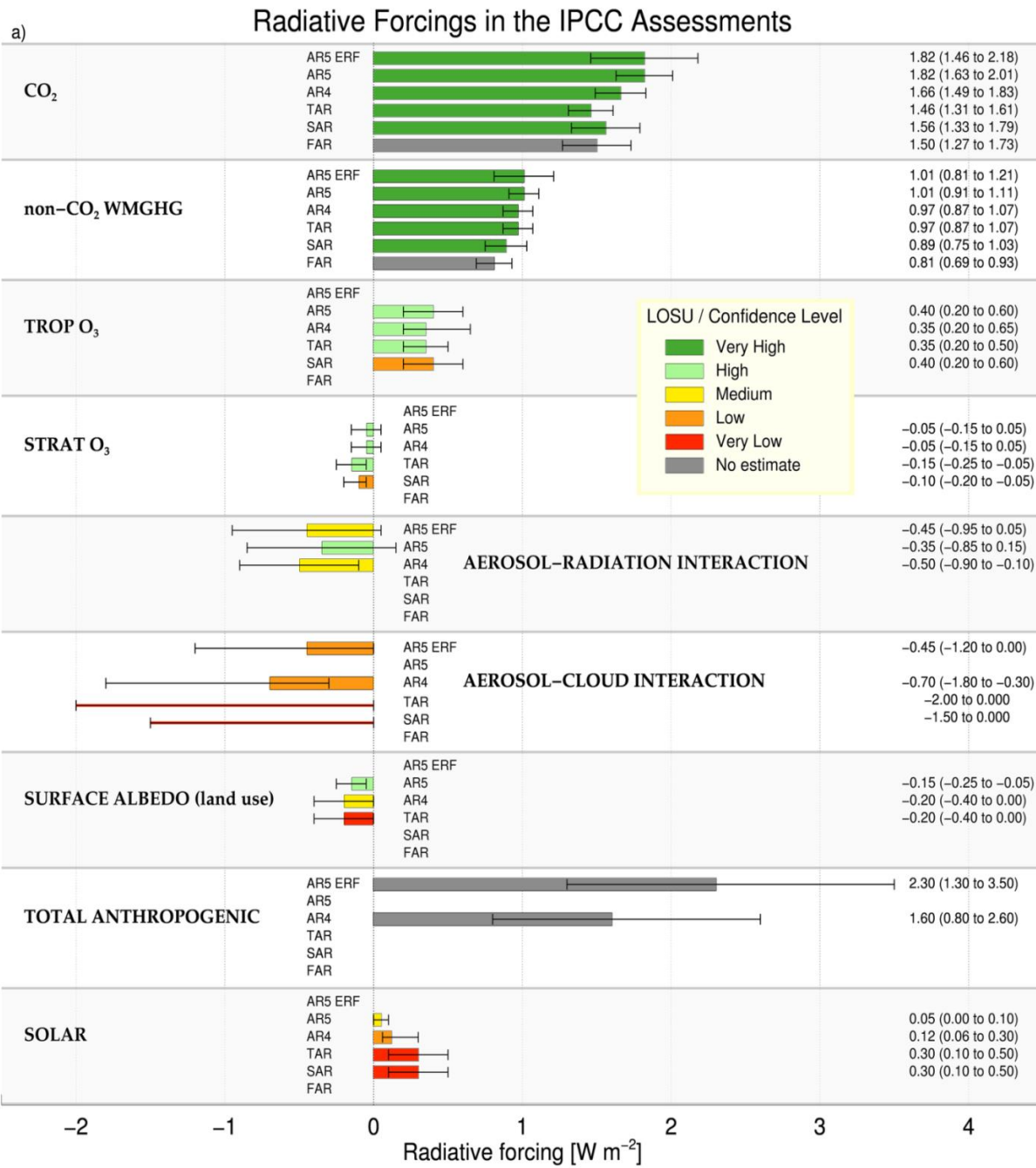
485

486 Figure 1.1: Comparison of one early estimate of the Earth's global-average energy budget (Dines
487 1917) with the contemporary estimates of L'Ecuyer et al. (2015) by annotating the original
488 figure from Dines (1917). All values are given in W m^{-2} , with Dines' values in plain font, and
489 L'Ecuyer et al. in bold font. Dines' value for the surface LW emission is low probably because
490 he adopted a value for Stefan's Constant which was "decidedly lower than that usually given"
491 although the assumed surface temperature is not stated either. For some components, Dines also
492 gave an estimate the uncertainty. The L'Ecuyer et al. (2015) values are from their Figure 4 which
493 applies energy and water balance constraints.

494

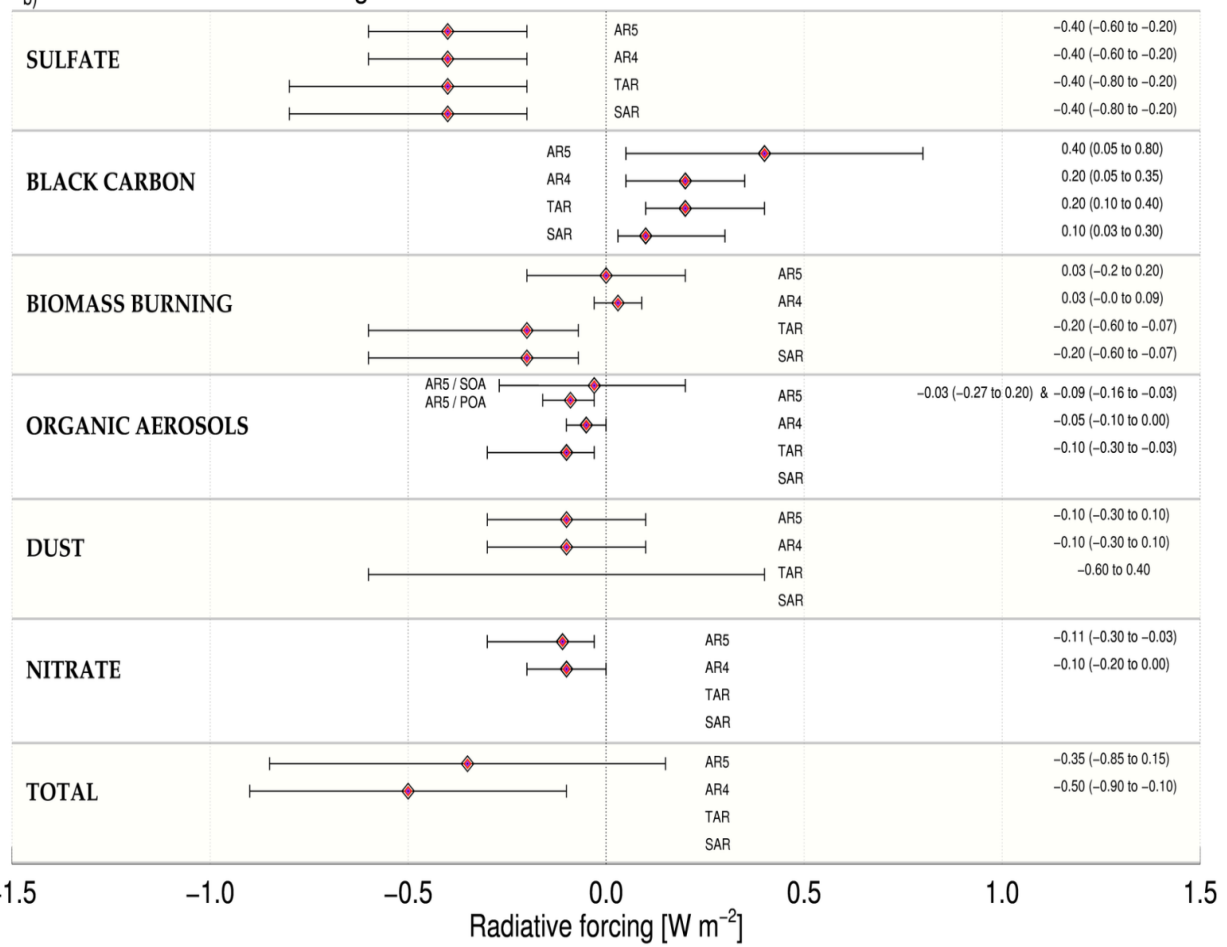
495

496



497
498
499
500

b) Radiative Forcing of aerosol–radiation interactions in the IPCC Assessments



-1.5 -1.0 -0.5 0.0 0.5 1.0 1.5
 Radiative forcing [W m⁻²]

501
 502
 503
 504
 505
 506

507 Figure 1.2: Summary of the evolution of the global-mean radiative forcings from IPCC reports,
508 where available, from FAR (1765-1990), SAR (1750-1992), TAR (1750-1998), AR4 (1750-
509 2005) and AR5 (1750-2011). The RF and/or the ERF presented in AR5 are included.
510 Uncertainty bars show the 5-95% confidence ranges.

511

512 (a) From top to bottom, the forcings are due to changes in CO₂, non-CO₂ well-mixed
513 greenhouse gases (WMGHGs), tropospheric ozone, stratospheric ozone, aerosol-radiation
514 interaction, aerosol-cloud interaction, surface albedo, total anthropogenic RF, and solar
515 irradiance. The forcings are color coded to indicate the “confidence level” (or “level of
516 scientific understanding (LOSU)”, as was presented in and before AR4, which used
517 “consensus” rather than “agreement” to assess confidence level). Dark green is “High
518 agreement and Robust evidence”; light green is either “High agreement and Medium evidence”
519 or “Medium agreement and Robust evidence”; yellow is either “High agreement and limited
520 evidence” or “Medium agreement and Medium evidence” or “Low agreement and Robust
521 evidence”; orange is either “Medium agreement and Limited evidence” or “Low agreement and
522 Medium evidence”; red is “Low agreement and Limited evidence”. Several minor forcings
523 (such as due to contrails, and stratospheric water vapor due to methane changes) are not
524 included. The information used here, and information on excluded components, can be mostly
525 found in Myhre et al. (2013) Tables 8.5 and 8.6 and Figure 8.14 and Shine et al. (1990) Table
526 2.6. The decrease in CO₂ RF between SAR and TAR was due to a change in the simplified
527 expressions used to compute its RF; the CO₂ concentration has increased monotonically
528 between each successive IPCC report. No central estimate was provided for aerosol-cloud
529 interaction in SAR and TAR, and a total aerosol-radiation interaction (see panel (b)) and a total

530 anthropogenic RF was not presented in assessments prior to AR4. Stratospheric aerosol RF
531 resulting from volcanic aerosols is not included due to their episodic nature; estimates can be
532 seen in Figure 10.3.

533

534 (b) Individual components of RF due to changes in aerosol-radiation interaction. From top to
535 bottom these are sulfate, black carbon from fossil fuel or biofuel burning, biomass
536 burning, -organic aerosols, dust, nitrate, and total (also shown on panel (a)). In AR5, the
537 organic aerosol RF was separated into primary organic aerosol (POA) from fossil fuel and
538 biofuel, and secondary organic aerosol (SOA), due to changes in source strength, partitioning
539 and oxidation rates. Separate confidence levels were not presented for individual components
540 of the aerosol-radiation interaction in AR4 and AR5, and hence none are shown-. The
541 information used here is mostly drawn from Myhre et al. (2013) Tables 8.4.

542

543
544

545

546 **2. Radiative Forcing – its origin, evolution and formulation**

547

548

549 **2.1 The utility of the forcing-feedback-response framework**

550

551

552 Radiative forcing provides a metric for quantifying how anthropogenic activities and natural
553 factors perturb the flow of energy into and out of the climate system. This perturbation initiates
554 all other changes of the climate due to an external forcing. The climate system responds to
555 restore radiative equilibrium through a change in temperature, known as the Planck response or
556 Planck feedback. A positive forcing (i.e., a net radiative gain) warms the climate and increases
557 the thermal emission to space until a balance is restored. Similarly, a negative forcing (i.e., a net
558 radiative loss) cools the climate, decreasing the thermal emission until equilibrium is restored.

559

560 The change in temperature required to restore equilibrium can induce other surface and
561 atmosphere changes that impact the net flow of energy into the climate system, and thus
562 modulate the efficiency at which the climate restores equilibrium. Borrowing terminology from
563 linear control theory, these secondary changes can be thought of as feedbacks that serve to
564 further amplify or dampen the initial radiative perturbation. The use of radiative forcings and
565 radiative feedbacks to quantify and understand the response of climate to external drivers has a
566 long and rich history (Schneider and Dickinson 1976; Hansen et al. 1984; Cess, 1976; Cess et
567 al., 1990, NRC 2005; Stephens 2005; Sherwood et al 2015).

568

569 Consider a perturbation in the global-mean net downward irradiance at the top-of-atmosphere,
570 $d\bar{F}$ (which we call the radiative forcing or RF) that requires a change in global-mean surface

571 temperature, $d\bar{T}$ to restore radiative equilibrium (overbars indicate a global-average quantity). If
572 the changes are small and higher order terms can be neglected, and $d\bar{F}$ is time independent, the
573 change in upward radiative energy, $d\bar{R}$ induced by the change in surface temperature, $d\bar{T}$, can
574 be decomposed into linear contributions from changes in temperature and other radiative
575 feedbacks X_i

576

577

578
$$d\bar{R} = \left[\frac{\partial \bar{R}}{\partial \bar{T}} + \sum_i \frac{\partial \bar{R}}{\partial X_i} \frac{\partial X_i}{\partial \bar{T}} \right] d\bar{T} \quad (2.1)$$

579

580

581 Equilibrium is restored when $d\bar{R} = d\bar{F}$. The ratio, $\alpha = d\bar{R} / d\bar{T}$, called the “climate feedback
582 parameter”, quantifies the efficiency at which the climate restores radiative equilibrium
583 following a perturbation. In the absence of feedbacks, the Planck response is $\alpha_i \approx 3.3 \text{ W m}^{-2} \text{ K}^{-1}$
584 (e.g. Cess 1976). In current climate models, radiative feedbacks from water vapor, clouds, and
585 snow/sea ice cover act to reduce α to a range $\approx 1-2 \text{ W m}^{-2} \text{ K}^{-1}$; this amplifies the change in
586 temperature in response to a given radiative forcing. Most of the intermodel spread in α is due
587 to differences in predicting the response of clouds to an external forcing (Cess et al. 1990).
588 Feedbacks from water vapor, clouds, snow and sea ice cover, have been well documented in
589 both models (Bony et al. 2006) and, to a lesser extent, in observations (Forster 2016). Less well
590 studied are feedbacks from the carbon cycle, ice sheets and the deep ocean that occur on much
591 longer time scales (e.g., Gregory et al. 2009; Forster 2016).
592 While attempting to characterize global climate changes using a single scalar quantity may seem
593 overly simplistic, many aspects of climate do respond in proportion to $d\bar{T}$, regardless of the
594 spatial and temporal scales being considered and are of much greater societal relevance than

595 global mean temperature (e.g., the magnitude of regional rainfall change). To the extent that
596 $d\bar{F}$ can be used to estimate $d\bar{T}$, radiative forcing then provides a simple but crude metric for
597 assessing the climate impacts of different forcing agents across a range of emission scenarios.
598 Here we write the relationship between $d\bar{T}$ and $d\bar{F}$ as

599
600
$$d\bar{T} \approx \lambda d\bar{F} \quad (2.2)$$

601
602 where λ is usually referred to as the “climate sensitivity parameter”, the inverse of α . It
603 is worth noting that equilibrium climate sensitivity is often written in terms of the
604 equilibrium surface temperature response, in K, to a doubling of CO₂ (about 3.7 W m⁻²).
605

606
607 An important driver in the early development of RF as a metric was the chronic uncertainty
608 in the value of λ , which persists to this day; this meant that quantifying the drivers of
609 climate change, and intercomparing different studies, was easier using $d\bar{F}$ rather than $d\bar{T}$.
610 However, such a comparison of different climate change mechanisms relies on the extent to
611 which λ is invariant (in any given model) to the mechanism causing the forcing; early
612 studies demonstrated similarity between the climate sensitivity parameter for CO₂ and solar
613 forcing (e.g. Manabe and Wetherald 1975) but subsequent work (see Section 2.3.4) has
614 indicated limitations to this assumption. The conceptual development in the subject, which
615 will be discussed in the following sections, has adopted progressively more advanced
616 definitions of RF with the aim of improving the level of approximation in Expression (2.2).
617

618
619
620
621

623 **2.2 Origin of the radiative forcing concept (1970s-1980s)**

624

625

626 Ramanathan (1975) presents the first explicit usage of the RF concept, as currently recognised
627 (although the term “radiative forcing” was not used), in an important paper quantifying, for the
628 first time, the potential climate impact of chlorofluorocarbons (CFCs). Ramanathan computed
629 the change in the top-of-atmosphere (TOA) irradiance due to increased CFC concentrations and
630 directly related this to the surface temperature change, via an empirical estimate of the
631 dependence of the irradiance on surface temperature; this is the climate feedback parameter
632 discussed in Section 2.1. Ramanathan noted that the surface temperature calculations using this
633 “simpler procedure” were identical to those derived using a “detailed” radiative-convective
634 model. Ramanathan and Dickinson (1979) extended the Ramanathan (1975) framework in
635 important ways, in a study of the climate impact of stratospheric ozone changes. First, there was
636 an explicit recognition that changes in stratospheric temperature (in this case driven by
637 stratospheric ozone change) would influence the tropospheric energy balance. Second, these
638 calculations were latitudinally-resolved. While the global-average stratosphere is in radiative
639 equilibrium (and hence temperature changes can be estimated via radiative calculations alone),
640 locally dynamical heat fluxes can be important. Ramanathan and Dickinson considered two
641 “extreme” scenarios to compute this temperature change without invoking a dynamical model.
642 One assumed that dynamical feedbacks were so efficient that they maintained observed
643 latitudinal temperature gradients; given subsequent developments, this is of less interest here.
644 The other scenario assumed that, following a perturbation, dynamical fluxes remain constant, and
645 temperatures adjust so that the perturbed radiative heating rates equal unperturbed heating rates
646 (and thus balance the unperturbed dynamical heat fluxes). This second method was originally

647 referred to as the “no feedback case” (the “feedback” referring to the response of stratospheric
648 dynamics to a forcing); it has since become more widely known as “Fixed Dynamical Heating”
649 (FDH) (Fels et al. 1980; WMO 1982) or more generally “stratospheric (temperature)
650 adjustment”. FDH has also been used for stratospheric temperature trend calculations, and shown
651 to yield reasonable estimates of temperature changes derived from a general circulation model
652 (GCM) (e.g. Fels et al. 1980; Kiehl and Boville 1988; Chanin et al., 1998; Maycock et al 2013;
653).

654
655
656 Ramanathan et al. (1979) applied the same methodology to CO₂ forcing. Their estimate of RF
657 for a doubling of CO₂ of about 4 W m⁻² was adopted in the influential Charney et al (1979)
658 report and has been an important yardstick since then. Although not explicitly stated until
659 subsequent papers in the 1980s (see later), one key reason for including stratospheric
660 temperature adjustment as part of RF, rather than as a climate feedback process, was that the
661 adjustment timescale is of order months; this is much faster than the decadal or longer timescale
662 for the surface temperature to respond to radiative perturbation, which is mostly driven by the
663 thermal inertia of the ocean mixed layer. A second, related, key reason is that the tight coupling
664 of the surface and troposphere, via convective heat fluxes, (and, conversely, the limited
665 coupling between the surface and the stratosphere) means that ΔT at surface is largely driven by
666 the RF at the tropopause. A consequence of applying stratospheric temperature adjustment
667 (which returns the stratosphere to global radiative equilibrium) is that tropopause and top-of-
668 atmosphere forcings are identical. This removes an important ambiguity in the definition of RF,
669 although the definition of the tropopause still has to be considered (see Section 2.3.5).

670
671

672 These timescales were made explicit by Hansen et al. (1981) who demonstrated the evolution of
673 the irradiance changes in their radiative-convective model, following a doubling of CO₂ (see Fig.
674 2.1). This tracked the changes from: (i) the immediate response (nowadays called the
675 instantaneous RF (IRF)); (ii) the response after a few months (which is close to the RF
676 incorporating stratospheric temperature adjustment); in the case of a CO₂ increase, the increased
677 emittance of the stratosphere leads to a cooling which increases the magnitude of the
678 perturbation of the top-of-atmosphere irradiance from -2.4 to -3.8 W m⁻²; and (iii) “Many years
679 later” when the surface temperature has equilibrated (following Expression (2.2)) and the
680 resulting irradiance change at the top of the atmosphere has cancelled out the forcing. Hansen et
681 al. (1981) seem to be the first to use the terminology “radiative forcing”, although they used it in
682 a general rather than a quantitative sense.

683

684 Several contributions to the edited volume by Clark (1982) also used the RF concept, at least in
685 an illustrative way, although using a variety of names. For example, Chamberlain et al. (1982)
686 compared different climate change mechanisms using what would now be called as surface
687 radiative forcing; their use of this (rather than tropopause or top-of-atmosphere RF) as a
688 predictor of surface temperature change was strongly disputed in the same volume by
689 Ramanathan (1982) (and earlier in Ramanathan et al., 1981), Hansen et al. (1982) and Luther
690 (1982). Hansen et al. (1982) briefly presented values of top-of-atmosphere radiative flux changes
691 for idealised changes in concentrations of 5 gases, and refer to these as “radiative forcings” in
692 their text. At around the same time, WMO (1982), in a brief report on a meeting on the potential
693 climate effects of ozone and other minor trace gases, refer explicitly to “the net outgoing

694 longwave flux at the tropopause" as determining "the radiative forcing of the surface-troposphere
695 system", and present values for idealised perturbations of 6 greenhouse gases.

696

697 Ramanathan et al (1985) also used the term "radiative forcing" in the context of Expression
698 (2.2) and Dickinson and Cicerone (1986) appear to be the first to use the concept to quantify the
699 climate impact of changes in concentrations of several greenhouse gases relative to pre-
700 industrial times in W m^{-2} (using the term "trapping" rather than RF).

701

702 "Radiative forcing" became firmly established as accepted terminology in Chapter 15 of the
703 1985 WMO Ozone Assessment (WMO 1985) (which was largely reproduced in Ramanathan et
704 al. (1987)) and the term was widely used in their discussion; however, much of their overall
705 comparison of the impacts of climate forcing agents was still posed in terms of surface
706 temperature change.

707

708

709
710

711 **2.3 The evolution of the radiative forcing concept during the IPCC era**

712

713 Assessment of RF has been firmly embedded in IPCC assessments from it's First Assessment
714 Report (FAR) onwards. FAR (Shine et al. 1990) took as its starting point the fact that the
715 climate impact of a range of different climate forcing agents could be compared using RF, in W m^{-2} , even though this was only starting to be done routinely in the wider literature at the time. A
716 significant motivator for the use of RF in all IPCC reports was as input to climate emissions
717 metrics (such as the Global Warming Potential, see Section 11). This section focuses mostly on
718 developments in understanding of anthropogenic forcings – more detailed discussions of the
719 evolution of the understanding of solar and volcanic aerosol forcings is given in Sections 8 and
720 9 respectively.

722

723
724

725

726 **2.3.1 The IPCC First Assessment Report 1990 (FAR)**

727

728

729 FAR discussed the concept of RF, stressing the utility of including stratospheric
730 temperature adjustment. Building on earlier work (e.g. Ramanathan et al. 1987) it also
731 emphasized the importance of indirect forcings, such as the impact of changes in methane
732 concentrations on ozone and stratospheric water vapor. The main focus was on greenhouse
733 gases, including extended tabulations of forcing due to CFCs and their potential replacements.
734 FAR also popularized the use of simplified expressions for calculating RF, which were
735 empirical fits to more complex model calculations. The expressions used in FAR were based on
736 two studies available at the time (Wigley et al. 1987; Hansen et al. 1988). Updated versions of
737 the simplified expressions are still widely used in simple climate models and for assessing
738 potential future scenarios of trace gas concentrations.

739

740 FAR also included, together in a single section, the roles of solar variability, direct aerosol
741 effects, indirect aerosol effects and changes in surface characteristics. The literature on these
742 was sparse. The section on direct aerosol forcing focused mostly on volcanic aerosol; it did not
743 attempt to quantify the impact of human activity because of “uncertainties in the sign, the
744 affected area and the temporal trend”. Perhaps surprisingly more attention was given to the
745 indirect aerosol effects (now more generally known as “aerosol cloud interactions”); although
746 FAR stated that “a confident assessment cannot be made”, due to important gaps in
747 understanding, a 1900-1985 estimate of -0.25 to -1.25 W m^{-2} (based on Wigley 1989) was

748 provided. FAR did not include estimates for pre-industrial to present-day RF across all forcing
749 agent, but restricted itself to two then-future periods (1990-2000 and 2000-2050).

750

751 Soon after FAR, an IPCC Supplementary Report provided an update (Isaksen et al. IPCC,
752 1992). Significant developments since FAR included more advanced RF estimates due to ozone
753 change (Lacis et al. 1990), and the first calculation of the forcing due to latitudinally-resolved
754 observed stratospheric ozone depletion (Ramaswamy et al., 1992). The indirect forcing due to
755 methane's impact on tropospheric ozone and stratospheric water vapour were quantified. The
756 first geographically-resolved estimates of sulphate aerosol direct forcing (now referred to as
757 aerosol-radiation interaction) (Charlson et al. 1991) had become available, indicating a
758 significant offset (in the global-mean sense) of greenhouse gas RF.

759

760

761

762
763
764
765

2.3.2 IPCC Special Report on Radiative Forcing and the IPCC Second Assessment Report (SAR)

766 The SAR discussion on RF was partly based on the analysis of Shine et al. (1995) in an IPCC
767 Special Report. Since FAR there had been several important developments. The 1992 Pinatubo
768 volcanic eruption had allowed unprecedented global-scale observations of the impact of such a
769 large eruption on the radiation budget (Minnis et al. 1993) and the subsequent climate response
770 was well predicted (Hansen et al. 1993 updated in Shine et al. 1995); because of the transient
771 nature of the forcing, this still arguably constitutes the most direct evidence of the linkage
772 between transient forcing and transient response to date. Understanding of ozone RF continued
773 to develop as a result of ongoing analyses of observational data and the advent of (then 2-D,
774 latitude-height) chemistry models allowing improved estimates of the longer-term increases in
775 tropospheric ozone (e.g. Wang et al., 1993; Hauglustaine et al. (1994)). More sophisticated RF
776 calculations due to sulphate aerosol-radiation interaction were becoming available (e.g. Kiehl
777 and Briegleb, 1993; Hansen et al. 1993; Taylor and Penner 1994), as were the first climate
778 model simulations of aerosol cloud-interaction (Jones et al. 1994). Early attempts to estimate the
779 direct RF from biomass burning (Penner et al. 1992; Hansen et al. 1993) were presented. Shine
780 et al. (1994) produced the first of IPCC's many figures of the pre-industrial to present-day
781 global-mean forcing incorporating both an estimate of the uncertainty range and a subjective
782 confidence level. Shine et al. (1994) also extended the discussion of the utility of the radiative
783 forcing concept; the chapter included clear demonstrations of the need to include stratospheric
784 temperature adjustment to compute ozone forcings, as IRF and RF could differ in sign.

785

786 Climate models were beginning to be used to test the forcing-response relationships for a wide
787 variety of forcings, including the impact of the spatial distribution of forcing; an unpublished
788 study by Hansen et al. (1993b) (a precursor to Hansen et al. (1997)) reported experiments with
789 an idealised GCM that indicated that extratropical forcings had almost double the impact on
790 global mean surface temperature change as the same (in the global-mean sense) tropical forcing;
791 ongoing work (e.g. Taylor and Penner 1994) also clearly demonstrated that while forcing in one
792 hemisphere was felt mostly in that hemisphere, there was still a large non-local response. By the
793 time of the SAR update (Schimel et al. 1996), attention had begun to focus on the (positive)
794 direct forcing due to soot (or black carbon) (Chylek and Wong 1995; Haywood and Shine 1995)
795 (see Section 5 for details), which highlighted the dependence of the computed forcing on
796 whether the aerosol population was internally or externally mixed. More studies of aerosol
797 indirect forcing were emerging (e.g. Boucher and Lohmann, 1995; Chuang et al, 1994) which
798 continued to indicate a significant negative forcing, as well as discussing indirect effects beyond
799 the impact on cloud effective radius. SAR updated the earlier RF figure most notably by
800 splitting the direct effect into its sulphate, biomass burning and soot components, but refrained
801 from giving a central estimate for the aerosol indirect forcing, “because quantitative
802 understanding of this process is so limited”.

803

804

805

806 **2.3.3 IPCC Third Assessment Report (TAR)**

807

808

809 After four IPCC reports with a focus on RF in the space of just 6 years, TAR's analysis
810 (Ramaswamy et al. 2001) was able to assimilate developments over a much longer period, using
811 a much larger body of literature. This was particularly so for tropospheric ozone and aerosol
812 forcing, as a result of many more chemistry-transport and GCM studies. These included early
813 studies investigating mineral dust and nitrate aerosols. The sophistication and range of studies
814 on aerosol indirect forcing had increased, with much more effort to separate out first (droplet
815 radii) and second indirect (liquid water path) effects. The associated uncertainty in the first
816 indirect effect could not be reduced beyond that given in SAR; no estimate was given for the
817 second indirect effect because it was "difficult to define and quantify" but it was noted that it
818 "could be of similar magnitude compared to the first (indirect) effect". Ramaswamy et al. (2001)
819 also reassessed the simple formulae used by IPCC to compute greenhouse gas RF, which led to
820 a 15% reduction in CO₂ forcing relative to the FAR formula; this and subsequent reports mostly
821 adopted the expressions presented by Myhre et al. (1998).

822

823

824 TAR also included in its RF summary figure, for the first time, the effect of contrails and
825 contrail-induced cirrus, partly based on work presented in the IPCC Special Report on Aviation
826 and the Global Atmosphere (Prather et al. 1999) and the effect of land-use change on surface
827 albedo.

828

829 TAR continued the important discussion on the utility of the RF concept. A larger number of
830 GCM studies, with a more diverse set of forcing mechanisms, were available, leading to the
831 important conclusion that "radiative forcing continues to be a good estimator of global-mean

832 surface temperature response, but not to a quantitatively rigorous extent as in the case of ...
833 radiative convective models". Most notably, Hansen et al. (1997) had presented a wide-ranging
834 study with a simplified configuration of their climate model which examined the response to
835 both latitudinally and vertically constrained forcings. They showed that forcings confined to
836 specific altitudes could lead to specific cloud or lapse rate responses, and these resulted in
837 marked variations in climate sensitivity for a given forcing. This weakened the perception that
838 the global-mean climate sensitivity for spatially inhomogeneous forcings could be used to
839 determine quantitative aspects of the spatial responses. This important work also presaged later
840 developments in the definition of RF, and appears to be the first explicit usage of the concept of
841 "efficacy" (although it was not given that name) that is discussed in the next subsection.

842
843

844

845 **2.3.4 IPCC Fourth Assessment Report (AR4)**

846

847

848 AR4's assessment of RF (Forster et al. 2007) brought together many important advances in both
849 its concept and utility of and the quantification of a number of new RF mechanisms. Notably, it
850 was the first report to formally combine all anthropogenic forcings via a Monte Carlo
851 simulation; it concluded that the net anthropogenic forcing since 1750 was "extremely likely" to
852 be positive (central estimate of 1.6 W m^{-2}) and that in the period since 1950, the impact of
853 natural forcings was considered "exceptionally unlikely" to have been comparable to the
854 anthropogenic forcings. A central estimate of the first indirect aerosol forcing (which was
855 labelled the "cloud albedo effect") was presented (-0.7 W m^{-2} with "low level of
856 understanding").

857

858 RF from changes in surface albedo due to black carbon on snow and stratospheric water vapor
859 from CH_4 oxidation were now included on the summary figure; it was noted that the total
860 stratospheric water vapor forcing, based on available observations, could be higher than the
861 methane-only component. In addition to the now-standard IPCC forcing diagram based on
862 changes in concentrations (see summary in Fig. 1.2), an emissions-based version (Fig 2.2) was
863 presented – this particularly served to highlight the fact that methane emissions (combining the
864 effect of methane change and the indirect forcings from changes in tropospheric ozone,
865 stratospheric water vapor and CO_2) led to a forcing equivalent to about half that of CO_2 . The
866 combined impact of NO_x emissions on tropospheric ozone, methane and nitrate aerosols, was
867 found to be negative.

868

869 Forster et al. (2007) detailed significant advances in the understanding of the utility of RF. In
870 particular, a number of GCM studies (e.g. Hansen et al. 2005; Shine et al. 2003; Gregory et al.
871 2004) had explored RF definitions which went beyond the then- standard RF with stratospheric
872 temperature adjustment; this framework allowed for rapid tropospheric adjustments (i.e. those
873 that occur independent of surface temperature change, and on timescales of up to a few months)
874 due to changes in clouds, water vapor and lapse rate, to be incorporated in the definition of
875 forcing. These were shown to have greater utility, in that the climate sensitivity showed less
876 dependence on the forcing mechanism. This framework would then lead to the AR5 definition of
877 effective radiative forcing (Section 2.3.5).

878
879 Forster et al. (2007) instead adopted the framework of efficacy, that had been developed in
880 earlier work discussed above, whereby Equation 2.1 is modified to

881

882 $d\bar{T} \approx E_i \lambda_{CO_2} d\bar{F}$ (2.3)

883

884

885 where $d\bar{F}$ still represents the (stratospheric-temperature-adjusted) radiative forcing, E_i
886 represents the efficacy of a given climate change mechanism, which is given by the ratio of the
887 climate sensitivity for that mechanism to that for CO₂; formally, since the CO₂ forcing varies
888 slightly with the magnitude of the CO₂ change (e.g. Hansen et al. 2005), a more robust
889 definition should be specific to the size of the CO₂ perturbation.

890

891 The product $E_i d\bar{F}$ was then labelled “effective radiative forcing”, a definition that would be
892 elaborated on in AR5 (Section 2.3.5). A significant number of climate modelling papers had, by
893 then, computed efficacies, with varying levels of agreement; this allowed Forster et al. (2007) to

894 draw tentative conclusions; for example, the combined efficacy for long-lived greenhouse gas
895 forcing was unity, to within 10%; solar forcing, tropospheric ozone and scattering aerosol
896 forcings had efficacies of 0.7 to 1.0, 0.6 to 1.1, and 0.7 to 1.1 respectively (all with “medium
897 confidence”). There was no consensus on an efficacy for black carbon.

898
899
900
901

902 **2.3.5 IPCC Fifth Assessment Report (AR5)**
903
904

905 In AR5 the effective radiative forcing (ERF) concept was introduced to allow rapid adjustment
906 processes in the troposphere but avoiding changes that are associated with climate feedbacks
907 (and in the conventional framework, mediated by surface temperature change – see Section
908 2.1) (Boucher et al., 2013; Myhre et al., 2013). ERF is defined in Myhre et al. (2013) as
909 “Change in the net top of atmosphere (TOA) downward radiative flux after allowing for
910 atmospheric temperatures, water vapour and clouds to adjust, but with surface temperature or a
911 portion of surface conditions unchanged”. Figure 2.3, from AR5, summarizes the progression
912 from instantaneous radiative forcing, through RF and ERF, to climate response. AR5 also
913 retained discussion of RF.

914

915 No new forcing mechanisms were included in AR5, but the confidence level was raised,
916 relative to earlier IPCC assessments for stratospheric water vapor, aerosol-radiation
917 interactions, surface albedo due to land use, contrails, contrail-induced cirrus, solar irradiance
918 changes and volcanic aerosols. The only ‘very low’ confidence level was given to rapid
919 adjustment of aerosol-cloud interactions (earlier denoted as aerosol indirect effects). See the
920 summary in Fig. 1.2.

921

922 The motivation for introducing the ERF concept was that efficacies (see expression 2.2) for
923 many climate drivers were different to unity when applying RF. This was particularly so for
924 black carbon (Ban-Weiss et al., 2011; Hansen et al., 2005; Ming et al., 2010) and for aerosol-
925 cloud interactions beyond the cloud albedo effect (Twomey effect) (e.g. Lohmann et al., 2010).
926 There was also a growing understanding that rapid adjustments were important for CO₂

927 (Andrews and Forster, 2008; Andrews et al., 2012; Doutriaux-Boucher et al., 2009).
928 Furthermore, a clearer distinction between the fast changes (including instantaneous radiative
929 perturbations and the rapid adjustments) and the slow climate feedback processes in terms of
930 their importance for the climate response was elaborated (Andrews et al., 2010; Bala et al.,
931 2010). Importantly, in single model studies, ERF was shown to provide an efficacy much
932 closer to unity than the traditional RF concept (Hansen et al., 2005; Shine et al., 2003). The
933 stratospheric temperature adjustment, which is included in the definition of RF, is also included
934 in ERF. An additional advantage of ERF compared to RF is that a tropopause definition is
935 avoided in the quantification of the forcing (e.g. Shine et al., 2003).

936

937 Two methods have been widely adopted to calculate the ERF. One method (Gregory et al.,
938 2004) regresses TOA net radiative imbalance against surface temperature change in coupled
939 climate model simulations. The extrapolation of that regression line to zero surface temperature
940 change then yields the ERF. The second method computes the TOA net radiative fluxes in
941 fixed sea surface temperature (SST) climate model simulations (Hansen et al., 2005); while it is
942 arguably more consistent to fix both land and surface temperatures (Shine et al. 2003), this is
943 difficult to implement in advanced climate models. Instead Hansen et al. (2005) suggested
944 adjusting the derived ERF to account for the impact of the land-surface temperature change on
945 TOA radiative fluxes.

946

947 The primary advantage of adopting ERF is that it reduces the level of approximation inherent
948 in Expression 2.2 across a wide range of climate forcing mechanisms. Nevertheless, there are
949 several limitations associated with its adoption. To some extent these are reflected in AR5

950 where the uncertainties in RF of WMGHGs were quantified as 10%, in agreement with earlier
951 IPCC assessments, whereas AR5 assessed WMGHG ERF to have uncertainties of 20%.

952

953 The necessity of climate model simulations to calculate tropospheric adjustments makes ERF
954 distinct from either IRF (see Section 2.2) or RF in several ways. IRF and RF can be quantified
955 using more sophisticated radiative transfer schemes than are typically available in climate
956 models, and, for example, can be more easily applied to a wider range of greenhouse gases. In
957 addition, the ERF technique is limited to forcing mechanisms that are of a sufficient size for
958 the impact on TOA fluxes to emerge from the noise of the climate model's own internal
959 variability (see Section 2.3.6).

960

961 Since rapid tropospheric adjustment processes are likely to be climate-model dependent this
962 introduces further uncertainties beyond those involved in more traditional forcing definitions.
963 For example, IRF are pure radiative transfer calculations that can be constrained reasonably
964 well with detailed models and a high degree of physical understanding. The stratospheric
965 temperature adjustment that is incorporated in the RF has a well-understood theoretical basis
966 (resulting from the balance between changes in absorption by and emission from the
967 stratosphere). By contrast, tropospheric adjustments are much more complicated. There is less
968 theoretical underpinning with which to constrain these adjustments; this is particularly so for
969 cloud adjustments which result from the complex interplay between different processes that
970 may or may not be well-represented in individual climate models. This complicates the
971 distinction between adjustments and feedbacks that are mediated by surface temperature
972 change and there is no obvious way to quantify the adjustments with observations.

973
974
975 One consequence of these shortcomings is a blurring of the lines between forcings and
976 feedbacks. While the tropospheric adjustments are defined to have a shorter time scale than
977 feedbacks, they also generally involve some coupling to the surface; e.g., land warming (in
978 the fixed-SST approach to ERF calculation) or pattern of SST change (in the regression
979 approach). Hence there is a need to further develop techniques that enable a robust
980 separation of adjustment and feedback processes.

981
982 A specific difficulty is that it is increasingly hard to compare different types of forcing.
983 IRF, which involves purely radiative transfer calculations, has generally not been computed
984 in climate model simulations (see section 2.3.6 for future efforts) due to computational
985 considerations; instead, ERF has become the preferred approach to quantifying RF.
986 Attempts to isolate IRF from ERF using radiative kernels have noted that most of the
987 intermodel spread in ERF from CO₂ forcing does not arise from differences in tropospheric
988 adjustments, but rather from differences in IRF (Chung and Soden 2015). Indeed,
989 intermodel differences in the calculation of IRF have been a persistent problem in GCMs
990 (Cess et al. 1993; Soden et al 2018) despite the presence of accurate and observationally
991 verified line-by-line calculations to constrain their counterparts in climate models (Collins
992 et al. 2006).

993

994

995 **2.3.6 Developments since AR5**
996
997

998 Marvel et al. (2015) and Shindell (2014) indicate that even for the ERF concept, efficacies (see
999 Expression 2.3) may be different for short-lived and regionally heterogeneous compounds like
1000 aerosols, ozone, and land use compared to greenhouse gases using various CMIP5 simulations.
1001 This would have implications for estimates of climate sensitivity using temperature changes
1002 over historical period. However, the cause of the findings on the efficacies in CMIP5 is under
1003 debate (Richardson et al., 2019). The ERF has been further described (Sherwood et al., 2015)
1004 and methods to calculate ERF have been better compared (Forster et al., 2016). Forster et al.
1005 (2016) find that uncertainties in ERF from fixed SST simulations are much lower than using the
1006 regression technique. ERF from the fixed SST simulations can be quantified to an accuracy of
1007 0.1 W m^{-2} at the 5-95% confidence interval in 30-year simulations. This implies that ERF from
1008 very small forcings ($<0.1 \text{ W m}^{-2}$) would require many ensembles or very long simulations.
1009
1010 The ERF framework has allowed a clearer understanding of the forcing and climate response of
1011 a climate driver; it is now constructive to distinguish into “instantaneous”, “rapid adjustment”,
1012 and “equilibrium”. Figure 2.4 shows how radiative fluxes and surface sensible and latent heat
1013 fluxes change for a doubling of CO₂ in multi-model simulations and is a modern version of
1014 Figure 2.1, explicitly using the ERF concept. The instantaneous radiative forcing due to CO₂ is
1015 well known to be primarily due to the longwave (LW), with a weak solar (shortwave (SW))
1016 effect (Fig 2.4 left) shown as the positive values at TOA. Positive values at the surface in Fig
1017 2.4 indicate that the surface gains energy. If the difference between the flux changes at TOA
1018 and surface is positive, it means the atmosphere gains energy. The SW absorption by CO₂

1019 reduces the solar absorption at the surface and causes a weak change at the TOA where it is
1020 very small compared to LW TOA.

1021
1022 By contrast, the SW contribution to atmospheric absorption is 35-40% of the LW trapping of
1023 energy in the atmosphere. The instantaneous part involves only the initial radiative perturbation.
1024 The rapid adjustments (Figure 2.4 middle) are processes that occur to equilibrate the atmosphere
1025 with no SST changes. A doubling of CO₂ gives an initial heating of the troposphere and a
1026 cooling of the stratosphere. The cooling of the stratosphere is well known (see Section 2.2) and
1027 the consequent adjustment in the radiative fluxes was included in the early applications of the
1028 RF concept. The initial radiative perturbation in the troposphere increases temperature and
1029 water vapor, and changes clouds. The increase in tropospheric temperature reduces the net
1030 atmospheric absorption (giving a radiative cooling) but the reduction in stratospheric
1031 temperature has a larger impact on the net atmospheric absorption. The overall rapid
1032 adjustments of temperature, water vapor and clouds lead to an enhanced atmospheric absorption
1033 of similar size to the initial heating (Myhre et al., 2018). The atmospheric equilibrium is
1034 achieved by reduction in the surface latent and sensible heat fluxes, thereby making a clear link
1035 between the atmospheric absorption and precipitation changes, at the global-mean level (e.g.
1036 Andrews et al., 2010). The fast response of global-mean precipitation can be estimated, to
1037 reasonable accuracy, from the atmospheric component of the ERF (e.g. Samset et al. 2016).

1038
1039 In the full climate response to doubling of CO₂ (Fig 2.4 right), the surface temperature changes
1040 to bring TOA and the atmosphere net fluxes into equilibrium (see section 2.1). Note that the
1041 initial atmospheric radiative heating (which leads to a precipitation decrease) when ERF is

1042 diagnosed, turns into a radiative cooling, when the full surface temperature response is allowed.
1043 Since AR5 there has been an improved quantification of the rapid adjustment processes and
1044 their inter-model diversity. Double radiation calls (Ghan, 2013) and radiative kernels (Soden et
1045 al., 2008) allow a differentiation of the instantaneous radiative perturbation and the rapid
1046 adjustment and individual rapid adjustment terms, respectively.

1047

1048 Smith et al. (2018) quantify the rapid adjustment contributions to ERF based on radiative
1049 kernels in multi-model simulations for various climate drivers. Figure 2.5 shows the rapid
1050 adjustment terms for two scenarios: a doubling of CO₂, and a tenfold increase in the black
1051 carbon (BC) abundance. In fact, the IRF at TOA for a doubling of CO₂ and tenfold increase in
1052 BC is very similar (Smith et al., 2018), but their total rapid adjustment (the bars on the yellow
1053 background in Fig 2.5) is strong and of opposite signs. Temperature increases enhance the
1054 outgoing longwave radiation and are thus a negative rapid adjustment, which can be seen both
1055 for land surface and tropospheric temperature for increase in CO₂ and BC.

1056

1057 The stratospheric cooling due to the CO₂ increase, on the other hand, gives a positive rapid
1058 adjustment. Increases in the tropospheric temperature increase water vapor, thus a positive rapid
1059 adjustment by increasing the greenhouse effect. For a doubling in CO₂, the high cloud cover
1060 increases with a reduction in the lower clouds, but these features are opposite for BC explaining
1061 the different sign of rapid adjustment of clouds for these two climate drivers. For CO₂ the rapid
1062 adjustments other than the stratospheric temperature adjustment happen to cancel each other
1063 out, making ERF and RF quite similar in that case. Based on available estimates for doubling of
1064 CO₂ this was already noted in AR5.

1065

1066 The total rapid adjustment for BC is strongly negative; nevertheless, individual rapid
1067 adjustments vary in sign, so that the net effect is a residual of these competing effects. Soden et
1068 al. (2018) indicate that the large diversity in ERF due to change in CO₂ among GCMs arise from
1069 differences in the instantaneous forcing. Results from Smith et al. (2018) support this by having
1070 a range of less than 10% (5-95% confidence interval) of the non-stratospheric temperature rapid
1071 adjustments. Combining the uncertainty in the tropospheric rapid adjustment with 10%
1072 uncertainty in RF derived from detailed off-line radiation schemes as given in AR5 provides an
1073 uncertainty in ERF of 14%. Section 10 describes the implication of a reduced uncertainty range
1074 of WMGHG forcing compared to that given in IPCC AR5 (20%) for the uncertainty in the total
1075 anthropogenic ERF.

1076

1077

1078

1079 **2.4 Summary and challenges**
1080
1081

1082 A future challenge with respect to the forcing concept is to quantify whether the efficacy is
1083 unity when adopting the current definition of ERF for all drivers of climate change and various
1084 models, and thus to understand the diversity among some previous results (Shine et al., 2003;
1085 Hansen et al., 2005; Shindell 2014; Marvel et al., 2015; Richardson et al., 2019).

1086

1087 Further there is a need to better understand the rapid adjustment processes in climate models,

1088 both the degree of influence of diversity in IRF as indicated in Smith et al. (2018), but also
1089 dedicated process studies comparing GCMs with high resolution models with weaker degrees of
1090 parametrization, such as convection permitting models. There is a high potential for progress to
1091 be made using results from the ongoing CMIP6 model intercomparison project, which is
1092 supporting IPCC AR6 (Eyring et al., 2016); efforts have been made to ensure that more
1093 diagnostics are available to enable the drivers of ERF to be better quantified and hence for inter-
1094 model diversity to be better characterized. Such studies will aid the understanding of whether
1095 uncertainties in ERF of CO₂ and other greenhouse gases are substantially larger than using RF,
1096 as was indicated in Myhre et al. (2013).

1097

1098 Lastly, there is a need to develop methodologies to compare weak radiative perturbations,
1099 which will continue to need to be quantified using RF, with the major climate drivers which are
1100 increasingly being quantified from various model simulations using the ERF concept. It is
1101 possible that once the generic understanding of the rapid adjustments has improved, it can be
1102 applied to the weak forcings and enable ERF to be estimated from their RFs.

1103

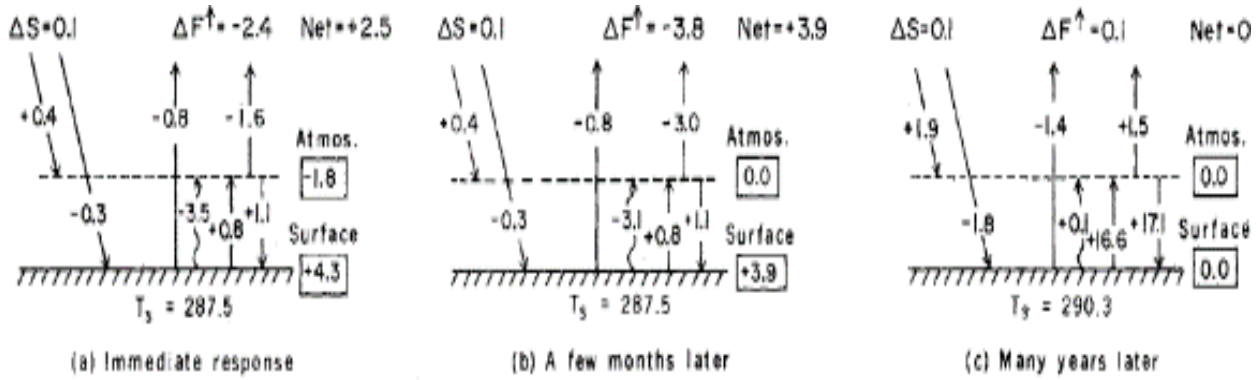


Fig. 4. Change of fluxes (watts per square meter) in the 1-D RC model when atmospheric CO₂ is doubled (from 300 to 600 ppm). Symbols: ΔS , change in solar radiation absorbed by the atmosphere and surface; ΔF^{\uparrow} , change in outward thermal radiation at top of the atmosphere. The wavy line represents convective flux; other fluxes are radiative.

Figure 2.1: Changes in top-of-atmosphere shortwave (ΔS) and longwave (ΔF^{\uparrow}) irradiances following a doubling of CO₂ from 300 ppm, in a one-dimensional radiative-convective model. Wavy lines represent changes in convective fluxes, with all other lines radiative. The values in boxes show the net flux changes at the surface and for the atmosphere. (a) the instantaneous flux change, (b) the change after a few months and includes the effect of stratospheric temperature adjustment and other rapid adjustments represented in the model and (c) the flux changes when the system has come to equilibrium following a change in surface temperature (T_s). Figure taken from Hansen et al. (1981).

Components of radiative forcing for principal emissions

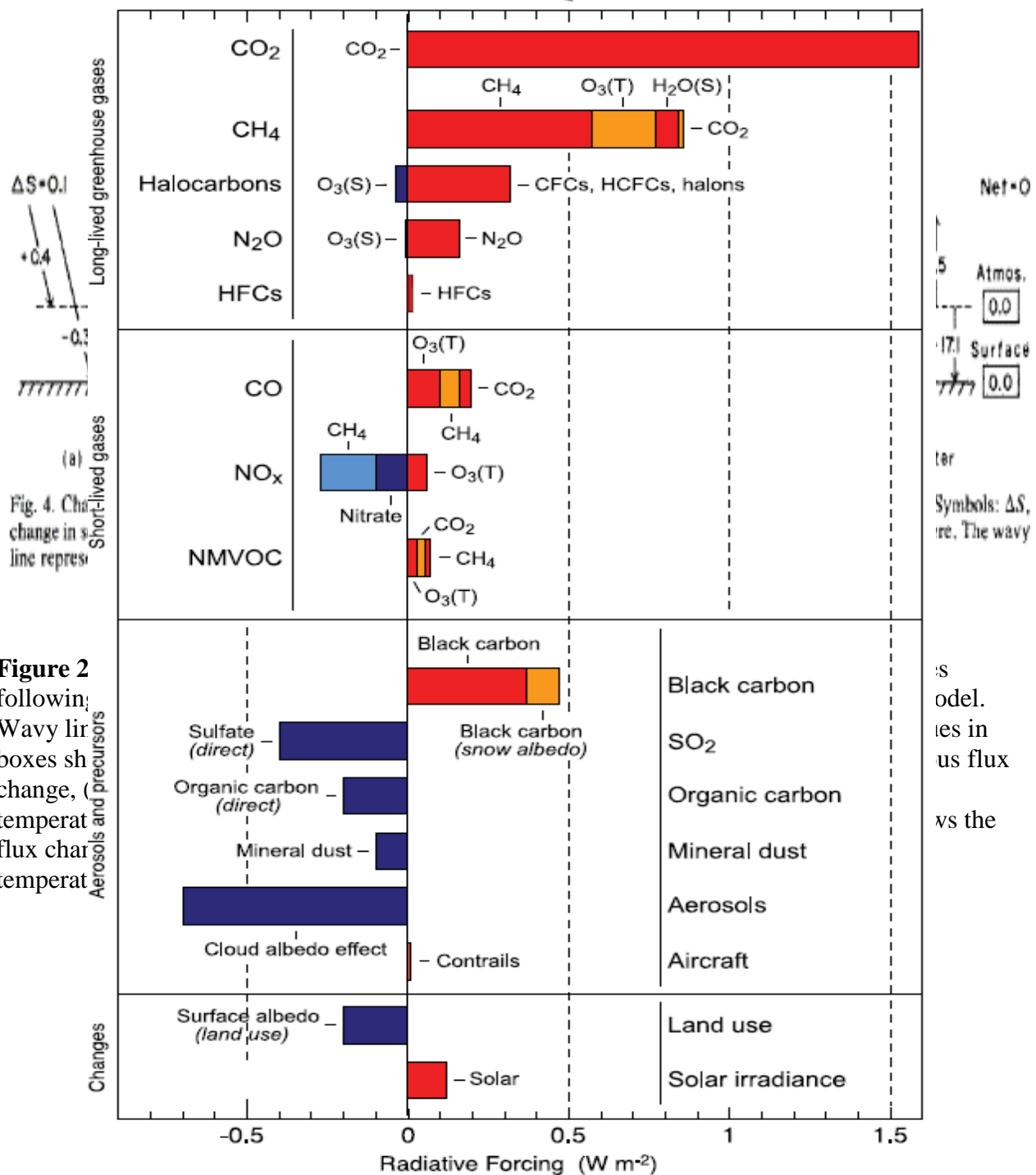


Figure 2.21. Components of RF for emissions of principal gases, aerosols and aerosol precursors and other changes. Values represent RF in 2005 due to emissions and changes since 1750. (S) and (T) next to gas species represent stratospheric and tropospheric changes, respectively. The uncertainties are given in the footnotes to Table 2.13. Quantitative values are displayed in Table 2.13.

1160 **Figure 2.2**

1161

1162

1163 Components of RF by emissions of gases, aerosols, or their precursors for the period 1750-

1164 2005. O₃(T) and O₃(S) indicate tropospheric and stratospheric ozone respectively. Figure from

1165 Forster et al. (2007).

1166

1167 [Jpeg can be obtained from

1168 <https://archive.ipcc.ch/report/graphics/images/Assessment%20Reports/AR4%20-%2>

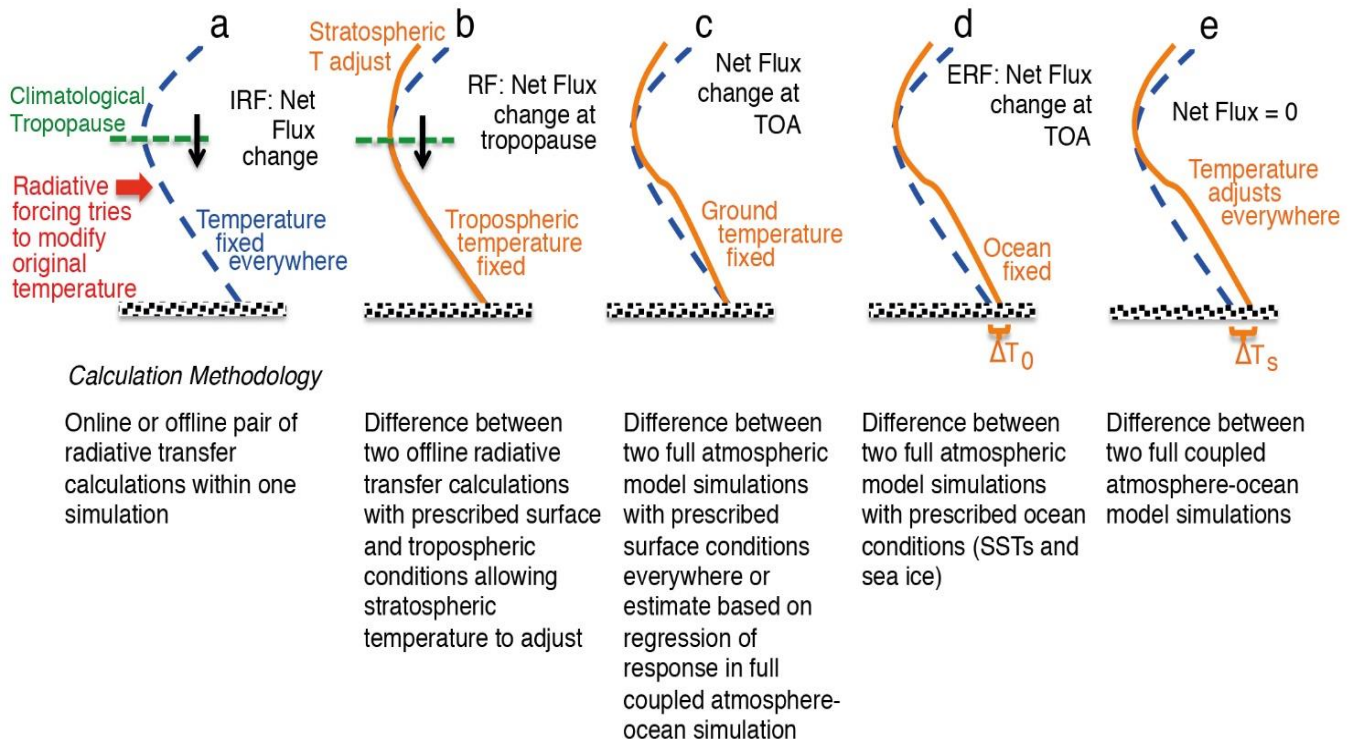
1169 WG1/Chapter%2002/fig-2-21.jpg].

1170

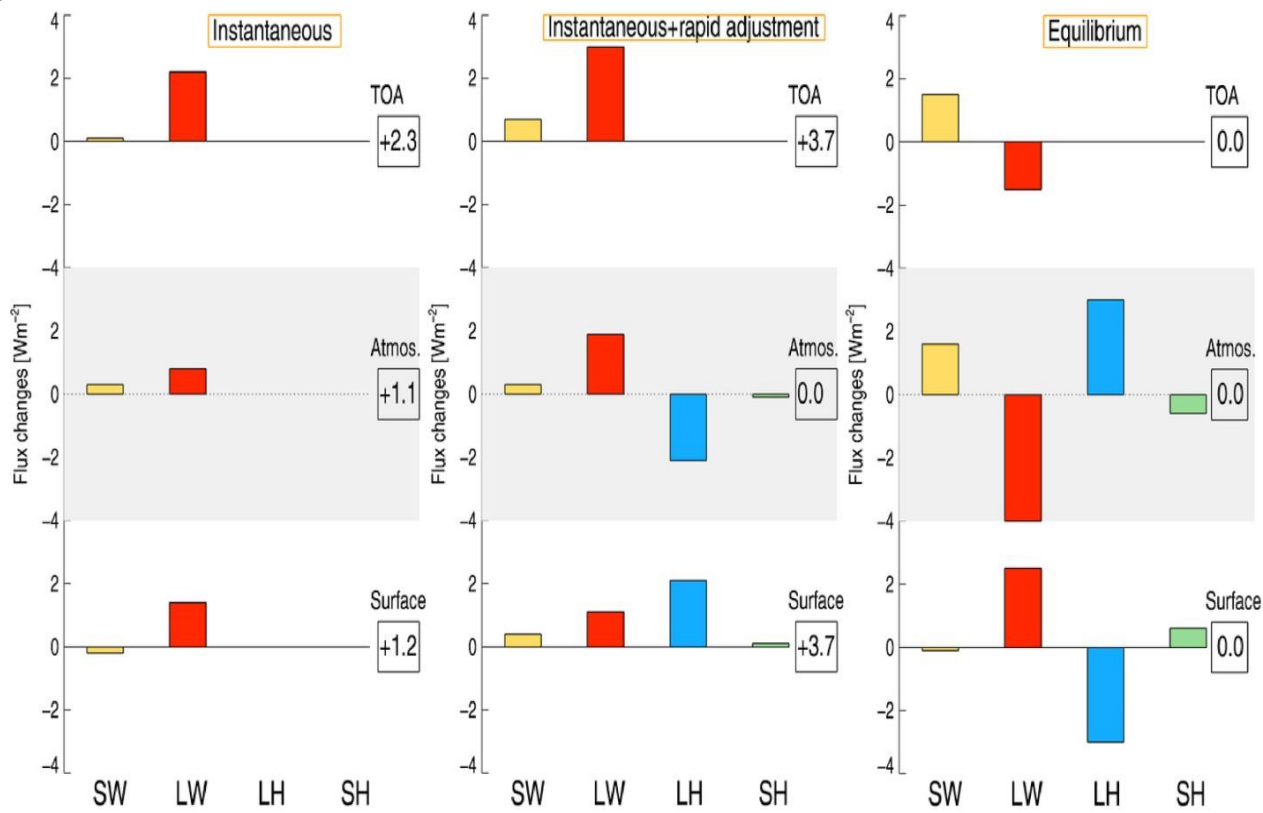
1171

1172

1173



1189



1190

1191

1192

1193

1194 **Figure 2.4:** Illustration of the change in the global energy balance (top of the1195 atmosphere -TOA, atmosphere - Atmos., and surface) from a doubling of the CO₂

1196 concentration for an instantaneous perturbation, instantaneous and rapid adjustment,

1197 and the climate system in new equilibrium. Changes in the energy fluxes of solar

1198 radiation (SW) is given in yellow bars, longwave (LW) in red bars, latent heat (LH) in

1199 blue bars and sensible heat (SH) in green bars. The net flux changes at TOA, Atmos.,

1200 and surface are given in numerical values in boxes. This figure can be considered as a

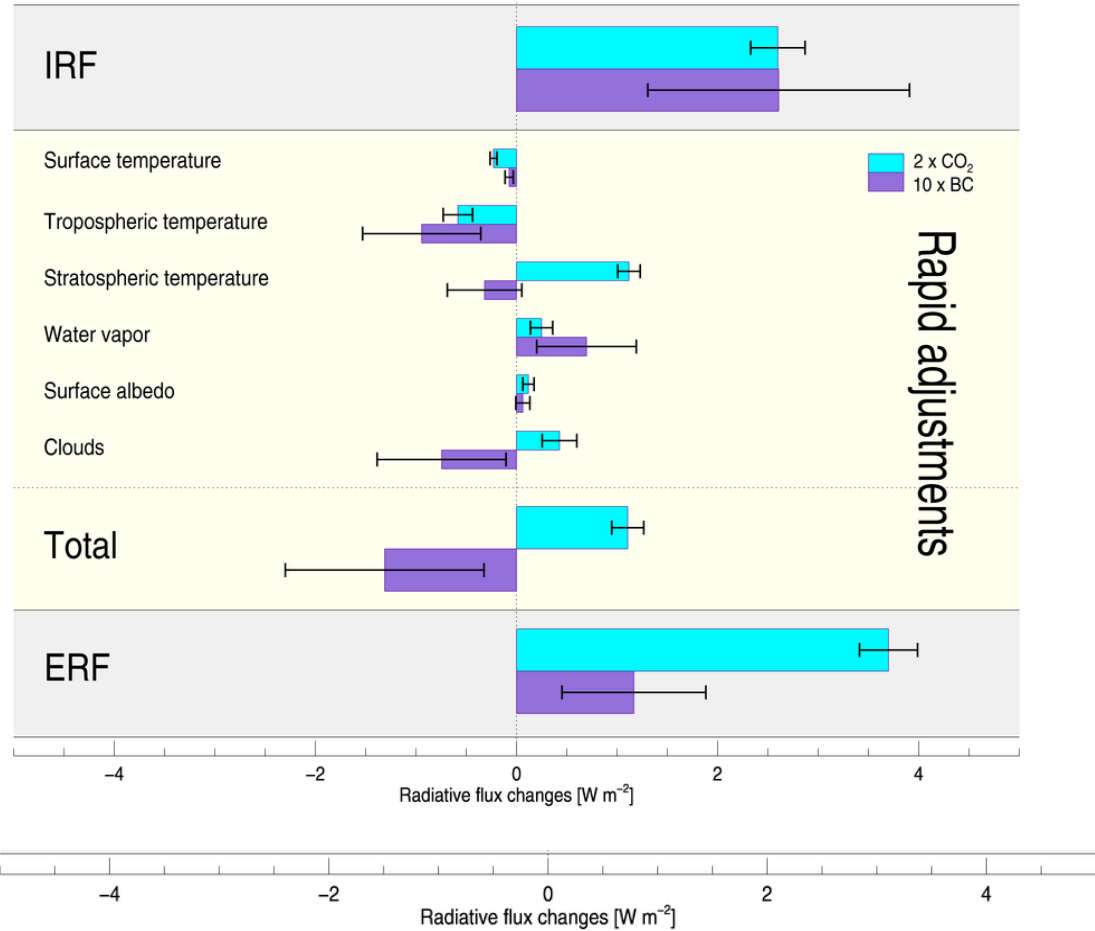
1201 modern day-version of Figure 2.1.

1202

1203

1204
1205

Figure 2.5: Instantaneous radiative forcing (IRF), individual and total rapid adjustments, and



1206 effective radiative forcing (ERF) at the top of the atmosphere for a doubling of CO₂ and a
1207 tenfold increase in the BC concentration. The total rapid adjustment is the sum of the individual
1208 terms of surface temperature change (only land), tropospheric temperature, stratospheric
1209 temperature, water vapor, surface albedo change, and clouds. The uncertainties are one standard
1210 deviation among the PDRMIP models. It is a coincidence that the IRF for CO₂ and BC is almost
1211 identical. The figure is modified from Smith et al. (2018).

1212

1213 **Section 3: CO₂ and other well-mixed greenhouse gases**

1214

1215

1216 Accurate computation of the radiative forcing by CO₂ and other gaseous constituents of the

1217 Earth's atmosphere only became possible with the advent of accurate spectroscopic

1218 measurements in the laboratory. While these measurements still serve as the primary

1219 foundation for calculations of the greenhouse effect, for some simple molecules the

1220 combination of quantum and statistical mechanics provides a complementary framework for

1221 interpreting the observations and extending them to conditions that have not been directly

1222 observed. The inputs to this framework are the energies, numbers (degeneracies), and

1223 occupation numbers of excited states of each constituent, the transitions among these

1224 excited states, and the interactions of these transitions with light and heat following

1225 Einstein's quantum theory of radiation. One of the first attempts to compute the effects of

1226 doubling CO₂ in an atmosphere in radiative-convective equilibrium produced a remarkably

1227 good estimate of 4 K (Hulbert, 1931). However, this finding and other supporting evidence

1228 was largely unappreciated due to prevailing assumptions prevalent that the strong broadband

1229 absorption of water vapor would dominate the regions of the spectrum where CO₂ is

1230 radiatively active and that the logarithmic curve of growth of CO₂ radiative effects in these

1231 regions would further constrain the impact of rising CO₂ on the climate system.

1232

1233

1234 Parameterizations of the rudimentary laboratory measurements of CO₂ with ambient and

1235 prescribed amounts of water vapor accumulated by the mid-20th century contradicted the

1236 assumption that water vapor would saturate the primary CO₂ bands (Callendar, 1941), but

1237 did little to change the balance of opinions held by the scientific community. Further, more

1238 detailed information on the bands of CO₂ based on its structure and more accurate
1239 spectrometers revealed the potential for additional absorption of terrestrial radiation at the
1240 edges of these bands and in the upper atmosphere, where the overlap among neighboring
1241 absorption lines is greatly reduced (Martin & Barker, 1932).

1242
1243
1244 Further progress had to await the need for operational weather forecasting and active and
1245 passive remote sensing during and after the Second World War together with the subsequent
1246 military investments in computing infrastructure, spectroscopic characterization of the
1247 Earth's atmosphere, and the theory of radiative transfer (see historical description by Weart,
1248 1997). One of the first applications of the new digital computers to atmospheric science
1249 revealed that the absorption by CO₂ of upwelling terrestrial radiation in the stratosphere had
1250 been systematically underestimated in prior studies based on manual calculations (Kaplan,
1251 1952). Subsequent computational solutions to the infrared radiative transfer for the whole
1252 atmosphere (Plass, 1956, 1956bb) revealed that the forcing by doubling CO₂ is sufficient to
1253 change the mean surface temperature of the Earth by about 3.6 K (Plass, 1956, 1956aa).

1254
1255
1256 In the 1960s, general circulation models of the atmosphere were developed that included
1257 reasonably complete parameterizations of solar and infrared radiative transfer together with
1258 detailed treatments of the radiative properties of the Earth's atmosphere and surface.
1259 Pioneering calculations with one-dimensional (Manabe & Wetherald, 1967) and three-
1260 dimensional (Manabe & Wetherald, 1975) models demonstrated the effects of CO₂ on the full
1261 climate system and suggested that the surface temperature would increase by approximately
1262 2.5 to 3 K for a doubling of carbon dioxide concentrations (Fig. 3.1). These models and other,

1263 simpler energy balance models (Ramanathan et al., 1979) formed the basis for one of the first
1264 comprehensive reviews of the state of climate change science for policy makers, the pivotal
1265 Charney Report (National Research Council, 1979).

1266

1267 Due to rapid increases in computing power, much more exact treatments of radiative transfer
1268 known as line-by-line (LBL) codes were developed starting in the 1970s. Early examples
1269 include the Fast Atmospheric Signature Code (Smith et al., 1978), a rapid method for
1270 computing the Voigt line shape profile that includes line broadening and Doppler shifting
1271 (Drayson, 1976) , and the Automated Atmospheric Absorption Atlas (Scott and Chedin 1981).
1272 These codes are based upon comprehensive tabulations of all known absorption lines for over
1273 fifty radiatively active gaseous species in the Earth's atmosphere. An early example that has
1274 grown significantly and is in widespread usage is the high-resolution transmission molecular
1275 absorption (HITRAN) database, which was first developed by the Air Force Cambridge
1276 Research Laboratories (McClatchey et al., 1973) and subsequently maintained and updated by
1277 the Harvard Smithsonian Center for Astrophysics; the most recent version is HITRAN2016
1278 (Gordon et al. 2017). A parallel European-led line database called GEISA (Gestion et Etude des
1279 Informations Spectroscopiques Atmosphériques) was launched in 1974 at the Laboratoire de
1280 Météorologie Dynamique (LMD) in France (Chédin et al, 1982; Husson et al, 1992) has been
1281 updated most recently in 2015 (Jacquinot-Husson et al, 2016). These LBL codes now serve as
1282 the reference radiative transfer codes for calculation of CO₂ forcing and its representation in
1283 Earth System Models (e.g., Collins et al., 2006).

1284

1285

1286

1287 While most climate models compute radiative transfer using full codes, in many applications
1288 simple formula, based on more detailed calculations, are useful for computing the global
1289 annual- mean greenhouse gas radiative forcing from changes in their concentration; such
1290 formulae appear in the First Assessment Report of the Intergovernmental Panel on Climate
1291 Change (IPCC; Shine, Derwent, Wuebbles, & J-J. Morcrette, 1990) and have been utilized and
1292 updated in subsequent IPCC Assessment Reports. For CO₂, to leading order, the forcing in the
1293 infrared is proportional to the logarithm of the concentration (Goody & Yung, 1989;
1294 Pierrehumbert, 2011), and in the Third Assessment Report (Ramaswamy et al. 2001) the IPCC
1295 formula was augmented to include absorption of solar radiation by CO₂ (Myhre et al., 1998).

1296

1297 One of the lingering uncertainties in the radiative forcing by CO₂ is due to remaining
1298 uncertainties in its spectroscopic characterization. If we assume that the energies associated
1299 with the most important excited states of the CO₂ molecule are known precisely, then three
1300 principal spectroscopic properties of CO₂ involved in computing its radiative forcing are its
1301 line strengths, line half widths, and line shapes, in addition to line overlaps with other
1302 absorbers. Systematic propagation of these uncertainties through to the radiative forcing
1303 from doubling CO₂ concentrations suggeststhat the combined effects of residual errors in
1304 these properties are less than approximately 0.7%; this suggests that current LBL models are
1305 more than sufficient for accurately computing the climate forcing from this WMGHG
1306 (Mlynczak et al., 2016).

1307

1308 **3.1 CH₄, N₂O, CFCs and halogenated compounds:**

1309
1310
1311 Since the atmospheric concentrations of CH₄ are two orders of magnitude lower than those
1312 of CO₂, it was historically difficult to detect through chemical sampling. Methane was first
1313 detected under ambient conditions in the 1940s using purely spectroscopic techniques
1314 (Migeotte, 1948). In turn, the atmospheric concentrations of N₂O, the third most important
1315 anthropogenic greenhouse gas, are three orders of magnitude lower than those for CO₂. The
1316 common assumption was that these trace species were present at insufficient levels to have
1317 an appreciable impact on the climate system.

1318
1319 As a result, the importance of the radiative forcings by long-lived greenhouse gases other
1320 than CO₂ went largely unappreciated. Wang et al. (1976) and Donner and Ramanathan
1321 (1980) were amongst the first to compute the impact of increasing concentrations of methane
1322 and nitrous oxide and show that the effect could be substantial. Wang et al (1976) computed
1323 the effects of doubling the concentrations of CH₄, N₂O (as well a NH₃ and HNO₃) as a
1324 simple proof-of-principle test of anthropogenic perturbations to the concentrations of these
1325 compounds.

1326
1327 They found that the combined effects of doubling concentrations of CH₄ and N₂O also
1328 approached 1K once the climate system had re-equilibrated to the elevated concentrations
1329 and forcing. To advance beyond these simpler tests required modeling the joint interactions
1330 between the physical climate system and the radiatively active species together with the
1331 associated networks of chemical sources and sinks for these species More advanced models
1332 that include these interactions can treat the nonlinear effects of spectral overlap among the

1333 well-mixed greenhouse gases, ozone, and water vapor. Ramanathan (1980) constructed a
1334 prototype of this class of coupled chemistry-climate model and showed that the non-CO₂
1335 WMGHGs could contribute nearly half the warming projected for 2025 assuming persistence
1336 of extant emissions trends. This conclusion was buttressed in subsequent studies starting with
1337 Ramanathan et al (1985) who concluded that the minor well-mixed greenhouse gases could
1338 contribute as much warming as projected increases in CO₂ concentrations. Indirect effects of
1339 CH₄ and N₂O were also uncovered in this time frame and are discussed in greater detail in
1340 Section 4.1.

1341
1342 Because chlorofluorocarbons (CFCs) have strong bands in the mid-infrared window, a region
1343 of the spectrum otherwise largely transparent to terrestrial infrared radiation, increasing
1344 concentrations of these gases leads to rapid increases in the Earth's greenhouse effect (Fig.
1345 3.2). Lovelock et al. (1973), after discovering the ubiquity of CFCs in the Earth's
1346 atmosphere, suggested that it might serve as a greenhouse gas. The implications of
1347 unchecked historical emissions of these gases (prior to the imposition of the Montreal
1348 Protocols in 1987) and the consequent increase in the total greenhouse effect for the mean
1349 surface temperature were first calculated by Ramanathan (1975). He found that continuing
1350 emissions unabated until the year 2000 would ultimately lead to increases in surface
1351 temperature approaching 1 K. Unlike CO₂, the major absorption bands of the CFCs are far
1352 from saturated, and therefore the forcing increases linearly and rapidly with increasing
1353 concentration.

1354

1355 Ramanathan et al (1985 investigated a larger set of compounds, including several CFCs, one
1356 HCFC and some fully fluorinated compounds (Fig 3.3). Fisher et al. (1990) expanded the
1357 number of halocarbons having a greenhouse effect by providing radiative forcing for a large
1358 group of CFC replacements including HCFCs and HFCs. Some of the halocarbons have
1359 major absorption bands outside the The mid-infrared window and thus have strong overlap
1360 with water vapor and even some with CH₄ and N₂O (Ramanathan et al., 1985). Pinnock et
1361 al. (1995) illustrated how the radiative forcing varies over the infrared spectral region for an
1362 increase in 1 ppb of an idealized halocarbon absorbing equally at all wavelengths (Fig. 3.4).

1363 The figure shows that halocarbons absorbing particularly in the region 800-1000 cm⁻¹ are
1364 very efficient compared to e.g. compounds like CF₄ with strong absorption band located
1365 closer to 1300 cm⁻¹.

1366

1367 Due to the weak absorption by the halocarbons and weak overlap by other gases in the mid-
1368 infrared window region Dickinson et al. (1978) showed that these compounds warm the
1369 lower stratosphere. This is unlike CO₂ and most halocarbons therefore have a positive
1370 contribution to radiative forcing from the stratospheric adjustment rather than the negative
1371 contribution from CO₂ (see section 2). The state of knowledge of radiative forcing per unit
1372 concentration change for halocarbons is discussed in section 11.3 on Radiative Efficiency.

1373 While much of the work to date had stressed the climatic effects of the infrared bands of
1374 these minor well-mixed gases, the fact that the shortwave bands also contribute non-
1375 negligible forcing was first highlighted by Collins et al. (2006).

1376

1377 Their study showed that all of the atmosphere-ocean global climate models participating in
1378 the Fourth Assessment Report of the IPCC omitted the shortwave effects of CH₄ and N₂O.
1379 This omission was starting to be corrected by the time of the Fifth Assessment, and these
1380 effects have now been incorporated into the simple bulk formulas for forcing by these
1381 greenhouse gases (Collins et al., 2018; Etminan et al., 2016). The simple formula in Etminan
1382 et al. (2016) includes in addition to direct shortwave effect the shortwave contribution due to
1383 stratospheric temperature adjustment and updated water vapor overlap with methane,
1384 resulting in a 25% enhancement in the radiative forcing of methane
1385
1386
1387
1388

1389 **3.2 Summary and Challenges**
1390
1391

1392 While current LBL models are more than sufficient for accurately computing the climate
1393 forcing from WMGHG (Mlynczak et al., 2016), unfortunately this accuracy has not been
1394 propagated to the radiation codes used in the ensemble of climate models used for climate
1395 projections. The first systematic quantifications of the spread in CO₂ radiative forcing were
1396 conducted using the generation of models used in the first IPCC assessment (Cess et al., 1993;
1397 Ellingson & Fouquart, 1991; Fels et al. 1991), followed by evaluations of modeled forcings
1398 used in the fourth (W. D. Collins et al., 2006) and fifth (Soden, Collins, & Feldman, 2018)
1399 IPCC assessments.

1400
1401
1402 The 1-sigma relative range in the TOA forcings for the latter two studies is 20%, approximately
1403 1.5 decades larger than the LBL uncertainty (Fig. 3.5). This has significant implications for the
1404 interpretation of historical climate change simulations. Reduction and ideally elimination of this
1405 large range in CO₂ radiative forcing remains an ongoing challenge for the climate modeling
1406 community, with efforts continuing under the WCRP/CMIP6 Radiative Forcing Model
1407 Intercomparison Project (RFMIP) (Pincus et al., 2016). Better agreement of ESM radiative
1408 parameterizations with LBL models is both feasible and highly desirable. It would help ensure
1409 more accurate interpretations of the historical climate record and more actionable projections of
1410 future climate and climate-change mitigation scenarios.

1411
1412
1413

1414
1415
1416
1417

Figures:

Figure 3.1: Vertical distributions of temperature in radiativeconvective equilibrium for various values of CO₂ content. (Manabe and Wetherald, 1967).

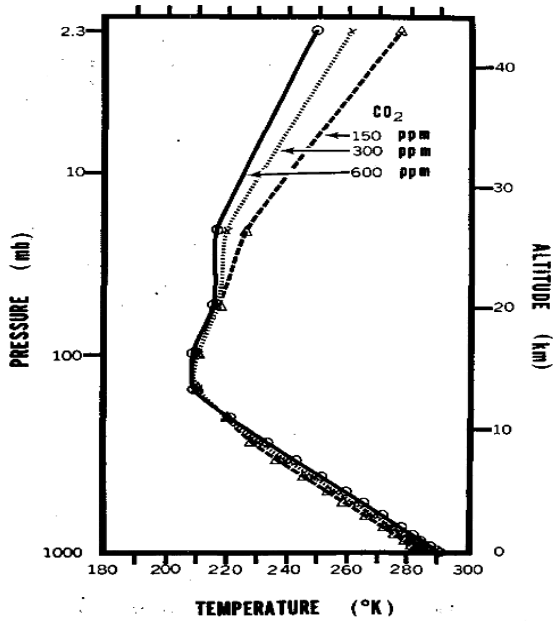


FIG. 16. Vertical distributions of temperature in radiative convective equilibrium for various values of CO₂ content.

1418

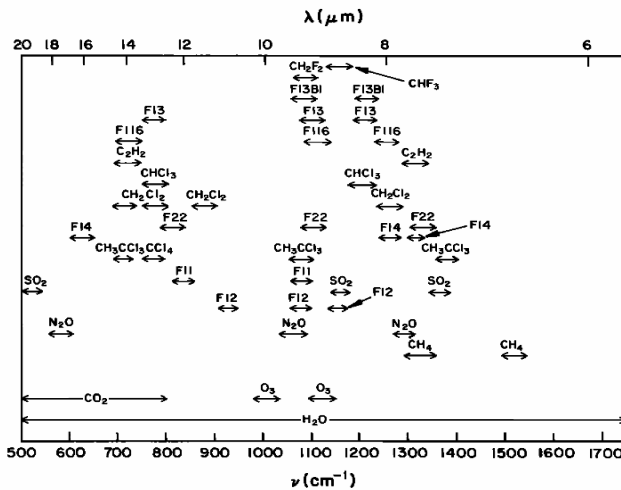


Fig. 3. Spectral locations of the absorption features of various trace gases. The spectral region between 7 and 13 μm is referred to as the atmospheric "window." The anthropogenic trace gases have the potentials for making it into a "dirty window." This figure was provided by J. T. Kiehl (private communication, 1986).

1419

Figure 3.2: Spectral locations of the absorption features of various trace gases. The spectral region between 7 and 13 μm is referred to as the atmospheric “window” because of its relative transparency compared to neighbouring spectral regions. The anthropogenic trace gases have the potentials for making it into a “dirtier window.” (Ramanathan et al, 1987).

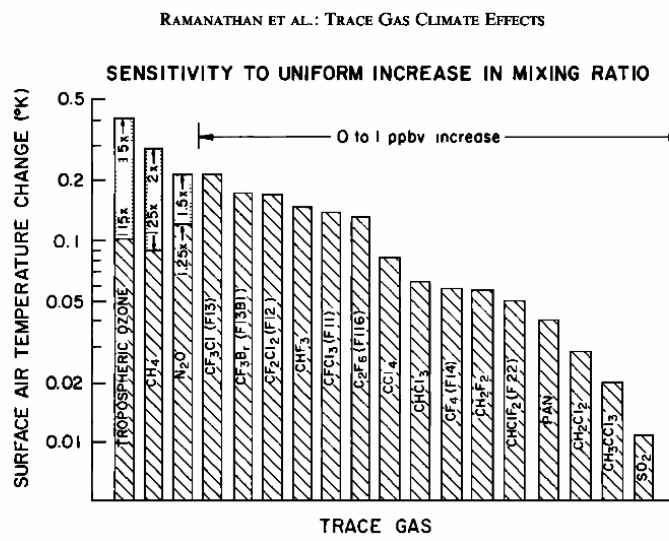


Fig. 1. Surface temperature increase due to a 0-1 ppbv increase in trace gas concentration. Tropospheric O₃, CH₄, and N₂O increases are also shown for comparison.

Figure 3.3: Surface temperature increase due to a 0-1 ppbv increase in

trace gas concentration. Tropospheric O₃, CH₄, and N₂O increases are also shown for comparison (Ramanathan et al, 1985).

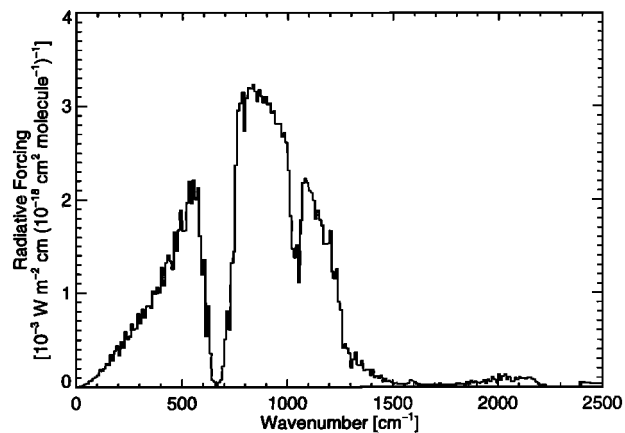


Figure 3. Radiative forcing per unit cross section for the GAM atmosphere including clouds, for a 0–1 ppbv increase in mixing ratio. This graph is repeated in tabular form in the Table 8.

1453 **Figure 3.4:** Radiative forcing per unit cross section for a 0–1 pp by increase
 1454 in mixing ratio of a gray-body absorber (Pinnock et al, 1995).

Reducing the uncertainty

Radiative forcing uncertainty in GCMs has remained high over the past 25 years. LBL calculations show that this uncertainty can be substantially reduced.

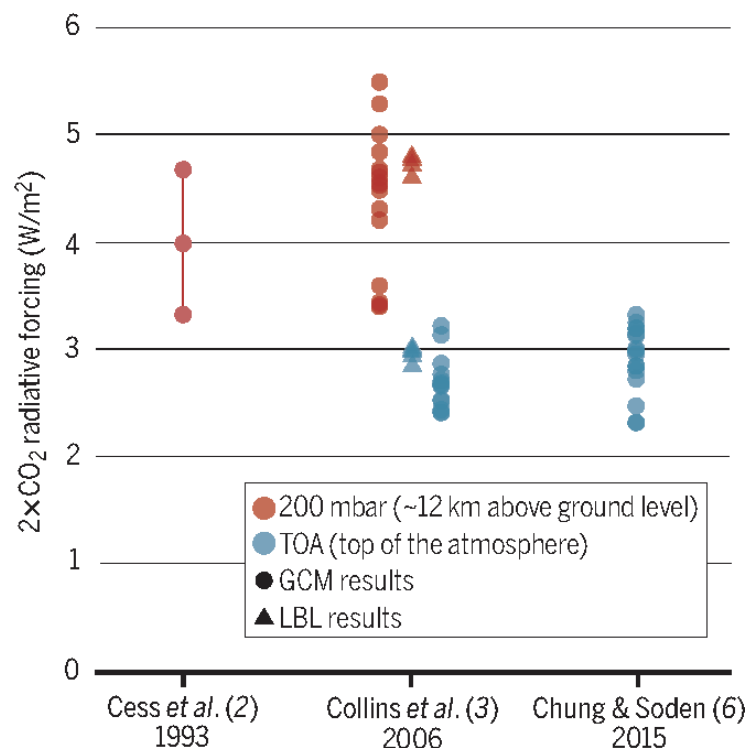


Figure 3.5: Estimates of radiative forcing from doubling CO₂ from three multi-model intercomparisons spanning 1993 to 2015, at the top of the atmosphere and a pseudo-tropopause at 200 mb (Soden et al., 2018).

1457

1458

1459

1460

1461

1462

1463

1464

1465
1466

1467 **Section 4: Short-lived trace gases and chemistry-climate interactions**
1468
1469
1470 The importance of atmospheric chemistry for climate began to be recognized after a
1471 multitude of advances in the early 1970s revealed a chemically active atmosphere that
1472 could be perturbed both by natural and anthropogenic activities (National Research
1473 Council, 1984). The foundation for these advances was laid over the preceding four to five
1474 decades. This included the knowledge of stratospheric ozone photochemistry (Chapman
1475 1930; Hampson 1965; Bates and Nicolet 1950), urban photochemical air pollution
1476 (Haagen-Smit 1952; Altshuller and Bufalini 1965) and tropospheric composition and
1477 photochemistry (Cadle and Allen 1970; Bates and Witherspoon (1952). Developments
1478 were also dependent on quantitative but (initially) highly uncertain estimates of
1479 atmospheric amounts of several trace gases including ozone (in the stratosphere only),
1480 nitrogen, oxygen, noble gases, CO₂, H₂O, CH₄ and N₂O (below the tropopause) (see
1481 section 1 for more details). We review below developments in atmospheric chemistry that
1482 set the stage for the recognition of chemistry as an integral part of the climate system and
1483 process- level advances made thereafter that have shaped our knowledge of radiative
1484 forcing from short- lived trace gases and chemistry-climate interactions.

1485
1486
1487
1488

1489 **Section 4.1 Atmospheric Chemistry and Climate Connections in 1970s-1980s**

1490

1491 The importance of chemistry for the radiative forcing of climate change was recognized
1492 by studies in the early 1960s that highlighted the important role of ozone in maintaining
1493 stratospheric temperature and the tropopause (Manabe and Möller 1961; Manabe and
1494 Strickler 1964). The seminal work of Manabe and Wetherald (1967) demonstrated that
1495 stratospheric ozone is not only important for maintaining stratospheric temperature but
1496 also influences tropospheric and surface temperature though the effect is small compared
1497 to that of CO₂.

1498

1499 A series of new developments in atmospheric chemistry through the 1970s and 1980s
1500 established the close links between stratospheric and tropospheric composition and
1501 chemistry and how human activities can perturb these linkages with consequences for
1502 climate change. The first of these developments was the discovery of human influence on
1503 stratospheric ozone through catalytic ozone destruction via nitrogen oxide (NO_x)
1504 (Crutzen 1970). Studies showed that increases in NO_x due to human activities leading to
1505 enhanced fossil fuel combustion (such as from a planned fleet of high-altitude supersonic
1506 transport planes) (Johnston 1971; Crutzen 1972a; McElroy et al. 1974) or changes in its
1507 primary source gas, N₂O (McElroy et al. 1977; Wang and Sze 1980) could cause
1508 significant stratospheric ozone loss in the future with consequences for climate
1509 (Ramanathan et al. 1976).

1510

1511 Around the same time, Molina and Rowland (1974) identified the role of
1512 chlorofluorocarbons (CFCs) as a major source of chlorine responsible for catalytic ozone
1513 destruction. Further developments in the understanding of the evolution of stratospheric
1514 ozone depletion during this time period are reviewed elsewhere (Wallington et al. 2018;
1515 Solomon 1999; Crutzen and Lelieveld 2001).

1516

1517 The next key development in atmospheric chemistry was the identification of the
1518 hydroxyl (OH) radical as the primary driver of tropospheric chemistry by Levy (1971).

1519 Observational evidence of large concentrations of tropospheric OH (Wang and Davis
1520 1974; Wang et al. 1975; Perner et al. 1976) combined with theoretical and modeling
1521 work established that OH plays an extremely important role in controlling the

1522 abundance and lifetime of several trace gases emitted at the Earth's surface were either
1523 directly radiatively active (e.g., methane, halogenated hydrocarbons) or affected the
1524 abundance of other radiatively active gases by influencing OH concentrations (e.g.,
1525 CO, NMHCs (McConnell et al. 1971; Wofsy et al. 1972; Singh 1977; Chameides and
1526 Cicerone 1978; Logan et al. 1981). Thus, OH came to be recognized as the chemical
1527 filter or cleansing agent in the troposphere with important consequences for
1528 calculations of radiative forcing.

1529

1530 Finally, a major development that solidified the focus on chemistry-climate
1531 interactions was the recognition of the essential role of tropospheric ozone in
1532 determining the chemical composition and the radiation budget of the Earth's
1533 atmosphere. Till the work of Levy (1971), ozone was assumed to be, except over

1534 polluted regions, injected into the troposphere from the stratosphere due to mixing
1535 processes, chemically inert, and destroyed at the Earth's surface (Regener 1938; Junge
1536 1962; Fabian and Pruchniewicz 1977). The understanding evolved as both theoretical
1537 and observational analysis showed that the photochemical source of tropospheric
1538 ozone from OH-initiated oxidation of CO, methane, and other hydrocarbons in the
1539 presence of NO_x dominates over that provided via transport from the stratosphere
1540 (Crutzen 1972b, 1973; Chameides and Walker 1973; Fishman et al. 1979b; Fishman
1541 and Crutzen 1978). Subsequently, Fishman (1979a) quantified the climate influence of
1542 tropospheric ozone using its observed distribution.

1543

1544 Advances in understanding of atmospheric chemistry in both the troposphere and
1545 stratosphere, therefore, led to better understanding of its interactions with climate.
1546 Before elaborating on the calculation of ozone radiative forcing, we summarize below
1547 the key chemical interactions leading to indirect radiative forcing of climate change
1548 that were recognized by the end of 1980s based on modeling studies with simplistic
1549 representation of physical, chemical, and dynamical processes (see Wang et al. 1986;
1550 Ramanathan et al. 1987; Wuebbles et al. 1989 for more details). Tropospheric
1551 hydroxyl radical, as the primary sink for many trace gases, was at the center of these
1552 chemistry-climate interactions as illustrated in Figure 4.1.

1553 • Since reaction with OH is the primary removal mechanism for methane, CO, non-
1554 methane hydrocarbons, many halogenated hydrocarbons, DMS, and SO₂ any
1555 changes in the abundance of these gases would alter OH with subsequent

1556 feedbacks on the lifetime and abundance, and therefore climate effects of methane
1557 and halogenated hydrocarbons.

1558

- 1559 • Changes in the emissions of NO_x, methane, CO and non-methane hydrocarbons
1560 would affect tropospheric ozone with subsequent climate effects via tropospheric
1561 ozone changes or OH induced changes in the abundances as mentioned above.

1562

- 1563 • Changes in stratospheric ozone would impact tropospheric OH concentrations by
1564 influencing the rate of photolysis of tropospheric ozone resulting in the formation
1565 of O₁(D) – the primary source of tropospheric OH.

1566

- 1567 • Increased water vapor in a warmer climate would enhance OH with impacts on
1568 abundances of tropospheric ozone (depending on the levels of tropospheric NO_x)
1569 and methane.

1570

- 1571 • Oxidation of methane is a major source of stratospheric water vapor. Hence, any
1572 changes in methane would also influence stratospheric water vapor with
1573 subsequent climate implications due to water vapor radiative effects.

1574

1575 By mid-1980s, the scientific community recognized that a full understanding of the
1576 possible changes in ozone distribution and its subsequent effects on climate and
1577 biologically important UV radiation would require not only consideration of
1578 stratospheric processes but also knowledge of often coupled and non-linear, physical,

1579 chemical and biological processes controlling the chemical composition of the
1580 troposphere. This was reflected in the first international scientific assessment of ozone
1581 sponsored by the World Meteorological Organization (WMO 1985).

1582

1583 The inhomogeneous distribution of ozone coupled with the different interactions of
1584 stratospheric and tropospheric ozone with solar and longwave radiation necessitated
1585 calculations of radiative forcing due to changes in stratospheric and tropospheric ozone
1586 separately. The net effect of a reduction in stratospheric ozone on surface temperature
1587 depends upon the balance between warming due to enhanced solar radiation reaching
1588 the surface-troposphere system and cooling due to reduced longwave radiation emitted
1589 by the stratosphere both because of the reduction in stratospheric ozone and the
1590 consequent cooling (the “stratospheric temperature adjustment” process described in
1591 section 2). Studies relying on model predictions of ozone distribution showed that the
1592 sign of surface temperature change depends on the vertical distribution of the
1593 stratospheric ozone change (Ramanathan and Dickinson 1979; Wang et al. 1980;
1594 Ramanathan et al. 1985). Further progress on the sensitivity of surface temperature to
1595 observed changes in the vertical distribution of ozone came in 1990 with the iconic
1596 work of
1597 Lacis et al (1990) who showed that ozone changes in the upper troposphere and lower
1598 stratosphere are most effective in forcing climate change. Surface temperature is much
1599 more sensitive to tropospheric ozone perturbations relative to stratospheric ozone
1600 changes because the longwave opacity of tropospheric ozone is nearly the same as that
1601 of stratospheric ozone, and the solar and longwave effects of tropospheric ozone change

1602 affect surface temperature in the same direction (Ramanathan et al. 1985). Studies
1603 estimated the net radiative effect of ozone changes from preindustrial up to 1980s to
1604 cause warming despite a net reduction in ozone column (driven by CFC induced
1605 stratospheric ozone depletion) because of the greater radiative efficiency of
1606 tropospheric ozone (Owens et al. 1985; Lacis 1985; Ramanathan and Dickinson 1979).

1607

1608

1609 **Section 4.2. Radiative Forcing due to Short-lived Trace Gases: 1990 to 2000**

1610

1611 By the early 1990s, a better understanding of the effect of ozone on radiative forcing and its
1612 strong dependence on the vertical profile of ozone change throughout the troposphere and
1613 stratosphere as well as on its total amount had emerged (Schwarzkopf and Ramaswamy 1993
1614 Lacis et al. 1990; Ramaswamy et al. 1991; Shine et al. 1990). Unlike sparse observational
1615 constraints on tropospheric ozone trends, better constraints on stratospheric ozone trends (e.g.
1616 Stolarski et al. 1991) facilitated quantitative assessment of its radiative forcing indicating that
1617 ozone reductions between 1979 to 1990 caused a negative radiative forcing (Ramaswamy et al.
1618 1991).

1619

1620 Estimates of radiative forcing due to ozone continued to be refined through the mid-1990s
1621 (IPCC 1994, 1995) though the level of confidence was low around this time (Figure 1.2 in
1622 section 1). Low confidence in stratospheric ozone forcing was largely driven by more than a
1623 factor of two spread in model computed values of stratospheric ozone forcing (Shine et al.
1624 1995a,c,b; Schimel et al. 1996). Similarly, for tropospheric ozone, studies based on modeled or
1625 limited observations of ozone trends agreed that increases in tropospheric ozone since
1626 preindustrial times have resulted in a positive forcing (e.g., Hauglustaine et al. 1994; Marenco et
1627 al. 1994; Mohnen et al. 1993) but there was large uncertainty as summarized in the IPCC 1994
1628 special report and SAR (Shine et al. 1995b; Schimel et al. 1996). The major difficulty in
1629 accurately estimating global ozone forcing was limitations in the knowledge of changes in
1630 vertical, horizontal and temporal distributions of ozone (Prather et al. 1995; Stordal et al. 1995;
1631 Ko et al. 1995). This was particularly true for tropospheric ozone whose distribution was

1632 difficult to capture in the two-dimensional models used widely until the mid 1990s (Prather et
1633 al. 1994; see Peters et al. 1995 for a review of tropospheric chemistry models until 1995).
1634 Furthermore, it was difficult to demonstrate confidence in model-derived trends because of the
1635 lack of strong observational constraints. Chemistry-climate interactions were recognized to have
1636 a significant effect on the total radiative forcing of climate and were deemed important to be
1637 accounted for in the assessment of potential future climate change as highlighted in Chapter 2 of
1638 the FAR (Shine et al. 1990) (Figure 4.1).

1639

1640

1641

1642 The first quantitative estimate of the indirect radiative effects, in terms of Global Warming
1643 Potentials (GWP_s; see section 11.2 for definition), from increases in emissions of methane, CO
1644 and NO_x was based on results from a two-dimensional model representing the fundamentals of
1645 atmospheric chemistry known at the time (Hough and Derwent 1990). Although there was a fair
1646 degree of confidence in the sign of the indirect effects (Isaksen et al. 1991), these early
1647 estimates were found to be too uncertain and likely overestimated (Johnson et al. 1992; Isaksen
1648 et al. 1992; Lelieveld and Crutzen 1992; Isaksen et al. 1991). Two-dimensional tropospheric
1649 chemistry models that had been primarily used until the mid-1990s were of limited scope in
1650 adequately characterizing the complex chemical and physical processes and the nonlinear
1651 interactions between them (Prather et al. 1995; Olson et al. 1997; Stordal et al. 1995) hampering
1652 the accurate quantification of indirect radiative forcing (Shine et al. 1995b,c; Schimel et al.
1653 1996). Limited atmospheric measurements on global scale for many species, including ozone,

1654 CO, NO_x, and NMHCs, needed to characterize historical trends and provide constraints on
1655 models, further restricted the ability to robustly quantify indirect radiative forcing..

1656

1657

1658 Progress was however made in better definition and quantification of indirect forcing
1659 from methane increases driven by theoretical (Prather 1994) and multi-model analysis (Prather et
1660 al. 1995; Stordal et al. 1995). Forcing due to the chemical feedback of methane increases on its
1661 own lifetime via reduced tropospheric OH (OH changes discussed in section 4.3) was no longer
1662 considered an indirect effect as this effect would be implicitly included in the estimates for the
1663 forcing due to historical methane changes (Schimel et al. 1996). The influence of methane
1664 increases on tropospheric ozone and stratospheric water vapor was estimated to add about 25%
1665 to the direct methane forcing (Schimel et al. 1996; Prather et al. 1995).

1666

1667 From the late 1990s onwards, the development and application of sophisticated global climate
1668 models with some representation of atmospheric chemistry (see Zhang 2008; Young et al. 2018
1669 for a historical overview of atmospheric chemistry in global models) combined with
1670 improvements in the knowledge of chemical and physical processes affecting the distributions
1671 of short-lived gases, and better atmospheric observations led to significant improvements in
1672 forcing estimates as assessed in the TAR (Ramaswamy et al. 2001). Results from several studies
1673 applying various approaches and observational evidence of ozone loss for a longer period (e.g.,
1674 MacKay et al. 1997; Forster 1999; F. Forster and Shine 1997; Hansen et al. 1997; Granier et al.
1675 1999) enhanced the level of scientific understanding of stratospheric ozone forcing of -0.15 ± 0.1
1676 Wm^{-2} for the period 1979 to 1997 (Ramaswamy et al. 2001). Approximate consistency between

1677 observed lower stratospheric temperature trends since the late 1970s and that simulated by global
1678 climate models forced with observed ozone losses confirmed that forcing from the decline in
1679 ozone is indeed negative (Hansen et al. 1997a). However, a clear attribution was complicated by
1680 the possible role of cooling from increasing stratospheric water vapor (Forster and Shine 1999),
1681 observations of which were limited.

1682

1683 Results based on global three-dimensional model studies of preindustrial to present-day
1684 tropospheric ozone changes driven by precursor emissions (e.g., Roelofs et al. 1997;
1685 Haywood et al. 1998; Dorland et al. 1997; Berntsen et al. 1997; Mickley et al. 1999;
1686 Brasseur et al. 1998; Stevenson et al. 1998) along with those based on satellite-inferred
1687 ozone column changes (Portmann et al. 1997; Kiehl et al. 1999) alleviated uncertainties
1688 in the tropospheric ozone forcing estimates (Granier et al. 1999; Ramaswamy et al.
1689 2001). Process studies provided better understanding of the sensitivity of surface
1690 temperature to the vertical distribution of ozone and clouds, and the spatial distribution
1691 of ozone forcing (e.g., Forster and Shine 1997; Hansen et al. 1997b; Hauglustaine and
1692 Brasseur 2001).

1693

1694 Although the level of confidence in tropospheric ozone forcing had increased,
1695 uncertainties remained because of the large model diversity in predicted historical ozone
1696 changes and limited observational constraints on ozone trends (Prather et al. 2001 and
1697 references therein). Limitations in our understanding of not only the complex non-linear
1698 chemical interactions between ozone precursors but also the historical evolution of the

1699 emissions of specific precursors impeded the quantitative attribution of ozone forcing up
1700 until this time (Prather et al. 2001 and references therein).

1701

1702 Studies also highlighted the importance of including feedbacks between climate and
1703 chemistry on the assessment of the climate impact of short-lived species (Prather et al.
1704 2001). Here, we do not cover the details of this feedback but refer to past IPCC reports
1705 and several review papers on this topic (Prather et al. 2001; Jacob and Winner 2009;
1706 Fiore et al. 2012, 2015; Isaksen et al. 2009; Denman et al. 2007; Von Schneidemesser et
1707 al. 2015; Brasseur 2009; Kirtman et al. 2013; Monks et al. 2015).

1708

1709 Much progress was made in the quantitative estimates of forcings from chemistry-
1710 climate interactions in the latter half of the 1990s as assessed in the TAR. The indirect
1711 forcing from methane changes continued to be the best studied, with explicit
1712 quantification of the individual effects on its own lifetime, tropospheric ozone,
1713 stratospheric water vapor, and CO₂ (e.g., Hauglustaine et al. 1995; Lelieveld et al. 1998;
1714 Fuglestvedt et al. 1996). Modeling studies also quantified indirect forcing from changes
1715 in CO and a suite of NMHCs through their influence on methane lifetime, tropospheric
1716 ozone and CO₂ (Daniel and Solomon 1998; Johnson and Derwent 1996).

1717

1718 Accurate calculation of the indirect forcing of NO_x remained challenging because of
1719 counteracting effects—increased NO_x emissions increase tropospheric ozone producing
1720 a short-lived regional positive forcing, but increase OH concentration lowering methane
1721 abundance (with a consequent decrease in ozone) that produces a longer-lived global

1722 negative forcing partially offsetting the short-lived positive ozone forcing (Ramaswamy
1723 et al. 2001 and references therein). Studies showed that the ozone and OH perturbations
1724 strongly depended on the location of NO_x emission perturbations because of the non-
1725 linear ozone chemistry and differences in mixing regimes (e.g., Fuglestvedt et al. 1999).

1726

1727 Diversity in results of model studies that resolved the complex and non-linear effects of
1728 emission changes on ozone and OH radical and limitations in observational constraints
1729 to build confidence in them remained a significant source of uncertainty in these
1730 estimates of indirect forcings (Ramaswamy et al. 2001).

1731

1732

1733

1734

1735 **Section 4.3. Emission-based radiative forcing for Short-lived Climate Forcers (SLCFs):**

1736 **2000-present**

1737

1738 Over the past two decades, the development of increasingly sophisticated comprehensive
1739 global chemistry models in terms of their design (e.g., models with coupled
1740 stratospheric-tropospheric chemistry, global climate model with online chemistry) and
1741 the representation of complex physical and chemical processes (e.g., trace gas-aerosol
1742 interactions, interactive natural emissions), combined with better estimates of trace gas
1743 emissions and the availability of longer observational records has facilitated advances in
1744 the attribution of the changes in short-lived trace gases and their forcings (Forster et al.
1745 2007; Myhre et al. 2013).

1746

1747 Consideration of coupled stratospheric and tropospheric chemistry in global models has
1748 facilitated greater understanding of the influence of changes in stratospheric ozone and
1749 ozone depleting substance (ODSs) on tropospheric ozone and the effect of tropospheric
1750 ozone precursors on stratospheric ozone (e.g., Shindell et al. 2006; Hegglin and Shepherd
1751 2009; Eyring et al. 2013; Young et al. 2013), which has led to better accounting of these
1752 impacts on the radiative forcing due to ozone (Gauss et al. 2006; Stevenson et al. 2013;
1753 Myhre et al. 2013; Forster et al. 2007; Shindell et al. 2013; Banerjee et al. 2016).

1754 Coupled chemistry-climate models have enabled assessment of the changes in ozone
1755 induced by climate change (i.e., chemistry-climate feedbacks; see Isaksen et al. 2009;
1756 more refs), and the resulting radiative forcing (e.g., Gauss et al. 2006; Stevenson et al.

1757 2013; Forster et al. 2007) and feedbacks on climate (e.g., Nowack et al. 2015; Chiodo et
1758 al. 2018; Marsh et al. 2016).

1759

1760 A major development in the quantification of forcing due to tropospheric ozone and
1761 chemistry-climate interactions over this period has been the adoption of an emissions-
1762 based approach (Shindell et al. 2009, 2005) to estimate the contribution of anthropogenic
1763 emissions of individual ozone (or aerosol) precursors to the preindustrial to present- day
1764 radiative forcing either via direct influences (e.g., ozone, methane, or aerosols) or
1765 indirect effects (Myhre et al. 2013; Forster et al. 2007). With this approach, model
1766 representation of couplings between gas-phase and aerosol chemistry in the troposphere
1767 has helped elucidate indirect effects of trace gases on aerosols via influences on ozone
1768 and OH and the resulting forcing (Shindell et al. 2009; Von Schneidemesser et al. 2015).
1769 Additionally, indirect forcing through detrimental ozone effects on vegetation (see
1770 section 6 for discussions on forcing from land and biogeochemical interactions) have
1771 also been explored (Sitch et al. 2007; Collins et al. 2010; Kvalevag and Myhre 2013).
1772 These emissions-based radiative forcing estimates (Figure 4.2) give a significantly
1773 different relative importance to various emissions (Forster et al. 2007; Myhre et al. 2013)
1774 than that suggested by abundance-based assessments in the past. Radiatively active short-
1775 lived trace gases (and aerosols; see section 5) and their precursors are now collectively
1776 termed as Short-lived Climate Forcers (SLCFs) as their climate impact is mainly felt
1777 within the first one to three decades (near term) of their emissions (Myhre et al., 2013;
1778 Fiore et al., 2015) in contrast to long-lived greenhouse gases. Furthermore, the short
1779 lifetimes of SLCFs result in spatially inhomogeneous abundances and associated forcings

1780 highly sensitive to the location of emissions. Consequently, climate influence from
1781 SLCFs is more important on a regional scale (e.g., Fry et al. 2012; Collins et al. 2013;
1782 Aamas et al. 2017) contrary to the relatively homogeneous spatial influence from well-
1783 mixed greenhouse gases.

1784

1785 The question of how global mean hydroxyl radical has evolved in the past and will
1786 change in the future in response to anthropogenic emission and climate change remains
1787 highly relevant to the estimates of SLCF radiative forcing given the dependence of SLCF
1788 atmospheric lifetimes on OH (section 4.1). Significant progress has been made in the
1789 understanding of fundamental atmospheric chemistry of OH with advances in both
1790 observations and modeling (e.g., Stone et al, 2012; Rohrer et al., 2014), however the
1791 answer to this question remains at an impasse. The atmospheric chemistry community
1792 has mostly relied on global chemistry models to derive past changes and predict future
1793 evolution of OH over long time scales, and on proxies, such as methyl chloroform, to
1794 derive OH variability over the past ~35 years during which we have observations (e.g.,
1795 Prinn et al., 2001; Bousquet et al., 2005; Montzka et al., 2011; Rigby et al., 2017; Turner
1796 et al., 2017). There is no consensus in the global model estimates of changes in
1797 tropospheric mean OH abundance from preindustrial to present-day based on studies
1798 over the past ~40 years as displayed in Table 4.1. The simulated change in present day
1799 OH relative to preindustrial ranges from a decline to no change to an increase due to
1800 varying levels of offsetting effects from increases in OH sinks (methane, CO, NMHCs)
1801 and increases in factors that increase OH (water vapor, tropospheric ozone, NOx, and
1802 UV radiation) (e.g., Naik et al., 2013). This is in contrast to the 30% decline in present-

1803 day OH relative to preindustrial inferred from ice core measurements, although with
1804 large uncertainties (Alexander and Mickley 2016). There are also large discrepancies in
1805 the projections of global OH levels with implications for estimates of future SLCF
1806 forcing (e.g., Voulgarakis et al. 2013). Changes in OH over the past ~35 years and their
1807 role in the renewed growth in atmospheric methane since 2007 are intensely debated in
1808 the literature with no consensus view (Turner et al., 2019).

1809

1810 Global chemistry-climate models have remained the tools of choice to quantify the
1811 contribution of SLCF emissions to radiative forcing of climate change as observational
1812 constraints are sparse (e.g., for tropospheric ozone Bowman et al., 2013). Multi-model
1813 intercomparison projects (MIPs) involving coordinated experiments with chemistry
1814 models provide a means of exploring structural uncertainty related to model
1815 representation of various physical and chemical processes determining the distribution
1816 and budgets of SLCFs and have informed IPCC as well as other international
1817 assessments (see Young et al. 2018 for a brief history of MIPs for chemistry).

1818

1819 Similar to climate model intercomparisons (e.g., Meehl et al., 2007), analysis is focused
1820 on multi-model means because the ensemble average across structurally different models
1821 shows better agreement with available observations with individual model biases
1822 canceling out, while the spread across models is considered a measure of uncertainty
1823 (e.g., Young et al. 2013). However, because these ensembles represent “ensembles of
1824 opportunity”, the spread across models does not necessarily span the full range of
1825 structural as well as process uncertainty (Tebaldi and Knutti 2007).

1826

1827 For chemistry models, early MIPs focused on exploring the uncertainty in model
1828 representation of specific processes affecting the distribution and budget of tropospheric
1829 ozone and related trace gases (e.g., PhotoComp in Olson et al., 1997 and OxComp in
1830 Prather et al., 2001). Computation of ozone radiative forcing within MIPs came about
1831 later in the 2000s beginning with the framework of Atmospheric Chemistry Composition
1832 Change: an European Network (ACCENT; Gauss et al. 2006) that informed the AR4
1833 report (Forster et al. 2007). The specifications of the simulations for MIPs improved with
1834 the development of a consistent set of gridded anthropogenic precursor emissions
1835 describing their preindustrial to present day evolution (Lamarque et al. 2010). This
1836 common dataset employed by the more recent ACCMIP (Atmospheric Chemistry and
1837 Climate Model Intercomparison Project) (Lamarque et al. 2013) allowed for increased
1838 comparability of model simulations of tropospheric ozone (and aerosols) abundances and
1839 resulting radiative forcings as assessed in AR5 (Myhre et al. 2013). Uncertainties in
1840 emission estimates (e.g., Granier et al., 2011; Bond et al., 2013) have consequences for
1841 SLCF radiative forcing. New and revised estimates of the historical evolution of SLCF
1842 and their precursor emissions (Hoesly et al, 2018; van Marle et al. 2017) provide a means
1843 of exploring the contribution of emission uncertainty to SLCF forcing uncertainty. The
1844 Aerosol Chemistry Model Intercomparison Project (AerChemMIP) in support of the
1845 forthcoming IPCC assessment (AR6) is designed to quantify and explore uncertainties in
1846 the forcing due to anthropogenic emissions of SLCFs thereby providing better constraints
1847 on the role of SLCFs in climate forcing (Collins et al. 2017).

1848

1849

1850 **Section 4.4. Summary and Challenges**

1851

1852 In this section, we have reviewed the evolution of our knowledge of radiative forcing from
1853 short-lived trace gases and chemistry-climate interactions over the past approximately four
1854 decades.

1855

1856 Significant progress has been made beginning with the recognition of the role of
1857 stratospheric ozone on climate change to the scientific understanding and quantitative
1858 estimate of the contribution of emissions of a suite of SLCFs to Earth's radiative forcing.

1859 The use of comprehensive global chemistry-climate models combined with observational
1860 constraints where available have enhanced our ability to capture complex chemical
1861 interactions in the computation of SLCF radiative forcing. However, challenges remain in
1862 quantifying the forcing due to anthropogenic emissions of SLCFs as outlined below:

1863

1864 • A persistent uncertainty in constraining the radiative forcing from SLCFs is
1865 the limited or no knowledge of preindustrial precursor emissions and atmospheric burdens
1866 (e.g., for tropospheric ozone as highlighted by Stevenson et al., 2013).

1867

1868 • The spatial distribution of ozone precursor emissions has undergone a
1869 dramatic change over the last couple of decades with emissions declining in the developed
1870 mid-latitude and rising in the developing tropical regions (e.g., Zhang et al., 2016). The
1871 consequences of such emission distribution for chemistry-climate interactions and
1872 consequent SLCF forcing is not clear.

1873
1874 • The debate over how global mean OH is changing in response to changing
1875 anthropogenic emissions and climate change, and the implications of this change for the
1876 abundance and lifetime of SLCFs is yet to be resolved. It has been a challenge to narrow
1877 down the reasons for differences in global model simulations of the evolution of
1878 atmospheric OH (e.g., Naik et al., 2013; Voulgarakis et al., 2013). Recent efforts
1879 combining observations and model results in novel ways show promise in understanding
1880 the causes of model disagreement (e.g., Nicely et al., 2017; Prather et al., 2018).

1881

1882

1883 **Tables:**

1884

1885 **Table 4.1.** Percent change in present day OH relative to preindustrial compiled from
1886 literature (based on Murray et al. 2014). The definition of present day varies depending
1887 on the year of publication of the study.

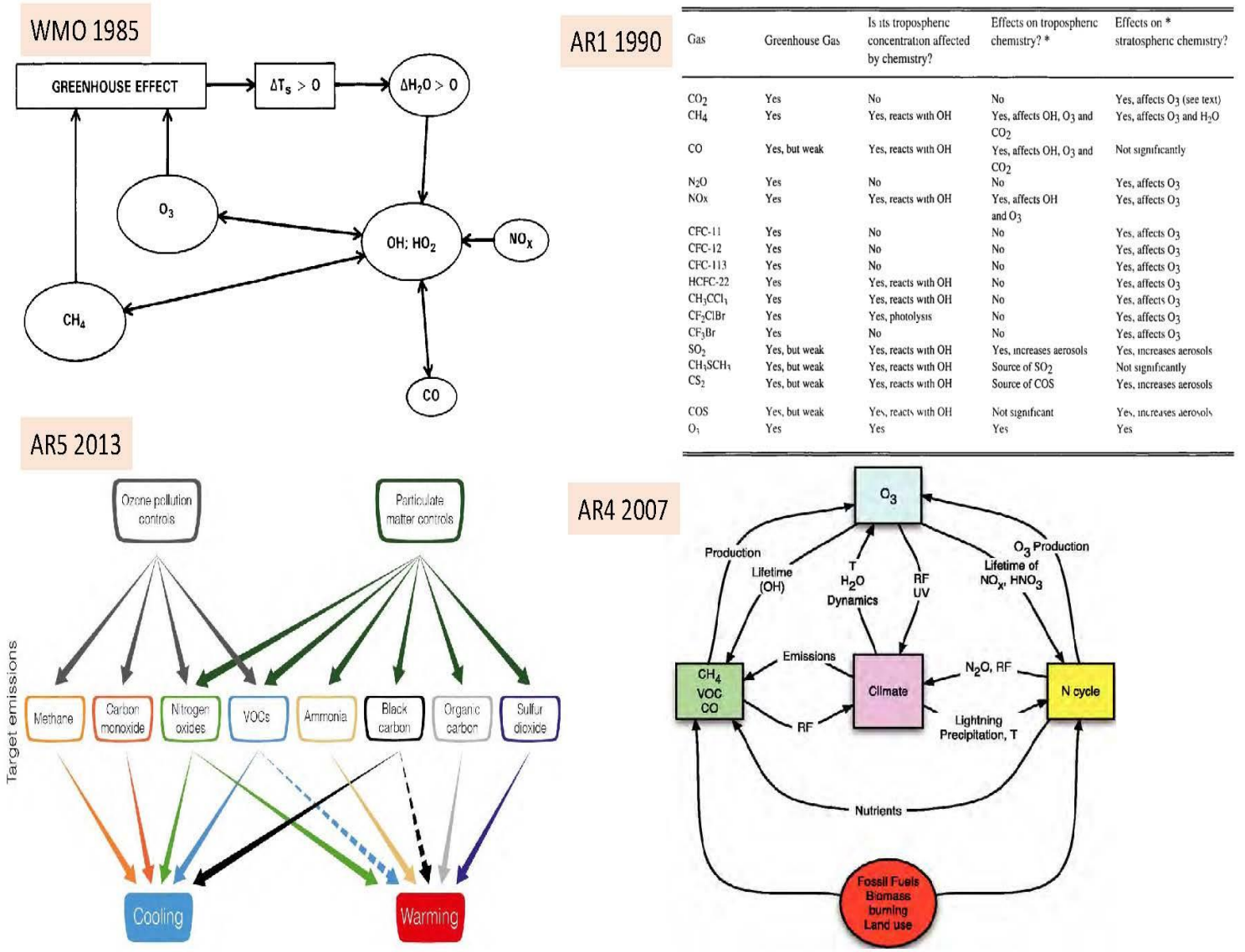
Reference	% Change in OH since preindustrial	Method
McElroy (1989)	+60%	1-D model
Hough and Derwent (1990)	-19%	2-D model
Valentin (1990)	-9%	2-D model
Law and Pyle (1991)	-13%	2-D model
Pinto and Khalil (1991), Lu and Khalil (1991)	-4%	1-D model, multi 1-D model
Staffelbach et al. (1991)	-30%	ice core measurements of formaldehyde
Crutzen and Zimmerman (1991)	-10% to -20%	3-D model
Thompson et al. (1993)	-20%	Multi 1-D model
Martinerie et al. (1995)	+6%	2-D model
Berntsen et al. (1997)	+6.8%	3-D model
Roelofs et al. (1997)	-22%	3-D model
Brasseur et al. (1998)	-17%	3-D model
Wang and Jacob (1998)	-9%	3-D model
Mickley et al. (1999)	-16%	3-D model
Grenfell et al. (2001)	-3.9%	3-D model, NMHCs
Hauglustaine and Brasseur (2001)	-33%	3-D model
Shindell et al. (2001)	-5.9%	3-D model
Lelieveld et al. (2002)	-5%	3-D model

Lamarque et al. (2005)	-8%	3-D model
Shindell et al. (2006)	-16%	3-D model
1888		
1889		
Sofen et al. (2011)	-10%	3-D model
John et al. (2012)	-6%	3-D model
Naik et al. (2013)	-0.6 \pm 8.8%	Multi 3-D model
Murray et al. (2014)	+7.7 \pm 4.3%	Multi 3-D model
Achakulwisut et al. (2015)	-8 to +17%	Multi 3-D Model

1890
1891
1892
1893
1894
1895
1896
1897
1898
1899
1900
1901
1902
1903
1904

1905

1906 **Figure 4.1** Historical evolution of the consideration of chemistry-climate interactions
 1907 in international assessments. The figure displays in clockwise order beginning from the
 1908 top left, the interactions of short-lived gases considered in WMO (1985), IPCC AR1
 1909 (1990), IPCC AR4 (2007), and IPCC AR5 (2013).



1910

1911

1912

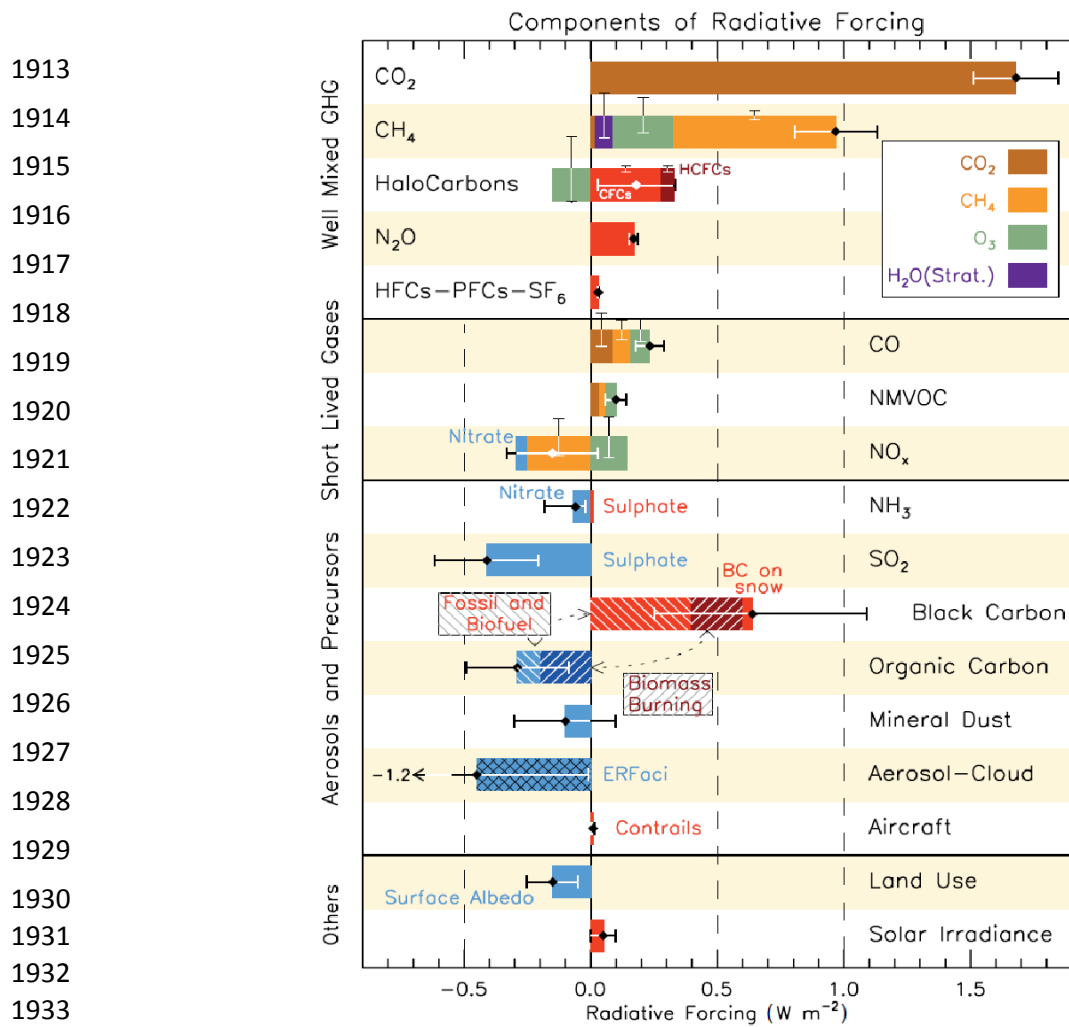


Figure 4.2. Best estimate of global average radiative forcing for the period 1750 to 2011 for emitted chemical species (well-mixed and short-lived gases, aerosols and their precursors) or other factors (from Myhre et al. (2013)). As shown in the inset in the top portion of the figure, many colors are used to represent RF from emitted species affecting several chemicals while red (positive forcing) and blue (negative forcing) are used for emitted components that affect fewer forcing agents. The vertical bars represent the relative uncertainty of the RF induced by each component. See Myhre et al. (2013) for more details.

1945 **Section 5. Tropospheric aerosols**

1946
1947
1948 Aerosols scatter and absorb radiation (the direct effect), and also act as cloud condensation
1949 nuclei whereby they modify the microphysical and macrophysical properties of clouds (the
1950 indirect effect). Increased concentrations of aerosols from anthropogenic activity therefore exert
1951 a radiative forcing of climate. The importance of atmospheric aerosols had been long
1952 established in the areas of atmospheric visibility (Koschmeider, 1924) and human health (e.g.
1953 Lippmann and Albert, 1969), but aerosols were originally considered to be of only minor
1954 consequence in terms of their impact on climate via direct and indirect effects (Twomey, 1959;
1955 McCormick and Ludwig, 1967; Bolin and Charlson, 1976). Simple models of the impact of
1956 aerosols on planetary albedo in terms of their absorptance and the reflectance of the underlying
1957 surface had been developed (e.g. Ensor et al., 1971; Reck, 1974, Chylek and Coakley, 1974),
1958 but the radiative forcing was not quantified owing to the lack of knowledge of the
1959 anthropogenic aerosol perturbation.

1960
1961 Observational evidence of aerosol-cloud interactions was hypothesized from observations of
1962 ship-tracks after satellite sensors were launched (Conover, 1966) but quantifying their radiative
1963 effect was only possible once detailed spectral information from satellites became available
1964 (Coakley et al., 1987). Observations of surface solar insolation suggested a widespread
1965 reduction in irradiance at the surface (Stanhill and Moreshet, 1992) although the causes were
1966 difficult to attribute. Thus, until the late 1980s, aerosols were considered insignificant in terms
1967 of radiative forcing when compared to that from changes in atmospheric concentrations of
1968 greenhouse gases. This view changed in the early 1990s. Global chemical transport models
1969 (CTMs) that were able to model the aerosol lifecycle of emission, chemical transformation,

1970 transportation and deposition and hence model the anthropogenic perturbation to aerosol
1971 concentrations were combined with relatively simple radiative transfer models.

1972

1973

1974

1975

1976 **5.1. Simple models of aerosol-climate interactions: the early 1990s**

1977

1978

1979 Sulfate aerosol was the first aerosol species to be comprehensively investigated owing to the

1980 anthropogenic emissions of the SO₂ gaseous precursor being ~100 Tg yr⁻¹, i.e. exceeding natural

1981 emissions by around a factor of five (Langner and Rodhe, 1991). These early global CTMs

1982 typically had a spatial resolution of 10°x10° latitude/longitude with ~10 coarsely-spaced

1983 atmospheric levels in the troposphere (Zimmermann et al., 1989). The impact of anthropogenic

1984 emissions of sulfur dioxide and the resulting sulfate aerosols on the radiative forcing of the

1985 Earth's climate was initially quantified by Charlson et al., (1991, 1992) who used a multiple

1986 scattering approximation to derive an equation for the change in the planetary albedo owing to a

1987 purely scattering aerosol and focused on the change in cloud free regions.

1988

1989 This related the direct radiative forcing of sulfate aerosol, F_{direct} , to the total solar irradiance, S_o ,

1990 the atmospheric transmission, T_{at} , the cloud fraction, A_c , the surface reflectance, R_s , the aerosol

1991 single scattering albedo, ω_0 , the fraction of light backscattered to space, β_{aer} , and the

1992 perturbation to the aerosol optical depth since pre-industrial times, $d\tau_{aer}$:

$$1993 F_{direct} = -\frac{1}{2} S_o T_{at}^2 (1 - A_c) (1 - R_s)^2 \beta_{aer} d\tau_{aer}$$

1999

1994 Charlson et al (1992) also derived an expression for the Twomey effect, which is the aerosol

1995 impact on the cloud droplet effective radius under the assumption of constant cloud liquid water

1996 (Twomey et al., 1977). Charlson et al (1992) used global mean estimates of the various

1997 parameters coupled to newly available estimates of the perturbation to the total aerosol

1998 concentrations caused by anthropogenic emissions (Langner and Rodhe, 1991) and concluded

2000 that the resulting global-mean radiative forcing for aerosols (pre-industrial to circa 1980s) was
2001 $F_{\text{direct}} = -1.3 \text{ W m}^{-2}$ and $F_{\text{Twomey}} = -1 \text{ W m}^{-2}$ with significant uncertainty owing to the neglect of
2002 subsequent impacts on cloud liquid water (i.e. the Albrecht effect, Albrecht, 1989), the
2003 simplicity of the models used and the lack of account of spatial correlation between the various
2004 parameters. Penner et al (1992) used a similar method to derive an initial estimate of the
2005 radiative forcing due to biomass burning aerosols from combined direct and indirect effects as
2006 strong as -2 W m^{-2} .

2007
2008 Simple representations of the direct radiative forcing of sulfate aerosol were straightforward to
2009 implement in fully coupled ocean-atmosphere models (Mitchell et al., 1995) because, for cloud-
2010 free regions, the local surface reflectance could simply be increased in proportion to $d\tau_{\text{aer}}$:-

2011
2012 $dR_s = (1 - R_s)^2 \beta_{\text{aer}} \frac{d\tau_{\text{aer}}}{\mu_0}$ _____
2013
2014
2015
2016
2017 Implementing this parameterization in the UK Met Office climate model showed a reduced rate
2018 of warming particularly in the northern hemisphere in their climate model simulations, bringing
2019 the simulated surface temperature change into better agreement with observations.
2020 Because the radiative forcing due to aerosols could conceivably outweigh that of increased
2021 concentrations of well-mixed greenhouse gases there were significant efforts to better quantify
2022 aerosol radiative forcing.

2023
2024
2025

2026 **5.2. Refinement of aerosol direct and indirect effect modelling studies: the mid-1990s**

2027
2028
2029 Simple models continued to play a significant role. Early simple theoretical models of radiative
2030 impacts of partially absorbing aerosols (e.g. Ensor et al., 1971; Reck, 1974; Chylek and Coakley,
2031 1974) were now extended (Haywood and Shine, 1995; Chylek and Wong, 1995) by accounting
2032 for aerosol absorption via the aerosol single scattering albedo, ω_0 , day-length fraction, D, and
2033 spatially resolved parameter values rather than global mean values:

2034
2035
$$F_{direct} = -DT_{at}^2(1 - A_c)[\omega_0\beta_{aer}(1 - R_s)^2 - 2(1 - \omega_0)R_s]d\tau_{aer}$$

2036
2037
2038
2039 Assuming a mass fraction between absorbing black carbon (BC) and scattering sulfate based on
2040 in-situ measurements weakened the sulfate F_{direct} from -0.34 W m⁻² (already much weaker than
2041 that diagnosed by Charlson et al., 1991, 1992) to between -0.10 to -0.30 W m⁻² depending on
2042 the assumed sulphate climatology and mixing state and that there was no direct radiative forcing
2043 in cloudy areas. This study established the importance of aerosol absorption, particularly when
2044 it was recognized that the positive radiative forcing impact would be amplified if absorbing
2045 aerosols resided above underlying cloud (e.g. Haywood and Shine, 1997). Regionally, dF_{direct}
2046 can be either positive (for low ω_0 and high R_s or above reflective cloud) or negative (for high ω_0
2047 and low R_s) as demonstrated by the 'real color' image (Fig 5.1). A more comprehensive estimate
2048 of F_{direct} for sulfate aerosol was performed by Kiehl and Briegleb (1993) who imposed
2049 monthly mean climatologies of sulfate mass burden (Langner and Rodhe, 1991), an aerosol size
2050 distribution and suitable refractive indices to derive aerosol optical properties. These optical
2051 properties were then included in off-line radiative transfer calculations using meteorological
2052 fields from observations. The F_{direct} of sulfate was evaluated as being a modest -0.3 W m⁻² (this



Fig 5.1. A real-colour MODIS satellite image showing the impact of smoke from biomass burning fires off the coast of Portugal on 3 August 2003. Fires are shown by the red spots and the smoke plume is shown in grey (from Haywood, 2016).

2053 affirmed the simple model of
 2054 Haywood and Shine (1995)).
 2055 Similarly, previous results for
 2056 biomass burning aerosol were
 2057 regarded as too strongly negative
 2058 owing to lack of account of aerosol
 2059 absorption, pre-industrial biomass
 2060 burning and the lack of a
 2061 discernible cooling trend in the
 2062 climatic record. GCM
 2063 investigations of the aerosol
 2064 indirect effect were also performed
 2065 (Jones et al., 1994; Boucher and
 2066 Lohmann, 1995) using the model-
 2067 simulated clouds.

2068 Climatological sulfate

2069 concentrations (Langner and Rodhe, 1991) were utilized together with parameterisations based
 2070 on airborne observations that related the cloud droplet effective radius to the aerosol number
 2071 concentration in marine and continental environments (Martin et al., 1994). These
 2072 simulations indicated a F_{Twomey} of -1.3 W m^{-2} (Jones et al., 1994) and -0.5 to -1.5 W m^{-2}
 2073 (Boucher and Lohmann, 1995), but the uncertainty remained significant. Boucher (1995)
 2074 made a first estimate using satellite observations of the difference between inter- hemispheric
 2075 cloud effective radius (northern hemisphere $11.0 \mu\text{m}$, southern hemisphere $11.7 \mu\text{m}$; Han et al.,

2076 1994) but acknowledged that the contribution of aerosols from natural land surfaces made the
2077 results difficult to interpret in the context of anthropogenic radiative forcing. Recognizing the
2078 fidelity of the refinements, IPCC (Schimel et al., 1996) suggested a best estimate for F_{direct} of -
2079 0.5W m^{-2} (range -0.25 to -1.0W m^{-2}) which was derived from a combination of the radiative
2080 forcing of sulfate (-0.4W m^{-2}), biomass burning (-0.2W m^{-2}) and fossil-fuel black carbon
2081 (FFBC; $+0.10 \text{W m}^{-2}$). IPCC (Schimel et al., 1996) recognized that a best estimate of F_{Twomey}
2082 was impossible to establish without further model simulations and observational constraints
2083 and suggested a range of 0 to -1.5W m^{-2}
2084
2085

2086

2087 **5.3. The proliferation of GCM-based estimates and the requirement for validation data:**

2088 **late 1990s to early 2000s**

2089

2090 The development of global model-based estimates of aerosol species other than sulfate

2091 continued apace. Tegen and Fung (1995) developed a global model of mineral dust and

2092 highlighted that, in addition to impacts in the solar region of the electromagnetic spectrum,

2093 coarse mode aerosols can have a significant impact by absorbing and re-emitting terrestrial

2094 radiation. Any anthropogenic fraction of mineral dust was recognized as being very uncertain.

2095 A first black carbon climatology was also produced (Cooke and Wilson, 1996) reiterating that

2096 global black carbon emissions ($\sim 14 \text{ Tg yr}^{-1}$ cf SO_2 at $\sim 100 \text{ Tg yr}^{-1}$) would lead to anthropogenic

2097 aerosol that was partially absorbing i.e. grey rather than white (Figure 5.1). The first estimates of

2098 nitrate aerosol direct radiative forcing were also produced (Van Dorland et al., 1997) but were

2099 highly uncertain owing to differences in the partitioning between the accumulation and coarse

2100 modes (Adams et al., 2001; Jacobson, 2001). The recognition that the different aerosol types

2101 needed to be represented for accurate determination of total aerosol radiative forcing led to a

2102 rapid expansion of GCM estimates based on aerosol climatologies derived from global CTMs.

2103

2104 Aerosol optical properties are determined by the (wavelength-dependent) refractive index of the

2105 particles and the particle size distribution. Recognizing that aerosol direct effects were be

2106 represented using more flexible radiative transfer codes that allowed integration over the full

2107 solar spectrum and range of solar zenith angles led to a comprehensive multi-model radiative

2108 transfer inter-comparison for sulfate aerosol (Boucher et al., 1998).

2109 This study showed a relatively modest variation in radiative effect between the radiative transfer
2110 models, indicating that the radiative transfer codes of reduced complexity in GCMs, but more
2111 refined than those used in the earlier simplified model calculations, could adequately describe
2112 aerosol direct radiative effects.

2113

2114 It was recognized that GCMs were a suitable tool for allowing representation of the variability
2115 in humidity, surface reflectance, aerosol and cloud but computational expense meant that CTMs
2116 were used for computing e.g. monthly mean distributions of sulfate aerosol and these monthly
2117 mean fields were then input to the GCMs, which computed the direct and indirect effects using
2118 their internal radiative transfer models (e.g. Kiehl and Briebleb, 1993; Boucher and Anderson,
2119 1995; Boucher and Lohmann, 1995; Kiehl and Rodhe, 1995; Haywood et al., 1997; Haywood
2120 and Ramaswamy, 1997; Hansen et al., 1998). However, CTMs and GCMs were increasingly
2121 combined so that the sulfur chemistry, transport, deposition and direct and indirect radiative
2122 forcing could be explicitly calculated. This method had the benefit that aerosol concentrations
2123 could be precisely correlated with fields determining aerosol production and removal i.e. clouds
2124 and precipitation (e.g. Graf et al., 1997; Feichter et al, 1997; Myhre et al., 1998; Iversen et al,
2125 2000; Ghan et al., 2001; Jacobson, 2001; Jones et al., 2001). Nevertheless, the limitations of
2126 model resolution were recognized; GCMs with their coarse resolution of ~100s of km were
2127 unable to represent the sub- gridscale details such as relative humidity and detailed distributions
2128 of gas phase and aqueous phase production of sulfate aerosol (Ghan et al., 2001).

2129
2130 Direct radiative forcing calculations were made for fossil-fuel BC (Haywood and Ramaswamy,
2131 1998; Penner et al., 1998; Cooke et al., 1999), fossil-fuel organic carbon (Penner et al., 1998;
2132 Cooke et al., 1999), biomass burning aerosol (Penner et al., 1998; Iacobellis et al., 1999), total

2133 BC (Hansen et al., 1998; Haywood and Ramaswamy, 1998; Jacobson, 2001) and fossil-and
2134 biomass- burning organic carbon (Hansen et al., 1998; Jacobson, 2001). These models treated
2135 each of the aerosol types separately (i.e. an external mixture) although some of these models
2136 began to represent multi-component aerosols as internal mixtures which can have particular
2137 relevance for inclusion of absorbing BC cores within scattering shells (e.g. Jacobson, 2001)
2138 producing a ‘lensing’ effect that enhances the absorption (e.g. Lesins et al., 2002).

2139

2140 GCM studies of indirect effects tended to rely on empirical relationships between aerosol
2141 number (e.g. Jones et al., 1994) or mass (Boucher and Lohmann, 1995) and cloud droplet
2142 number concentrations (CDNC), but prognostic mechanistic parametrizations that attempted to
2143 explicitly account for aerosol activation and cloud nucleation began to appear (e.g. Lohmann et
2144 al. (2000), Ghan et al. (2001)). By contrasting polluted and unpolluted clouds, comprehensive
2145 aircraft-based observational measurement campaigns (e.g. ACE-2, Brenguier et al., 2000) were
2146 able to show clear evidence of aerosol Twomey effects, but definitive evidence of Albrecht
2147 effects remained elusive.

2148

2149 Until this point, there was little/no information available from observational sources with a
2150 global reach (i.e. satellites or global surface networks) with which the global models could be
2151 challenged. The first satellite retrievals of τ_{aer} (at midvisible wavelength) appeared, based on
2152 the reflectance from a single visible spectral channel from the AVHRR satellite sensor (Husar et
2153 al., 1997; Fig 5.2).

2154
2155 These retrievals were restricted to cloud-free regions over ocean owing to difficulties in
2156 accurately characterizing surface reflectance properties over land and cloudy regions, but for the

2157 first time these retrievals were able to detect the geographic distribution of aerosols, and how
2158 these distributions shifted according to the season. These observations emphasized that, to
2159 compare model results against those from observations, both natural and anthropogenic aerosols
2160 need to be modelled, particularly those of mineral dust (e.g. Woodward, 2001) and sea-salt
2161 aerosol (Fig 5.2).

2162

2163

2164

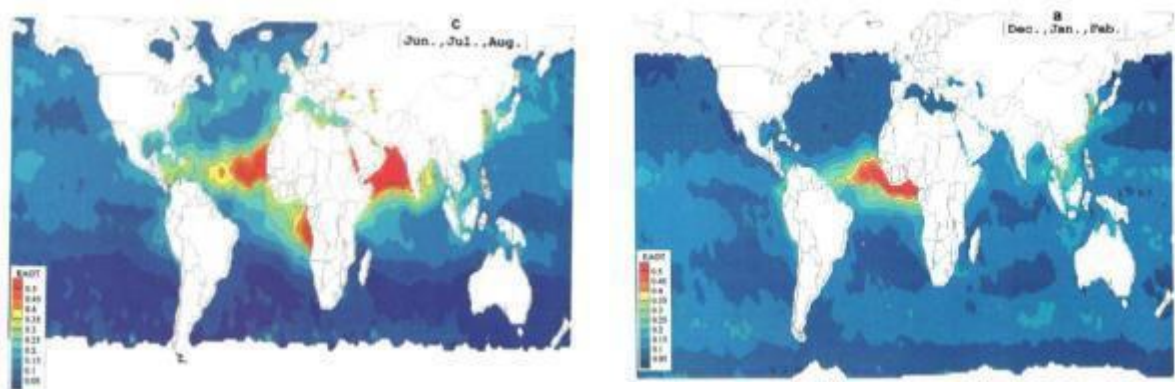
2165

2166 **Fig 5.2.** The equivalent aerosol optical thickness EAOT) derived from a single channel
2167 (algorithm of the AVHRR satellite sensor (reproduced from Husar et al., 1997).

2168

2169

2170



2171

2172

2173 Improved detection algorithms soon followed using 2-channels (AVHRR; Mishchenko et al.,
2174 1999) or polarization (POLDER; Deuzé et al., 1999). The use of 2-channel retrievals and
2175

2180 polarization allowed, for the first time, separation between coarse and fine mode aerosol
2181 particles based on the measured Angstrom exponent (i.e. the wavelength dependence of τ_{aer})
2182 and depolarization respectively. Initial estimates of the direct radiative effect were also made
2183 over the cloud-free oceans (e.g. Haywood et al., 1999; Boucher and Tanré, 2000), but the
2184 problem of deriving a radiative forcing (i.e. the change in the radiative effect since pre-
2185 industrial times) remained. Concurrently with satellite observations, significant investment was
2186 made in the global network of aerosol sun-photometers (Holben et al., 1998) that were able to
2187 measure τ_{aer} from direct sun measurements. The first sun photometer was deployed in 1993, but
2188 this network was to blossom over the next two decades with the number of sites operational in
2189 June 1998/2008/2018 increasing from 33/200/400 globally. AERONET has become a
2190 mainstay for checking both the calibration of satellite τ_{aer} retrievals and modelled τ_{aer} .

2191
2192 Given the rapid growth in model estimates of direct and indirect effects, IPCC (2001)
2193 commissioned an Intercomparison workshop (Penner et al., 2001) to provide global model
2194 estimates of various aerosol parameters such as speciated natural and anthropogenic burdens,
2195 direct and indirect radiative forcings; in many ways this may be considered the forerunner of the
2196 Aerosol Comparisons between Observations and Models project (AeroCom; Kinne et al., 2006).
2197 Because of the rapid expansion of estimates of both direct and indirect effects, IPCC
2198 (Ramaswamy et al., 2001) expanded the number of aerosol species assigned a direct radiative
2199 forcing; sulfate (- 0.40W m⁻², x2 uncertainty), biomass burning aerosols (-0.20W m⁻², x3
2200 uncertainty), BC from fossil fuel use (FFBC) (+0.2W m⁻², x2 uncertainty), organic carbon from
2201 fossil-fuel use (FFOC; -0.10W m⁻², x3 uncertainty), mineral dust (range -0.6 to +0.40W m⁻²)
2202 and estimated the total combined Fdirect to be -0.6W m⁻² (range -0.1 to 1 W m⁻²). While

2203 diagnosing aerosol direct radiative effects within GCMs was straightforward, diagnosing aerosol
2204 indirect forcing beyond the Twomey effect became problematic because the strict definition of
2205 radiative forcing required “surface and tropospheric temperatures and state held fixed at the
2206 unperturbed values” (Ramaswamy et al., 2001). This definition precluded allowing changes in
2207 cloud macrophysical properties such as cloud liquid water path (Albrecht, 1989) and subsequent
2208 impacts on cloud fraction, cloud height etc. Thus, in a strict radiative forcing sense, only
2209 FTwomey could be calculated within GCMs, although some studies simply used the difference
2210 between two simulations with pre-industrial and present-day aerosols with fixed sea-surface
2211 temperatures to attempt to diagnose aerosol-cloud impacts beyond Twomey effects
2212 (Rotstayn, 1999; Jones et al, 2001). These studies can be thought of as forerunners of the
2213 “Effective RadiativeForcing (ERF) concept” (section 2). The fidelity and utility of ERF was far
2214 from proven however,so IPCC (2001) assigned only the Twomey effect with a radiative forcing,
2215 with an increased uncertainty range of 0 to -2 W m⁻². A comprehensive discussion of the basis
2216 and quantitative estimates of the direct and indirect radiative forcing is provided by Haywood
2217 and Boucher (2000).

2218

2219

2220

2221
2222 **5.4. Explicit treatment of aerosols within GCMs and improved observational capability:**
2223 **2000s.**

2224
2225 As computing power increased and advances were made through observations and fundamental
2226 developments in the physics of aerosols, GCMs increasingly incorporated detailed aerosol
2227 chemistry, transport and microphysics schemes, frequently on a species-by-species basis under
2228 the assumption of external mixing. Models began to incorporate enough of the natural and
2229 anthropogenic species prevalent in the atmosphere to make meaningful inter-comparisons
2230 against observations from e.g. surface-based AERONET sun photometer sites and satellite
2231 retrievals. However, determining differences in performance between the models was
2232 complicated by the impacts of differing emissions, differing time-periods of analysis, and
2233 different analyses of observational constraints (Textor et al., 2007). Hence, many modelling
2234 centres joined the AeroCom initiative (Kinne et al., 2006, Schulz et al., 2006) which provided
2235 a platform for consistent model-model and model-observation intercomparisons. AeroCom
2236 initially focused on inter-comparison of aerosol optical properties (Kinne et al., 2006) and
2237 aerosol direct radiative forcing (Schulz et al., 2006). AeroCom's remit rapidly expanded
2238 considerably to include a wide range of intercomparisons such as aerosol indirect effects
2239 (Penner et al., 2006; Quaas et al., 2009) along with more specific objectives such as
2240 comparisons of model derived vertical profiles against satellite-borne lidars (Koffi et al., 2011)
2241 and in-situ black-carbon profiles (Schwarz et al., 2010), enabling refinements of model
2242 performance.

2243

2244 The majority of aerosol schemes at this time treated aerosols in ‘bulk’ form i.e. aerosol mass
2245 was transported, but the detailed description of aerosol microphysics was not included. Aerosol
2246 size distributions and hygroscopic growth factors were assumed based on in-situ measurements
2247 of aerosol properties from surface sites, in-situ aircraft-based measurements, or validated
2248 AERONET sky-radiance-based retrievals (Dubovik and King, 2000, Haywood et al., 2003). At
2249 the time, the impacts of relative humidity on the radiative forcing of aerosols via their influence
2250 on optical properties and in particular the specific extinction coefficient were frequently
2251 accounted for via measurements of the hygroscopic growth using e.g. airborne humidified
2252 nephelometer systems. For example, Kotchenruther and Hobbs (1998) and Kotchenruther et al.
2253 (1999) provided hygroscopic growth parameterisations for biomass burning aerosols in Brazil
2254 and industrial pollution off the east coast of the USA, respectively.

2255
2256 In addition to aerosol direct effects and aerosol indirect effects, the aerosol semi-direct effect
2257 started to receive some considerable attention. The semi-direct effect is the mechanism
2258 whereby aerosol absorption leads to heating of the atmospheric column, increasing atmospheric
2259 stability and decreasing the relative humidity. These impacts were postulated to inhibit cloud
2260 formation in the layer of absorbing aerosols, but also alter cloud cover in other parts of the
2261 troposphere (e.g. Ackerman et al., 2000; Johnson et al., 2004; Hansen et al., 1997). Diagnosing
2262 the semi-direct effect of aerosols using the strict definition of radiative forcing (holding all
2263 other atmospheric variables fixed) was not possible; as for aerosol indirect effects beyond the
2264 Twomey effect this posed a significant problem in quantification of radiative forcing.

2265

2266 MODIS TERRA started producing τ_{aer} data in 2002, with MODIS AQUA following in 2002
2267 (Remer et al., 2002); they are still providing essential data for validation and data assimilation
2268 to this day. Other satellite sensors provided considerable additional information (e.g. MISR,
2269 Kahn et al., 2002; AATSR/AATSR-2, Table 2.2 of Forster et al., 2007). However, the
2270 combination of the near-global daily coverage, developments of retrievals over land surfaces
2271 (Hsu et al., 2006), cross calibration with the highly accurate AERONET network, ease of data
2272 access and the longevity of this data-set has resulted in MODIS becoming the mainstay for
2273 model validation for both τ_{aer} and for examining aerosol indirect effects via relationships
2274 between aerosol and clouds (Quaas et al., 2009). Development of near-global coverage of τ_{aer}
2275 from satellites and accumulation mode fraction from the MODIS instrument augmented by in-
2276 situ aircraft-based measurements allowed the first mainly observational estimate of aerosol
2277 direct effects (Bellouin et al., 2005) compared to the earlier efforts using model-observation
2278 analysis. The anthropogenic fraction was recognized as being almost entirely in the
2279 accumulation mode, while natural aerosols in the form of sea-salt and mineral dust are typically
2280 in the coarse mode allowing a first observational estimate of the perturbation of τ_{aer} by
2281 anthropogenic emissions and an associated F_{direct} of -0.8 W m^{-2} . Similar methods followed
2282 (Chung et al., 2005, -0.35 W m^{-2} ; Yu et al., 2006, -0.5 W m^{-2}); these estimates were generally
2283 rather stronger than those from models, potentially due to the fact that absorbing aerosols (e.g.
2284 anthropogenic biomass burning aerosols above clouds) were neglected which can frequently
2285 produce positive radiative forcings (e.g. Keil and Haywood, 2003)

2286
2287 More sophisticated estimates of the direct radiative effect of aerosol in cloud-free skies over
2288 oceans were also developed by correlating the cloud-free TOA upward solar irradiance
2289 (frequently derived from CERES) against the aerosol optical depth derived from other

2290 instruments such as VIRS or MODIS (Loeb and Kato, 2002; Zhang et al., 2005, Loeb and
2291 Manalo-Smith, 2005). These estimates provide additional validation data for testing
2292 relationships in GCMs, but cannot be used to infer the radiative forcing by themselves owing to
2293 lack of knowledge of pre-industrial conditions.

2294

2295 Aerosol indirect forcing based on satellite retrievals were also developed. Typically these
2296 studies developed relationships between CDNC and fine mode aerosol concentrations or optical
2297 depth (Quaas, 2005; Quaas and Boucher, 2005). For example, Quaas and Boucher (2005)
2298 developed relationships between observed cloud properties from MODIS and observed aerosol
2299 properties from POLDER for stratiform marine clouds and for convective clouds over land and
2300 utilized these relationships within GCMs. Various methods for partitioning the observed
2301 relationships as a function of meteorology, above cloud moisture, and SSTs were to be
2302 developed to account for the impacts of meteorology that can confound derived relationships in
2303 observational studies. However, a persistent problem with these correlative studies is the mutual
2304 exclusivity of aerosol and cloud satellite retrievals and the lack of account of the relative
2305 vertical profile of aerosol and cloud.

2306

2307 IPCC (2007) and Forster et al (2007) recognized that the growing number of different aerosol
2308 species that were being considered in climate models was becoming unwieldy; while aerosol
2309 components were still assigned individual radiative forcing values, only the total aerosol direct
2310 effect and cloud albedo effect were included on the bar chart. Direct radiative forcing estimates
2311 were predominately model-based relying on a combination of AeroCom/non-AeroCom
2312 estimates and revealed $F_{\text{direct}} = -0.5 \pm 0.4 \text{ W m}^{-2}$ (5% to 95% confidence), while the Twomey effect

2313 was estimated to be -0.7W m^{-2} (best estimate) with a 5% to 95% range of -0.3 to -1.8W m^{-2}
2314 (Forster et al., 2007). For the first time, Forster et al (2007) presented the spread in the long-
2315 lived GHG, aerosol and total radiative forcing using a Monte-Carlo simulation of the
2316 uncertainties associated with each of the forcing mechanisms (Boucher and Haywood, 2001) to
2317 demonstrate that the uncertainty in the total radiative forcing was dominated by that of aerosols,
2318 particularly owing to uncertainties in the aerosol indirect effects, and that the total radiative
2319 forcing was positive, consistent with the observed warming of climate. Forster et al (2007)
2320 recognized that interactions of aerosols with mixed-phase and ice-clouds continued to be
2321 impossible to quantify on a global mean basis owing to the even greater complexity of these
2322 clouds when compared to warm liquid- phase clouds.

2323

2324

2325

2326

2327
2328
2329

5.5.Increases in aerosol model complexity – 2nd generation models: 2010s

2330 As aerosol modelling matured, further refinements of aerosol direct and indirect effects were
2331 included in GCMs. Further components of aerosol were included; Bellouin et al (2011) included
2332 nitrate aerosol and pointed out that as sulphur dioxide emissions decrease in the future owing to
2333 emission control, the radiative forcing of nitrate will likely increase owing to the availability of
2334 excess ammonia in the atmosphere. However, nitrate continues to remain a difficult aerosol to
2335 model owing to the dissociation to nitric acid and ammonia under ambient temperature and
2336 humidities.

2337

2338 The development of aerosol mass spectrometers and their location at surface sites and airborne
2339 platforms enabled, for the first time, a full appreciation of the complexity of optically active sub-
2340 micron aerosol composition as a function of location and altitude to be deduced (Jimenez et al.,
2341 2011) with sulphate, organic and nitrate highlighted as the dominant sub-micron components. The
2342 problems of the mutual exclusivity of satellite-retrievals of aerosol and cloud can be avoided using
2343 active satellite sensors such as CALIPSO lidar aerosol data collocated with MODIS cloud data
2344 (e.g. Costantino and Bréon, 2013). However, in-situ airborne platforms with dedicated
2345 instrumentation such as nephelometers, and aerosol optical particle counters continued to provide
2346 vital information on the aerosol vertical profiles at a level of detail and vertical resolution
2347 impossible to achieve with satellite mounted lidars.

2348

2349

2350

2351 In modelling, dual-moment schemes became more common, treating both aerosol number and
2352 aerosol mass prognostically (Stier et al., 2005) and both internal and external mixtures. This has
2353 particular relevance to estimates of aerosol-cloud-interactions because, for single-moment
2354 schemes with prognostic mass only, any increase in the aerosol mass (e.g. via condensation or
2355 coagulation), must artificially increase the aerosol number and hence CCN which then produces
2356 stronger aerosol indirect effects. The use of dual-moment state-of-the-art aerosol schemes in
2357 GCMs is now common-place.

2358

2359 Lohmann et al. (2010) examined the differences between i) the radiative flux perturbation (RFP;
2360 Haywood et al., 2009) which is calculated as the difference in the top-of-the-atmosphere
2361 radiation budget between a present-day simulation and a preindustrial simulation, both using the
2362 same sea surface temperatures and ii) the radiative forcing computed from two-calls to the
2363 radiative transfer code in GCMs holding the atmospheric state fixed. The RFP calculation allows
2364 for rapid responses (e.g. in clouds), that occur on a faster time-scale than the large-scale shifts in
2365 climate response that are induced through SST responses. RFP has become more commonly
2366 known as the effective radiative forcing (ERF – see Section 2.3.6). Allowing rapid adjustment to
2367 occur in diagnosing the ERF allowed isolation of both the Twomey (1977) and the Albrecht
2368 (1989) aerosol indirect effects and also aerosol semi-direct effects.

2369

2370

2371

2372 Myhre (2009) suggested that the discrepancy between observational (stronger) and modelled
2373 (weaker) estimates of aerosol direct forcing highlighted in IPCC (2007) was due to the lack of
2374 account of aerosol absorption above clouds and (ii) relatively larger fractional increase in BC
2375 containing absorbing than scattering aerosols since pre-industrial times. Analysis of models
2376 reported an aerosol direct radiative forcing of -0.3W m^{-2} which was found to be consistent with
2377 observational estimates. Aerosol absorption was again highlighted as a major uncertainty in
2378 accurate determination of aerosol direct radiative forcing (Bond et al., 2013) owing to aspects such
2379 as the morphology of the black carbon as a function of age and the impact of coatings of organic
2380 and inorganic components, the heating in the atmospheric column and subsequent rapid
2381 adjustment. Again this suggested that diagnosing the radiative forcing in a strict sense could not
2382 capture the rapid adjustment associated with atmospheric processes.

2383

2384 Boucher et al. (2013), Myhre et al (2013) and IPCC (2013) recognized that retaining the strict
2385 definition of radiative forcing as in previous IPCC reports was becoming untenable because it
2386 did not reflect the growing consensus that rapid responses can and should be isolated in any
2387 metric of climate change, but also because of the ease of application to GCM simulations. Hence
2388 the growth of ERF as the preferred metric for assessing potential climate impacts. Indeed, IPCC
2389 also chose the term aerosol-radiation-interactions over the aerosol direct forcing and aerosol-
2390 cloud interactions over aerosol indirect with rapid adjustment of aerosol-radiation interaction as a
2391 term for the semi-direct effect (Boucher et al., 2013). By this time there were many mature
2392 estimates of the impact of aerosol-radiation-interactions and aerosol-cloud-interactions from

2393 sophisticated GCMs and satellite-based estimates (e.g. Fig 5.3; see also Table 7.4 and 7.5 of
2394 Boucher et al. , 2013) allowing Myhre et al (2013) to estimate the magnitude of pre-industrial to
2395 present-day aerosol-radiation-interactions (-0.45W m⁻² with a 95% uncertainty range of -0.9 to
2396 +0.05W m⁻²) and aerosol-cloud-interactions (-0.45W m⁻² with a 95% uncertainty range of -1.2
2397 to 0 W m⁻²).

2398
2399
2400

2401
2402
2403
2404 **5.6. Current promising lines of research**
2405

2406 We have seen that the radiative forcing (or effective radiative forcing, ERF) has changed
2407 significantly from best estimates of stronger than -2 W m^{-2} (Charlson et al., 1991; 1992)
2408 to weaker than -1 W m^{-2} . Much of this reduction in magnitude of the radiative forcing via the
2409 direct effect (aerosol-radiation-interactions) was captured by the late 1990s owing to the use of
2410 GCMs (e.g. Kiehl and Briegleb, 1993) and by accounting for the effects of aerosol absorption by
2411 black carbon (Haywood and Shine, 1995). However, uncertainties in both the aerosol-radiation
2412 and aerosol-cloud interactions have remained stubbornly difficult to reduce owing to structural
2413 and parametric uncertainties. Here we ask what progress has been made in the 5-years since
2414 IPCC (2013) in terms of promising avenues of research.

2415
2416 The direct radiative effect/forcing of aerosols above clouds has remained a contentious issue
2417 with some very strong instantaneous positive radiative effects (greater than $+130$ to $+150 \text{ W m}^{-2}$)
2418 being diagnosed from various satellite instruments (e.g. de Graaf et al., 2012; Meyer et al., 2015;
2419 Peers et al., 2016) over the S.E. Atlantic; values that are stronger than those from climate models
2420 (de Graaf et al., 2014). Zuidema et al (2016) highlights that global models diverge when
2421 determining the direct radiative effect in the region. This is because the direct radiative forcing of
2422 a partially absorbing aerosol such as biomass burning aerosol depends not just on determination of
2423 the aerosol optical depth and aerosol absorption properties, but on the cloud amount, cloud reflectance
2424 and the relative vertical profile of cloud relative to the aerosols (see Fig 5.4). The ORACLES, LASIC,

2425 CLARIFY and AeroClo-SA in-situ aircraft-based measurement campaigns have targeted deriving
2426 better estimates of the direct effect

2427

2428

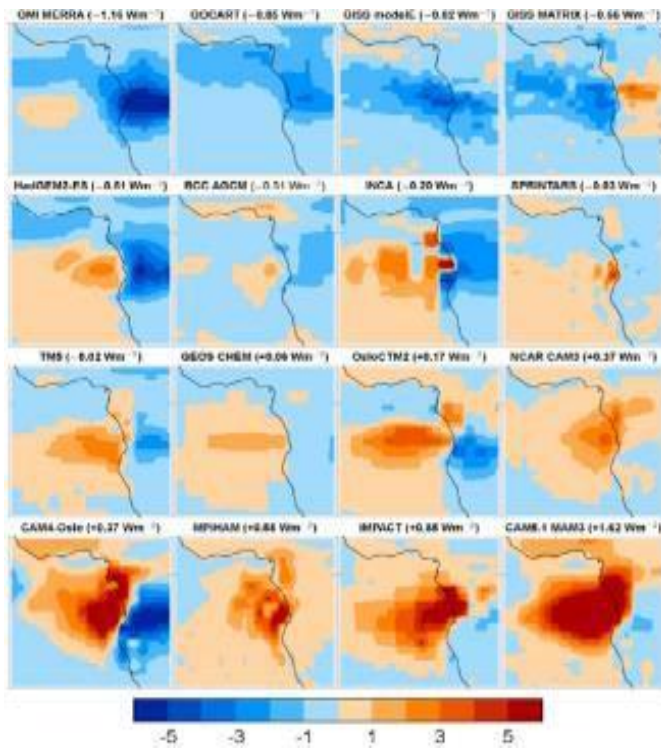


Figure 5.3. Showing the direct radiative effect of partially absorbing biomass burning aerosols diagnosed from 16 different climate models. The model with the strongest negative direct radiative effect is shown on the top left, while that with the strongest positive forcing is on the bottom right.

2429 of absorbing aerosols over clouds as one of their primary objectives (Zuidema et al., 2016).
2430 These measurement campaigns will undoubtedly give a better understanding of direct radiative
2431 effects of partially absorbing aerosols above clouds in the key-region of the SE Atlantic, but the
2432 change in concentration from pre-industrial times may well preclude accurate determination of
2433 the radiative forcing.

2434

2435

2436

2437

2438 Accurate representation of pre-industrial aerosol concentrations is also highlighted as a key
2439 uncertainty by Carslaw et al. (2013), who used a statistical emulator approach to examine the
2440 sensitivity of the aerosol forcing to a wide range of parameters including uncertainties in
2441 anthropogenic and natural emissions. The variance caused by uncertainties in natural aerosol
2442 concentrations accounted for around 45% of the variance, while uncertainty in anthropogenic
2443 emissions accounted for around 35% of the variance due to the impact that natural
2444 background aerosols have on the susceptibility of clouds to anthropogenic perturbations. Based
2445 on the limited paleodata, desert dust may have increased by almost 40% over the twentieth
2446 century due to a combination of climate change and land use (Mahowald et al., 2010; Ginoux et
2447 al., 2012). An important and likely source of higher preindustrial aerosols, which is currently
2448 poorly constrained, are wildfires. Recent studies have suggested that due to uncertainties in
2449 preindustrial wildfire emissions alone, the range of anthropogenic indirect effects could be
2450 between -0.1 W/m² to -1.1 W/m² (Hamilton et al., 2018). If these estimates are supported by
2451 more studies, we would have to rethink how we constrain estimates of both aerosol indirect
2452 effects from anthropogenic aerosols and climate sensitivity (see Section 6.0 for more discussion).

2453

2454 Progress been made in understanding the impact of anthropogenic emissions on mixed-phase
2455 cloud by contrasting observations of their behavior against liquid-phase clouds. Christensen et
2456 al., (2014) examined ship-track data in mixed-cloud environments and found a more muted
2457 indirect radiative forcing impact owing to enhanced glaciation induced precipitation that limited
2458 the total water path of the clouds. Christensen et al. (2016) extended these observations by using
2459 multiple sensors over millions of atmospheric profiles and concluded that liquid clouds

2460 dominate any negative radiative forcing for the aerosol indirect effects owing to the muted
2461 impacts of mixed-phase clouds and a counterbalancing positive radiative forcing from
2462 convective clouds. These observations call into question whether net aerosol indirect effects
2463 have been overestimated.

2464

2465 Ghan et al. (2016) performed an intercomparison to isolate the strength of the Twomey and
2466 Albrecht aerosol-cloud-interaction effects in GCMs, and showed that while all models exhibited
2467 a reasonably consistent Twomey effect, the strength of the Albrecht effect essentially fell into
2468 two clusters. The cluster were i) an almost negligible impact, ii) a strong positive forcing that
2469 acted to reinforce the radiative forcing from the Twomey effect, but observational evidence
2470 remained lacking as to which one of these responses was correct. However, one interesting line
2471 of evidence to elucidate the strength of the Albrecht effect was the use of large-scale SO₂-
2472 degassing volcanic eruptions in relatively pristine environments to examine the impact on
2473 satellite-derived cloud properties. This technique was first used by Gasso (2008), on relatively
2474 modest degassing events and has been the subject of further research (Toll et al., 2017). These
2475 smaller scale degassing eruptions can be used to examine relationships between cloud and
2476 aerosol in a similar way to ship- tracks (Christensen et al., 2014; Chen et al., 2015), but are
2477 frequently on too small a scale for the impacts to be directly compared against GCMs capable of
2478 diagnosing a radiative forcing. This situation changed in 2014 with the fissure eruption at
2479 Holuhraun, Iceland which emitted a huge plume of SO₂ across the entire north Atlantic
2480 (Gettelman et al., 2015) causing a clear, statistically significant reduction in the cloud effective
2481 radius in the MODIS satellite record (McCoy and Hartmann, 2015, Malavelle et al., 2017), but
2482 no discernible impact of the cloud liquid water path. Malavelle et al. (2017) were able to show

2483 that only models with a modest Albrecht effect were consistent with observations for a host of
2484 liquid-water cloud conditions. In a similar vein, Chen et al (2014) showed that variations in
2485 cloud liquid water paths are dominated by other meteorological factors such as the state of
2486 precipitation, humidity and atmospheric stability rather than aerosol microphysical processes
2487 making definitive detection and attribution difficult.

2488

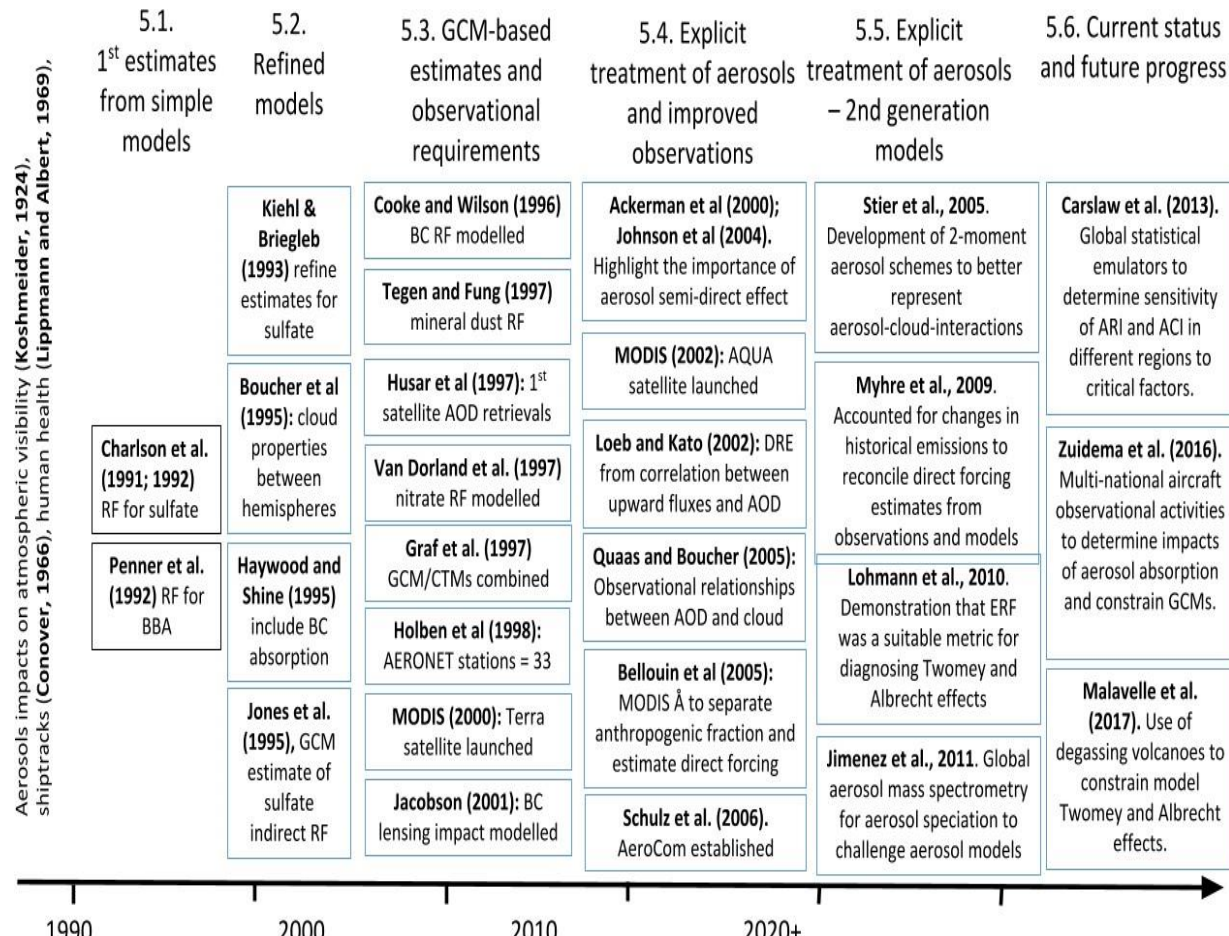
2489 These advances provide an opportunity to better constrain aerosol indirect effects in the future;
2490 without pursuing these opportunities to confront model performance, an accurate
2491 characterization of aerosol radiative forcing is likely to prove elusive. There is however, a
2492 growing consensus that, in the future, the importance of the radiative forcing of aerosols will
2493 begin to be a less important uncertainty as the radiative forcing from greenhouse gases continues
2494 to increase. Global emissions of sulphur dioxide have plateaued at around 1990, and have begun
2495 to fall on a global mean basis owing to effective clean-air policies targeted at reducing
2496 particulate pollution. Areas such as the US and Europe have already seen reductions in sulphur
2497 dioxide emissions of around a factor of 5 since their peak. This reduction in emissions, coupled
2498 with the ever increasing radiative forcing from greenhouse gases may result in significant rates of
2499 global warming over the next few decades (e.g. Andreae et al., 2005).

2500

2501 Where aerosols may start to play an increasing role is in the, currently theoretical, field of
2502 geoengineering i.e. the deliberate injection of aerosols or their precursors into the stratosphere to
2503 mimic the cooling impacts of explosive volcanic eruptions such as Pinatubo or the deliberate
2504 injection of aerosols into stratocumulus clouds to mimic the impacts of natural degassing
2505 volcanoes. The use of such techniques would have many, many consequences (e.g. Robock et al.,

2506 2008), not least that, if proven effective, it could reduce the drive for reduced use of fossil-fuels
 2507 (see Section 13 for a comprehensive discussion).

2508
 2509



2510 1990 2000 2010 2020+ →

2511

2512

2513 **Figure 5.4.** Illustrating the time evolution of some of the most significant findings that
 2514 are discussed in the text. Keil, A., and Haywood, J.M., Solar radiative forcing by
 2515 biomass aerosol particles over marine clouds during SAFARI-2000. *J. Geophys. Res.*,
 2516 8467, 108(D13), doi:10.1029/2002JD002315, 2003.

2517
 2518
 2519

2520 **6. Land and biogeochemistry interactions**

2521
2522
2523 Human activities do not only directly emit gases and aerosols which impact climate, as
2524 described above, they also modify the land surface, which can directly change the surface
2525 properties, and both directly and indirectly change the emissions of different gases and aerosols
2526 (Feddema et al., 2005; Heald and Spracken, 2015; Myhre et al., 2013; Pielke, 2005; Ward et al.,
2527 2014). Land conversion of forests, for example to croplands, emits carbon dioxide immediately,
2528 and the land cover change and the land management has many implications for albedo changes,
2529 and emissions Feddema et al., 2005; Heald and Spracken, 2015; Myhre et al., 2013; Pielke,
2530 2005; Ward et al., 2014). Changes in land surface, such as urbanization or deforestation, can
2531 also change the local experience of climate in substantial ways, but these are not contributing to
2532 changes in the top of atmosphere radiative forcing directly, and thus are not discussed here
2533 (Field et al., 2014; Hartmann et al., 2013; Lejeune et al., 2018). We also do not consider longer
2534 term feedbacks, such as the fertilization of land or ocean ecosystems by anthropogenic aerosols,
2535 which could be as large as the direct radiative effects of anthropogenic aerosols (Mahowald,
2536 2011). Generally speaking, understanding and quantifying how changes to the land surface are
2537 impacting the climate are more difficult than some of the direct emissions from human activities
2538 described previously (Boucher et al., 2013; Myhre et al., 2013).

2539 The most important impact of human land use and land cover change (LULCC), in terms of
2540 radiative forcing of climate, and one of the first processes included in the IPCC assessment
2541 reports are the direct emissions of CO₂ from deforestation, and the indirect emissions of CO₂
2542 from forest degradation and land management (IPCC, 1990). Other processes, such as the
2543 albedo changes, interactions with wildfires and other processes, were mentioned in the first

2544 report, but not quantified (IPCC, 1990). In subsequent AR, these processes were expanded upon
2545 and quantified, as described below.

2546
2547 For long-lived gases, which can be assumed to be relatively well-mixed across the troposphere,
2548 such as carbon dioxide, methane or nitrous oxides, estimates of changes in the atmospheric
2549 composition rely on ice core and other observational records, as discussed previously (Forster et
2550 al., 2007; Myhre et al., 2013). But for short-lived gases and aerosols, an important difficulty in
2551 understanding how human activities have changed past atmospheric conditions, especially for
2552 example, in understanding base line preindustrial chemistry or aerosol conditions, is that there
2553 are no direct observations of preindustrial conditions for short lived gases or aerosols, since the
2554 ice core records from just a few sites cannot characterize the global average for short-lived
2555 constituents (Myhre et al., 2013). For short-lived gases and aerosols, their emissions are
2556 estimated based on simple assumptions or modeling studies (Boucher et al., 2013; Collins et al.,
2557 2017; Lamarque et al., 2010; Van Marle et al., 2017; Myhre et al., 2013; Shindell et al., 2013).
2558 Recent studies have highlighted the importance of potential changes in emissions from ‘natural’
2559 sources due to human activities, especially on the land surface (Carslaw et al., 2010, 2013;
2560 Hamilton et al., 2018; Mahowald et al., 2011, 2010; Myhre et al., 2013; Ward et al., 2014), so
2561 here we review the state of knowledge on how humans can perturb natural sources. We will also
2562 review evolution of the representation of human land use forcings of climate in the IPCC
2563 reports, as an indication of how the understanding of how human activities on the land surface
2564 impacting natural sources of different important radiative constituents has evolved.

2565

2566
2567

2568 **6.1 Land use and land cover change climate forcers**

2569
2570
2571 The interactions of land use and land cover change are shown in Figure 1 and described in
2572 more detail in each section below.

2573
2574
2575 **6.1.1 Albedo impacts from land use and land cover change**

2576
2577 The direct modification of the surface from land use, land management or land cover change
2578 can be through albedo changes or through changes in the energy fluxes locally (Andrews et al.,
2579 2017; Bonan, 2008; Feddema et al., 2005; Myhre et al., 2013; Pielke, 2005). The surface albedo
2580 (ratio of the reflected and incoming solar radiation) varies between dark forests, lighter
2581 grasslands or crops, and often even lighter barren deserts or snow covered surfaces.
2582 Consequently, deforestation tends to increase the Earth's albedo, and cause more light to be
2583 reflected, cooling the Earth. The largest impacts of land use and deforestation will occur at
2584 higher latitudes because snow covered forests retain a low albedo, while snow covered crop-
2585 lands will have a high albedo (IPCC, 2001). Recently satellite measurement have been used to
2586 estimate the impact of land use on radiative forcing (Myhre et al., 2013; Zhao and Jackson,
2587 2014). Estimates of the changes since preindustrial require the use of models, and the
2588 biophysical impacts of LULCC are sensitive to the model's used; a Land Use Model Inter-
2589 comparison project (LUMIP) is underway to better constrain the impacts on radiative forcing
2590 (Lawrence et al., 2016). Changes in the land surface, such as changes in vegetation, and their
2591 impact on the surface albedo have been included in the assessments since the first report (IPCC,
2592 1990), but not quantified until the third report, to be $-0.2 \pm 0.2 \text{ W/m}^2$ (IPCC, 2001). The

2593 estimates and uncertainty stayed the same in the AR4, but became slightly smaller, with smaller
2594 uncertainties in the AR5 (-0.15 +/- 010 W/m²) (Myhre et al., 2013).

2595

2596

2597 **6.1.2. Carbon dioxide emissions**

2598

2599 The gross carbon dioxides emissions or uptake from natural ecosystems, both land and
2600 ocean, are much larger than the fluxes from anthropogenic emissions but the net emissions
2601 are close to zero (Ciais et al., 2013; Le Quere et al., 2013; Le Quéré et al., 2016; Sitch et al.,
2602 2015). Deforestation and conversion of natural lands for human management tend to
2603 directly release carbon dioxide into the atmosphere, while reforestation, afforestation, or
2604 carbon dioxide fertilization will increase the uptake of carbon dioxide into the terrestrial
2605 system, including soils (Ciais et al., 2013; Friedlingstein et al., 2006; Houghton, 2018; Le
2606 Quere et al., 2013). In addition, the change in land cover and land management changes the
2607 longer term uptake of carbon dioxide (Ciais et al., 2013; Friedlingstein et al., 2006;
2608 Houghton, 2018; Le Quere et al., 2013). Over all of the IPCC assessment reports, ice core
2609 data is used for carbon dioxide changes, which does not require the attribution of the change
2610 in carbon dioxide from land surface changes versus direct emission (Ciais et al., 2013;
2611 Denman et al., 2007; IPCC, 1996, 2001; Stocker et al., 2013). However, starting already in
2612 the FAR, there was an important division between land use emissions and other emissions
2613 identified in the reports (IPCC, 1990). The 2000 Special report on land use, land use change
2614 and forestry was written in support of the Kyoto Protocol and provided

2615
2616 **6.1.3 Wildfires and biomass burning**

2617

2618 Natural ecosystems can emit short-lived gases and aerosols through a variety of processes, and
2619 these processes can be modified by human activities (Carslaw et al., 2010, 2013; Hamilton et
2620 al., 2018; Mahowald et al., 2011, 2010; Myhre et al., 2013; Ward et al., 2014) (Figure 6.1). Of
2621 the most important is likely to be changes in wildfire regimes (Arneth et al., 2010; Carslaw et

2622 al., 2010; Ward et al., 2014). Intermittent wildfires release substantial amounts of carbon
2623 dioxide, carbon monoxide, sulfur dioxide, methane and other organic gases, and carbonaceous
2624 aerosols (Andreae and Merlet, 2001). Wildfire sources of methane were identified already in the
2625 FAR. Biomass burning aerosols were one of the first three aerosols considered in the TAR
2626 (along with industrial sources of sulfate and black carbon). For AR4 and AR5, studies suggested
2627 that preindustrial wildfires were much less than in current climate, as they attributed wildfires to
2628 deforestation fires (Boucher et al., 2013; Forster et al., 2007; Lamarque et al., 2010). Recent
2629 evidence suggests strong changes in wildfire over the last 250 years, with a large increase in
2630 fires about 200 years ago, and then a decrease (Kloster et al., 2010; Marlon et al., 2008, 2012;
2631 Pechony and Shindell, 2010; Zennaro et al., 2014). Recently, evidence from satellites has
2632 suggested a 25% decrease in fires over the last 18 years, likely to due to the expansion of
2633 agriculture (Andela et al., 2017). While increases in biomass burning due to deforestation and
2634 climate change are assumed to have occurred since preindustrial times in the standard estimates
2635 used for CMIP6 (Van Marle et al., 2017), some estimates suggest a decline instead, due largely
2636 to a change in human fire and land management (Hamilton et al., 2018; Marlon et al., 2008;
2637 Zennaro et al., 2014). These large decreases in wildfire emissions, over the Anthropocene are
2638 large enough to have an impact on indirect and direct aerosol radiative forcing so that they
2639 offset those from direct anthropogenic emissions (Hamilton et al., 2018). For example, that
2640 study suggested that new wildfire emission estimates increase estimated anthropogenic aerosol
2641 indirect forcing from -1.1 W/m² using the CMIP6 emission datasets to 0.1 W/m² using LMfire
2642 estimates of wildfire (Figure 6.1; using global averages from Hamilton et al., 2018). In other
2643 words, because the preindustrial wildfire emissions are poorly constrained,
2644 current day anthropogenic aerosol radiative forcing could be -1.1 W/m² or 0.1 W/m² using the

2645 same model but different emission estimates. This has profound implications for our
2646 understanding, not only of anthropogenic aerosol radiative forcing, but also climate sensitivity,
2647 which is very sensitive to assumptions about the size of the anthropogenic aerosol radiative
2648 forcing (Knutti et al., 2002; Myhre et al., 2013).

2649

2650

2651 **6.1.4. Agricultural activity and soils**

2652

2653 Soils naturally release nitrogen oxides, nitrous oxide and ammonia: changes in nitrogen inputs
2654 or temperature can radically modify the amount of nitrogen oxides or ammonia released (Ciais
2655 et al., 2013; Fowler et al., 2013). Since agriculture, and especially the green revolution, there
2656 has been a substantial modification of the nitrogen budgets of regions with land use, modifying
2657 substantially the nitrogen inputs (Ciais et al., 2013; Fowler et al., 2013). In terms of direct
2658 radiative forcing of nitrogen-based species, nitrous oxide is the most important and is a long-
2659 lived greenhouse gas, with a lifetime on the order of 100 years (Ciais et al., 2013). Already in
2660 the FAR, the agricultural sources of nitrous oxide were identified, if not quantified (IPCC,
2661 1990), while in the SAR and later reports, estimates for the agricultural sources of nitrous
2662 oxides were quantified (Ciais et al., 2013; Denman et al., 2007; Forster et al., 2007; IPCC, 1996,
2663 2001; Myhre et al., 2013). The ice core changes over the last hundred years in nitrous oxide
2664 have been attributed to changes in land management (Ciais et al., 2013; Ward et al., 2014).
2665 Nitrogen oxide and ammonia emissions from soils are thought to be enhanced by agricultural
2666 activities, especially nitrogen fertilizers (Fowler et al., 2013; Myhre et al., 2013), and the role of
2667 human land use in modifying these emissions from soils is first mentioned in the TAR (IPCC,
2668 2001). Nitrogen oxide emissions are important climatically for their impact on tropospheric

2669 ozone and methane lifetime (section 4), but the anthropogenic part is dominated by combustion
2670 sources (Myhre et al., 2013; Shindell et al., 2017). On the other hand, ammonia emissions are
2671 predominantly from nitrogen fertilization as part of agriculture or pasture usage, which
2672 contribute to a change in ammonium aerosols (Myhre et al., 2013; Riddick et al., 2016; Shindell
2673 et al., 2017; Sutton et al., 2013).

2674
2675
2676
2677

2678 **6.1.5. Methane**

2679
2680 In inundated regions, methanogens thrive, producing methane from organic material in the soil
2681 (Mathews and Fung, 1987). Changes in the area of inundated areas (for example, due to
2682 expansion of rice paddies or filling of wetlands), productivity of these regions, temperatures and
2683 carbon dioxide itself have impacted the methane emissions from these regions (Kirschke et al.,
2684 2013; Myhre et al., 2013; Paudel et al., 2016; Zhang et al., 2017). In addition to changes in
2685 natural wetland area, rice paddy expansion and ruminant animal husbandry has increased land
2686 use methane production (Kirschke et al., 2013; Myhre et al., 2013). Emissions of methane from
2687 land use change were already considered early in the IPCC process (IPCC, 1990, 2000).

2688
2689 **6.1.6. Mineral aerosols (Dust)**

2690
2691 Dry, unvegetated land subject to strong winds allow the entrainment of soils into the
2692 atmosphere, causing the largest source of aerosols by mass into the atmosphere (Mahowald et
2693 al., 2011). Desert dust is one of the few aerosols for which we have paleo-records, since it can be
2694 retrieved from ice, marine, terrestrial and land records (Albani et al., 2018; Kohfeld and
2695 Harrison, 2001; Mahowald et al., 2010). AR4 assumed that <10% of mineral aerosols were from
2696 anthropogenic sources (Forster et al., 2007). A reconstruction based on paleo-data suggests that
2697 dust may have increased by a factor of almost two across the 20th century (Mahowald et al.,
2698 2010), due to either aridification from climate change (Mahowald, 2007) or land use (Ginoux et
2699 al., 2012). However, between the AR4 and AR5, estimates of the radiative forcing from mineral
2700 aerosols became closer to zero because of a shift in dust properties (Albani et al., 2014;
2701 Mahowald et al., 2010; Perlitz et al., 2001; Sinyuk et al., 2003), suggesting small
2702 contributions from anthropogenic desert dust to radiative forcing. Mineral aerosols absorb and

2704 scatter in both the short wave and long wave, making them complicated in their impacts
2705 (Sokolik and Toon, 1996). The shift to a smaller magnitude radiative forcing for mineral
2706 aerosols is due to both an improved estimate that mineral aerosols are likely more absorbing in
2707 the short wave than previously thought from remote sensing data (Sinyuk et al., 2003), as well
2708 as a consensus that mineral aerosols tends to be larger than previously thought (Kok et al., 2017;
2709 Mahowald et al., 2014). Future projections vary depending on whether they include climate
2710 change impacts (Evan et al., 2016), land use impacts or both (Ward et al., 2014). While the SAR
2711 included the possibility of anthropogenic land use sources of desert dust, (IPCC, 2001; Tegen et
2712 al., 1996) the radiative forcing of this constituent was not included in the report until the TAR
2713 (Forster et al., 2007).

2714
2715
2716 **6.1.7 Organic compounds**
2717
2718 Some plants emit volatile organic compounds (Guenther et al., 2006), which can interact with
2719 nitrogen oxides to change the cycling of tropospheric ozone (Collins et al., 2017; Myhre et al.,
2720 2013), as well as produce secondary organic aerosols (Arneth et al., 2010; Carslaw et al., 2010;
2721 Mahowald et al., 2011; Myhre et al., 2013). Natural ecosystems also emit primary biogenic
2722 aerosols, from fungi, pollen or plant or insect pieces (Despres et al., 2012; Graham et al., 2003;
2723 Mahowald et al., 2011). Deforestation, climate change or changes in fire frequency can
2724 modify the amount of forests, thereby modifying the emissions from natural forests of these
2725 important constituents (Arneth et al., 2010; Mahowald et al., 2011; Unger, 2014; Ward et al.,
2726 2014). The importance of biogenic derived organics for modifying both ozone and secondary
2727 organic aerosol formation was established by the TAR, although no explicit calculation of the
2728 impact of human land use or fires onto the radiative forcing was performed until after the last

2729 assessment (Forster et al., 2007; IPCC, 2001; Myhre et al., 2013), and is thought to be a small,
2730 but important feedback (Unger, 2014; Ward et al., 2014)

2731
2732
2733
2734
2735
2736

2737 **6.2 Snow albedo changes**

2738

2739

2740 Anthropogenic aerosol deposition of black carbon onto snow can change the albedo of the
2741 snow, darkening the snow and warming the globe (Hansen and Nazarenko, 2004) as well as
2742 modifying the melting of the snow and glaciers (Painter et al., 2013). This effect was first
2743 included in the AR4 as a slight warming: +0.1 [0.0 to 0.2] W/m² (Forster et al., 2007). The
2744 AR5 estimate is slightly smaller at +0.04 (0.02 to 0.09) W/m².

2745

2746

2747

2748

2749 **6.3. Estimates of the net effect of land use land cover change (LULCC) on radiative**
2750 **forcing.**

2751

2752

2753

2754 In order to better understand the relative role of LULCC compared to other sources of radiative
2755 forcing, one set of studies split the emissions into those from LULCC from non-LULCC based
2756 on standard CMIP5 and IPCC AR5 input datasets and approaches, including using the ERF
2757 concept (Mahowald et al., 2017; Ward et al., 2014; Ward and Mahowald, 2015). Similar to most
2758 climate models, the model used in this set of studies overpredicted aerosol direct and indirect
2759 effects compared to IPCC AR5 assessed RF, and thus the aerosol radiative forcings from
2760 LULCC results were tuned to the AR5 estimates (Mahowald et al., 2017; Ward et al., 2014;
2761 Ward and Mahowald, 2015). Radiative forcing from LULCC sector represents 40% of the
2762 current anthropogenic forcing (Figure 6.3a). This is due to the carbon dioxide emissions from
2763 conversion of natural lands to managed lands, in addition to substantial radiative forcing from
2764 methane and nitrous oxide emitted from agriculture and changes in land (Mahowald et al., 2017;
2765 Ward et al., 2014; Ward and Mahowald, 2015). Anthropogenic aerosol changes from land use
2766 are thought to be large individually, due to changes in desert dust, agricultural aerosols, forest
2767 biogenic aerosol emissions and wildfires, but have a net zero impact on radiative forcing in this
2768 set of studies (Ward et al., 2014), so that most of anthropogenic aerosol radiative forcing is due
2769 to non-LULCC (Figure 6.3a), which is a net negative radiative forcing. The fraction of the
2770 Total radiative forcing from LULCC (40%) is larger than the fraction of the CO₂ radiative
2771 forcing attributable to LULCC (20%). Over time, the LULCC radiative forcing has grown
2772 gradually over the 20th century, while non-LULCC radiative forcing was close to zero until

2773 1970s, and now is growing very quickly to positive values as CO₂ is accumulating the
2774 atmosphere (Figure 6.3b).

2775
2776
2777
2778
2779
2780
2781

2782 **6.4. Future projections**
2783
2784

2785 LULCC RF for future are even more difficult to estimate than that for past, and are highly
2786
2787 dependent on driving assumptions, especially how much land use conversion will occur (Ward
2788 et al., 2014). Integrated assessment models which were used to create the forcing scenarios for the
2789 earth system models (Gidden et al., 2018; Hurtt et al., 2011; Moss et al., 2010), tended to
2790 underestimate current deforestation rates in the AR5, especially in the tropics, and tended to
2791 have very similar deforestation rates, compared with possible futures (Ciais et al., 2013; Ward
2792 et al., 2014). This suggests that future estimates from IAMs or IAMs coupled to earth system
2793 models may underestimate the impact of LULCC (Mahowald et al., 2017). The land use model
2794 intercomparison (LUMIP) has the goal to explore more fully the possible LULCC pathways as
2795 well as the radiative forcing resulting from the land biophysics component (Lawrence et al.,
2796 2016).

2797

2798 The emission datasets used in the CMIP5 and CMIP6 include some of processes which might
2799 impact radiative forcing from LULCC: generally only direct emissions from agriculture are
2800 included in emission changes, including some estimates of changes in wildfires in the past and
2801 future but with no changes in desert dust (Collins et al., 2017; Gidden et al., 2018; Lamarque et
2802 al., 2010, 2011). However the CMIP6 studies, currently underway, will include idealized
2803 sensitivity studies for the different natural aerosols to understand their impact on current
2804 radiative forcing, providing some bounding on their current and future role (Collins et al.,
2805 2017).

2806

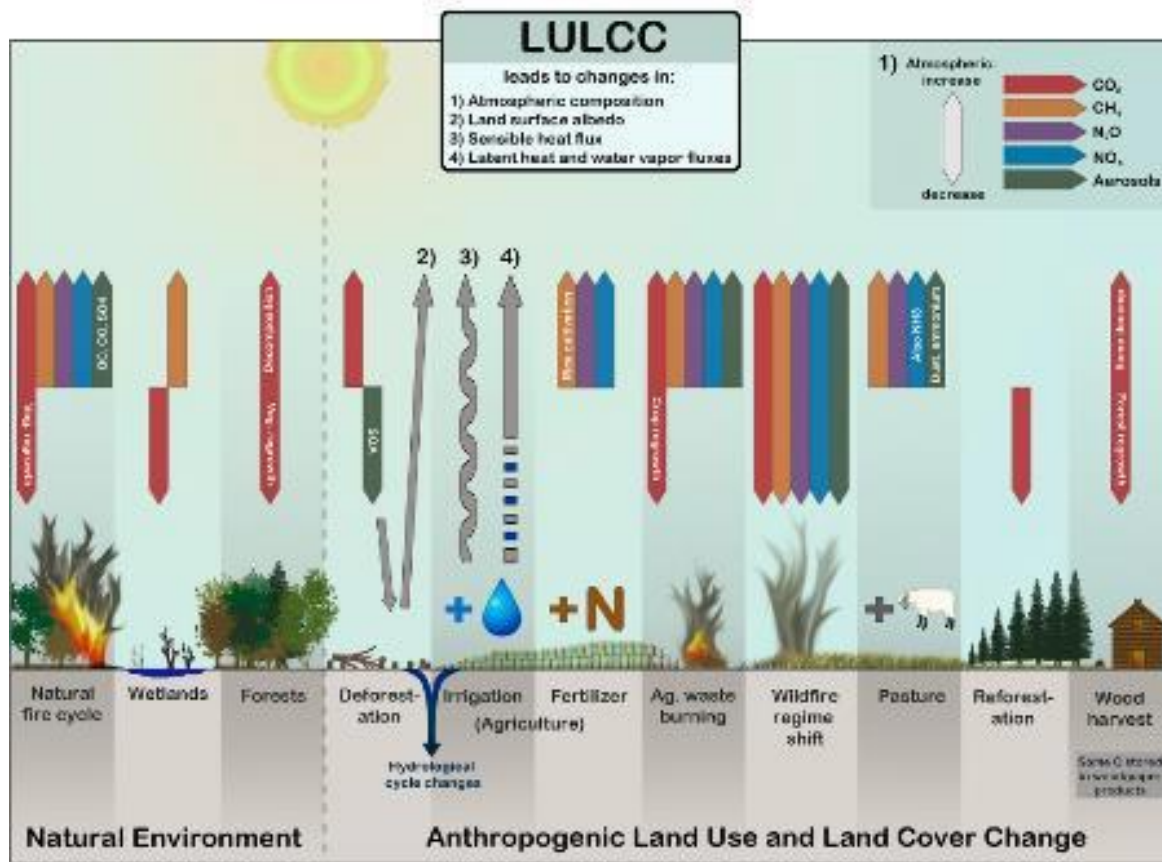
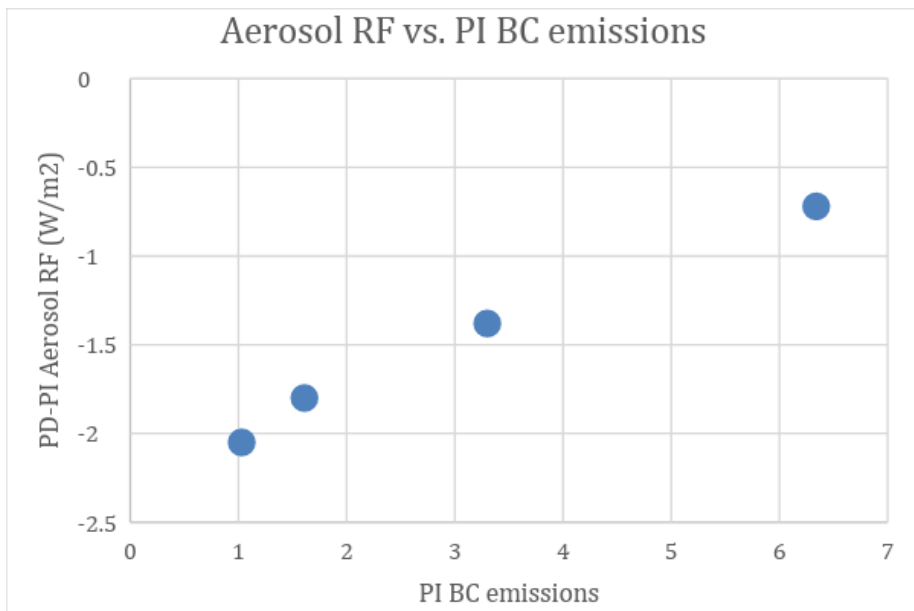


Figure 6.1: A schematic illustration of the climate impacts of land use and land cover change

from Ward et al., 2014.

2816
2817
2818
2819
2820
2821
2822
2823
2824
2825
2826
2827
2828
2829
2830
2831
2832
2833



2834
2835
2836 **Figure 6.2:** Graph showing the relationship between estimated preindustrial black
2837 carbon missions (PI BC) from different fire models and the total indirect
2838 anthropogenic radiative forcing based on Hamilton et al., 2018 numbers. Notice
2839 that estimates of current anthropogenic indirect radiative forcing are linearly
2840 dependent on estimates for preindustrial emissions of
2841
2842
2843

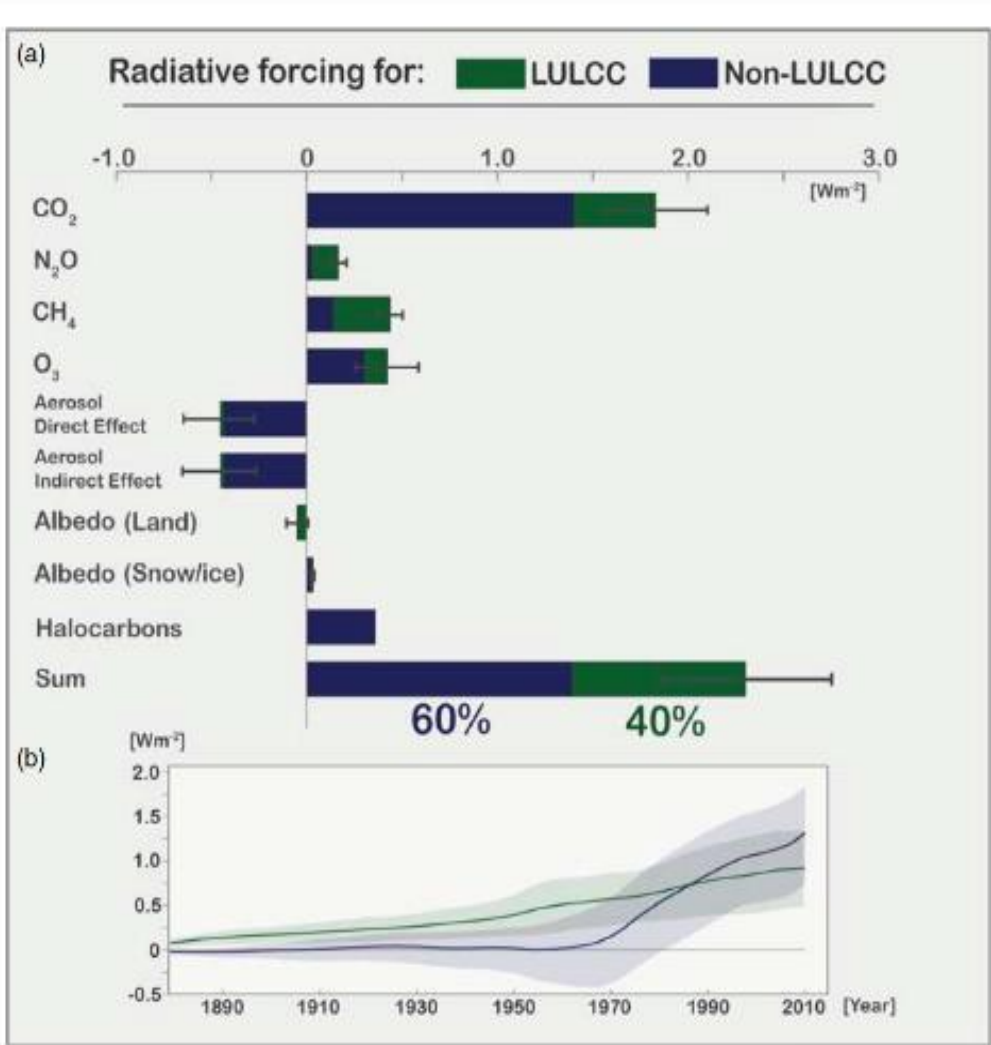


Figure 6.3: a) Anthropogenic radiative forcing (W/m^2) for the year 2010 relative to 1850 partitioned into LULCC and non-LULCC sources for different forcing agents, with uncertainty in the portion of total radiative forcing due to LULCC given by the error bars (adapted from Ward et al., 2014). b) time series of anthropogenic radiative forcing (W/m^2) for LULCC and non-LULCC sources with uncertainty represented by the shading. (from Mahowald et al., 2017).

2884 **Section 7. Contrails and contrail-induced cloudiness**

2885

2886

2887 One important component to the RF from subsonic and supersonic aircraft operations (in
2888 addition to its direct emissions of CO₂ and the indirect effects of NO_x emissions) arises from
2889 the ejection of hot moist air (and aerosols and their precursors) from jet engines into air which
2890 is supersaturated (with respect to ice) in the upper troposphere and lower stratosphere (e.g.
2891 Heymsfield et al. 2010; Kärcher 2018). This leads to the formation of persistent linear
2892 condensation trails (contrails) that can evolve into persistent cirrus (e.g. Minnis et al., 1998;
2893 Boucher, 1999; Fahey et al., 1999), comprised mostly of ice condensates. Contrail
2894 characteristics are influenced by humidity and temperature along aircraft flight tracks. In
2895 addition, aerosols from aviation can alter the properties of existing clouds or influence their
2896 subsequent formation. The potential impact of aviation contrails on climate was recognized in
2897 the early 1970s. Machta and Carpenter (1971) presented evidence of changes in high cloud
2898 cover over Denver and Salt Lake City, USA, which they tentatively attributed to aviation; in
2899 the same volume Matthew et al. (1971) noted that while this would increase the albedo, a
2900 compensating change in longwave emissivity could reverse the sign of the climate effect.

2901

2902 Assessments of contrail RF have mostly concluded that, when diurnally averaged, the net
2903 effect of contrails is a positive, due to the dominance of the longwave component. An early
2904 quantification of persistent linear contrails consisted of using meteorological and air traffic
2905 data scaled to regional observations of contrail cover (Minnis et al., 1999; Fahey et al., 1999).
2906 These studies yielded an estimate of 0.02 W m⁻².
2907 (with Fahey et al. (1999) estimating a range: 0.005 to 0.06 W m⁻²) (IPCC, 1999, 2001). The
2908 uncertainty factors included contrail cover, optical depth and cloud microphysical properties

2909 which runs true even today. Sausen et al. (2005) updated the IPCC estimate, giving a year 2000
2910 forcing of 0.01 W m^{-2} for persistent linear contrails and a total (including the impact on cirrus)
2911 of 0.05 W m^{-2} . Soot emissions from aircraft can also affect the cirrus cloud processes
2912 especially the nucleation of ice crystals, but the effects are deemed highly uncertain.
2913 Sedimentation of ice crystals from contrails may remove water vapor from the upper
2914 troposphere with resultant impacts on vertical profiles of cloud condensates and humidity.
2915
2916
2917
2918 Boucher et al. (2013) used more advanced model results to support the view that the longwave
2919 forcing dominates over the shortwave (e.g. Stuber and Forster, 2007); however, models
2920 disagree on the relative importance of the two effects. Contrails have been observed to spread
2921 into cirrus sheets which can persist for several hours, and observations confirm their overall
2922 positive RF (Haywood et al., 2009). Boucher et al. (2013) gave a global-mean RF estimate of
2923 0.01 (0.005 to 0.03) W m^{-2} for persistent linear contrails. Based on Schumann and Graf (2013)
2924 and Burkhardt and Kärcher (2011), the combined linear contrails and contrail-induced cirrus
2925 ERF for the year 2011 was assessed to be 0.05 (0.02 to 0.15) W m^{-2} , with the principal
2926 uncertainties still occurring due to gaps in the knowledge of the spreading rate, physical
2927 properties including optical depth and shape, radiative transfer, as well as the lack of
2928 knowledge of actual aircraft trajectories. This emphasizes the importance of ongoing
2929 measurement campaigns that target contrail properties (e.g. Voigt et al. 2017) as well as the
2930 systematic collation of existing knowledge emerging from such campaigns (Schumann et al.
2931 2017). Analysis of satellite data, especially in the context of detecting line-shaped contrails,

2932 remains important in the assessment of contrail RF. The recent estimate of Duda et al. (2019),
2933 using MODIS data for the period 2006-2012, yielded global-mean RF of $0.008 - 0.009 \text{ W m}^{-2}$,
2934 supporting the values assessed earlier in Boucher et al. (2013).

2935

2936 Bock and Burkhardt (2016) have produced a more-refined model estimate of contrail-induced
2937 cirrus (including line-shaped contrails) forcing of 0.056 W m^{-2} for a 2006 aviation inventory.
2938 Although this seemed in good agreement with the earlier Burkhardt and Kärcher (2011) results,
2939 it arose from a different balance between the longwave and shortwave RF components.

2940
2941 Both Chen and Gettelman (2016) and Bock and Burkhardt (2019) have performed detailed
2942 modelling studies of the possible contrail RF in 2050. There are formidable challenges in
2943 making such estimates, in addition to those that are relevant to estimating present-day forcing.
2944 These include assumptions on the growth in air traffic, and the regional distribution of that
2945 growth, changes in engine technology and fuel type, and how changes in climate may impact
2946 the occurrence of ice supersaturated regions in which contrails form. Chen and Gettelman
2947 (2016) predict a seven-fold increase in contrail forcing from 2006 to 2050, which is
2948 substantially more than the four-fold increase in global-flight distance - they attribute this to
2949 stronger growth in flight distances in low latitudes. Bock and Burkhardt (2019) obtain a more-
2950 modest factor of 3 increase in global-mean forcing and find that growth in air traffic is the
2951 predominant cause, with other effects only impacting the regional distribution. The absolute
2952 2050 forcing differs significantly between these studies, with Chen and Gettelman (2016)
2953 obtaining a value of 87 mW m^{-2} while Bock and Burkhardt (2019) obtain 160 to 180 mW m^{-2} .
2954 Bock and Burkhardt (2019) attribute the differences to different assumptions of ice crystal

2955 size in newly-formed contrails; additional effects include differences in the simulation of
2956 changes in the distribution of ice supersaturated regions in a future climate in the two models.

2957

2958 A significant issue in understanding the importance of contrail RF arises from uncertainty in
2959 the efficacy of that forcing (see Section 2.3.4). There is a sparse literature on the topic. In GCM
2960 studies, Ponater et al. (2006) found an efficacy of 0.6, while Rap et al. (2010) obtained a value
2961 of 0.3. Both studies pre-date the uptake of ERF as a concept and the reason/
2962 s for these low values remains unclear; however, if confirmed by later work, it would imply a
2963 significantly lower impact of contrails on surface temperature than implied by the radiative
2964 forcing. Schumann and Mayer (2017), using results from a simple global-mean model,
2965 speculate that the climate sensitivity to the (negative) shortwave contrail forcing may exceed
2966 that due to the (positive) longwave forcing, because of differences in the partitioning of the
2967 surface and top-of-atmosphere forcings in the two cases. As they note, there is a need to test
2968 this hypothesis in a comprehensive global model.

2969

2970

2971

2972

2973 **Section 8. Solar Radiative Forcing**

2974

2975

2976 Three primary foci compose contemporary solar radiative forcing research; 1) space-based
2977 measurements of solar irradiance, which explicitly define the forcing over the past 40 years, 2)
2978 modelling observed irradiance variability in terms of proxies that expand understanding across
2979 wavelengths and to multi-centennial time scales, and 3) detection and understanding of
2980 terrestrial responses to solar irradiance variability for indirect assessment of the forcing.

2981 Following an historical overview, this section addresses the development and current status of
2982 these three primary topics, concluding with a summary of successes, uncertainties and
2983 challenges.

2984

2985

2986

2987 **8.1 Historical Overview**
2988
2989
2990 Solar photons at all wavelengths of the electromagnetic spectrum interact with the terrestrial
2991 system over a range of altitudes, via multiple processes that depend on the composition of
2992 Earth's land, atmosphere, ice and ocean. The processes couple radiatively, chemically and
2993 dynamically to distribute incoming solar energy from low to high latitudes and among different
2994 altitude regimes. Solar radiation is Earth's primary energy source, and pursuit of possible
2995 terrestrial influences of its variability has a long history. The discovery in 1843 of an 11-year
2996 cycle in the occurrence of dark sunspots on the Sun's surface initiated efforts to detect,
2997 understand and specify variability in solar radiative output and Earth's response that continue
2998 today (see e.g., reviews by Hoyt & Schatten, 1997; Gray et al., 2010; Lean 2017).
2999
3000
3001
3002
3003
3004
3005
3006
3007
3008
3009 From the mid 19th century until the late 20th century, correlations between solar indices such as
3010 sunspots and climate indices such as temperature afforded the primary evidence in support of a
3011 solar influence on climate. However, the phase and magnitude of correlations from individual
3012 sites sometimes differed from each other and during different epochs, making their significance
3013 difficult to establish. Moreover, the Sun's total irradiance was assumed to
3014 be invariant; solar-related changes at the level of 0.1% detected in a few decades of ground-
3015 based observations made in the early-to-mid 20th Century were attributed to changes in
3016 atmospheric transmission and speculated to be due to changes in ozone concentrations in
3017 response to the Sun's more variable ultraviolet radiation (Foukal, Mack & Vernazza, 1977).
3018 Sporadic balloon and rocket-borne measurements did detect variations in solar ultraviolet
3019 irradiance but with large uncertainties. Exploratory studies of the terrestrial impacts of solar
3020

3021 variability using physical models of climate and, independently, of ozone suggested that an
3022 increase in total solar irradiance of 2% was equivalent to doubling CO₂ concentrations
3023 (Wetherald & Manabe, 1975) and that a 30% increase in solar UV irradiance would increase
3024 total ozone by 5% (Penner & Chang, 1978).

3025

3026 Space-based observations of the Sun transformed knowledge of solar radiative forcing. They
3027 quantify unequivocal changes in the Sun's total irradiance over the past forty years (Fröhlich &
3028 Lean, 2004; Dudok de Wit et al., 2017) and characterize concurrent spectral irradiance changes
3029 at all wavelengths (Haberreiter et al., 2017). Models successfully simulate the observed
3030 irradiance changes in terms of the occurrence of dark sunspots and bright faculae on the solar
3031 disc (Fröhlich & Lean, 2004, Lean et al., 2005) and estimate solar radiative forcing during past
3032 millennia using solar activity proxies (Jungclaus et al., 2017; Matthes et al., 2017; Lean, 2018a).
3033 In 2015 NOAA implemented a Solar Irradiance Climate Data Record (CDR, Coddington et al.,
3034 2016) in support of multiple solar-terrestrial endeavors.

3035

3036 Space-based and expanded ground-based observations of Earth's surface and atmosphere
3037 provide compelling terrestrial evidence for solar radiative forcing (Gray et al., 2010; Liliensten
3038 et al., 2015; Lean, 2017). Solar signals are affirmed in surface and atmospheric temperature and
3039 ozone concentrations over multiple recent decades, providing a new framework for verification
3040 and interpretation of site-specific sun-climate paleo connections evident in multiple
3041 paleoclimate records, especially of hydrological variables (e.g., Haug et al., 2003; Antico &
3042 Torres, 2015). State-of-the-art physical general circulation climate models, such as those used in
3043 recent IPCC assessments, couple surface, atmosphere and ocean processes, include interactive

3044 ozone, and input spectral – not just total – irradiance. They indicate detectable responses to
3045 solar radiative forcing throughout the ocean, surface and atmosphere (Mitchell et al., 2015;
3046 Misios et al., 2015; Hood et al., 2015), as do statistical models of the direct observations (Lean
3047 & Rind, 2008; Lean 2017; Foster & Rahmstorf, 2011).

3048
3049
3050

3051 **8.2 Space-Based Observations of Solar Irradiance Variability**
3052
3053

3054 The launch into space of electrical substitution “active” cavity radiometers enabled the
3055 detection of real changes in total solar irradiance, beginning with the Hickey-Friedan
3056 radiometer on the Nimbus 7 satellite in November 1978 (Hickey et al., 1980). The radiometers
3057 compare solar radiant heating of a black cavity of known aperture area with equivalent
3058 electrical power. The Active Cavity Radiometer Irradiance Monitor (ACRIM) on the Solar
3059 Maximum Mission (SMM, 1980-1989), Upper Atmosphere Research Satellite (UARS, 1992-
3060 2005) and ACRIMSAT (1999-2013) comprised multiple cavities each with different solar
3061 exposure (Willson, 1979, 2014), thereby isolating real solar irradiance changes during the 11-
3062 year solar cycle from changes in radiometer sensitivity. Radiometers with different
3063 configurations of cavity geometry, surface coating, baffles and aperture placement continue to
3064 measure total solar irradiance on the Solar and Heliospheric Observatory (SOHO) since 1996
3065 (Fröhlich et al., 1995; Fröhlich, 2013), the Solar Radiation and Climate Experiment (SORCE)
3066 since 2003 (Kopp & Lawrence, 2005; Kopp & Lean, 2011) and on the International Space
3067 Station since 2018 (ISS, Richard et al., 2011). By virtue of advanced radiometric design and
3068 signal detection, etched cavity surface, extensive characterization and ground-based absolute
3069 calibration, the Total and Spectral Solar Irradiance Sensor (TSIS) on the International Space
3070 Station (ISS) is expected to measure total solar irradiance with <100 ppm uncertainty and 10
3071 ppm per year repeatability (Richard et al., 2011; Pilewskie et al., 2018).

3072

3073 Space-based observations show unequivocal total solar irradiance variability on time scales
3074 from days to decades as the sun rotates on its axis (every 27-days) and in concert with the 11-
3075 year activity cycle. Initial ACRIM observations readily detected the day-to-day variations

3076 (Willson et al., 1981; Hudson et al., 1982), with solar cycle changes subsequently established
3077 in the longer ACRIM dataset (Foukal & Lean, 1988). Total solar irradiance can decrease by a
3078 few tenths percent over a few days but the Sun is brighter overall when solar activity is higher,
3079 as indicated by higher sunspot numbers.

3080

3081 Figure 8.1 shows monthly mean values of sunspot numbers and total solar irradiance since
3082 1978 according to five different composite records constructed by cross-calibrating and
3083 combining multiple observations. The absolute value of total solar irradiance during the 2008
3084 solar minimum period is $1360.8 \pm 0.5 \text{ W m}^{-2}$ (Kopp & Lean, 2011) and the change in total
3085 solar irradiance, ΔTSI , of 1.3 W m^{-2} (0.1%) in solar cycles 22 (1986-1996) and cycle 23
3086 (1996-2008) produced decadal solar radiative forcing $\Delta F_S = 0.7\Delta TSI/4 = 0.23 \text{ W m}^{-2}$ (Hansen
3087 & Lacis, 1990). For comparison, radiative forcing by greenhouse gases over the five-year
3088 period of solar irradiance's increase from solar minimum to maximum is less than 0.25 W m^{-2} .
3089 Such forcing estimates assume full adjustment of terrestrial climate processes to a new
3090 "equilibrium" state.

3091

3092 Absolute solar spectral irradiance is less well specified observationally, especially at infrared
3093 wavelengths (Meftah et al., 2018), than is its integral, the total solar irradiance and spectral
3094 irradiance variability, which also depends (differently) on wavelength, is similarly less well
3095 specified observationally than is total solar irradiance variability. This is especially true over the
3096 solar cycle because drifts in spectral radiometer sensitivity during space operation can produce
3097

3098 measurement uncertainties that are larger than the magnitude of the solar cycle changes (Lean
3099 & DeLand, 2012; Mauceri et al., 2018). Conclusive detection of real spectral irradiance
3100 changes was achieved initially at ultraviolet wavelengths, where the relative changes are about
3101 an order of magnitude larger than at visible wavelengths. Spectroradiometers onboard the Solar
3102 Mesosphere Explorer (SME, 1980-1989), UARS (1992-2005) (Lean et al., 1997; Rottman,
3103 2006) and SORCE (2003-), as well as Solar Backscatter Ultraviolet (SBUV) instruments on
3104 multiple NASA and NOAA spacecraft (DeLand & Cebula, 1998) all record spectral irradiance
3105 variability at wavelengths less than 400 nm. The launch of SORCE in 2003 successfully
3106 extended the detection of solar spectral irradiance variability to visible and near infrared
3107 wavelengths (Rottman et al., 2005; Mauceri et al., 2018).

3108

3109 Figure 8.1 shows monthly mean variations in solar spectral irradiance in four broad wavelengths
3110 bands measured by SORCE since 2003 (green lines); 11-year cycle variability is in the range
3111 0.7% to 1.4% in the wavelength band 200-300 nm, 0.1% to 0.2% in the band 300-600 nm,
3112 0.06% to 0.1% in the band 600-900 nm and <0.05% in the band 900-1200 nm. Composite
3113 records of solar UV irradiance have been constructed by combining observations over multiple
3114 solar cycles (DeLand and Cebula, 2008; Haberreiter et al., 2017) but their repeatability is
3115 generally insufficient to reliably specify the magnitude of solar cycle variability because of
3116 instrument sensitivity drifts and the lack of overlap needed to cross calibrate spectroradiometers
3117 with different absolute scales. The exception is the H I Lyman \langle emission line whose variability
3118 has been constructed since 1947 (Woods et al., 2000); solar Lyman \langle irradiance (at 121.5+0.5
3119 nm) increased 3.5 mW m^{-2} (60%) in solar cycle 22 and 2.5 mW m^{-2} W m^{-2} (40%) in cycle 24
3120 (Snow et al., 2018).

3121

3122 **8.3 Modelling Solar Irradiance Variability**

3123

3124

3125

Climatological time scales, on which radiative forcing is typically defined, are considerably
3126 longer than the four-decades of space-based solar irradiance observations. Models that relate the
3127 observed irradiance variations to historical indices of solar activity are therefore necessary to
3128 reconstruct solar radiative forcing prior to 1978. The primary causes of solar irradiance
3129 variability are dark sunspots and bright faculae which respectively reduce and enhance the Sun's
3130 local radiative output (Foukal, 1981), by different amounts at different wavelengths (Unruh et
3131 al., 2000; Lean et al., 2005). Solar rotation imposes a 27-day cycle on solar irradiance by
3132 altering the heliographic locations of dark sunspots and bright faculae on the disk, and the
3133 growth, transport and decay of sunspots and faculae in response to a sub-surface solar dynamo
3134 generates 11-year irradiance cycles. Models that utilize indices of sunspot darkening and facular
3135 brightening reproduce the observed variations in total solar irradiance with high fidelity,
3136 including decreases up to a few tenths percent during solar rotation and cycle increases of 0.1%
3137 (Foukal & Lean, 1988, 1990; Fröhlich & Lean, 2004, Lean, 2017).

3138

3139

Examples of solar irradiance variability models are those of the Naval Research Laboratory
3140 (NRLTSI2, NRLSSI2, Lean et al, 2005), which the NOAA CDR utilizes to estimate present and
3141 historical irradiance variations (Coddington et al., 2016), and the Spectral and Total Irradiance
3142 Reconstructions (SATIRE, Krivova & Solanki, 2008; Krivova et al., 2010). The NRL models
3143 input a sunspot darkening function calculated from direct observations of sunspot areas and
3144 locations on the Sun's surface and the Mg irradiance index facular proxy; multiple regression

3145

3146 against observations determines the relative contributions of the two influences bolometrically
3147 and at individual wavelengths. The SATIRE model derives its two sunspot (dark sunspot umbra
3148 and penumbra) and two facular (bright faculae and network) inputs from solar magneto grams; a
3149 theoretical stellar atmosphere model specifies their wavelength-dependent contrasts relative to
3150 the background “quiet” Sun (Unruh et al., 2000).

3151

3152 To assess the fidelity of such models by comparisons with extant, albeit imperfect,
3153 observations, Figure 8.1 also shows monthly values of total solar irradiance and spectral
3154 irradiance in four broad wavelength bands according to the NRLSSI2 and SATIRE models.
3155 Figure 8.2 compares their total solar irradiance reconstructions over multiple solar cycles and
3156 corresponding spectral irradiance changes in selected epochs. Compared with the SATIRE
3157 model the NRL model has a negligible downward trend during recent cycle minima (e.g., from
3158 1986 to 2008 in Figure 8.1), somewhat smaller solar cycle increases at near ultraviolet
3159 wavelengths and larger increases at longer wavelengths. In solar cycle 23, for example (Figure
3160 8.2), irradiance from 300 to 400 nm increases 0.4 W m^{-2} in the NRLSSI2 model and 0.59 W
3161 m^{-2} in the SATIRE model while visible irradiance from 500 to 750 nm increases 0.42 W m^{-2}
3162 in the NRLSSI2 model and 0.35 W m^{-2} in the SATIRE model.

3163

3164 Reliable historical reconstructions of solar irradiance depend on the availability of suitable
3165 sunspot and facular indices and on understanding plausible irradiance variability mechanisms.
3166 The lack of sunspots on the Sun’s disk for several years during the Maunder Minimum (1645-
3167 1715) indicates anomalously low solar activity relative to the contemporary epoch (Eddy,
3168 1976). The possibility that solar irradiance was reduced during such periods relative to

3169 contemporary minima derives from the overall higher levels of ^{14}C in tree-rings and ^{10}Be in
3170 ice-cores (respectively) during the Spörer, Maunder and Dalton Minima. Cosmogenic isotope
3171 levels increase when solar activity decreases because the reduced solar magnetic flux in the
3172 heliosphere facilitates a great flux of galactic cosmic rays at Earth (McCracken et al., 2013).
3173 That cycles near 80, 210 and 2400 years manifest in cosmogenic isotope records of solar
3174 activity suggests the likelihood of similar periodicities in irradiance (e.g., Damon & Jirikowic,
3175 1992).

3176

3177 Initial estimates of the reduction in solar irradiance during the Maunder Minimum below
3178 contemporary solar minima considered two different scenarios (Lean et al., 1992; White et al.,
3179 1992). In one scenario total irradiance decreased 1.5 Wm^{-2} (about 0.1%) due to the
3180 disappearance of faculae; a second scenario estimated a larger decrease of 2.6 Wm^{-2} (about
3181 0.2%) because of an additional reduction in the background “quiet” Sun, inferred from the
3182 reduced emission in non-cycling Sun-like stars (assumed to be in states of suppressed activity
3183 similar to the Maunder Minimum) relative to overall higher emission in cycling stars. Questions
3184 about the applicability of Sun-like stars for solar variability made these initial estimates
3185 speculative (Foukal et al., 2004). Current estimates of the solar irradiance increase from the
3186 Maunder Minimum to the present derive from a model of the transport of magnetic flux on the
3187 Sun’s surface. The simulations suggest an increase of 0.5 Wm^{-2} (about 0.04%) in total solar
3188 irradiance at cycle minima over the past ~ 300 years, from the accumulation of magnetic flux
3189 during successive 11-year cycles of increasing strength (Wang et al., 2005). This estimate of
3190 long-term solar irradiance variability is a factor of five smaller than inferred from Sun-like stars
3191 (Lean et al., 2005, Table IV summarizes estimates of total solar irradiance reduction in the

3192 Maunder Minimum). Figure 8.2 shows reconstructions of total solar irradiance from 850 to
3193 2300 using the ^{14}C cosmogenic isotope record of Roth & Joos (2013), assuming a reduction in
3194 the Maunder Minimum of 0.5 Wm^{-2} . Figure 8.2 also shows spectral irradiance changes in the
3195 NRLSSI2 and SATIRE models from the Maunder Minimum to the present and to the Medieval
3196 Maximum.

3197

3198 Both the magnitude and temporal structure of longer-term irradiance changes remain uncertain.
3199 The only direct index of solar activity prior to 1882 is the sunspot number, which is undergoing
3200 renewed scrutiny and debate (Clette & Lefèvre, 2016; Kopp et al., 2016). The two historical
3201 irradiance reconstructions in Figure 8.2 differ notably prior to 1882 because of their different
3202 parameterizations of irradiance in terms of sunspot numbers and cosmogenic isotopes (Lean,
3203 2018a). The relationship between solar irradiance and cosmogenic isotopes is complex and
3204 poorly known, in part because the magnetic fields that produce sunspots and faculae at the
3205 Sun's surface are not the same as those that modulate galactic cosmic rays in the heliosphere
3206 (Lean et al., 2002). As well, distinctly different terrestrial processes produce cosmogenic
3207 archives in tree- rings and ice-cores (Delaygue & Bard, 2011; Steinhilber, et al., 2012; Roth &
3208 Joos, 2013).

3209
3210
3211

3212 **8.4 Climate Response to Solar Radiative Forcing**

3213

3214

3215 Just as the detection of terrestrial responses to solar activity initially signified the relevance of
3216 solar radiative forcing for understanding climate change, in lieu of direct observations of the
3217 forcing itself, so too does ongoing analyses of ever-lengthening terrestrial observations and
3218 newly extracted, high fidelity paleoclimate records continue to strengthen and expand the
3219 evidence. Using indicators such as sunspots and cosmogenic isotopes to identify times of high
3220 and low solar activity during the 11-, 80- and 210-year cycles, solar-related changes are
3221 identified in diverse climate parameters that range from low latitude drought and rainfall (e.g.,
3222 Verschuren et al., 2000; Neff et al., 2001; Haug et al., 2003; Antico & Torres, 2015), associated
3223 with Intertropical Convergence Zone displacement (Novello et al., 2016) and a La-Nina type
3224 response in the tropical Pacific (Mann et al., 2005), to mid-and high latitude ‘centers of action’
3225 (Christoforou & Hameed, 1997), storm tracks and winter intensity (e.g., Barriopedro et al., 2008;
3226 Mann et al., 2009; Lockwood et al., 2010), associated with the North Atlantic Oscillation and
3227 the circumpolar vortex.

3228

3229 On global scales, climate signals related to the 11-year solar cycle were detected first in basin-
3230 wide ocean temperatures (White et al., 1997) then in global lower tropospheric temperature
3231 (Michaels & Knappenberger, 2000). Observational temperature and ozone databases are now
3232 sufficiently long that statistical analyses readily isolate in them solar responses, both globally
3233 and regionally, from other concurrent influences (Douglass & Clader, 2002; Lean and Rind,
3234 2008; Foster & Rahmstorf, 2011). Figure 8.3 shows the solar cycle component, thus extracted,
3235 of $<0.1^{\circ}\text{C}$ in global surface temperature and <3 DU (1%) in total ozone compared with natural
3236

3237 (volcanic, ENSO, QBO) and anthropogenic (greenhouse gases and ozone depleting substances)
3238 components and Figure 8.4 shows the corresponding geographical response patterns. These
3239 estimates of climate's response to solar forcing are attained by linearly regressing indices of the
3240 simultaneous natural and anthropogenic influences against (de-seasonalized) monthly mean surface
3241 temperature (Figure 8.3a) and total ozone (Figure 8.3b) observations from 1979 to 2017 (Lean,
3242 2017, 2018b).

3243

3244 Time dependent simulations of climate's response to solar radiative forcing on climatological
3245 time scales became possible with the reconstruction of historical solar irradiance. Simulations
3246 using energy balance models initially suggested that the global surface temperature response to
3247 reconstructed solar irradiance cycles since 1874 (Foukal & Lean, 1990) was likely undetectable,
3248 the transient response of 0.03°C being notably smaller than the equilibrium response because of
3249 attenuation ($\sim 80\%$) by the thermal inertia of the ocean (Wigley & Raper, 1990). But subsequent
3250 analysis of historical surface temperature observations did detect a solar cycle response of
3251 0.06°C by statistically extracting the modelled spatial pattern of the response to the forcing
3252 (Stevens & North, 1996).

3253

3254 The first general circulation model simulations of climate's response to time-dependent solar
3255 radiative forcing found a global surface temperature increase of $\sim 0.5^{\circ}\text{C}$ since the Maunder
3256 Minimum (Cubasch et al., 1997; Rind et al., 1999). Decreased solar irradiance during the
3257 Spörer, Maunder and Dalton solar activity minima (Eddy, 1976) and enhanced volcanic activity
3258 are posited causes of anomalously cold surface temperatures from ~ 1300 to 1850, during the
3259 Little Ice Age (e.g., Mann et al., 2005, 2009). Even though the simulations input a factor of five
3260 – or more – larger increase in total solar irradiance (Lean et al., 1995) than current estimates

3261 (Wang et al., 2005), they nevertheless identified that water vapor feedbacks, cloud cover
3262 changes and land-sea contrasts contribute to the surface response to solar radiative forcing, with
3263 enhanced warming in sub-tropical regions similar to that forced by increasing greenhouse gas
3264 concentrations. The simulations further established that variations in solar irradiance were
3265 unlikely to be the primary cause of global warming in the postindustrial period, as some
3266 statistical correlations between solar cycle length and northern hemisphere temperature had
3267 suggested (Friis-Christensen & Lassen, 1991).

3268

3269 State-of-the-art general circulation models now include couplings between the land, ocean and
3270 atmosphere, functional middle atmospheres with ozone chemistry, and the ability to input
3271 realistic solar spectral irradiance changes. Analyses of ensembles of simulations made with
3272 various such models, designed to isolate responses of different terrestrial regimes to solar
3273 radiative forcing, demonstrate both a direct response of the land and ocean, dependent in part on
3274 the regional distribution of clouds, and an indirect response facilitated by stratospheric ozone
3275 and temperature changes (Rind et al., 2008; Meehl et al., 2009). Convective and dynamical
3276 processes disperse the forcing geographically and altitudinally, altering extant dynamical
3277 patterns such as the Hadley and Walker circulations and impacting, in particular, the
3278 hydrological cycle. IPCC's AR5 climate assessment included simulations made with 13 models
3279 that resolve the stratosphere (Mitchell et al., 2015), 6 of which include interactive ozone
3280 chemistry (Hood et al., 2015). Modeled responses to solar cycle irradiance changes are evident
3281 at the surface, in the ocean (Misios et al., 2015) and in the troposphere, stratosphere and ozone
3282 layer (Hood et al., 2015). While the simulated responses are generally of smaller magnitude
3283 than in observations (e.g., global mean surface warming of 0.07°C), the processes and patterns

3284 are qualitatively similar, including changes in precipitation and water vapor leading to weaker
3285 Walker circulation (Misios et al., 2015) and a stratosphere-related North Atlantic surface
3286 response (Mitchell et al., 2015).

3287

3288 Figure 8.4 compares statistically-extracted geographical patterns of the terrestrial response to
3289 solar radiative forcing with estimates made by a physical climate model (Rind et al., 2008).
3290 Differences between the physical and statistical model patterns suggest that deficiencies remain
3291 in one or both. Uncertainties in the hundreds of parameterizations that seek to account for the
3292 multiple integrated processes that heat the land and ocean, and redistribute this heat regionally
3293 and vertically, compromise physical model simulations. Statistical models suffer from
3294 uncertainties in the predictors and covariance among them (such as between solar and
3295 anthropogenic indices), including distinguishing whether covariance is physically based or
3296 random. The limited duration of the most reliable observations and indices exacerbate such
3297 uncertainties. Articulating and reconciling differences between the statistical and physical
3298 models is expected to improve understanding of process that facilitate terrestrial responses to
3299 solar radiative forcing, and may help improve physical model parameterizations of these
3300 processes. It is increasingly apparent that solar radiative forcing initiates a continuous spectrum
3301 of coupled interactions throughout Earth's land, ocean and atmosphere on multiple time scales
3302 with different and interrelated regional dependencies. Differential heating of the land and
3303 oceans, equator and poles, and surface and atmosphere drive these responses; the processes
3304 involved are those by which climate responds to other radiative forcings, including by
3305 increasing greenhouse gas concentrations, albeit with different, magnitude, timing and regional
3306 detail.

3307

3308 **8.5 Summary: Successes, Uncertainties, Challenges**

3309

3310 *Successes*

3311

3312 Both measurements and models have now established that solar irradiance varies at all
3313 wavelengths, with different magnitudes at different wavelengths. Total (spectrally integrated)
3314 solar irradiance increased $1.3+0.2 \text{ Wm}^{-2}$ (0.1%) in solar cycle 23 (1996-2008) producing radiative
3315 forcing of 0.22 Wm^{-2} . Spectrally, the energy change maximizes at 300-400 nm, which increased 0.4 W
3316 m^{-2} in solar cycle 23.

3317

3318 Solar irradiance variability is a result of the Sun's magnetic activity, which alters radiative
3319 output locally in dark sunspots and bright faculae. Models of the net, global influence of
3320 sunspots and faculae reproduce observed total solar irradiance variability with high fidelity on
3321 time scales of the Sun's 27-day rotation.

3322

3323 Observations and models of Earth's surface and atmospheric temperature and ozone amount
3324 indicate that terrestrial responses to solar radiative forcing have detectable magnitudes during
3325 the 11-year solar cycle. Global responses are $\sim 0.1^\circ\text{C}$ in surface temperature, $\sim 0.3^\circ\text{C}$ in lower
3326 stratospheric temperature and $\sim 3 \text{ DU}$ (1%) in total ozone; the response patterns are regionally
3327 inhomogeneous and differ from that of the incident solar radiative forcing. There is abundant
3328 terrestrial evidence in paleoclimate records and solar activity proxies for solar radiative forcing
3329 with cycles near 80 and 210 years, in addition to the 11-year cycle.

3330

3331 *Uncertainties*

3332

3333 Not yet known with the needed certainty is the magnitude of spectral irradiance changes in the
3334 solar cycle. This is because observations lack the long-term stability to establish this
3335 unequivocally and models disagree about the apportioning of the changes to near-UV versus
3336 visible-near IR wavelengths. Less certain still are the magnitudes of multi-decadal irradiance
3337 variations and their possible mechanisms. Yet to be proven is the assumption in historical
3338 reconstructions that solar irradiance varies on time scales longer than the 11-year activity
3339 cycle, and whether observations of Sun-like stars can provide useful estimates of the
3340 magnitude of this variability.

3341
3342 Physical processes that connect variations in solar irradiance and cosmogenic isotopes,
3343 including modulation by solar magnetic flux, the flow of galactic cosmic rays through the
3344 heliosphere and production of isotopes in terrestrial archives are conceptually established but
3345 not yet quantified with the needed certainty. Similarly, the terrestrial processes and model
3346 parameterizations thereof that facilitate the multiple pathways that transform solar radiative
3347 forcing to climate variability are generally recognized but their specifications require validation
3348 and improvement. This includes the deposition of incident solar in c) for total ozone and in d)
3349 for surface temperature spectral energy, direct chemical and dynamical responses to this
3350 forcing, and the modulation of extant circulation patterns throughout the integrated system.

3351

3352 *Challenges*

3353

3354

3355 The highest priority going forward is the continuous monitoring of solar irradiance with the
3356 highest possible accuracy and repeatability to extend the extant record of solar radiative
3357 forcing, exemplified by the launch in 2018 of the Total and Spectral Solar Irradiance Sensor
3358 (TSIS) on the International Space Station.

3359

3360 Differences among observed and modelled absolute irradiance and irradiance variations,
3361 require resolution, including the magnitude of inter-minima changes in the space era and the
3362 spectral dependence of the variability.

3363

3364 Physical climate models of the future are challenged to fully capture and parameterize the
3365 multiple pathways by which solar radiation enters and alters the integrated terrestrial
3366 environment, including under different conditions of other natural and anthropogenic forcings.
3367 The reconciliation of the magnitude, pattern and time lags of terrestrial responses to solar
3368 radiative forcing extracted statistically from observations with those calculated by physical
3369 models may aid the pursuit of this challenge.

3370

3371

3372

3373 **Figure captions**

3374

3375

3376 **8.1.** Shown are monthly means in the space era of a) sunspot numbers, b) total solar irradiance,
3377 TSI, and solar spectral irradiance in broad bands from c) 100-300 nm, d) 300-600 nm, e) 600-
3378 900 nm and f) 900-1200 nm. The five green lines in b) are composite records of TSI constructed
3379 from different combinations of observations. Also shown are estimates of the irradiance
3380 variations by two models, the NRLTSI2 and NRLSSI2 models (black lines) and the SATIRE
3381 model (orange lines).

3382

3383 **8.2.** Reconstructed historical and projected future variations in total solar irradiance are shown
3384 in a) from 850 to 2300 according to two different models, the NRLTSI2 model (black lines)
3385 and the SATIRE model (orange lines, recommended for use in PMIP4). Shown in b), c) and d)
3386 are the spectral irradiance changes for three selected periods, specifically solar cycle 23 (1996
3387 to 2009), the Maunder Minimum (1645–1715) to Modern Maximum (1950-2009) and the
3388 Maunder Minimum to the Medieval Maximum (1100-1250).

3389

3390

3391 **8.3.** Shown as the black lines are observed changes from 1979 to 2017 in a) monthly-averaged
3392 global surface temperature and b) monthly-averaged global total ozone. Also shown by the
3393 blue lines in a) and b) are the changes in the respective observations according to statistical
3394 models. The statistical models are constructed by using linear least squares regression of the
3395 observations against indices of the known sources of their variability. The relative
3396 contributions of the individual components to the observed changes are identified in the lower

3397 two panels; these include the El Niño southern oscillation (ENSO), quasi biennial oscillations
3398 (QBO), volcanic aerosols, the solar irradiance cycle, changes in the concentrations of
3399 anthropogenic greenhouse gases (GHG) and the effective equivalent stratospheric chlorine
3400 (EESC) of ozone-depleting substances (adapted from Lean, 2017, 2018b).

3401

3402 **8.4.** Shown in the top image is the annually averaged relative distribution of received solar
3403 radiation at Earth. The regional patterns of terrestrial responses to changes in solar radiation
3404 during the 11-year cycle, statistically extracted from observations (Lean, 2017, 2018b), are
3405 shown in a) for total ozone and in b) for surface temperature. For comparison, the terrestrial
3406 responses to the solar cycle simulated by a general circulation model (GISS Model 3; Rind et
3407 al., 2008) are shown.

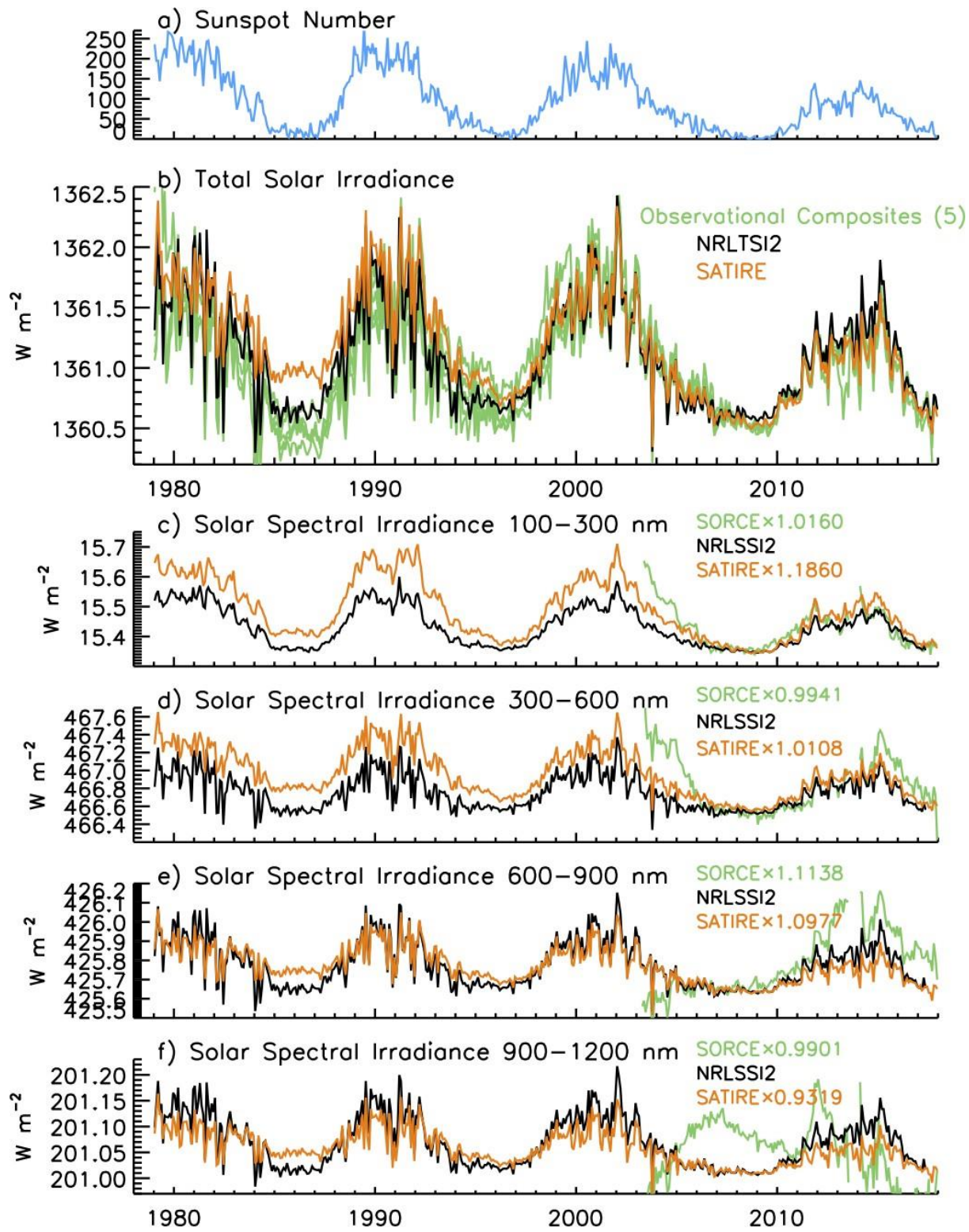
3408

3409

3410

3411

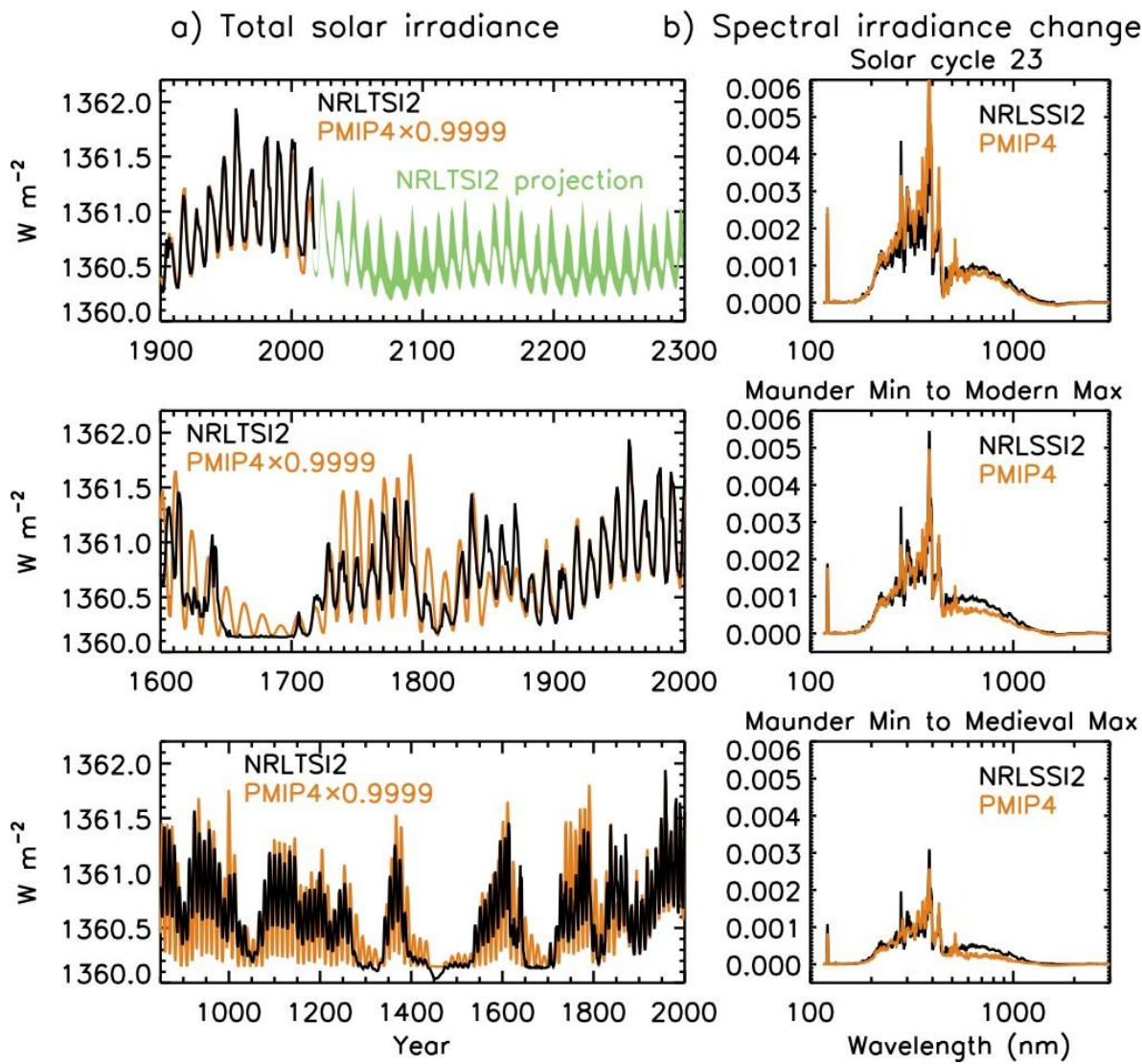
3412 **Figure 8.1**
3413



3414
3415

3416
3417
3418
3419

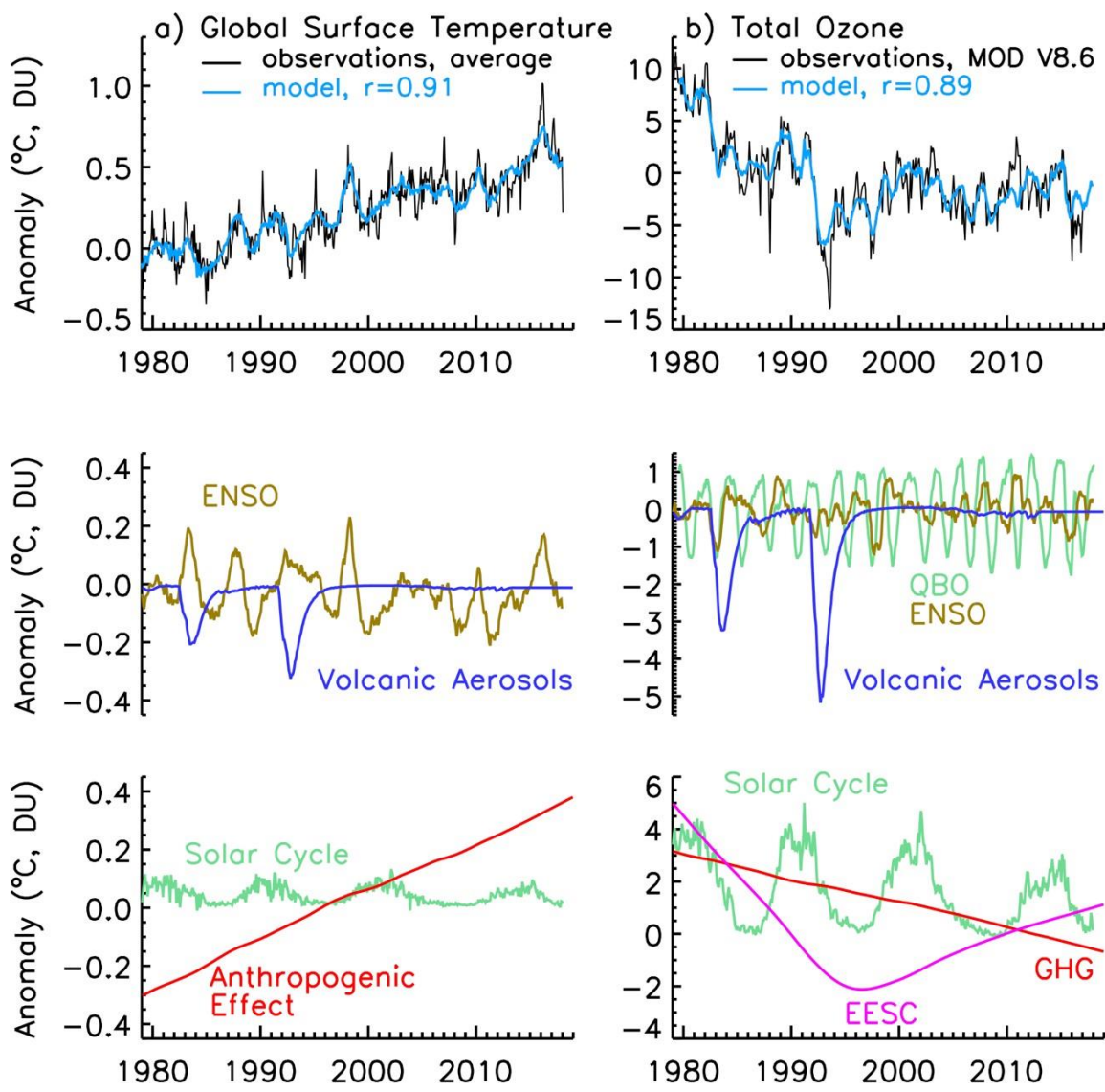
Figure 8.2



3420
3421

3422 **Figure 8.3**

3423



3424

3425

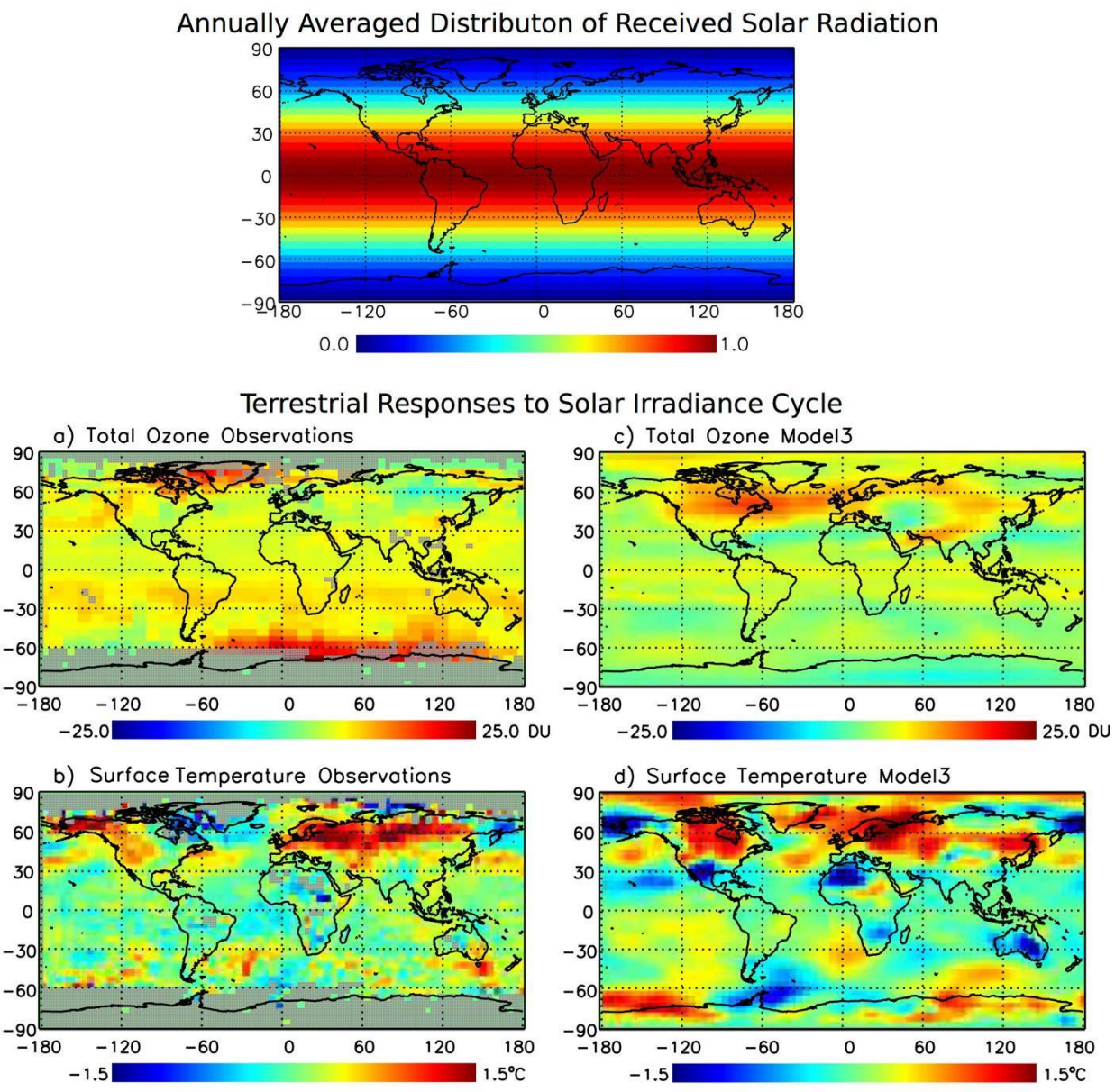
3426

3427

3428

3429
3430

Figure 8.4



3431
3432
3433
3434
3435

3436

3437 **9. Stratospheric Aerosols**

3438

3439

3440 **9.1 Introduction**

3441

3442 An important discovery of the 20th century is that some amount of submicron sulfate
3443 particles are permanently present in the stratosphere perturbing the Earth's radiative balance,
3444 climate, and weather (Junge et al., 1961; Turco et al., 1982; Pueschel, 1996; Hamill et al.,
3445 1997). The abundance of stratospheric aerosols greatly increases after explosive volcanic
3446 eruptions that inject materials directly in the stratosphere. The tremendous success in
3447 observations and theoretical understanding of stratospheric aerosols achieved during recent
3448 decades is briefly reviewed in this Section.

3449

3450 Volcanic hazards have been documented since antiquity. Pompeii in the ancient Roman
3451 Empire was destroyed by the eruption of Vesuvius in 79 AD (Zeilinga de Boer and Sanders,
3452 2002). Plutarch mentioned that the Etna eruption in 44 B.C. dimmed the Sun and killed the
3453 crops causing famine in Rome and Egypt (Forsyth, 1988). The systematic compilation of
3454 active volcanoes and past volcanic eruptions started in the mid-nineteenth century (Scope,
3455 1862). Coming to the present times, there is now available a comprehensive database of
3456 active volcanoes (Simkin et al, 1981; Simkin, 1993).

3457

3458 It was long suspected that explosive volcanic eruptions affect the weather, climate, and
3459 human health through the injection into the atmosphere of large amounts of solid particles
3460 (i.e., volcanic ash) and gases (Coakley, 1981; Robock, 2000; Timmreck, 2012; Stenchikov,
3461 2016). Benjamin Franklin, then a US ambassador to the court of Louis XVI, related the 1783

3462 Laki eruption in Iceland with the dry fog and anomalously cold weather in Europe (Franklin,
3463 1784). Grattan et al. (1998) found an increase in mortality caused by the Laki's plume. Sereno
3464 Bishop was the first who described the diffuse halo that forms around the sun due to the
3465 optical effect of volcanic aerosols (now called Bishop's ring) after the eruption of Krakatau
3466 in Indonesia in 1883. Much later Humphreys (1913, 1940) correctly pointed out the radiative
3467 effect of volcanic aerosols as a physical cause of volcanically-induced cold weather.

3468
3469
3470

3471

3472 **9.2 Origin of Stratospheric Aerosols**

3473

3474

3475 During the sufficiently prolonged volcanically quiescent periods, stratospheric aerosols do
3476 not disappear but reduce to background levels. Gruner and Kleiner (1927) first suggested the
3477 existence of a persistent non-volcanic aerosol layer in the stratosphere. It was instrumentally
3478 confirmed in 1961 (Junge et al., 1961; Junge and Manson, 1961) 59 years after the
3479 stratosphere itself was documented by a pioneering balloonist Leon Tisserenc de Bort in 1902
3480 (Greene, 2000). Currently, the stratospheric aerosol layer is often referred to as Junge layer
3481 both for volcanically quiescent and active periods, although the aerosol abundance, vertical
3482 extent, and horizontal spread drastically change after an explosive volcanic eruption.

3483

3484 In the volcanically quiescent periods, the background Junge layer height varies around 20 km
3485 and is modulated by the quasi-biennial oscillation (QBO). The aerosol abundance is
3486 maintained by the mostly tropical cross-tropopause transport (Fueglistaler et al., 2009) of
3487 sulfur-containing gases, carbonyl sulphide (OCS) (Crutzen, 1976) and SO₂ (Bruhl et al.,
3488 2012; Sheng et al., 2015), as well as aerosols of natural and anthropogenic origin (Brock et
3489 al., 1995). Deep convective cells could also overshoot tropospheric materials into the
3490 stratosphere (Stenchikov et al., 1996). The much-debated contribution of anthropogenic sulfur
3491 from highly polluted East Asia is found to be of minor importance (Deshler et al., 2006;
3492 Vernier et al., 2011; Thompson and Peter, 2006). This is consistent with the observation
3493 that despite the increase in anthropogenic emissions there is no measurable long-term trend
3494 in background aerosols (Deshler et al., 2006; Vernier et al., 2011; Thomson and Peter, 2006)
3495 during 1970-2005. The estimated total net flux of sulfur into the stratosphere is about 180

3496 GgS/year but this figure has an uncertainty of at least 50% (Thompson and Peter, 2006;
3497 Kremser et al., 2016). The input of other aerosols, meteoric from the middle atmosphere,
3498 organic from troposphere, and mixed from air traffic and rocket exhaust, is little by mass but
3499 may affect aerosol microphysics (Turco et al., 1982; Bardeen et al., 2008; Kremser et al., 2016;
3500 Gomez Martin et al., 2017).

3501

3502 The diameters of background aerosol particles range from 10 to 100 nm and their total
3503 optical depth is of the order of 0.001 in visible (Vernier et al., 2011) resulting in radiative
3504 forcing (compared to zero concentrations) of about -0.01 to -0.05 W/m². So, although
3505 background stratospheric aerosols are important indicators of the stratosphere-troposphere
3506 chemical exchange and chemical processes in the stratosphere itself, their radiative effect is
3507 relatively small, but not completely negligible. Note that radiative forcing in the present
3508 paper is with reference to preindustrial times when there was likely a small but non-zero
3509 background concentration.

3510 However, the pure background Junge layer is rarely observed as it is frequently perturbed by
3511 explosive volcanic eruptions that directly inject into the lower stratosphere volcanic ash,
3512 sulfur-containing gases, mostly SO₂ and H₂S, water vapor, CO₂, halogens, nitrogen (N₂),
3513 and other species. After such emissions the thermal and chemical relaxation of the
3514 stratosphere to background level takes 7-8 years (Brasseur and Granier, 1992; Thomason and
3515 Peter, 2006). So during the observation period that started in the 1970s there are only a few
3516 time-windows when the background Junge layer could be sampled.

3517

3518

3519

3520 Volcanic ash particles, mainly re-condensed silicates, usually exceed 2 μm in diameter.
3521 Although ash immediately after eruption develops a measurable radiative forcing, it does not
3522 produce a long- term climate effect as it gravitationally deposits in an about a week or two.
3523 The finest ash particles might be present in the stratosphere for a few months but their
3524 radiative effect is negligible (Niemeier et al., 2009; Guo et al., 2004a, 2004b).

3525

3526

3527 The model studies suggest that the aerosol plume from a strong equatorial volcanic eruption
3528 could heat the tropical tropopause layer (TTL) facilitating the tropospheric water vapor
3529 penetration into the stratosphere (Joshi and Shine, 2003; Robock et al., 2009; Löffler et al.,
3530 2016). The heating of the TTL after volcanic eruptions appears challenging to detect in
3531 observations even for the most recent strong eruption of Mt. Pinatubo (Fueglistaler et al.,
3532 2013; Randel et al., 2004; Chiou et al., 2006). This is because the TTL temperature and
3533 water vapor flux into the stratosphere are also affected by QBO, El Nino Southern
3534 Oscillation (ENSO), and the strength of the Brewer-Dobson Circulation. Dessler et al.
3535 (2014) used multiple regression analysis to account for all those factors and have shown the
3536 increase of the water vapor mixing ratio in the air entering the tropical stratosphere both for
3537 El Chichon and Pinatubo eruptions.

3538

3539

3540

3541 Volcanic SO₂ and H₂S are oxidized in the stratosphere by a photochemically produced
3542 hydroxyl radical to form sulfate aerosols with a characteristic conversion time of about one
3543 month (Bluth et al., 1992, 1993; Read et al., 1993), although, this rate could vary at different
3544 stages of the process (LeGrande et al., 2016). Initially, aerosol particles are formed due to
3545 binary nucleation of sulfuric acid and water vapor and are subject to coagulation and
3546 diffusional growth as well as gravitational settling (Turco et al., 1982; Pueschel, 1996;
3547 Hamill et al., 1997). They exert substantial perturbation of the radiative energy budget of the
3548 planet (Lambert et al., 1993; Baran and Foot, 1994; Minnis et al., 1993; Barns and Hoffman,
3549 1997; Lacis et al., 1992; Stenchikov et al., 1998).

3550

3551 Volcanic aerosols are dispersed in the stratosphere by wave-driven Brewer-Dobson
3552 circulation (Holton et al., 1995) modulated by the QBO phase (Trepte and Hitchman, 1992)
3553 to be deposited at high latitudes. The stratospheric e-folding residence time of equatorial
3554 injections with respect to Brewer-Dobson transport is about two years (Hamill et al., 1997).
3555 The lifetime of high-latitude volcanic injections is somewhat shorter than the low-latitude
3556 ones because of proximity to a pole and absence of the slowly emptying aerosol equatorial
3557 reservoir blocked by the subtropical barrier (Oman et al., 2006b). For large eruptions,
3558 gravitational settling of quickly growing sulfate particles intensifies aerosol removal
3559 restricting the magnitude of the climate impact of super-eruptions (Pinto et al., 1989;
3560 Timmreck et al., 2010). Volcanic aerosols deposited to Antarctica and/or Greenland snow
3561 affect the chemical composition of ice, thus recording the history of the Earth's volcanism
3562 for thousands of years (Zielinski, 2000; Cole-Dai, 2010).

3563
3564

3565

3566 **9.3 Observations Of Stratospheric Aerosols**

3567

3568

3569

3570 The first generation of aerosol viewing instruments provided invaluable empirical
3571 knowledge about stratospheric loadings and optical properties, however, with some
3572 significant gaps in space and time (Deshler, 2008; Deshler et al., 2003; Hofmann et al., 1975;
3573 Baumgardner et al., 1992; Borrmann et al., 2000; Fiocco and Grams, 1964; Stothers, 1996;
3574 1997; 2001a, 2001b; Krueger et al., 2000; Carn et al., 2003; McCormick et al., 1987;
3575 Antuña et al., 2003; Thomason and Taha, 2003; Randall et al., 2000; 2001). Thomson and
3576 Peter (2006) and Kremser et al. (2016) overview extensively the available observations.

3577

3578 The recognized deficiency of existing observations is that aerosol size distribution, which
3579 affects both aerosol optical characteristics and sedimentation velocities, suffers from
3580 significant retrieval uncertainties (Kremser et al., 2016; Bingen et al., 2004a, 2004b;
3581 Bourassa et al., 2008; Malinina et al., 2018). During the recent decade, a new generation of
3582 instruments for monitoring aerosols and precursor gases has emerged. Among them are the
3583 Michelson Interferometer for Passive Atmospheric Sounding (MIPAS), Ozone Mapping
3584 Profiler Suite (OMPS), Ozone Monitoring Instrument (OMI), InfraRed Atmospheric
3585 Sounding Interferometer (IASI), Cloud-Aerosol Lidar and Infrared Pathfinder Satellite
3586 Observations (CALIPSO), Cloud-Aerosol Transport System (CATS), Optical Spectrograph
3587 and InfraRed Imager System (OSIRIS), SCanning Imaging Absorption SpectroMeter for
3588 Atmospheric CHartographY (SCIAMACHY). OMI and OMPS continue the Total Ozone

3589 mapping Spectrometer (TOMS) measurement record providing SO₂ loadings used to
3590 document the global volcanic degassing (Carn et al., 2016). MIPAS sees the
3591
3592 vertically resolved SO₂ and aerosol volume (Hopfner et al., 2013; 2015). The vertically
3593 resolved aerosol extinctions are detected by the limb profiling SCHIAMACHY (Burrows et
3594 al., 1995; Bovensmann et al., 1999; von Savigny et al., 2015), OSIRIS (Bourassa et al.,
3595 2007), and Lidar instruments, CATS (Yorks et al., 2015) and CALIOP (Vernier et al.,
3596 2009). The new limb-scattering instruments observe aerosol plume more frequently than
3597 those based on the solar occultation technique and allow reliably retrieve more parameters
3598 of aerosol Particle Size Distribution (PSD) then were possible in the past (Malinina et al.,
3599 2018). For the forcing calculations, it is important to smoothly merge the past and current
3600 aerosol observations to produce seamless datasets of stratospheric aerosol parameters for an
3601 extended period of time (Thomason et al., 2018).

3602
3603
3604

3605

3606 **9.4 Radiative Forcing Of Stratospheric Aerosols**

3607

3608

3609

3610 Stratospheric aerosols, both volcanic and background, scatter the incoming shortwave
3611 radiation depleting the direct and enhancing the diffuse downward solar fluxes; they also
3612 absorb shortwave near infrared, and absorb and emit outgoing terrestrial radiation. The
3613 cumulative radiative effect of stratospheric aerosols is to cool the Earth's surface and heat
3614 the aerosol layer in the lower stratosphere.

3615

3616 Volcanic eruptions that have historically exerted the strongest radiative forcing, have i)
3617 significant SO₂/H₂S injected into the stratosphere (although there is growing evidence of
3618 non-linearity of injections strength and radiative forcing (e.g. Niemeier and Tilmes, 2017) ,
3619 ii) tend to occur in tropical regions where both hemispheres of the globe are impacted by the
3620 subsequent perturbation to the aerosol optical depth and iii) inject SO₂ to sufficiently high
3621 altitudes within the stratosphere (e.g. Jones et al., 2017).

3622

3623 The large perturbations of the Earth's radiative balance caused by explosive volcanic
3624 eruptions e.g., Pinatubo, are discernible in observations; however, this does not lend itself
3625 readily to quantifying their actual radiative forcing (Dutton and Christy, 1992; Minnis et al.,
3626 1993; Russell et al., 1993). The theoretical calculations of the radiative forcing of
3627 stratospheric aerosols were first attempted using conceptual models (Lacis et al., 1992;
3628 Harshvardhan, 1979; Toon and Pollack, 1976). Because aerosol microphysical and optical

3629 characteristics, which have to be compiled from observations or calculated within the
3630 model, are the major input into the radiative forcing calculations, we discuss both these
3631 aspects together here.

3632

3633 The first generation of the atmospheric general circulation models simulated the impact of
3634 volcanic aerosols using simplified approaches, i.e., assuming a reduction of the solar
3635 constant, increase of planetary albedo, or representing stratospheric aerosols by a single
3636 reflecting layer (e.g., Broccoli et al., 2003; Soden et al., 2002).

3637

3638 The existing aerosol observations were used to build the global aerosol datasets with pre-
3639 calculated aerosol optical/microphysical characteristics that could be implemented in
3640 climate models (Stenchikov et al., 1998; Stenchikov, 2016; Ramachandran et al., 2000; Sato
3641 et al., 1993; Hansen et al., 2002; Schmidt et al., 2011; Tett et al., 2002; Ammann et al.,
3642 2003). One approach is to use the observed/reconstructed aerosol optical depth (usually in
3643 visible) and assume aerosol composition and size distribution to calculate aerosol extinction,
3644 single scattering albedo, and asymmetry parameter required for radiative transfer models as
3645 input (Stenchikov et al., 1998; Sato et al., 1993). Another approach uses the empirical
3646 estimates of SO₂ emissions and a simplified model to distribute them globally and to obtain
3647 the aerosol optical parameters (Ammann et al., 2003; Gao et al., 2008). Ammann et al.
3648 (2003) and Sato et al. (1993) datasets have essentially provided the bases for

3649

3650 implementing volcanic aerosols in virtually all of the climate models that have performed the
3651 20th-century climate integrations within IPCC AR4 (Stenchikov et al., 2006; Forster et al.,
3652 2007).

3653

3654 For the IPCC AR5 and CMIP6, the improved “gap-filled” SAGE II Version 6 aerosol
3655 product from (Thomason and Peter, 2006) was employed (Arfeuille et al., 2013; Zanchettin
3656 et al., 2016). All three stratospheric optical depths (SATO, AMMAN, and CMIP6) in Figure
3657 9.1 vary by about 30%, with Amman’s optical depth being the largest and CMIP6 being the
3658 smallest.

3659

3660 Figure 9.2 and 9.3 compare the all-sky shortwave (SW), longwave (LW), and SW+LW
3661 instantaneous radiative forcing at the top of the atmosphere and perturbations of heating rates
3662 calculated using SATO and CMIP6 inputs within the GFDL CM2.1 (Delworth et al., 2006)
3663 employing a double radiation call. To calculate optical characteristics of stratospheric
3664 aerosols for the SATO case, it was assumed that the aerosol has lognormal distribution with
3665 the time-and-latitude-varying effective radii and a fixed geometric width of 1.8 μm
3666 (SATO1.8) or 2.0 μm (SATO2). Despite the differences in the input information and
3667 assumptions, the changes in total radiative balance for the three datasets appear to be quite
3668 close. Both SATO’s datasets slightly overestimate the SW radiative forcing in comparison
3669 with (Minnis et al. 1993). The CMIP6 heating rates appear to be higher than expected
3670 (Stenchikov et al., 1998) and shifted toward the SW heating. Typical stratospheric sulfate
3671 particles absorb SW radiation only in near-IR starting

3672

3673 from 2.5 μm where solar flux is weak. This is why LW heating is expected to prevail
3674 contributing about 70% of the effect (Stenchikov et al., 1998). The stratospheric heating is
3675 important, as it controls stratospheric dynamic responses (Ramaswamy et al., 2006).

3676

3677 The complexity of radiative, microphysical, and transport processes forced by volcanic
3678 aerosols suggests that it is important to calculate aerosol radiative effects interactively with
3679 the aerosol plume development rather than use a pre-calculated set of aerosol optical
3680 parameters. To accomplish this, it is necessary to know the SO₂ volcanic emissions (Krueger
3681 et al., 2000; Hopfner et al., 2013; 2015) and be able to calculate development, transport, and
3682 decay of a volcanic aerosol layer.

3683

3684 The “bulk” aerosol models calculate SO₂ to H₂SO₄ conversion and transport their bulk
3685 concentrations. Sulfate aerosols are assumed to form instantaneously with the prescribed size
3686 distribution (Timmreck et al., 1999; Oman et al., 2006a; and Aquila et al., 2012) that defines
3687 aerosol optical properties and deposition rates. Modal aerosol models keep track of
3688 aerosol number-density approximating the aerosol size distribution by a few log-normal
3689 modes with the prescribed width and varying modal radii, accounting for coagulation,
3690 condensation growth, and size-dependent gravitational settling (Niemeier et al., 2009; Bruhl
3691 et al., 2015; Dhomze et al., 2014; LeGrande et al., 2016; Sekiya et al., 2016). The aerosol
3692 sectional microphysical models are the most accurate but computationally more demanding
3693 (English et al., 2013; Mills et al., 2016).

3694

3695

3696 There are still significant discrepancies between models, and between the models and
3697 observations. This remains a challenging issue. The 1991 Pinatubo case-study is an important
3698 testbed where different approaches have been compared and could be further investigated.
3699 For example, in (Bruhl et al., 2015) the aerosol optical depth relaxes too fast, but in (Mills et
3700 al., 2016) the stratospheric aerosol plume decays too slowly and the initial SO₂ loading has
3701 to be decreased by almost a factor of two to make the results consistent with observations.

3702

3703 **9.5 Small Volcanoes, Climate Hiatus, and Geoengineering Analogs**

3704

3705 The slowing of global warming, or climate hiatus, in 2000-2013, despite continued emission
3706 of greenhouse gases, attracted widespread attention (Meehl et al., 2011; Myhre et al., 2013).
3707 Many mechanisms were suggested as causal factors. These included natural variability
3708 associated with increased ocean heat uptake (Balmaseda et al., 2013) and cooling forced by
3709 small volcanic eruptions (Fyfe et al., 2013; Haywood et al., 2014; Santer et al., 2014;
3710 Solomon et al., 2011). The latter refers to eruptions of Kasatochi in August of 2008,
3711 Sarychev in June 2009, and Nabro in June 2011. They were the most significant recent
3712 events, however, 15-20 times weaker in terms of SO₂ injection than for the Pinatubo
3713 eruption. The estimated global mean surface temperature perturbations that they could cause
3714 range from 0.02 K to 0.07 K (Haywood et al., 2014; Santer et al., 2014). However,
3715 Andersson et al. (2014) reported that about 30% of aerosols from these small
3716 volcanoes were retained in the lowermost stratosphere and their total optical depth was
3717 underestimated in observations.

3718

3719 The deliberate injection of aerosols and aerosol precursors in the lower stratosphere
3720 suggested to reduce greenhouse warming (Crutzen, 2006; Wigley, 2006; Govindasamy and
3721 Caldeira, 2000; Robock et al., 2010; Heckendorn et al., 2009) is discussed in detail in
3722 Section 17. The associated processes have much in common with the effects of volcanic
3723 aerosols. Therefore the understanding of all aspects of stratospheric aerosols and climate links,
3724 which we gain from investigating the climate consequences of volcanic eruptions, is important for a
3725 feasibility assessment of solar management schemes (Pitari et al., 2014; Tilmes et al., 2009; Aquila

3726 et al., 2014; Haywood et al, 2013; Aquila et al., 2012; Kravitz et al., 2013; Tilmes et al.,
3727 2013).

3728

3729 **9.6 Dynamic and Thermal Responses To Volcanic Eruptions**

3730

3731 Improvements in our understanding of volcanic forcing help to better understand past climate
3732 and make a better climate prediction. It also enables the radiative forcing and accompanying
3733 transient response due to volcanic aerosols to be placed in perspective, relative to the forcing
3734 and responses due to the increases in the anthropogenic well-mixed greenhouse gas emissions.
3735 Since 1850 volcanic forcing has offset the ocean heat content increase due to the global-mean
3736 warming by about 30% (Delworth et al. 2005). Comparison of simulated and observed climate
3737 responses to the major volcanic eruptions helps to evaluate volcanic forcing itself. The
3738 relatively large transient forcing by volcanic aerosols offers a platform to test climate model
3739 simulations of stratospheric and surface temperature perturbations against observations.

3740 The net radiative effects of volcanic aerosols on the thermal and hydrologic balance (e.g.,
3741 surface temperature and moisture) have been highlighted in (Kirchner et al., 1999; Free and
3742 Angell, 2002; Jones et al., 2004; Trenberth and Dai, 2007). Atmospheric temperature after
3743 volcanic eruptions relaxes for 7-10 years, while the deep ocean retains a thermal perturbation
3744 for about a century (Stenchikov et al., 2009; Delworth et al., 2005). Gregory et al. (2013)
3745 indicated the importance of the pre-industrial volcanic forcing to predict future climate
3746 correctly. The prolonged volcanic activity could be a reason for a long-term climate cooling as
3747 it had arguably happened during the medieval Little Ice Age in 1300-1850 (Free and Robock,
3748 1999) when in the middle of this period the cooling was enhanced by the Maunder Minimum
3749 in Solar Irradiance (Eddy, 1976).

3750

3751 In addition, the differential heating/cooling due to volcanic aerosols affect atmospheric
3752 circulation. It is believed these circulation responses could cause a positive phase of the
3753 Arctic oscillation and winter warming in high northern latitudes (Ramaswamy et al., 2006;
3754 Shindell et al., 2003, 2004; Stenchikov et al., 2002, 2004, 2006; Perlwitz and Graf, 2001;
3755 Toohey et al., 2014;), prolong or even initiate El Nino (Adams et al., 2003; Pausata et al.,
3756 2015; Predybaylo et al., 2017; McGregor et al., 2011; Ohba et al., 2013), or damp monsoon
3757 circulations (Trenberth and Dai, 2007; Anchukaitis et al., 2010; Iles et al., 2013; Schneider et
3758 al., 2009). There are still large discrepancies between the models on the magnitude and the
3759 leading mechanism that forces those dynamic responses, and observations are not long
3760 enough to provide empirical proof of a concept. E.g., (Polvani et al., 2019) argued that the
3761 positive phase of Arctic Oscillation in winter of 1991/1992 was not casually forced by the
3762 1991 Pinatubo eruption, as it was not associated with the strong northern polar vortex.
3763 However, one has to take precaution making a far-reaching conclusion from their analysis as
3764 the authors only considered one volcanic winter that does not exhibit a statistically
3765 significant climate signal.

3766

3767 One robust finding in terms of dynamical response to high latitude eruptions that
3768 preferentially load one hemisphere relative to the other, is that tropical precipitation
3769 associated with the Inter-Tropical Convergence Zone is shifted towards the unperturbed
3770 hemisphere in both observations and global climate models (Oman et al., 2006 Haywood et al.,
3771 2013). Thus, significant high latitude eruptions in the northern hemisphere (e.g., Katmai which
3772 erupted in 1913) can lead to drought in sub-Saharan Africa and cause the North Atlantic
3773 hurricane frequency to dramatically reduce in years subsequent to the eruptions (Evan, 2012;

3774 Jones et al., 2017). These impacts are relatively well understood from theoretical constraints
3775 on cross equatorial energy and moisture transport (e.g. Bischoff and Schneider, 2014; 2016).
3776 Equatorial eruptions also can affect the position of African rain-belt by the combined effect
3777 of the preferential hemispheric summer cooling and damping of Indian Monsoon (Dogar et
3778 al., 2017).

3779
3780
3781
3782

3783 Stratospheric aerosols exert a substantial, albeit transient, impact on climate after the Junge
3784 layer is replenished by strong volcanic injections. For the equatorial eruptions, the radiative
3785 forcing peaks in about a half a year after a volcanic explosion and relaxes with the e-folding
3786 time of one-two years. For the high-latitude eruptions, the e-folding time is shorter than for
3787 tropical ones. Despite the transient nature of the volcanic forcing, the global ocean integrates
3788 the cooling from multiple eruptions extending the climate response to decades and even
3789 centuries (Delworth et al., 2005; Stenchikov et al., 2009).

3790

3791 Our understanding of the effect of stratospheric aerosols has grown substantially over the last
3792 century, from descriptive and intuitive knowledge base to the full-scale first-principle
3793 modeling supported by ground-based and satellite observations. Despite this progress, the
3794 error bars in volcanic radiative forcing probably remain larger than 20-30%. Because we
3795 have a limited ability to reconstruct volcanic forcing in the past, it is extremely important to
3796 further develop models that could interactively simulate volcanic plume development and its
3797 radiative effect. The best models so far demonstrate a sizable discrepancy with available

3798 observations that also may bear a significant uncertainty. One important bottle-neck is
3799 aerosol particle size distribution that is controlled by fine-scale microphysical processes.
3800 Particle sizes are important as they define both radiative effects of aerosols and their
3801 lifetime with respect to gravitational settling. The accumulation of the effect of small
3802 volcanic eruptions has to be better understood as it contradicts the expectation of a smaller
3803 lifetime of above-tropopause emissions. The pre-calculated, based on observations, aerosol
3804 datasets have their value in helping to better calibrate simulated climate
3805 responses to volcanic forcing.

3806
3807 It is important to consider radiative forcing and climate responses in combination, as this
3808 gives important feedback on how well a model reproduces the observed climate variations.
3809 The climate models are capable of calculating the thermodynamic responses to the volcanic
3810 aerosols forcing, but fail to consistently reproduce the circulation anomalies forced by
3811 volcanic eruptions. Further development of model capabilities and stratospheric aerosol
3812 monitoring are necessary to reduce uncertainties in past and future climate simulations

3813
3814
3815

3816

3817 **Figure captions**

3818

3819 **Figure 9.1**

3820 Global mean optical depth of stratospheric sulfate aerosols for 0.55 μm calculated using
3821 CMIP6, Sato et al. (1993) with (Schmidt et al., 2011) corrections, and Amman et al.
3822 (2003) data sets

3823

3824 **Figure 9.2.**

3825 Global mean radiative forcing (clear-sky and all-sky) at top of the atmosphere after the
3826 1991 Pinatubo eruption as a function of time calculated using different volcanic aerosol
3827 datasets

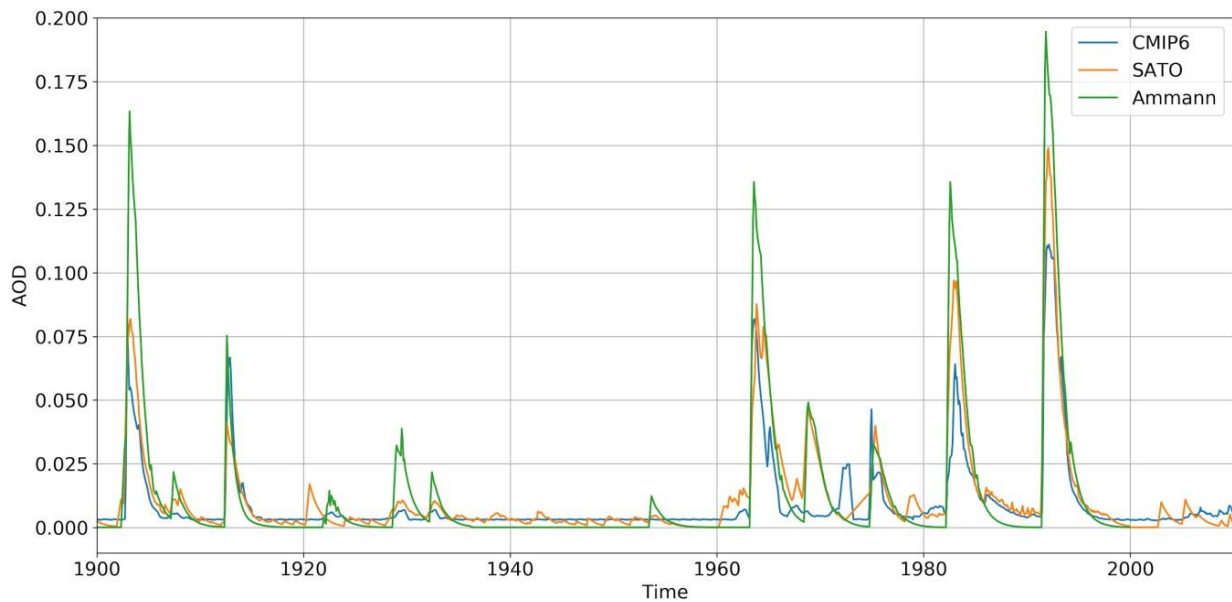
3828

3829 **Figure 9.3.**

3830 Zonal mean SW (top row) and LW (bottom row) Heating Rates after the 1991 Pinatubo
3831 eruption calculated using CMIP6 (left column), Sato1.8 (middle column), and Sato2
3832 (right column) datasets averaged over the equatorial belt of 5S-5N as a function of time
3833 and pressure.

3834

3835



3836
3837
3838
3839
3840
3841
3842
3843
3844
3845
3846
3847
3848
3849
3850
3851

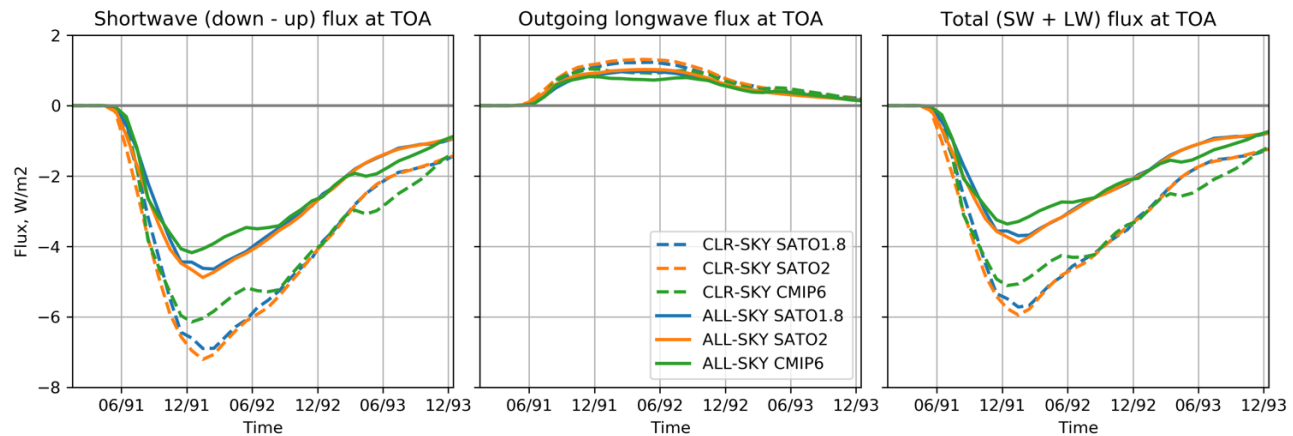
3852

3853 **Figure 9.1**

3854

3855

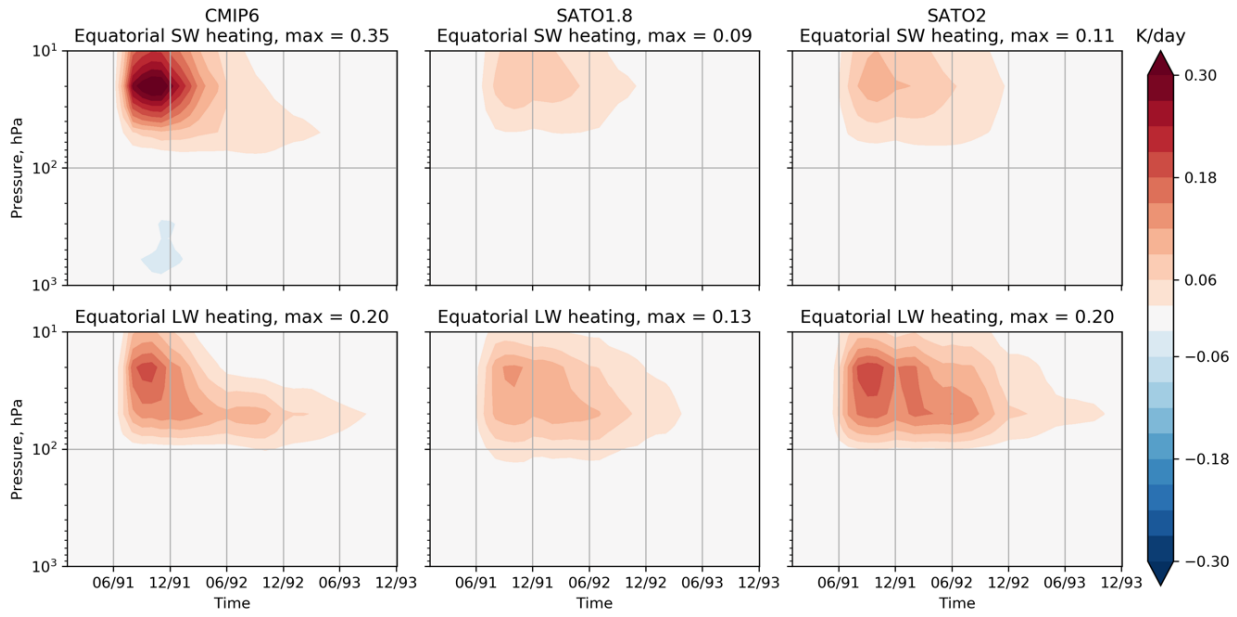
3856



3857

3858 **Figure 9.2.**

3859



3860

3861

3862 **Figure 9.3.**

3863

3864

3865

3866 **10. Total natural and anthropogenic radiative forcing**

3867

3868 This section describes developments in the comparison of different forcing agents which then

3869 naturally leads to estimates of the total forcing and its time evolution, and thus acts as a

3870 synthesis of the material in the previous Sections. The nature of the forcing agents is

3871 very different in terms of magnitude, uncertainty, spatial distribution and time evolution

3872 (see sections 2-9).

3873

3874

3875

3876

3877

3878 **10.1 Complexity in comparing forcing agents**
3879
3880

3881 Kiehl and Briegleb (1993) were the first to provide model estimates of the geographical
3882 distribution of the net forcing of WMGHGs and the direct sulfate aerosol effect. The results
3883 showed that the WMGHG forcing in northern industrialized regions at mid-latitudes was
3884 strongly offset by the direct aerosol effect, but the offset was much weaker in the tropics where
3885 WMGHG forcing is at maximum. A distinct spatial distribution was also found in modelling
3886 studies for tropospheric ozone and biomass burning by Penner et al. (1992) with a maximum
3887 near the emission regions located over the continents, and for stratospheric ozone forcing by
3888 Ramaswamy et al. (1992) with a negative forcing in the middle to high latitudes but near-zero
3889 or small negative in the low latitudes.

3890
3891 Geographical distributions of various climate drivers, and further estimates of RF and their
3892 uncertainties, were given in Shine and Forster (1999), Hansen et al. (2000), and assessed in
3893 TAR. All these estimates showed a large difference in the uncertainty of WMGHG forcing and
3894 other climate drivers, in particular, aerosol effects. The much larger uncertainties are due to
3895 known factors such as the aerosol distribution and optical properties, as well as uncertainties in
3896 the physical process of aerosol-cloud interactions. Compared to relatively low uncertainties for
3897 WMGHGs, this made it difficult to provide a net RF. In addition to providing uncertainty
3898 ranges for the climate drivers, TAR presented the “Level of Scientific Understanding” which
3899 showed large difference among the climate drivers. This illustrated the difficulty at that time of
3900 providing a net forcing for both global and annual means and geographical distributions.
3901 Ramanathan et al. (2001) and Kaufman et al. (2002) on regional scale and AR4 globally pointed
3902 out the distinct differences in the net anthropogenic forcings at TOA and surface, which

3903 demonstrates the sharp differences between the relatively homogeneous WMGHG forcings and
3904 the much more spatially inhomogeneous aerosol forcing.

3905

3906 **10.2 Applications of probability distribution functions to derive total anthropogenic
3907 forcing**

3908

3909 Boucher and Haywood (2001) provided a method to estimate a net global-mean RF from
3910 components with different uncertainties, a method which has since been used in IPCC
3911 assessments beginning with AR4. The method used probability distribution functions (PDFs) for
3912 the individual climate drivers and a Monte-Carlo approach to estimate the net RF. In Boucher
3913 and Haywood (2001) various assumptions on the shape of the PDFs such as normal and log-
3914 normal distributions were investigated. They found a higher sensitivity to how uncertainty ranges
3915 should be interpreted than to the shape of the PDFs. This has led to an improved quantification of
3916 uncertainty range and confidence levels in later research and whether RF numbers are given as
3917 e.g. one standard deviation or 5-95% confidence intervals. The method of Boucher and Haywood
3918 (2001) allows the calculation of a mean net RF (with an uncertainty range) and the quantification
3919 of the probability of the RF falling outside a certain range, e.g. the probability for a negative RF
3920 given the time period for the selection of climate drivers.

3921

3922 Fig 10.1 shows PDFs for global-mean forcing, relative to 1750, due to total aerosols, total
3923 WMGHGs, and the net of all climate drivers for IPCC AR4 and AR5 as well as two scenarios for
3924 2030 (RCP2.6 and RCP8.5). RFs are presented for AR4 PDFs. All the other results use ERF, but
3925 the AR5 WMGHG RF is also shown to illustrate the larger uncertainty in ERF (20%) relative to
3926 RF (10%). The mean estimates of ERF and RF for WMGHGs in AR5 are the same, but the much
3927 wider PDF for ERF relative to RF is evident.

3928

3929

3930 The change in net forcing between AR4 (1750-2005) and AR5 (1750-2011) results partly from
3931 the introduction of ERF, partly from the increase in the WMGHG forcing of 8% due to changes
3932 in concentrations between 2005 and 2011, and partly from a wide range of other updates based
3933 on a better understanding of processes important for forcing

3934

3935 The change in the forcing for the two RCPs compared to AR5 (1750-2011) is solely due to the
3936 trends in atmospheric composition. The main change in the scenarios are due to aerosols and
3937 WMGHGs; the changes to other climate drivers are small (less than 0.1 W m^{-2}) (Myhre et al.,
3938 2015). The weaker aerosol forcing and increased WMGHG forcing enhance the net forcing quite
3939 substantially in 2030 (for both RCPs) relative to AR5 (1750-2011) forcing. Furthermore, the
3940 weaker contribution from aerosols (with its high uncertainty) and a stronger dominance of
3941 WMGHGs (with its relatively low uncertainty) contributes to a smaller uncertainty in the future
3942 forcing in both absolute and relative terms. The increase in CO₂ in the two scenarios is
3943 responsible for between 80 and 100% of the increase in WMGHG forcing, and is a strong
3944 contributor to the lower uncertainty in the net forcing. The reduction in the magnitude of the
3945 aerosol forcing is consistent with recent developments in trends of aerosol abundance (e.g.
3946 Paulot et al., 2018).

3947

3948 Since AR5, the WMGHG concentration has increased and there have been updates to RF and
3949 the quantification of rapid adjustments (see sections 2 and 3). The upper bar in Figure 10.2
3950 shows the net anthropogenic ERF from AR5 (which was for the period 1750-2011) with an
3951 absolute (5-95%) uncertainty range of 2.2 W m^{-2} (1.1 to 3.3 W m^{-2}). Keeping everything the

3952 same as in the upper bar, except updating WMGHG concentrations (to 2018) using the growth
3953 rates from NOAA (<https://www.esrl.noaa.gov/gmd/aggi/aggi.html>) and the methane forcing
3954 expression (to include the solar absorption component from Etminan et al. 2016) gives the
3955 middle bar of Figure 10.2. The best estimate increases from 2.3 W m^{-2} in AR5 to 2.7 W m^{-2} .
3956 With a better quantification of rapid adjustments (see Smith et al., 2018 and section 2) the
3957 uncertainties in tropospheric rapid adjustment to ERF of CO₂ is about 10% leading to a total
3958 ERF uncertainty of 14% compared to the 20% uncertainty assumed in AR5. A large part of the
3959 diversity in the ERF of CO₂ is likely to be from the instantaneous RF (Soden et al., 2018). The
3960 lower bar in Figure 10.2 combines the contribution of uncertainties in detailed off-line
3961 calculations (10%) with the 10% uncertainty from climate model simulated rapid adjustment.
3962
3963

3964 **10.3 Time evolution of forcing**

3965
3966 The natural climate drivers from volcanic eruptions and solar irradiance changes have large
3967 interannual variations (Section 8 and 9) and because of that, it is difficult to include these in the
3968 PDF of climate drivers for a time period. The time evolution of the natural climate drivers
3969 represents their relation to anthropogenic drivers much better than providing forcing over a
3970 fixed time period. Hansen et al. (1993) provided, for the first time, the evolution of various
3971 forcing agents and the net RF (Figure 10.3). Figure 10.3 shows that there is a remarkable
3972 similarity between the evolution of net forcing until 2000 between Hansen et al. (1993) and the
3973 estimate in IPCC AR5, given all the new insights since early 1990s. A strengthening in the
3974 aerosol forcing especially in the period 1950 to 1980 is further illustrated in Figure 10.3 as is the
3975 strengthening of WMGHG forcing since 1960.

3976
3977
3978
3979
3980

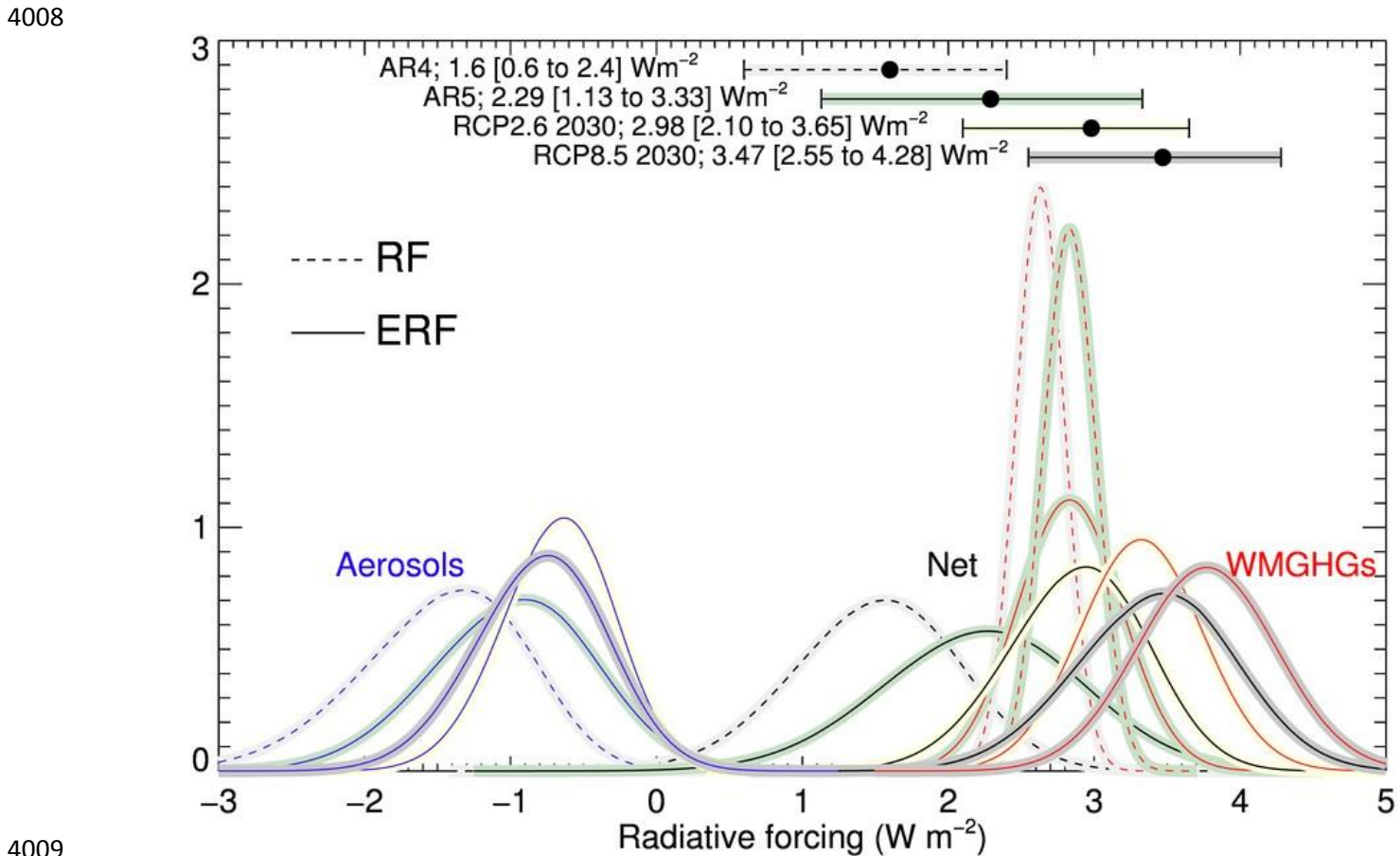
3981 **10.4 Summary and challenges**
3982

3983 The AR5 result shown in Figure 10.1 led Myhre et al. (2013) to conclude that “it is certain that
3984 the total anthropogenic forcing is positive” strengthening the “extremely likely” wording used
3985 in AR4 (Forster et al. 2007). Nevertheless, despite this strengthened language, the AR5 1750-
3986 2011 net anthropogenic forcing (2.3 (1.1 to 3.3) W m^{-2}) indicates that uncertainties remain
3987 very large compared to the best-estimate net forcing; this significantly hinders efforts to derive,
3988 for example, climate sensitivity given observed temperature changes, and inhibits understanding
3989 of the effectiveness of proposed mitigation pathways, with consequent impacts on the
3990 confidence in the advice given to policymakers.

3991

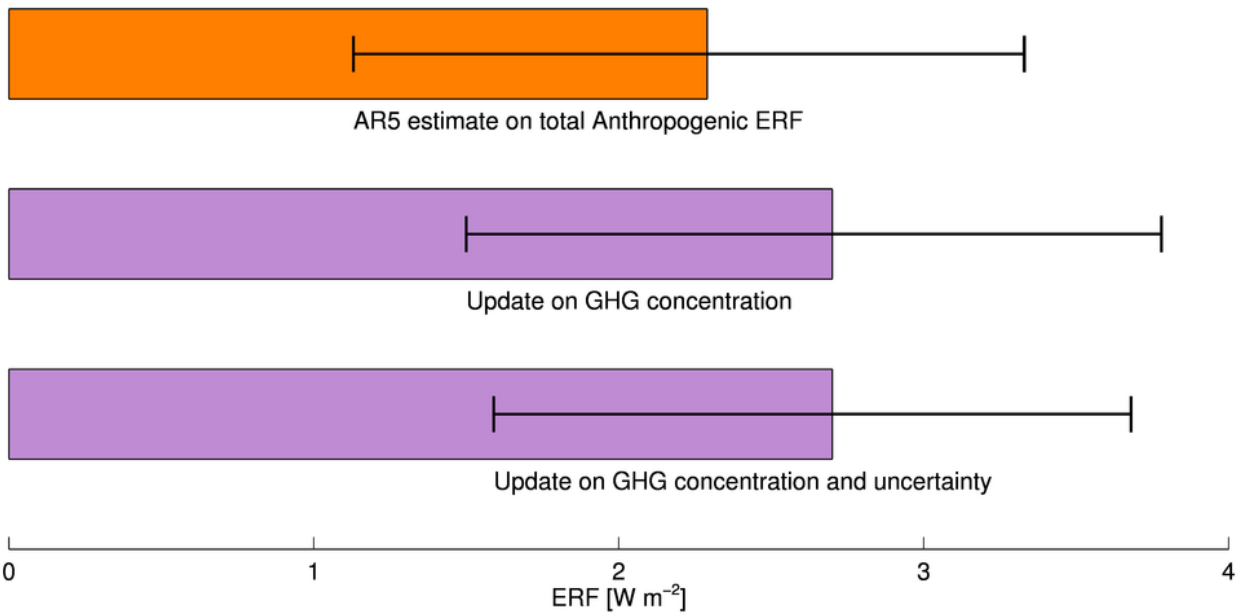
3992 Challenges to decreasing the spread in the estimated net forcing include (i) ensuring adequate
3993 monitoring of changes in concentrations of drivers of forcing, and improved understanding of
3994 the pre-industrial background values, especially for aerosols and ozone and (ii) improving
3995 methods of calculating the forcing, given these constituent changes. It is particularly notable
3996 that the introduction of ERF in AR5 led to an increase in the uncertainty of the WMGHG
3997 forcing. While the relative uncertainty in WMGHG is lower than other components, Myhre et
3998 al. (2013) give the absolute 5-95% % uncertainty for the 1750-2011 ERF as 1.14 W m^{-2} ; this is
3999 only slightly less than the corresponding values for the aerosol-cloud interaction (1.2 W m^{-2}).
4000 Recent results indicate progress in understanding rapid adjustment. Given the expected
4001 increasing dominance of WMGHG forcing in coming decades (Figure 10.1) this indicates the
4002 importance of improved estimates of the rapid adjustments in order to reduce the WMGHG
4003 ERF uncertainty, as well as efforts to better characterize the other remaining uncertainties in
4004 WMGHG forcing. It is also clear that, to date, most efforts on estimating the net forcing have

4005 focused on the global-mean; further attempts to provide geographical distributions of the net
4006 forcing, and the associated confidence levels, would allow additional insights into the drivers of
4007 climate change.

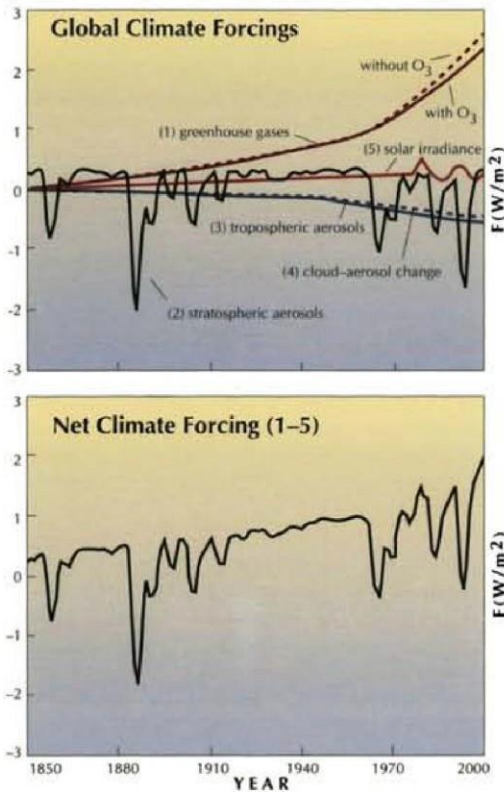


4009
4010
4011
4012 **Figure 10.1:** Probability distribution functions of forcing from IPCC AR4 (1750-
4013 2005) (Forster et al., 2007), IPCC AR5 (1750-2011) (Myhre et al., 2013) and two
4014 scenarios for year 2030 relative to 1750 (RCP2.6 and RCP8.5) (Prather et al., 2013).
4015 Black lines show net forcing, blue lines show total aerosol forcing, and red lines
4016 show WMGHG forcing. The colors around the lines provide information on AR4,
4017 AR5 and RCPs. Unlike AR5, the red line includes solely the WMGHGs and does
4018 not include ozone and stratospheric water vapor.

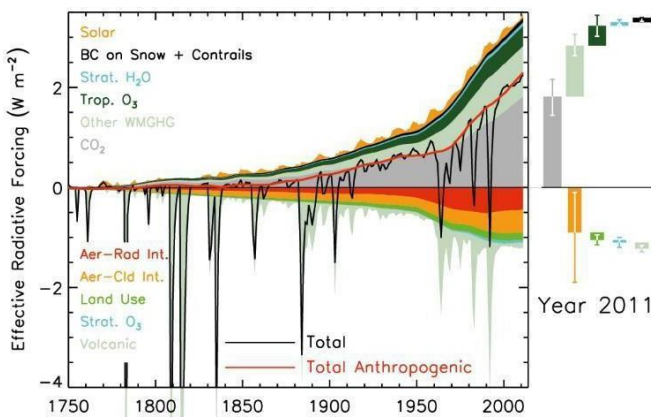
4019
4020



4021
4022
4023
4024 Figure 10.2: Estimates of the net anthropogenic ERF from AR5 (1750-2011)
4025 (upper bar), the effect of updates to WMGHG concentrations (1750-2018)
4026 and to the methane RF expression (middle bar), and updates to the uncertainty
4027 range due to improved understanding of rapid adjustments (lower bar).
4028
4029
4030



4031
4032



4033

4034 **Figure 10.3:** Time evolution of radiative forcing for individual and net forcings 1850-
4035 2000 (Hansen et al., 1993) (left) and IPCC AR5 estimates of individual and net forcings
4036 1750-2011 (right).
4037
4038

4039 **11. Emission metrics and radiative efficiencies**

4040

4041

4042 As described in previous sections, RF has great utility in quantifying the radiative impact of
4043 changes in concentrations of different atmospheric constituents, and in assessing their relative
4044 importance. RF has also found an important usage in serving climate policy, by enabling
4045 methodologies, which are simple to apply in a policy context, to compare the climate impact of
4046 *emissions* of different species; this role is discussed in this section.

4047

4048

4049

4050 **11.1 Background**
4051
4052

4053 RF at a given time (e.g. present day), relative to some past time (e.g. pre-industrial), is an
4054 important indicator of the absolute and relative importance of different drivers of climate
4055 change. That forcing depends on the past history of emissions. In the case of CO₂, because of
4056 the long persistence times of atmospheric perturbations, emissions over a century ago are still
4057 impacting present-day RF; at the other extreme, the present-day RF due (directly) to aviation
4058 contrails is mostly the result of contrails formed in the preceding few hours. The influence of
4059 the lifetime of perturbations is implicit in, for example, the standard IPCC forcing bars (Fig
4060 1.2), but this provides little guide to future influence of present-day forcing agents. Fig 11.1
4061 (from Fuglestvedt et al. 2010) illustrates this point for an extreme scenario when a selection of
4062 emissions from the transport sector are instantaneously reduced to zero. The forcing due to CO₂
4063 emissions persists for centuries, while most of the forcing due to short-lived species reduces to
4064 zero within a few weeks.

4065

4066 From a policy perspective, the explicit consideration of these timescales is important, for
4067 example in assessing the future impact of present-day emissions. In addition, in the context of
4068 climate agreements which cover emissions of a range of different gases (sometimes called multi-
4069 gas agreements), it is necessary to place the climate impact of different emissions on a common
4070 scale. Via the application of a climate emission metric (henceforth “metric”), it is (at least in
4071 principle) possible to aggregate all emissions into a single “CO₂-Equivalent” value.

4072

4073 There are many aspects and choices, some contentious, to consider in the design and application
4074 of such metrics and there is no agreed metric which is suitable for all purposes. The issues have
4075
4076

4077 been extensively discussed in various reviews and assessments and
4078
4079 has continued through all IPCC ARs (e.g. Fuglestvedt et al. 2010, Myhre et al. 2013). Some
4080
4081 of the issues extend beyond physical science, and reflect policy choices on, for example the
4082
4083 appropriate timescales and the extent to which the chosen metric serves the aims of a particular
4084
4085 policy. Here the focus will be on the role of RF in computing these metrics.
4086

4087
4088
4089

4090

4091 **11.2 The Global Warming Potential**

4092

4093

4094 By way of illustration, one metric, the Global Warming Potential (GWP), is considered briefly

4095

4096 here; it is the most widely used metric in international policymaking

4097

4098 . The GWP was presented in FAR, based on rather

4099

4100 few precursor studies (Derwent, 1990; Fisher et al., 1990; Lashof and Ahuja 1990; Rodhe 1990)

4101

4102 and has been assessed in all IPCC assessments since then. The GWP is, for example, used by

4103 parties to the 1997 Kyoto Protocol to the United Nations Framework Convention on Climate

4104 Change (UNFCCC) to place emissions of more than 20 gases on a common CO₂-equivalent

4105 scale, and in the UNFCCC's 2015 Paris Agreement. It is also used within the 2016 Kigali

4106 Amendment to the UN's Montreal Protocol on Substances that Deplete the Ozone Layer, to

4107 place targets on emissions of many hydrofluorocarbons.

4108

4109

4110 The GWP measures the time-integrated RF of a pulse emission of a unit mass of a

4111

4112 climate forcing agent (or its precursor) relative to the time-integrated RF of a pulse

4113

4114 emission of a unit mass of CO₂. For each agent, it is necessary to know the radiative efficiency

4115

4116 (i.e. the RF per molecule or per kilogram) and its lifetime, which determines the

4117

4118 decay of the pulse after emission. In addition, indirect forcings resulting from that emission

4119

4120 should be incorporated; one example is the impact of methane emissions on ozone, stratospheric

4121 water vapour and CO₂. In almost all policy applications of the GWP, the integration is

4122 performed over 100 years (the "time horizon"), and denoted GWP(100). However, there is no

4123

4124 compelling scientific reason for that choice, and the perceived importance of emissions of a gas

4125

4126 (i.e. their contribution to CO₂-equivalent emissions) can depend markedly on that choice,

4127

4128 especially for short-lived species. For example, for methane, AR5 (Myhre et al. 2013) reports
4129 values of GWP(20) and GWP(100) of 84 and 28 respectively.
4130
4131
4132
4133

4134 All IPCC assessments have presented values of GWPs for a range of gases (more than 200 are
4135 included in Myhre et al. (2013)) and have discussed scientific issues in determining the input
4136 parameters. The reported values of GWP(100) for some species have varied quite strongly over
4137 time. For example, the GWP(100) for methane has increased from 21 to 28 between FAR (Shine
4138 et al., 1990) to AR5 (Myhre et al. 2013) as a result of changes in the recommended values of
4139 methane's radiative efficiency, lifetime and indirect effects, as well as changes in the radiative
4140 efficiency and lifetime of CO₂. Advances in understanding since AR5 (for example, the effect of
4141 methane's near-infrared
4142 absorption bands (Section 3)), and the incorporation of the influence of carbon-climate feedbacks
4143 (e.g. Gasser et al. 2016, Sterner and Johansson 2017), could see the recommended
4144 GWP(100) value for methane change significantly in future.

4145
4146
4147
4148
4149

4150 **11.3 Radiative efficiency**

4151
4152

4153 Radiative efficiency (RE) is a key input to all the main emission metrics that have been
4154 proposed to support multi-gas agreements. By convention, IPCC assessments have computed
4155 the RE for a small perturbation to present-day concentrations for the more major greenhouse
4156 gases (CO₂, CH₄, N₂O), for which forcing does not increase linearly with
4157 concentration; for more minor species, present in sub-ppbv concentrations, the forcing
4158 is assumed to be linear in concentration. RE calculations need to be
4159 representative of global-average conditions including the effects of clouds (e.g. Myhre and
4160 Stordal 1997). Irrespective of its use in metrics, the RE gives insights into the role of different
4161 gases. For CO₂, Myhre et al. (2013) report a value of 1.37x10⁻⁵ W m⁻² ppb⁻¹. The RE of methane
4162 is 26 times higher and nitrous oxide's is 220 times higher. Halocarbons are often greater than
4163 10,000 times more effective, per molecule. There are multiple reasons for these differences in
4164 RE (e.g. Shine 1991). These include the fundamental spectroscopic intensity of each molecule,
4165 which is determined by the probabilities of vibration-rotation transitions, the wavelengths of
4166 absorption features relative to the Planck function at typical atmospheric temperatures, the pre-
4167 existing atmospheric concentrations of the molecule (as RE decreases with concentration), and
4168 overlap with absorption features of other atmospheric gases (notably water vapor and CO₂).
4169 Hodnebrog et al. (2013) attempted to characterize the sources of uncertainty in calculating REs,
4170
4171 focusing particularly on the halocarbons. The overall conclusion was that REs were accurate to
4172 within 15% for longer-lived gases and to within about 25% for the
4173 shorter-lived gases.

4174

4175

4176 Compilations of halocarbon REs and the associated emission metrics in many earlier
4177 IPCC assessments drew values from different sources which used various techniques to
4178 compute the forcing. This inhibited a reliable comparison of the RE of different gases. AR5
4179 (Myhre et al. (2013)), using the Hodnebrog et al. (2013) calculations, tried to enhance the
4180 consistency between gases, by adopting a single method for calculating the RE.

4181

4182 To date REs have mostly been computed using RF (i.e. accounting for stratospheric temperature
4183 adjustment in some way), rather than using ERFs for several reasons. First, computing ERFs for
4184 such large numbers of gases using GCMs would be a formidable task; in future, a simpler
4185 generic framework for estimating rapid adjustments could be developed if it was shown to be
4186 applicable to a wide range of gases. Second, , GCM radiation codes do not have the spectral
4187 resolution that is necessary for reliable RE calculations for gases with generally quite narrow
4188 spectral features. Finally, because of the noise inherent in GCM calculations of ERF, estimation
4189 of REs for sub-ppbv concentrations (and hence radative forcings below about 0.2 W m^{-2}
4190 (Forster et al. 2016) would be difficult; while artificially high perturbations could be imposed in
4191 GCMs, this would raise questions about the applicability of the results to more realistic
4192 concentrations found, or likely to be found, in the atmosphere.

4193

Molecule	Radiative Efficiency ($\text{W m}^{-2} \text{ ppb}^{-1}$)	Radiative Efficiency relative to CO_2
CO_2	1.37×10^{-5}	1
CH_4	3.63×10^{-4}	26
N_2O	3.00×10^{-3}	219
CFC-12	0.32	23,360

HFC134a	0.16	11,680
SF ₆	0.57	41,600

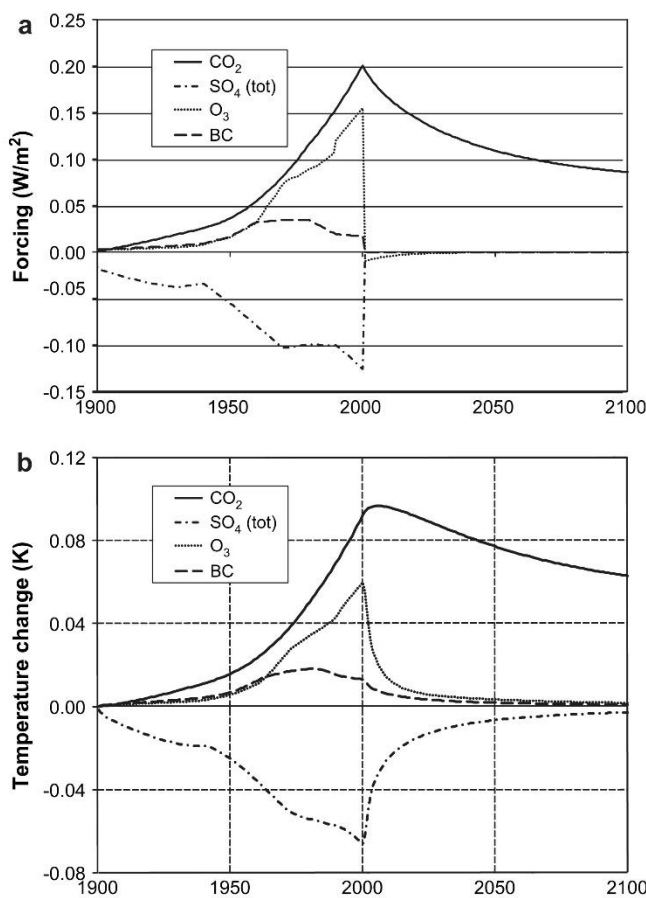
4194

4195 Table 11.1 Radiative efficiencies (in W m^{-2} ppb⁻¹, and relative to CO₂) for a selection

4196 of gases (values from Myhre et al. 2013).

4197

4198



4199

4200

4201 Figure 11.1: Consequences for RF of different agents and associated temperature response over
4202 time from an assumed scenario when a selection of emissions from the transport sector is
4203 instantaneously reduced to zero in 2000.

4204

4205

4206
4207

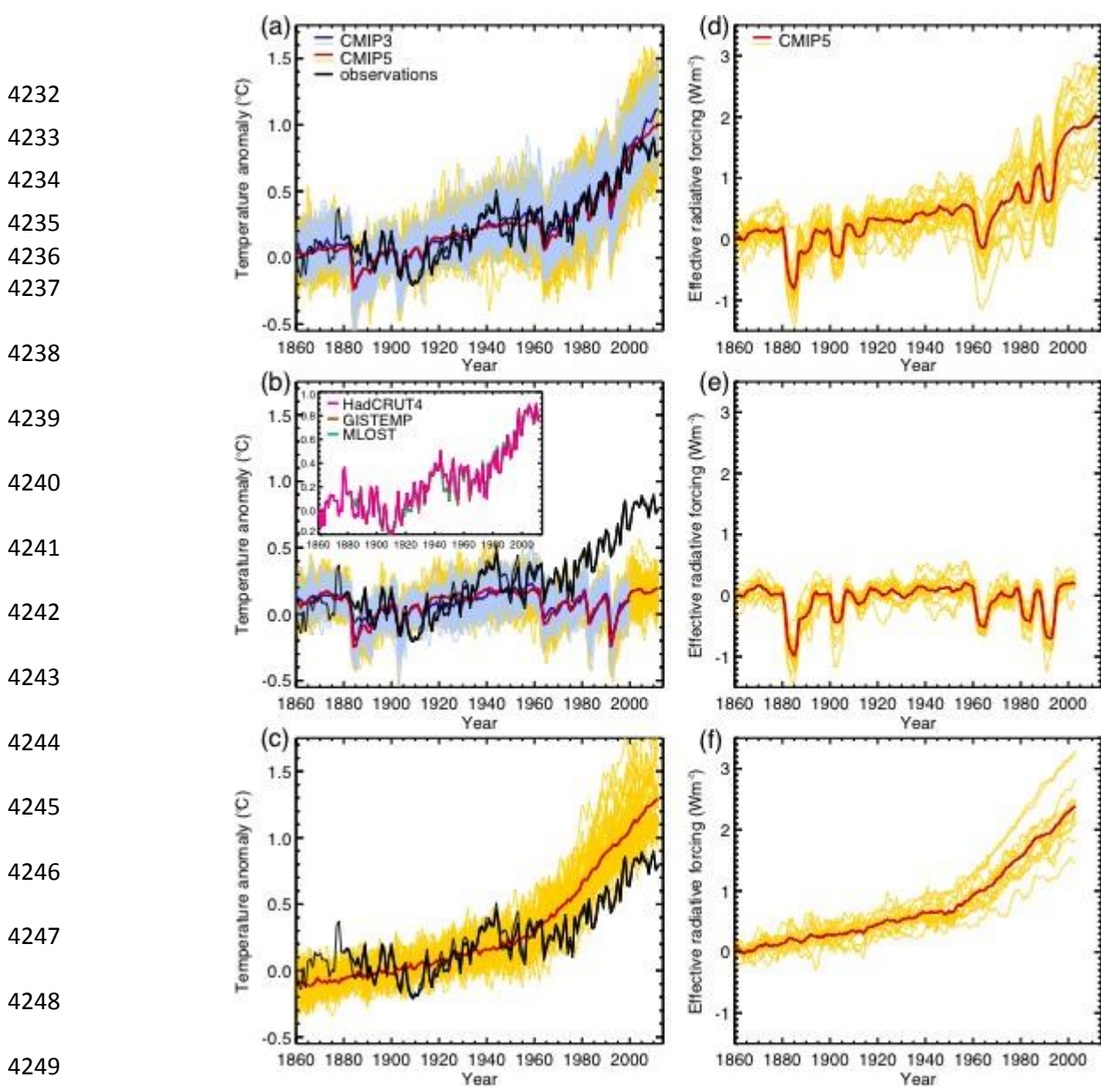
4208 **12. Climate Response to Radiative Forcings**

4209
4210
4211
4212
4213
4214
4215
4216
4217
4218
4219
4220

Radiative forcing is an essential component in understanding historical changes in climate and their attribution to both natural and anthropogenic causes. Attribution of anthropogenic climate change requires both models and observations and consists of three steps: (i) detecting a change in climate; (ii) establishing that this change is consistent with the expected response to the estimated anthropogenic net forcing; and (c) establishing that this change cannot be explained by other mechanisms, such as internal variability or natural forcings. Without quantitative information on the magnitude, spatial structure and temporal evolution of both natural and anthropogenic radiative forcings, understanding the causes of historical changes in climate, from glacial-interglacial periods to the change in climate over the past century, would not be possible.

4221
4222
4223
4224
4225
4226
4227
4228
4229
4230
4231

As an illustration of this process, Figure 12-1 (left column) compares the observed and model simulated global-mean temperature anomalies from 1860-2012 with that predicted from a multi-model ensemble of coupled ocean-atmosphere models from CMIP3 (gray lines) and CMIP5(yellow lines) that are integrated under three different forcing scenarios: historical natural and anthropogenic forcings (top), natural forcings only (middle), and anthropogenic greenhouse gas forcings only (bottom). The right columns show the corresponding ERF for each of these forcing scenarios derived from the CMIP5 simulations following Forster et al. (2013)



4253 **Figure 12-1: Left-hand column:** A comparison of observational estimates of global mean
 4254 surface temperature (GMST, black lines) and climate model simulations [CMIP3 – blue lines;
 4255 CMIP5 models – yellow lines] using both anthropogenic and natural forcings (a), natural
 4256 forcings only (b) and greenhouse gas (GHG) forcing only (c). Thick red and blue lines depict the

4257 multi-model ensemble mean across all CMIP5 and CMIP3 simulations respectively. Note that
4258 CMIP3 simulations are not available for GHG forcing only (c). Inset to (b) shows the three
4259 observational data sets distinguished by different colours. **Right-hand column:** The effective
4260 radiative forcing (ERF) in CMIP5 models due to anthropogenic and natural forcings (d), natural
4261 forcings only (e) and GHGs only (f). Individual ensemble members are shown by thin yellow
4262 lines, and CMIP5 multi-model means are shown as thick red lines. From Bindoff et al. 2013.

4263
4264
4265
4266 This set of simulations highlight the basis for the attribution of recent warming to human-
4267 influenced activities. The simulations with natural forcing alone (center left panel) are unable to
4268 explain the rise in global mean temperature from the mid 20th Century to present. However,
4269 when natural and anthropogenic forcings are combined (top left panel), the model simulations
4270 are in excellent agreement with the observed temperature anomalies. Contrasting these
4271 simulations with the GHG only simulations (bottom panels), serves to illustrate how aerosols
4272 have partially offset a significant fraction of the GHG warming; without aerosols forcing, the
4273 present day global-mean temperatures would have increased another ~0.5 K. Since
4274 anthropogenic aerosols occur primarily in the Northern Hemisphere, these differences also have
4275 a distinct signature on the hemispheric contrast in temperature and precipitation as discussed
4276 below. Thus, accurate knowledge of both GHG and aerosol forcings is critical to understanding
4277 past and projecting future changes in climate, both globally and regionally.

4278
4279 Early attribution studies focused primarily on the changes in global-mean surface temperature
4280

4281 (e.g., Wigley and Raper 1990; Stouffer et al. 1994). These evolved into more complex studies
4282 that considered the spatial pattern or ‘fingerprints’ of climate change that were predicted by
4283 climate models and used more elaborate statistical methods to search for their presence in the
4284 observed record (Santer et al. 1996b). The fingerprints of anthropogenic climate change were
4285 expanded beyond simply the regional pattern of surface temperature, to consider the vertical
4286 structure of temperature change in the atmosphere and oceans, temperature extremes, and the
4287 diurnal and seasonal cycles of temperature, as well as other variables such as precipitation and
4288 sea level pressure (Santer et al., 1995, Hegerl et al., 1996, 1997, 2006; Stott et al., 2000, 2004;
4289 Vecchi et al. 2006; Meehl et al. 2009; Min et al. 2011; Zhang et al 2007). While each of these
4290 quantities have a defined response to anthropogenic forcing, the use of multivariate changes
4291 enhances the confidence in the attribution process. For example, both solar and GHG forcings
4292 can warm the surface, however they have very different impacts on the diurnal temperature
4293 cycle, precipitation change, and the temperature response in the stratosphere. Across all of these
4294 quantities, the observed changes are only explained through the inclusion of anthropogenic
4295 forcing. Thus, the concept of radiative forcing is fundamental to methods used to identify a
4296 human influence on climate.

4297
4298
4299

4300 **12.1 The Spatial Structure of Forcing and Response**

4301
4302
4303 As noted in Sections 2, 5, anthropogenic forcing from well-mixed GHGs and aerosols over the
4304 historical period have distinctly different spatial patterns – the former being positive and more
4305 spatially uniform, whereas the latter is a net negative and largely confined to the Northern
4306 Hemisphere. As noted above, this hemispheric asymmetry in the pattern of forcing, has significant
4307 impacts on both the detection and attribution of anthropogenic climate change (Bindoff et al.,
4308 2013) as well as the transient climate response to forcing in both historical simulations and future
4309 projections (Shindell, 2014).

4310
4311 For example, rainfall observations reveal a coherent southward shift of the tropical rain belt
4312 over the latter half of the 20th Century, which has been associated with severe droughts over the
4313 Sahel and portions of South America (Folland et al. 1986; Allen et al 2002). Observations in the
4314 last few decades of the 20th Century have revealed a weakening of the monsoon (Ramanathan
4315 et al., 2005, Chung and Ramanathan, 2006; Lau and Kim, 2006). This tropical precipitation shift
4316 has been linked to changes in the cross-equatorial energy transport driven by the
4317 interhemispheric contrast in the warming of the surface temperatures that arise from the
4318 combination of a spatially inhomogeneous shortwave forcing by aerosols and a relatively more
4319 homogeneous longwave forcing by WMGHGs (Kang et al. 2008). This type of a spatial
4320 structure in the radiative forcing leads to a decrease of the shortwave flux, primarily felt at the
4321 surface in the northern hemisphere (e.g., Chen and Ramaswamy, 1996; IPCC, 2001), and an
4322 increase in the heating of the atmosphere and surface

4323

4324 globally due to the longwave effects of the WMGHGs (e.g., Ramanathan et al., 1981). The
4325 model- simulated response to this pattern of hemispheric asymmetry in the forcing enhances the
4326
4327 temperature gradient, induces a change in the meridional circulation and intensifies the heat and
4328 moisture exchange between the two hemispheres across the equator, effectively moving the
4329 tropical precipitation belt towards the warmer hemisphere (Ramaswamy and Chen, 1997).
4330
4331 Subsequent studies with improved models have affirmed this characteristic for realistic aerosol
4332 and WMGHG forcings (Rotstayn and Lohman 2002; Ming and Ramaswamy, 2009; Hwang et
4333 al. 2013; Shindell et al. 2015; Wang 2015).

4337
4338
4339 Both aerosols and WMGHG influence the spatial pattern of warming. Anthropogenic aerosols
4340 introduce hemispheric asymmetry by preferentially cooling the northern hemisphere, while
4341 WMGHG warms the northern hemisphere more than the southern hemisphere due to the
4342 differing thermal inertia between the two hemispheres (Friedman et al. 2013). When forced by
4343 historical changes in both anthropogenic aerosols and greenhouse gases, the cooling effect of
4344 the aerosols dominates and climate models simulate less warming in the northern hemisphere
4345 compared to the southern hemisphere.

4346
4347 Aerosols induce an anomalous meridional circulation, which reduces the ascent in the northern
4348 tropics and opposes the local Hadley circulation. The hemispheric temperature gradient initiated
4349 reduces the southward cross-equatorial energy transport accompanying the weakening of the
4350 Hadley circulation (Hwang et al 2013; Allen et al. 2002; Bollasina et al. 2011; Soden and
4351 Chung 2017). This change in the large-scale atmospheric circulation, in turn, drives meridional
4352 shifts in the tropical precipitation bands; most notably a southward shift in tropical precipitation

4353 compared to simulations in which only GHG or natural forcings are included. The aerosol-
4354 induced effect on the cross-equatorial circulation and precipitation changes emerges as a strong
4355 spatial feature vis-à-vis WMGHG effects. In addition the poleward transport of heat in both
4356 atmosphere and ocean are affected by aerosols differently

4357
4358 than in the case of the WMGHGs (Ocko et al., 2013). Polson et al. (2014) note a correlation
4359 between the trend of precipitation in the last few decades of the 20th Century and sulfur
4360 emissions. Recent work has also highlighted the role of aerosol-cloud interactions that induce
4361 adjustments in cloud interactions in amplifying this response. Aerosol forcing is found to induce
4362 secondary changes in the model simulated cloud radiative properties through both microphysical
4363 (Chung and Soden 2017) and large-scale dynamical changes. These changes act to further
4364 increase the hemispheric contrast in forcing, thereby amplifying both the circulation and
4365 precipitation changes. However, the broad spatial pattern of the climate response to aerosols and
4366 well mixed GHG forcings is more similar than would be expected given the differing
4367 geographic distributions of their emissions and forcings (e.g. Boer and Yu, 2003; Levy et al.,
4368 2013; Xie et al., 2013).

4369
4370 Boer and Yu (2003) showed that the CO₂ forcing spatial pattern (with maxima in the sub-tropics
4371 and a minima at high latitudes) explains very little of the surface temperature response pattern
4372 (generally increasing with latitude). While the aerosol forcing pattern explained more of the
4373 aerosol response pattern, the correlation remained small; indeed, the CO₂ and aerosol surface
4374 temperature responses were better correlated with each other than with their “parent” forcing
4375 pattern. Recent studies suggest that atmospheric feedbacks to the different patterns of forcing
4376 serve to homogenize the radiative perturbations, resulting in a more spatially similar pattern of

4377 response for both temperature and precipitation (Ganguly et al., 2012; Xie et al., 2013; Hill et
4378 al., 2015; Tian et al., 2016; Persad et al. 2018;). The rapid atmosphere-only adjustments to the
4379 forcing have been found to be particularly effective at homogenizing the response to aerosols
4380 and GHG forcings.

4381
4382

Another spatial dimension to be considered is the vertical. An important parameter to consider in
the presence of WMGHG, tropospheric aerosol, and stratospheric ozone forcings is the manner of
changes in the vertical structure of the thermal profile, and comparison of model simulations with
observations (Santer et al., 1996). In the troposphere, there is a warming of the surface and
troposphere primarily due to the combined effect of the positive forcings primarily by WMGHGs
(with smaller contributions from short-lived gases and tropospheric ozone), and negative forcing
by tropospheric aerosols (Mitchell et al., 1990). In the stratosphere, there is a reduction of
temperature due to loss of stratospheric ozone, and increases in CO₂, tropospheric ozone and
stratospheric water vapor (Shine, 1991; Hansen et al., 1995; Ramaswamy et al., 1996; Forster and
Shine, 1997). The confirmation of the model simulations by observed temperature trends, from the
troposphere to the stratosphere and the temporal evolution of the vertical profile of temperature
changes, has helped affirm our knowledge of the radiative forcing agents, the radiative
perturbations they exert on the atmosphere and surface, and the manner of their influences on the
spatial dimensions of the climate system (Hansen et al., 1995; Santer et al., 2005; Fu et al., 2011;
Stott et al., 2004; Ramaswamy et al., 2006).

4383
4384
4385
4386

4387 **13. Solar and terrestrial radiation management**

4388

4389 **13.1 Introduction**

4390

4391

4392 The growth in the understanding and quantification of RF, its consequences for climate

4393 change, and the attribution of observed phenomena to forcings, as described in the prior

4394 sections, has initiated conceptual thinking on potential management of the forcing/s to

4395 mitigate climate change. The principal pursuit is on how the long-term WMGHG forcings

4396 can be partially offset or mitigated. The idea of solar and terrestrial radiation

4397 management (STRM), sometimes also referred to as geoengineering, has over the last decade

4398 become one of the research areas in which the concept of radiative forcing has been applied. t

4399 But, the idea is by no means new. As early as the 1960s, Budyko wrote about "...the possibility

4400 of implementing in future some projects of active influence on the climate..." (Budyko 1969).

4401 Ironically, Budyko discussed this possibility as a way to prevent a new ice age, while the current

4402 discussion is focused chiefly on the possibility of intentionally imposing a negative radiative

4403 forcing on the Earth System, and thus introducing a cooling tendency. Specifically, current

4404 research mainly explores the potential of using a few different STRM strategies to counter some

4405 or all of the warming from increasing greenhouse gas concentrations in the atmosphere. While

4406 the first research on this controversial topic began as early as the 1980s (Keith and Dowlatabadi

4407 1992), it was not until Crutzen (2006) that extensive research on various types of solar and

4408 terrestrial radiation management began. The field represents one of the most recent examples of

4409 how the radiative forcing concept can be useful for a range of research topics. Several

4410 comprehensive reviews and assessments of this literature have been written (Royal society 2009;

4411 Caldeira et al. 2013; Ocean Studies Board 2015). They all share the conclusion that more
4412 research on the risks and benefits of STRM is urgently needed.

4413
4414 To date, research on the topic has been carried out almost exclusively with numerical models,
4415 and assessment has been based on the modeling activity organized by the Geoengineering
4416 Model Intercomparison Project (GeoMIP) (Kravitz et al. 2013). In the following, we review the
4417 major findings that have emerged from numerical modeling to date, with a focus on the
4418 *viability* and *climate response* of the three types of STRM that have gained the most attention
4419 : Stratospheric Aerosol Injection (SAI), Marine Sky Brightening (MSB) and Cirrus
4420 Cloud Thinning (CCT). While the former two strategies fall in the category of Solar
4421 Radiation Management (SRM), the latter belongs to what we can be labeled as Terrestrial
4422 Radiation Management (TRM). Viability in this context refers to the likelihood that the STRM
4423 mechanism in question can produce negative forcings of a magnitude sufficient to counter a
4424 considerable proportion of anthropogenic greenhouse gas forcing (currently at approximately 3
4425 Wm^{-2} , see Section 3).

4426
4427 Here we focus exclusively on the physical science related to STRM, and thus review the
4428 literature to-date and identify important knowledge gaps related to that aspect only. We do
4429 not discuss here any aspect of potential implementation concepts nor factors underlying them.

4430
4431

4432 **13.2 Solar radiation management (SRM)**

4433

4434

4435 In the following, studies on the two types of SRM that have so far received the most attention

4436 are discussed (Sections 13.2.1 and 13.2.2). SRM strategies that have been proposed but received

4437 limited attention thus far, including surface albedo enhancements and the introduction of

4438 mirrors in space, will not be reviewed here. A review of literature on the climate response to

4439 SRM, with a focus on changes to the hydrological cycle, is presented in Section 13.2.3.

4440

4441

4442

4443

4444 **13.2.1 Stratospheric Aerosol Injection (SAI)**

4445

4446 Extensive research focused on the major volcanic eruptions of the last century have clearly
4447 demonstrated the conceptual viability of stratospheric aerosol injection as an SRM strategy (see
4448 Section 9). However, reported forcings from GCM studies of SAI over the last decade span a
4449 wide range, with differences

4450 that can mainly be attributed to differing assumptions regarding

4451 injection location and height, injection rates and aerosol sizes; estimates of RF range from -

4452 8.5 to -1.2 Wm^{-2} , and the associated global mean cooling ranges from 0.5 to 3.2 K 0.5 to 3.2 K

4453 (e.g., Rasch et al., 2008, Robock et al., 2008, Jones et al. 2010, Berdahl et al., 2014, Crook et
4454 al., 2015 and Timmreck and Niemeier, 2015). Thus, even the most conservative estimates
4455 suggest that SAI likely has the potential to offset an appreciable proportion of anthropogenic
4456 GHG forcing to date.

4457

4458 Most studies to date have considered stratospheric injection of SO_2 , which in many respects
4459 mimic the climate impact of major volcanic eruptions. The advantage of this is that the
4460 global-mean response of the climate system to large injections of sulfur into the stratosphere
4461 is well understood, largely due to studies of the 1991 Mt Pinatubo eruption and other well-
4462 observed volcanic eruptions (see Section 9). However, the spatial responses due to the
4463 volcanic aerosol perturbations are not well-understood and there are knowledge gaps with
4464 respect to the climate feedback processes operating on the time scale of duration of the
4465 stratospheric particles (e.g., cloud interactions, air-sea interactions). Further, the relationship
4466 between the sulfur injection rates and the resulting forcing remains poorly understood and is

4467 expected to be nonlinear. The non-linearity with increasing emission rates arises in part
4468 because of the corresponding increase in aerosol size, which decreases aerosol lifetime and
4469 scattering efficiency. As a result, studies with prescribed aerosol sizes, regardless of emission
4470 rate, may overestimate forcing, especially for high emission rates. A major uncertainty in
4471 this respect is the aerosol coagulation rate in a freshly injected plume under stratospheric
4472 conditions.

4473
4474
4475
4476
4477
4478 Solid materials have also been considered for the purpose of SAI (Weisenstein et al. 2015;
4479 Jones et al. 2016) and could
4480 considerably reduce the stratospheric ozone destruction that follows from injection of sulfur in
4481 the stratosphere. But apart from a few isolated
4482
4483 studies, the associated forcing is largely
4484 unexplored. Irrespective of the injected material, there is broad agreement that large and
4485 negative forcings are achievable through SAI, but considerably less agreement when it comes
4486 to the climate response beyond the intended global mean cooling, which will be discussed
4487 further in Section 13.2.3.

4492
4493

4494

4495

4496

4497

4498

4499

4500

4501
4502
4503
4504
4505
4506
4507
4508
4509
4510
4511
4512
4513
4514
4515

4516 **13.2.2 Marine sky brightening (MSB)**

4517

4518

4519 While the very first STRM studies focused on SAI, research to explore the alternative strategy
4520 of marine cloud brightening (MCB) also emerged almost three decades ago. Notably, Slingo
4521 (1990) demonstrated how even modest perturbations of cloud properties could induce strong
4522 radiative forcings. This understanding triggered the idea of intentionally perturbing marine
4523 stratocumulus clouds for the purpose of cooling the climate (Latham 1990). Follow-up research
4524 based on satellite observations has since identified the most susceptible regions for the purpose
4525 of MCB as the subtropical regions off the west coasts of the major continents (Alterskjær et al.
4526 2012). By injecting cloud condensation nuclei into the marine boundary layer of these regions,
4527 cloud albedo could be increased through the creation of artificial ship tracks, through the
4528 mechanisms discussed in Section 5. Hill and Ming (2012) employed a coupled-mixed-layer-
4529 ocean-atmosphere GCM to conduct marine stratocumulus brightening experiments and found
4530 that over half of the radiative cooling is due to scattering of solar radiation by the added sea-salt
4531 aerosols while the rest arose from enhancement of the local cloud albedo. This finding was
4532 recently supported by Ahlm et al. (2017), and suggests that the term *Marine Sky Brightening* is
4533 more appropriate for this STRM strategy, as the forcing would manifest both under clear and
4534 cloudy skies.

4535

4536 While no studies of SAI to date have produced positive forcings, Alterskjær & Kristjánsson

4537 (2013) reported from a GCM study that depending on the size of the injected particles (usually
4538 assumed to be sea salt), the competition for the available water vapor could actually lead to a
4539 reduction in cloud droplet number concentrations, leading to a positive forcing. The opposite of
4540 the desired brightening effect has also been reported from studies using large-eddy-simulations,

4541 depending on the background aerosol concentration and humidity (Wang et al. 2011).
4542 Therefore, despite the 17 GCM studies included in Figure 2 supporting the conceptual viability
4543 of MCB as a STRM strategy, important knowledge gaps remain. Notably, many of the early
4544 GCM studies on MCB, which produced very large negative radiative forcings, simply
4545 prescribed an increase in cloud droplet number in marine clouds, and thus could not capture
4546 buffering effects like the one described above.

4547

4548 .

4549

4550

4551

4552

4553

4554

4555
4556

4557

4558 **13.3 Climate response to SRM**

4559

4560 Beyond the global mean cooling which SRM strategies are designed to produce, the following
4561 common features of the simulated climate response to SRM have been identified:

4562
4563 i) SRM naturally yields negative forcings that maximize in the tropics, where insolation is
4564 strong. Consequently, SRM tends to cool the low latitudes more than it cools the polar regions,
4565 and for a global mean cancellation of a given GHG forcing it will generally produce over-
4566 cooling in the tropics while only partly cancelling the high-latitude GHG warming. This would
4567 in turn reduce the equator-to-pole temperature gradient and generate atmospheric circulation
4568 changes.

4569
4570 ii) Along with the cooling comes a reduction in global mean precipitation, as expected. There
4571 is consensus among GCMs that a complete cancellation of GHG warming by SRM in the
4572 global mean will lead to an over-compensation in global mean precipitation. This net
4573 precipitation reduction is a consequence of the relative changes to the surface- and atmospheric
4574 radiation budgets in a climate with both increased GHG forcing and SRM (Bala et al. 2008). It
4575 may therefore prove more beneficial to only partly compensate for the increase in GHG forcing
4576 (MacMartin et al. 2013).

4577
4578 iii) A novel finding is that the reduction of shortwave radiation to the surface that would result
4579 from SRM may have detrimental effects on agriculture, in contrast to what has been reported in
4580 previous studies (Proctor et al. 2018). This finding warrants further investigation.

4581

4582 **13.3 Terrestrial radiation management (TRM)**

4583

4584

4585 Only one TRM method has so far received sufficient research attention to merit review

4586 here, namely cirrus cloud thinning (CCT). In the following, the research on CCT and the

4587 associated climate response are reviewed.

4588

4589

4590 **13.3.1 Cirrus cloud thinning (CCT)**

4591
4592

4593 Taking advantage of the fact that most cirrus clouds exert a net positive cloud radiative effect,
4594 this TRM strategy proposes to reduce cirrus cloud coverage and lifetime, and thus generate a
4595 negative forcing. The mechanism by which this could be achieved is through seeding of the
4596 cold (< 40 C) upper troposphere with ice nucleating particles (INPs), which would allow ice
4597 crystals to nucleate and grow even for very slight supersaturations, and thus prevent the
4598 abundance of ice crystals that results if saturation ratios becomes high enough for ubiquitous
4599 tiny solution droplets to freeze spontaneously (~150%). The resulting large ice crystals would
4600 sediment out and reduce cirrus cloud cover and upper tropospheric water vapor, both producing
4601 a negative ERF (Mitchell and Finnegan 2009). In theory, this should produce the desired
4602 cooling effect, but GCM studies to date produce conflicting results on the matter. The
4603 mechanism relies on assumptions about the balance between the dominant ice nucleating
4604 mechanisms in the upper troposphere, which is poorly understood in the present. The fact that
4605 different studies yield different ERFs should therefore not be surprising.

4606

4607 An additional concern with CCT is the risk of “over seeding”, that is, injecting too many
4608 artificial INPs which ultimately yield higher cirrus ice crystal concentrations than would have
4609 occurred in an unperturbed case, and thus a positive ERF (Storelvmo et al. 2013). For this
4610 TRM mechanism, the viability is thus still a topic of ongoing research, but recent cloud-
4611 resolving modeling results appear to support viability (Gruber et al. 2019) and reinforce the
4612 idea that CCT appears to be most promising in the instance of wintertime cirrus clouds at high
4613 latitudes.

4614
4615
4616
4617
4618
4619
4620
4621
4622
4623
4624
4625
4626
4627
4628
4629
4630
4631
4632
4633
4634
4635
4636

4637 **13.3. 2 Climate response to TRM**

4638

4639

4640 CCT does not reduce global mean precipitation to the same extent as SRM. The few GCM
4641 studies on the climate response to CCT that have been carried out to date suggest that the
4642 global mean hydrological sensitivity (i.e., the precipitation change for a unit temperature
4643 change) is similar for CCT and GHG forcing, and that simultaneous compensation of
4644 temperature and precipitation changes could thus be possible (Kristjánsson et al. 2015). This
4645 appears to hold primarily for mid- and high latitudes (Kristjánsson et al. 2015). The
4646 geographical distribution of cooling also more closely mirrors that of GHG warming. With
4647 the caveat that the literature on this topic is still limited, it therefore appears that the climate
4648 response to TRM is better suited to compensate for GHG warming than SRM. However, as
4649 noted above, whether CCT is in fact a viable STRM strategy remains unclear.

4650

4651

4652

4653 **13.4 Conclusion, key unknowns, outlook**

4654
4655

4656 STRM remains a scientifically pursued but controversial topic, and arguments have been
4657 presented in the literature for why even theoretical and modeling studies on the topic should be
4658 conducted with caution. The current understanding of the forcings associated with STRM
4659 strategies can be summarized as follows:

4660
4661 1) Stratospheric Aerosol Injection (SAI) can produce strong negative forcings, but the non-
4662 linear relationship between the injected mass and forcing is poorly understood.

4663
4664 2) Marine Sky brightening (MSB) through, for example, sea salt injection will very likely
4665 achieve negative forcings of the desired magnitude, but there is a non-negligible chance that
4666 forcing of the opposite sign could result under some conditions. Forcing per mass of injected
4667 sea salt aerosol is poorly understood, and is highly dependent on the injected aerosol size.

4668
4669 3) Ocean albedo modification could generate strong negative forcings but does not seem
4670 viable because of the likely interference with ocean ecosystems. A multi-disciplinary team of
4671 experts is needed to fully address its viability.

4672
4673 4) Proposed land surface albedo modifications are deemed ineffective for the purpose of
4674 STRM.

4675
4676 5) Mirrors in space can produce negative forcings of the desired magnitude, but viability
4677 depends on the engineering question of whether it is feasible to arrange for sufficient reflective
4678 material at the location in space where this would be optimal .

4679

4680 6) In part due to conflicting modeling results, it is still unclear whether cirrus cloud thinning
4681 (CCT) can produce sufficiently strong negative forcings to be a viable TRM strategy.

4682
4683 7) Using SAI and MCB to completely cancel global-mean GHG warming would likely cause
4684 a net reduction of precipitation relative to pre-industrial conditions. A partial compensation of
4685 global mean GHG warming could lead to a lesser effect on precipitation.

4686
4687 8) Should it prove viable as a STRM strategy, CCT appears more suited for an an offset of the
4688 climate response to increased GHG concentrations.

4689
4690 Common for many of the unknowns related to STRM strategies is that they are related to
4691 uncertainties about the unperturbed atmosphere, and to processes that are highly relevant for our
4692 understanding of the present atmosphere and anthropogenic perturbations to it. STRM research
4693 efforts are best directed towards activities which have the dual benefit of increasing
4694 understanding both of how past inadvertent and potential future advertent forcings affect the
4695 Earth's global climate system.

4696
4697

4698

4699 **14. Overall Summary and Challenges**

4700

4701

4702 **14.1 Summary**

4703

4704

4705 This paper has traced the evolution of the concept of radiative forcing over the past century. It
4706 has also described the historical milestones in the scientific community's understanding of the
4707 RF agents, their quantification including the total or net RF, and some important applications
4708 stemming from the concept. Beginning with the fundamentals of radiation physics, principally
4709 with the developments in the late 18th and through the 19th and 20th centuries to the present,
4710 that growth has established a powerful framework to quantify the factors that force the climate
4711 system by perturbing the shortwave and longwave energy disposition in the Earth System. We
4712 have focused on the forcing as defined from pre-industrial time (~1750) to present,
4713 approximately the mid-2010s. (We note that IPCC AR6 will be completing a major assessment
4714 in 2021 which will represent a major full update since the IPCC (2013) assessment). We have
4715 treated the fundamental developments by considering the major inflection points of scientific
4716 advances, more particularly as they relate to the quantification of the estimates together with the
4717 uncertainties. For some agents, such periods are well marked by times prior to approximately
4718 the 1950s (say, before the International Geophysical Year, 1957), between 1950s and the advent
4719 of the satellite era of global measurements (1979), and the onset of the major international
4720 assessments since mid-1980s. We have highlighted especially those points in time when the
4721 literature saw more robustness added to the knowledge especially with regards to quantification.
4722 The stages in growth evolved differently for the different forcing agents, with the complexity of

4723 some still hindering a rapidity of growth in confidence in the quantitative estimates (e.g.,
4724 aerosol indirect forcing).

4725
4726 The forcing concept has been conceptualized and applied with the intent to define a metric that
4727 would be helpful in providing a first-order estimate of the global-mean climate impact, and
4728 most specifically the effect on surface temperature. Perhaps the most important application has
4729 been the use of the RF estimates to comparatively estimate the climate responses due to
4730 different agents, both for policy decisions concerning mitigation and adaptation, and for the
4731 scientific understanding of the relative importance of the forcing agents. In recent years, the
4732 forcing concept has been extended to investigate the comparative impact of forcings on changes
4733 on circulation patterns, including consideration of both anthropogenic and natural forcings, and
4734 taking into account the internal variability of the climate system. The RF concept has also been
4735 used to formulate simple metrics for the warming potential of various agents and for ideas in
4736 radiation management.

4737
4738 There are several limitations encountered with both the RF and the more recent ERF concepts.
4739 These include: accounting for the growing recognition of the complexity of some of the forcers;
4740 inadequacies in characterizing and narrowing uncertainties in the determination of the forcings;
4741 uncertainties in precursor parameters to determining the forcing (e.g., preindustrial emissions);
4742 reliance on numerical models for estimates of forcing; and difficulties in achieving consistency
4743 across different numerical models and their estimates. The above issues in turn affect the
4744 synthesis of the estimate and uncertainty of the total RF of climate.

4745
4746 RF and ERF remain theoretical concepts well-suited to computational estimates and computer
4747 modeling of the climate system including the agents that drive climate change. However, there

4748 are shortcomings. These include: inability to observe/measure/quantify parameters of relevance
4749 in forcing estimates; and inability to monitor on a continuous basis key radiative flux and
4750 associated parameters to a high degree of accuracy; difficulties in verifying the theoretically-
4751 formulated radiative forcing against practically measurable observations since the latter are not
4752 rigorously able to measure the changes in the state of the system without feedbacks; theoretical
4753 (and laboratory measurement) gaps inhibiting the knowledge of the processes that lead to the
4754 agent's forcing of climate.

4755
4756 Weaknesses in the application of the concept include propagation of the uncertainties in
4757 different factors leading to the forcing estimate. This in turn affects the evaluation of the
4758 feedbacks and response due to the forcing. It also impacts linkages to detection-and-attribution
4759 of climate change, ability to link observed phenomena (e.g., extreme events) to forcing of the
4760 climate system, and narrowing uncertainties in climate projections.

4761
4762 It is important to note that the RF concept has been more than just an arbitrary or an academic
4763 formulation. It has gone beyond just a routine definition to express a metric concerning climate
4764 driving/forcing agent. Despite its limitations, there have been remarkable successes with this
4765 metric in understanding the way global climate responds to different forcings. Many findings
4766 have been demonstrated to be highly useful, e.g.: links to emissions/sources/precursors and
4767 relative effectiveness of the different forcers; ability to inter-compare models to quantify the
4768 changes in climate parameters; policy applications (e.g., GWP)s. .

4769
4770
4771 Additional relevance with regards to climate impacts are the following points:
4772

4773 • The RF concept has found usefulness in the policy context as a precursor to Global Warming
4774 Potential – paralleling Ozone Depletion Potentials in the ozone loss context. It has become
4775 possible to link RFs of forcers to their influences on surface temperature, thus allowing cross-
4776 comparison of the climate change effectiveness of different forcers. It has also enabled
4777 thinking to develop along the lines of mitigation of anthropogenic greenhouse gas effects such
4778 as in Solar Radiation Management (Royal Society, 2009).

4779
4780
4781 • RF has become intertwined in the linkage from emissions to responses. A degree of robustness
4782 has been obtained using 3D global climate models to connect RF and responses in a simple
4783 manner. This started with global-means but has also included regional-based quantitative
4784 estimates in the case of some forcers. The variable in question has been principally surface
4785 temperature, but extensions have been made to other climate parameters through physical
4786 connections (hydrologic cycle and precipitation, sea-level rise).

4787
4788 • Forcing at the TOA/tropopause, that at the surface, and their physical relevance have been
4789 identified with changes in parameters describing the physical climate change. While surface
4790 flux change does not relate easily to surface temperature change, it can be linked to
4791 hydrological cycle and precipitation. (e.g., Asian monsoon and hemispheric/global spin-down
4792 of precipitation caused by aerosols).

4793
4794 • Significance of the question: what is the Earth's climate sensitivity to radiative forcings?
4795 Estimating climate sensitivity from observed temperature changes depends crucially on our
4796 knowledge of RF. If net anthropogenic RF over the past century has been the result of a
4797 significant offset of the positive forcings by negative forcings, that would suggest a strong

4798 climate sensitivity. But if positive forcing has been the dominant type, then the system is
4799 relative less sensitive. The dependence on an accurate RF to obtain a good estimate of climate
4800 sensitivity crucially determines in turn how severe climate impacts are likely to be under the
4801 influence of increased GHG emissions in the 21st Century estimates. Accompanying this task
4802 should be the sustained monitoring of changes in aerosol and related properties e.g., aerosol
4803 optical depths, vertical profile, clear- and all-sky spectral and total radiative fluxes.

4804

4805 • Characterizing and, to the extent possible, narrowing the uncertainties in the pre-industrial state
4806 especially for short-lived climate forcers (e.g., ozone, aerosols). Non-linearities and interactions
4807 between forcings and its invariable relation to feedbacks (e.g. dependencies on cloud, water
4808 vapor, surface albedo).

4809

4810 • Continue to explore the potential for direct observation of radiative forcing (e.g., stratospheric
4811 aerosols in the aftermath of a volcanic eruption, solar irradiance, spectrally- resolved TOA and
4812 surface observations).

4813

4814 • As the ERF concept advances, clarifying and documenting the nuances that differentiate his
4815 from RF e.g., the uncertainties arising due to different treatments of physical processes in
4816 different models, efficacy factors etc.

4817

4818

4819

4820 **14.2 Important research challenges in the coming decades**
4821
4822

4823 **14.2.1 Improving the accuracy of the forcing estimate**
4824
4825

4826 The principal challenge in arriving at a definitive estimate of the net forcing since preindustrial
4827 times is made starkly evident by the IPCC Assessments. The last IPCC assessment report
4828 (2013) conclusion that the 1750-2011 net anthropogenic forcing (best estimate of 2.3 W m⁻²,
4829 with a range from 1.1 to 3.3 W m⁻²) indicates that the remaining uncertainties are very large
4830 compared to the best-estimate net forcing; this significantly hinders efforts to derive, for
4831 example, climate sensitivity given observed temperature changes, and inhibits understanding of
4832 the effectiveness of proposed mitigation pathways, with knock-on impacts on the confidence in
4833 the advice that can be given to policymakers.

4834
4835 • Ensuring GCM radiation codes faithfully represent radiative processes – with linkages to
4836 available observations. One particularly demanding task is to reduce the undesirable spread in
4837 the CO₂ forcing especially for the purposes of computing accurate climate responses in climate
4838 models. The World Climate Research Program Radiative Forcing Model Intercomparison
4839 Projects have enabled the community to calibrate models against robust reference calculations.
4840 The latest venture (Pincus et al., 2017) is expected to sustain the momentum and push the
4841 frontiers further forward.

4842
4843 • Deployment and utilization of observations from multiplicity of platforms for characterizing
4844 fully the four-dimensional distribution of forcing agents and their time evolution, especially for
4845 natural forcers such as solar irradiance and volcanic aerosols, and for short-lived climate forcers
4846 such as aerosols and related cloud microphysics, and ozone.

4847

4848 • A better process understanding of aerosol forcing and in particular aerosol-cloud interactions,
4849 which has been a main contributor to uncertainty in anthropogenic forcing.

4850

4851 **14.2.2 Computational and observational determinations that need to be carried out**
4852 **include:**

4853

4854

4855 ● Taking advantage of the rapid advances in the past few years in computational
4856 architectures, algorithmic formalisms, and computing capacities. Recent advances include the
4857 facilitation of machine learning and neural networks (e.g., Krasnopolksy et al., 2005),
4858 performing line-by-line benchmark computations over the entire global scale of a model (e.g.,
4859 Jones et al., 2017).

4860

4861 ● Processes and model parameterizations that enable translating the radiative forcing to
4862 climate change, including the physical, chemical, and dynamical responses to the forcing, and
4863 the modulation of extant circulation patterns throughout the integrated system.

4864

4865 ● Continuous monitoring of the agents (concentrations, radiative properties) with the
4866 highest possible accuracy and repeatability.

4867

4868 ● Resolution of differences among observed (to the degree feasible) and modelled absolute
4869 variations and changes in forcings.

4870

4871 ● Improving the ability of climate models to capture the responses to the natural and
4872 anthropogenic forcings, and evaluate the resulting responses to climate.

4873

4874

4875 It is sobering to realize that RF largely evolved as a theoretical concept, a simple metric to
4876 compare effects due to different forcers initially formulated for well-mixed greenhouse gases,
4877 and shown to be somewhat easily relatable to simulated surface temperature change. In the

4878 past, when running climate model calculations was computationally taxing, RF proved to be an
4879 invaluable quantifying capability. With increased computational resources now to run climate
4880 responses of single forcings or subsets of forcings or all forcings somewhat inexpensively, is
4881 RF or ERF a redundant concept? Recognizing the caveats and deficiencies noted above, and
4882 with the newer nuances in the forcing definition (e.g., adoption of ERF as the new forcing
4883 metric, Section 2), a legitimate question arises – what is the future of the radiative forcing
4884 concept?

4885
4886

4887 **14.3 Grand Challenge**

4888

4889

4890 The answer to the above question is that investigations into forcing and estimating it may no
4891 longer be independent of considerations of the rest of the climate system. For instance,
4892 adjustments (feedbacks) in climate parameters may need to be increasingly considered in order
4893 to relate to surface temperature change, which was the initial quest in determining RFs. RF and
4894 ERF remain useful physically-based constructs that, despite the fact that they cannot be in
4895 general observationally verified, still retain a simple link to climate responses, at least in the
4896 context of global-mean surface temperature.

4897

4898 Going forward, the *Grand Challenge* lies in viewing RF and forcing in general not as a separate
4899 entity in the trinity of forcing, feedback, and response, but to put it into a broader perspective. A
4900 picture of this might comprise looking at the Earth System in its broader scope than just
4901 temperature and only the physical climate system. Instead, in combining forcing, feedback, and
4902 response – we are entering the era of an Earth System challenge that needs to account for
4903 feedbacks e.g., ERF departs from RF in allowance for fast feedbacks to be factored into the
4904 forcing estimate (Section 2). This increase in complexity is manifest for the various forcing
4905 agents (Sections 3-9). These complexities then add to the body of uncertainties in the net
4906 forcing and its applications (Sections 10-13), with concomitant impacts on societal adaptation
4907 and mitigation planning and measures. There are thus significant facets to the Grand Challenge
4908 regarding the application of RF and ERF in the future and the societal utilization of this science
4909 for decision-making.

4910

4911 Radiative forcing in the climate science and climate change context is emerging after a century
4912 of exploration and investigations with a firm qualitative sense but still with limitations in its
4913 quantitative certainty. There is considerable ground still to be covered in order to achieve a
4914 comprehensive resolution of the remaining uncertainties while retaining the simplicity of the
4915 concept, and meeting the demand for more accurate quantification of both the agent-wise and
4916 net anthropogenic forcing.

4917

4918

4919 **APPENDIX**

4920

4921 AATSR: Advanced Along Track Scanning Radiometer

4922 ACCENT: Atmospheric Composition Change: the European NeTwork of excellence

4923 ACCMIP: Atmospheric Chemistry and Climate Model Intercomparison Project

4924 ACE: [Aerosol Characterization Experiment](#)

4925 ACI: Aerosol cloud interactions

4926 ACP: Atmospheric Chemistry and Physics

4927 ACRIM: Active Cavity Radiometer Irradiance Monitor

4928 ACRIM3: ACRIM 3

4929 ACRIMSAT: Active Cavity Radiometer Irradiance Monitor Satellite

4930 AERONET Aerosol Robotic Network

4931 AFCRL: [Air Force Cambridge Research Laboratory](#)

4932 AGCM: Atmospheric General Circulation Model

4933 AIRS: Atmospheric Infrared Sounder

4934 AMOC: Atlantic Meridional Overturning Circulation

4935 AMS: Aerosol Mass Spectrometer

4936

4937 AOD: Aerosol Optical Depth

4938 AQUA: an Earth observing satellite mission

4939 MODIS AQUA in the name of the platform

4940 AR: Assessment Report

4941 AR4: Fourth Assessment Report

4942 AR5: Fifth Assessment Report

4943 AR6: Sixth Assessment Report

4944 ARM: Atmospheric Radiation Measurements

4945

4946 ARs: Assessment Reports

4947

4948 AVHRR: Advanced Very High Resolution Radiometer

4949 AerChemMIP: Aerosols and Chemistry Model Intercomparison Project

4950 BAMS: Bulletin of the American Meteorological Society

4951 BC: Black Carbon

4952 BGC: Biogeochemistry

4953

4954 C4MIP: Coupled Climate-Carbon Cycle Model Intercomparison Project

4955 CALIOP: Cloud-aerosol Lidar with Orthogonal Polarization

4956 CALIPSO: Cloud-Aerosol Lidar and Infrared Pathfinder Satellite Observation

4957	CAM: Community Atmospheric Model
4958	CATS: Cloud-Aerosol Transport System
4959	CCM: chemistry-climate model
4960	CCN: Cloud condensation nuclei
4961	CCSP: Climate Change Science Program
4962	CCT: Cirrus cloud thinning
4963	CDNC: Cloud droplet number concentration
4964	CDR: Carbon dioxide Removal
4965	CERES: Clouds and the Earth's Radiant Energy System
4966	CF4: Carbon tetrafluoride
4967	CFC:chlorofluorocarbon
4968	CFCs: chlorofluorocarbons
4969	CH4: methane
4970	
4971	CICERO: Centre for International Climate and Environmental Research
4972	CLARIFY Cloud aerosol interaction and forcing
4973	CLM4: Community Land Model Version 4
4974	CM2: GFDL's Coupled Model version 2
4975	CMIP: Coupled Model Intercomparison Project

4976 CMIP3: Coupled Model Intercomparison Project Phase 3

4977 CMIP5: Coupled Model Intercomparison Project Phase 5

4978 CMIP6: Coupled Model Intercomparison Project Phase 6

4979 CO: carbon monoxide

4980 CO2: Carbon dioxide

4981 CTM: Chemistry Transport Model

4982

4983

4984 DIRTMAP: The geological map of dust

4985 DMS: Dimethyl Sulfide

4986 DU: Dobson Unit

4987 ECHAM: climate model developed at the Max Planck Institut fur Meteorologie,

4988 Hamburg

4989 ECHAM4: ECHAM version 4

4990 ECHAM5: ECHAM version 5

4991 ECMWF: European Centre for Medium-Range Weather Forecasting

4992 EESC: effective equivalent stratospheric chlorine

4993 ENSO: El Nino Southern Oscillation

4994 ERF: effective radiative forcing

4995 ERFs: effective radiative forcings

4996	ESM: Earth System Model
4997	
4998	FAR: First Assessment Report
4999	FDH: Fixed Dynamical Heating
5000	FFBC – fossil fuel black carbon
5001	FFOC – fossil fuel organic carbon
5002	
5003	GCM: General Circulation Model
5004	GCTMs: Global Chemical Transport Models
5005	GEISA – Gestion et Etude des Informations Spectroscopiques Atmosphériques
5006	GFDL: Geophysical Fluid Dynamics Laboratory
5007	GHG: Greenhouse gas
5008	GISS: Goddard Institute for Space Studies
5009	GWP: Global Warming Potential
5010	GWP _s : Global Warming Potentials
5011	GeoMIP: geoengineering model intercomparison project
5012	
5013	H ₂ S Hydrogen Sulfide
5014	H ₂ SO ₄ Sulfuric Acid

5015	HALOE: Halogen Occultation Experiment
5016	HCFC -- Hydrochlorofluorocarbons
5017	HCFCs -- Hydrochlorofluorocarbons
5018	HFCs -- Hydroflourocabons
5019	
5020	HIRS: High resolution Infrared Sounder
5021	HITRAN -- High-resolution transmission molecular absorption
5022	HITRAN2016 – HITRAN version issues in 2016
5023	HNO ₃ : Nitric Acid
5024	HO ₂ : Peroxy hydroxyl
5025	HadGEM2: UK Hadley Centre Global Environment Model version 2
5026	
5027	IEEE: Institute of Electrical and Electronic Engineers
5028	IGY: International Geophysical Year
5029	
5030	IPCC: Intergovernmental Panel on Climate Change
5031	IR: Infrared Radiation
5032	IRF: Instantaneous radiative forcing
5033	IRIS: Interface Region Imaging Spectrograph

5034	IS92: An emissions scenario
5035	ISAMS: Improved Stratospheric and Mesospheric Sounder
5036	ISCCP: International Satellite Cloud Climatology Project
5037	ISS: international Space Station
5038	ITCZ: InterTropical Convergence Zone
5039	
5040	JAS: Journal of the Atmospheric Sciences
5041	
5042	LASIC: Layered Atlantic Smoke Interactions with Clouds
5043	LBL: Line-by-line
5044	LH: Latent heat
5045	LMD – Laboratoire de Meteorologie Dynamique
5046	
5047	LOSU: level of scientific understanding
5048	LULCC: Land Use Land Cover Change
5049	LUMIP Land use model intercomparison Project
5050	LW: Longwave radiation
5051	
5052	MEGAN Model of Emissions of Gases and Aerosols from Nature

5053	MIPAS: Michelson Interferometer for Passive Atmospheric Sounding
5054	MIPs: Model Intercomparison Projects
5055	MISR: multi-angle imaging spectroradiometer
5056	MIT: Massachusetts Institute of Technology
5057	ML: Mixed Layer
5058	
5059	MODIS: moderate resolution imaging spectrometer
5060	MSB: Marine sky brightening
5061	MSU: microwave sounding unit
5062	
5063	NASA: National Aeronautics and Space Administration
5064	NATO: North Atlantic Treaty Organization
5065	NCAR: National Center for Atmospheric Research
5066	NERC: Natural environment research council
5067	NH ₃ : ammonia
5068	NMHCs: Non-methane hydrocarbons
5069	NO: nitrogen oxide
5070	NO ₂ : nitrogen dioxide
5071	NOAA: National Oceanic Atmospheric Administration

5072	NOx: nitrogen oxides
5073	N2: Nitrogen
5074	NRC: National Research Council
5075	NRLTSI2: Naval Research laboratory Total Solar Irradiance 2
5076	NRLSSI2: Naval Research Laboratory Solar Spectral Irradiance 2
5077	
5078	
5079	OCS: Carbonyl Sulfide
5080	ODSs: Ozone Depleting Substances
5081	OH: hydroxyl
5082	OK: Oklahoma
5083	OMI: ozone monitoring instrument
5084	OMPS: ozone mapping and profiling suite
5085	ORACLES: ObseRvations of Aerosols above CLouds and their intEractiOnS
5086	OSIRIS: Optical Spectrograph and InfraRed Imaging System
5087	
5088	PARASOL: Polarization and Anisotropy of Reflectances for Atmospheric Sciences
5089	PD: present-day
5090	PDF: probability distribution function

5091

5092 PI: pre-industrial

5093 PMIP: Paleoclimate Model Intercomparison Project

5094 PMIP4: Paleoclimate Model Intercomparison Project (version 4)

5095 PMOD: Physikalisch-Meteorologisches Observatorium Davos

5096 PNAS: Proceedings of the National Academy of Sciences

5097 POAM: Polar Ozone and Aerosol Measurement

5098 POLDER: POLarization and Directionality of the Earth's Reflectances

5099 PSD: Particle Size Distribution

5100

5101

5102 QBO: Quasi-Biennial Oscillation

5103

5104 RCP2.6: Representative Concentration Pathway 2.6

5105 RCP8.5: Representative Concentration Pathway 8.5

5106 RCPs: Representative Concentration Pathways

5107 RE: Radiative efficiency

5108 REs: Radiative efficiencies

5109 RF: Radiative forcing

5110 RFMIP: Radiative Forcing Model Intercomparison Project

5111 RFP: Radiative Flux Perturbation

5112 RFs: Radiative forcings

5113 RH: Relative Humidity

5114

5115 SA: South Africa

5116 SAFARI: Southern African Regional Science Initiative

5117 SAGE: Stratospheric Gas and Aerosol Experiment

5118 SAI: Stratospheric aerosol injection

5119 SAR: Second Assessment Report

5120 SATIRE: Spectral and Total Irradiance Reconstruction

5121

5122 SBUV Solar Backscatter Ultraviolet

5123 SCHIAMACHY (this is wrong abbreviation)

5124 SCIAMACHY SCanning Imaging Absorption SpectroMeter for Atmospheric

5125 CHartographY SCanning

5126

5127 SF6: sulfur hexafluoride

5128 SH: sensible heat

5129 SKYHI: generic name for a general circulation model at NOAA/Geophysical Fluid
5130 Dynamics Laboratory

5131 SLCF: short-lived climate forcer

5132

5133 SME Solar Mesosphere Explorer

5134 SMIC: Study of Man's Impact on Climate (a report)

5135 SMM Solar Maximum Mission

5136 SO2: Sulfur Dioxide

5137 SOHO Solar Heliospheric Observatory

5138 SORCE Solar Radiation and Climate Experiment

5139 SPARC: Stratospheric Tropospheric Processes and their Role in Climate

5140 SRM: solar radiation management

5141 SST: sea surface temperature

5142 SSTs: sea surface temperatures

5143

5144 STRM: Solar and terrestrial radiation management

5145 SUCCESS

5146 SW: Shortwave radiation

5147

5148 TAR: Third Assessment Report

5149	TERRA: name of MODIS satellite
5150	TIM Total Irradiance Monitor
5151	TOA: top of atmosphere
5152	TOMS: total ozone mapping spectrometer
5153	TRM: Terrestrial radiation management
5154	TSI Total Spectral Irradiance
5155	TSIS Total and Spectral Irradiance Sensor
5156	TTL Tropical Tropopause Layer
5157	
5158	UARS Upper Atmosphere Research Satellite
5159	UK: United Kingdom
5160	UKCA: UK chemistry and aerosol
5161	UM: Unified Model
5162	UN: United Nations
5163	UNFCCC: United Nations Framework Convention on Climate Change
5164	US : United States
5165	USA: United States of America
5166	UV: Ultraviolet
5167	VIRGO: a French-Italian project

5168 VIIRS: Visible Infrared Imaging Radiometer Suite

5169 VolMIP: Volcanic Forcings Model Intercomparison Project

5170 WACCM: Whole Atmosphere Community Climate Model

5171 WCRP – World Climate Research Programme

5172 WGI – Working Group I

5173 WMGHG: Well-mixed greenhouse gas

5174 WMGHGs: Well-mixed greenhouse gases

5175 WMO: World Meteorological Organization |

5176

5177

5178

REFERENCES

5179

5180 Aamaas, B., T. K. Berntsen, J. S. Fuglestvedt, K. P. Shine, and W. J. Collins, 2017: Regional
5181 temperature change potentials for short-lived climate forcers based on radiative forcing
5182 from multiple models, *Atmos. Chem. Phys.*, **17**, 10795-10809, <https://doi.org/10.5194/acp-17-10795-2017>

5184 Abbott, C.G. and Fowle, F.E. (1908). Recent determination of the solar constant of
5185 radiation. *Terr. Magnetism and Atmos. Electricity* 13: doi: 10.1029/TE013i002p00079. issn:
5186 0096-8013.

5187 Ackerman, Andy S., O. B. Toon, D. E. Stevens, A. J. Heymsfield, V. Ramanathan, and E. J.
5188 Welton. Reduction of tropical cloudiness by soot. *Science* 288, no. 5468 (2000): 1042-1047.

5189 Adams, J. B., M. E. Mann, and C. M. Ammann (2003), Proxy evidence for an El Nino-like
5190 response to volcanic forcing. *Nature*, 426, 274-278.

5191 Adams, P. J., Seinfeld, J. H., Koch, D., Mickley, L., & Jacob, D. (2001). General circulation
5192 model assessment of direct radiative forcing by the sulfate-nitrate-ammonium-water
5193 inorganic aerosol system. *Journal of Geophysical Research: Atmospheres*, 106(D1), 1097-
5194 1111.

5195 Ahlm, L., A. Jones, W. C. Stjern, H. Muri, B. Kravitz, and J. E. Kristjánsson, 2017: Marine
5196 cloud brightening - As effective without clouds. *Atmos. Chem. Phys.*, doi:10.5194/acp-17-
5197 13071-2017.

5198 Albani, S., Balkanski, Y., Mahowald, N., Winckler, G., Maggi, V. and Delmonte, B.: Aerosol-
5199 Climate Interactions During the Last Glacial Maximum, *Curr. Clim. Chang. Reports*, 4(2),
5200 99–114, doi:10.1007/s40641-018-0100-7, 2018.

5201 Albrecht, B. A. Aerosols, cloud microphysics, and fractional cloudiness. *Science* **245**, 1227-1230
5202 (1989).

5203 Alexander, B., and L. J. Mickley, 2015: Paleo-Perspectives on Potential Future Changes in the

5204 Oxidative Capacity of the Atmosphere Due to Climate Change and Anthropogenic
5205 Emissions. *Curr. Pollut. Reports*, **1**, 57–69, doi:10.1007/s40726-015-0006-0.

5206 Allen, R. J., Evan, A. T. & Booth, B. B. Interhemispheric aerosol radiative forcing and tropical
5207 precipitation shifts during the late twentieth century. *J. Clim.* **28**, 8219-8246 (2015).

5208 Alterskjær, K., and J. E. Kristjánsson, 2013: The sign of the radiative forcing from marine cloud
5209 brightening depends on both particle size and injection amount. *Geophys. Res. Lett.*,
5210 doi:10.1029/2012GL054286.

5211 —, —, and Ø. Seland, 2012: Sensitivity to deliberate sea salt seeding of marine clouds –
5212 observations and model simulations. *Atmos. Chem. Phys.*, **12**, 2795–2807, doi:10.5194/acp-
5213 12-2795-2012. <https://www.atmos-chem-phys.net/12/2795/2012/> (Accessed December 20,
5214 2018).

5215 Altshuller, A. P., and J. J. Bufalini, 1965: Photochemical aspects of air pollution: a review.
5216 *Photochem. Photobiol.*, **4**, 97–146, doi:doi:10.1111/j.1751-1097.1965.tb05731.x.
5217 <https://doi.org/10.1111/j.1751-1097.1965.tb05731.x>.

5218 Amman, C., G. Meehl, W. Washington, and C. Zender (2003), A monthly and latitudinally varying
5219 forcing dataset in simulations of 20th century climate. *Geophys Res Lett*, **30**, 1657.

5220 Anchukaitis, K. J., B. M. Buckley, E. R. Cook, B. I. Cook, R. D. D'Arrigo, and C. M. Ammann
5221 (2010), Influence of volcanic eruptions on the climate of the Asian monsoon region.
5222 *Geophysical Research Letters*, **37**, L22703.

5223 Andela, N., Morton, D. C., Giglio, L., Chen, Y., Van Der Werf, G. R., Kasibhatla, P. S., DeFries,
5224 R. S., Collatz, G. J., Hantson, S., Kloster, S., Bachelet, D., Forrest, M., Lasslop, G., Li, F.,
5225 Mangeon, S., Melton, J. R., Yue, C. and Randerson, J. T.: A human-driven decline in global
5226 burned area, *Science* (80-.), **356**(6345), 1356–1362, doi:10.1126/science.aal4108, 2017.

5227 Anderson, T. R., E. Hawkins, and P. D. Jones, 2016: CO₂, the greenhouse effect and global
5228 warming: from the pioneering work of Arrhenius and Callendar to today's Earth
5229 System Models. *Endeavor*, **40**, 3, pp178-187.
5230 <https://doi.org/10.1016/endeavour.2016.07.002>

5231 Andersson, S., B. Martinsson, J.-P. Vernier, J. Friberg, C. A. M. Brenninkmeijer, M. Hermann, P.
5232 van Velhoven, and A. Zahn (2014), Significant radiative impact of volcanic aerosol in the
5233 lowermost stratosphere, *Nature Communications*, doi:10.1038/NCOMMS8692.

5234 Andreae, M. O. and Merlet, P.: Emission of trace gases and aerosols from biomass burning,
5235 *Global Biogeochem. Cycles*, 15(4), 955–966, 2001.

5236 Andrews, T. and Forster, P.: CO₂ forcing induces semi-direct effects with consequences for
5237 climate feedback interpretations, *Geophysical Research Letters*, 35, L04802, 2008.

5238 Andrews, T., Forster, P., Boucher, O., Bellouin, N. and Jones, A.: Precipitation, radiative forcing
5239 and global temperature change, *Geophysical Research Letters*, 37, L14701, 2010.

5240 Andrews, T., Gregory, J. M., Forster, P. M. and Webb, M. J.: Cloud Adjustment and its Role in
5241 CO₂ Radiative Forcing and Climate Sensitivity: A Review, *Surveys in Geophysics*, 33(3-4),
5242 619-635, 2012.

5243 Andrews, T. (2014). Using an AGCM to diagnose historical effective radiative forcing and
5244 mechanisms of recent decadal climate change. *Journal of Climate*, 27(3), 1193-1209.

5245 Angel, R., 2006: Feasibility of cooling the Earth with a cloud of small spacecraft near the inner
5246 Lagrange point (L1). *Proc. Natl. Acad. Sci.*, doi:10.1073/pnas.0608163103.

5247 Antico, A., and M. E. Torres, 2015: Evidence of a decadal solar signal in the Amazon River:
5248 1903 to 2013, *Geophys. Res. Lett.*, 42, doi:10.1002/2015GL066089.

5249 Antuña, J. C., A. Robock, G. L. Stenchikov, J. Zhou, C. David, J. Barnes, and L. Thomason (2003),
5250 Spatial and temporal variability of the stratospheric aerosol cloud produced by the 1991
5251 Mount Pinatubo eruption. *J Geophys Res*, 108, 4624.

5252 Aquila, V., L. D. Oman, R. S. Stolarski, P. R. Colarco, and P. A. Newman (2012), Dispersion of
5253 the volcanic sulfate cloud from a Mount Pinatubo-like eruption. *Journal of Geophysical
5254 Research-Atmospheres*, 117, D06216.

5255 Aquila, V., C. I. Garfinkel, P. A. Newman, L. D. Oman, and D. W. Waugh (2014), Modifications
5256 of the quasi-biennial oscillation by a geoengineering perturbation of the stratospheric aerosol
5257 layer. *Geophysical Research Letters*, 41, 1738-1744.

5258 Archer, D., and S. Ramstorf, 2010: The Climate Crisis, ISBN 978-0-521-73255-0
5259 (paperback version). Cambridge University Press, 250 pages.

5260 Arfeuille, F., and Coauthors (2013), Modeling the stratospheric warming following the Mt.
5261 Pinatubo eruption: uncertainties in aerosol extinctions. *Atmos Chem Phys*, 13, 11221-11234.

5262 Armour, K. C., C. M. Bitz, and G. H. Roe (2013), Time-varying climate sensitivity from regional
5263 feedbacks, *J. Clim.*, 26, 4518–4534, doi:10.1175/jcli-d-12-00544.1.

5264 Arneth, A., Harrison, S., Zaehle, S., Tsigaridis, K., Menon, S., Bartlein, P., Feichter, J., Korhola,
5265 A., Kulmala, M., O'Donnell, D., Schurgers, G., Sorvari, S. and Vesala, T.: Terrestrial
5266 biogeochemical feedbacks in the climate system, *Nature-geoscience*, 3, 525–532; DOI:
5267 10.1038/NGEO905, 2010.

5268 Arrhenius, S., 1896: On the influence of carbonic acid in the air upon the temperature of the
5269 ground. *Phil. Mag. and J. Science*, Ser. 5, vol. 41, pp 237-276.

5270

5271 Bala, G., Caldeira, K. and Nemani, R.: Fast versus slow response in climate change: implications
5272 for the global hydrological cycle, *Climate Dynamics*, 35(2-3), 423-434, 2010.

5273 Bala, G., P. B. Duffy, and K. E. Taylor, 2008: Impact of geoengineering schemes on the global
5274 hydrological cycle. *Proc. Natl. Acad. Sci.*, doi:10.1073/pnas.0711648105.

5275 Balmaseda, M. A., K. Mogensen, and A. T. Weaver (2013), Evaluation of the ECMWF ocean
5276 reanalysis system ORAS4. *Quarterly Journal of the Royal Meteorological Society*, 139,
5277 1132-1161.

5278 Baran, A. J., and J. S. Foot (1994), New application of the operational sounder HIRS in
5279 determining a climatology of sulphuric acid aerosol from the Pinatubo eruption, *J. Geophys.*
5280 *Res.*, 99(D), 25,673–25,679, doi:10.1029/94JD02044.

5281 Ban-Weiss, G., Cao, L., Bala, G. and Caldeira, K.: Dependence of climate forcing and response
5282 on the altitude of black carbon aerosols, *Climate Dynamics*, 897-911, 2011.

5283 Banerjee, A., A. C. Maycock, A. T. Archibald, N. L. Abraham, P. Telford, P. Braesicke, and J.
5284 A. Pyle, 2016: Drivers of changes in stratospheric and tropospheric ozone between year
5285 2000 and 2100. *Atmos. Chem. Phys.*, **16**, 2727–2746, doi:10.5194/acp-16-2727-2016.
5286 <https://www.atmos-chem-phys.net/16/2727/2016/> (Accessed October 1, 2018).

5287 Bardeen, C. G., O. B. Toon, E. J. Jensen, D. R. Marsh, and V. L. Harvey (2008), Numerical
5288 simulations of the three-dimensional distribution of meteoric dust in the mesosphere and
5289 upper stratosphere, *J. Geophys. Res.*, 113, D17202, doi:10.1029/2007JD009515.

5290 Barnes, J. E., and D. J. Hofmann (1997), Lidar measurements of stratospheric aerosol over Mauna
5291 Loa, *Geophys. Res. Lett.*, 24, 1923-1926.

5292 Barriopedro, D., R. García-Herrera, and R. Huth, 2008: Solar modulation of Northern
5293 Hemisphere winter blocking, *J. Geophys. Res.*, 113, D14118, doi:10.1029/2008JD009789.

5294 Bates, D. R., and M. Nicolet, 1950: The photochemistry of atmospheric water vapor. *J. Geophys.*
5295 *Res.*, **55**, 301–327, doi:doi:10.1029/JZ055i003p00301.
5296 <https://doi.org/10.1029/JZ055i003p00301>.

5297 Bates, D. R., and A. E. Witherspoon, 1952: The photochemistry of some minor constituents of
5298 the Earth's atmosphere (CO₂, CO, CH₄, N₂O)*. *Geophys. J. Int.*, **6**, 324,
5299 doi:doi:10.1111/j.1365-246X.1952.tb03020.x. <https://doi.org/10.1111/j.1365-246X.1952.tb03020.x>.

5301 Baumgardner, D., J. E. Dye, R. G. Knollenberg and B. W. Gandrud (1992), Interpretation of
5302 measurements made by the FSSP-300X during the Airborne Arctic Stratospheric Expedition,
5303 *J. Geophys. Res.*, 97, 8035-8046.

5304 Bellouin, N. Boucher, O., Haywood, J.M., and Reddy, M.S., Global estimate of aerosol direct
5305 radiative forcing from satellite measurements, *Nature*, 428, doi: 10.1038/nature04348, 2005.

5306 Bellouin, N., J. Rae, A. Jones, C. Johnson, J.M. Haywood , O. Boucher Aerosol forcing in the
5307 CMIP5 simulations by HadGEM2-ES and the role of ammonium nitrate, *J Geophys. Res.*,
5308 doi:10.1029/2011JD016074, 2011.

5309

5310

5311 Berdahl, M., Alan Robock, Duoying Ji, John C. Moore, Andy Jones, Ben Kravitz, and Shingo
5312 Watanabe, 2014: Arctic cryosphere response in the Geoengineering Model Intercomparison
5313 Project G3 and G4 scenarios, *J. Geophys. Res. Atmospheres*.
5314 <https://doi.org/10.1002/2013JD020627>

5315

5316 Berntsen, T. K., I. S. A. Isaksen, G. Myhre, J. S. Fuglestvedt, F. Stordal, T. A. Larsen, R. S.
5317 Freckleton, and K. P. Shine, 1997: Effects of anthropogenic emissions on tropospheric
5318 ozone and its radiative forcing. *J. Geophys. Res. Atmos.*, **102**, 28101–28126,
5319 doi:doi:10.1029/97JD02226. <https://doi.org/10.1029/97JD02226>.

5320 Bindoff, N.L., P.A. Stott, K.M. AchutaRao, M.R. Allen, N. Gillett, D. Gutzler, K. Hansingo, G.
5321 Hegerl, Y. Hu, S. Jain, I.I. Mokhov, J. Overland, J. Perlitz, R. S. and X. Z., 2013:
5322 Detection and attribution of climate change: From global to regional. *Climate Change 2013*
5323 *the Physical Science Basis: Working Group I Contribution to the Fifth Assessment Report*
5324 *of the Intergovernmental Panel on Climate Change*.

5325 Bingen, C., D. Fussen, and F. Vanhellemont (2004a), A global climatology of stratospheric aerosol
5326 size distribution parameters derived from SAGE II data over the period 1984 – 2000: 1.
5327 Methodology and climatological observations, *J. Geophys. Res.*, 109, D06201.

5328 Bingen, C., D. Fussen, and F. Vanhellemont (2004b), A global climatology of stratospheric aerosol
5329 size distribution parameters derived from SAGE II data over the period 1984–2000: 2.
5330 Reference data, *J. Geophys. Res.*, 109, D06202.

5331 Bischoff T, Schneider T (2014), Energetic constraints on the position of the intertropical
5332 convergence zone, *J Clim.*, 27(13), 4937–4951

5333 Bischoff T, Schneider T (2016), The equatorial energy balance, ITCZ position, and double-ITCZ
5334 bifurcations, *J Clim.*, 29(8), 2997–3013.

5335 Bock, L., and U. Burkhardt (2016), Reassessing properties and radiative forcing of contrail cirrus
5336 using a climate model, *J. Geophys. Res. Atmos.*, 121, 9717–9736,
5337 doi:10.1002/2016JD025112.

5338 Bock, L. and Burkhardt, U.: Contrail cirrus radiative forcing for future air traffic, *Atmos. Chem.*
5339 *Phys.*, 19, 8163-8174, <https://doi.org/10.5194/acp-19-8163-2019>, 2019.

5340 Bolin, B. and Charlson, R. J. (1976), On the role of the tropospheric sulfur cycle in the
5341 shortwave radiative climate of the earth, *Ambio* 5,47-54.

5342 Bollasina, M. A., Ming, Y. & Ramaswamy, V. Anthropogenic aerosols and the weakening of the
5343 South Asian summer monsoon. *Science* **334**, 502-505 (2011).

5344 Bonan, G.: Forests and climate change: Forcings, Feedbacks and the Climate Benefits of Forests,
5345 *Science* (80- .), 320, 1444–1448; DOI: 10.1126/science.1155121, 2008.

5346 Bond, T. C., and Coauthors, 2013: Bounding the role of black carbon in the climate system: A
5347 scientific assessment. *J. Geophys. Res. Atmos.*, **118**, 5380–5552, doi:10.1002/jgrd.50171.

5348 Bony, S., and Coauthors, 2006: How Well Do We Understand and Evaluate Climate Change
5349 Feedback Processes? *J. Clim.*, 19, 3445–3482, doi:10.1175/JCLI3819.1.
5350 <https://doi.org/10.1175/JCLI3819.1>.

5351 Borrmann S., A. Thomas, V. Rudakov, V. Yushkov, B. Lepuchov, T. Deshler, N. Vinnichenko,
5352 V. Khattatov, L. Stefanutti (2000), Stratospheric aerosol measurements in the Arctic winter
5353 of 1996/1997 with the M-55 Geophysika high-altitude research aircraft, *Tellus B*, 52 (4),
5354 1088-1103.

5355 Boucher, O., and J. Haywood, 2001: On summing the components of radiative forcing of climate
5356 change. *Clim. Dyn.*, **18**, 297–302.

5357 Boucher, O. *et al.* Clouds and Aerosols. In: *Climate Change 2013: The Physical Science Basis.*
5358 *Contribution of Working Group I to the Fifth Assessment Report of the Intergovernmental*
5359 *Panel on Climate Change* (eds Stocker TF, et al.) (Cambridge Univ. Press, 2013).

5360 Boucher, O., and U. Lohmann, 1995: The sulfate-CCN-cloud albedo effect - a sensitivity study
5361 with 2 general-circulation models. *Tellus Ser. B-Chemical Phys. Meteorol.*, 47, 281–300.

5362 Boucher, O., Randall, D., Artaxo, P., Bretherton, C., Feingold, G., Forster, P., Kerminen, V.-M.,
5363 Kondo, Y., Liao, H., Lohmann, U., Rasch, P., Satheesh, S. K., Sherwood, S., Stevens, B.
5364 and Zhang, X.-Y., Clouds and Aerosols. In: *Climate Change 2013: The Physical Science*
5365 *Basis. Contribution of Working Group I to the Fifth Assessment Report of the*
5366 *Intergovernmental Panel on Climate Change.* T. F. Stocker, D. Qin, G.-K. Plattner, M.
5367 Tignor, S. K. Allen et al. (Editors), Cambridge University Press, Cambridge, United
5368 Kingdom and New York, NY, USA, pp. 571-657, 2013.

5369 Boucher, O. (1995). GCM estimate of the indirect aerosol forcing using satellite-retrieved cloud
5370 droplet effective radii. *Journal of climate*, 8(5), 1403-1409.

5371 Boucher, O., & Anderson, T. L. (1995). General circulation model assessment of the sensitivity of
5372 direct climate forcing by anthropogenic sulfate aerosols to aerosol size and chemistry. *Journal*
5373 *of Geophysical Research: Atmospheres*, 100(D12), 26117-26134.

5374 Boucher, O., & Lohmann, U. (1995). The sulfate-CCN-cloud albedo effect. *Tellus B: Chemical*
5375 *and Physical Meteorology*, 47(3), 281-300.

5376 Boucher, O., et al., 1998. Intercomparison of models representing direct shortwave radiative
5377 forcing by sulfate aerosols. *J. Geophys. Res.*, 103, 16979-16998.

5378 Boucher, O., & Tanré, D. (2000). Estimation of the aerosol perturbation to the Earth's radiative
5379 budget over oceans using POLDER satellite aerosol retrievals. *Geophysical research letters*,
5380 27(8), 1103-1106.

5381 Boucher, O., and Haywood, J.M., 2001. On summing the components of radiative forcing of
5382 climate change. *Climate Dynamics*, 18, 297-302.

5383 Boucher, O., Randall, D., Artaxo, P., Bretherton, C., Feingold, G., Forster, P., Kerminen, V.-M.,

5384 Kondo, Y., Liao, H., Lohman, U., Rasch, P., Satheesh, S., Sherwood, S., Stevens, B.,
5385 Zhang, X.-Y., Lohmann, U., Rasch, P., Satheesh, S., Sherwood, S., Stevens, B. and Zhang,
5386 X.-Y.: Clouds and Aerosols, in Climate Change 2013: The Physical Science Basis.
5387 Contribution of Working Group I to the Fifth Assessment Report of the Intergovernmental
5388 Panel on Climate Change, edited by V. B. and P. M. M. Stocker, T.F., D. Qin, G.-K.
5389 Plattner, M. Tignor, S.K. Allen, J. Boschung, A. Nauels, Y. Xia, pp. 573–657, Cambridge
5390 University Press, United Kingdom., 2013.

5391 Bourassa, A. E., Degenstein, D. A., Gattinger, R. L., and Llewellyn, E. J. (2007), Stratospheric
5392 aerosol retrieval with OSIRIS limb scatter measurements, *J. Geophys. Res.*, 112, D10 217,
5393 doi:10.1029/2006JD008079.

5394 Bourassa, A. E., Degenstein, D. A., and Llewellyn, E. J. (2008), Retrieval of stratospheric aerosol
5395 size information from OSIRIS limb scattered sunlight spectra, *Atmos. Chem. Phys.*, 8, 6375-
5396 6380.

5397 Bousquet, P., D. A. Hauglustaine, P. Peylin, C. Carouge, and P. Ciais, 2005: Two decades of OH
5398 variability as inferred by an inversion of atmospheric transport and chemistry of methyl
5399 chloroform. *Atmos. Chem. Phys.*, 5, 2635–2656, doi:10.5194/acp-5-2635-2005.
5400 <https://www.atmos-chem-phys.net/5/2635/2005/>.

5401 Bovensmann, H. Burrows, J. P., Buchwitz, M., Frerick, J., Noël, S., Rozanov et al. (1999),
5402 SCIAMACHY: Mission Objectives and Measurement Modes, *J. Atmos. Sci.*, 56, 127 – 150,
5403 doi: 10.1175/1520-0469.

5404 Brasseur, G. P., 2009: Implications of Climate Change for Air Quality. *WMO Bulletin*, 10–15.

5405 Brasseur, G., and C. Granier (1992), Mount Pinatubo aerosols, chlorofluorocarbons and ozone
5406 depletion. *Science*, 257, 1239–1242.

5407 Brasseur, G. P., J. T. Kiehl, J.-F. Müller, T. Schneider, C. Granier, X. Tie, and D. Hauglustaine,
5408 1998: Past and future changes in global tropospheric ozone: Impact on radiative forcing.
5409 *Geophys. Res. Lett.*, 25, 3807–3810, doi:doi:10.1029/1998GL900013.
5410 <https://doi.org/10.1029/1998GL900013>.

5411 Brenguier, J.-L., P. Y. Chuang, Y. Fouquart, D. W. Johnson, F. Parol, H. Pawlowska, J. Pelon, L.
5412 Schueller, F. Schroeder, and J. Snider, An overview of the ACE-2 CloudyColumn Closure
5413 Experiment, *Tellus, Ser. B*, 52, 815–827, 2000a.

5414 Brimblecombe, P., Bowler, C. (1990) Air pollution history, York 1850–1900,
5415 in: Brimblecombe, P., Pfister, C. (editors), *The Silent Countdown*, pp. 182–195,
5416 Springer Verlag.

5417 Brock, C. A., P. Hamill, J. C. Wilson, H. H. Jonsson, and K. R. Chan (1995), Particle formation
5418 in the upper tropical troposphere: A source of nuclei for the stratospheric aerosol, *Science*,
5419 270(5242), 1650–1653, doi:10.2307/2887916.

5420 Broccoli, A., K. Dixon, T. Delworth, T. Knutson, and R. Stouffer (2003), Twentieth-century
5421 temperature and precipitation trends in ensemble climate simulations including natural and
5422 anthropogenic forcing. *J Geophys Res*, 108, 4798.

5423 Bryan, K., S. Manabe, and M. Spelman, 1988: Interhemispheric asymmetry in the transient
5424 response of a coupled ocean-atmosphere model to a CO₂ forcing. *J. Phys.*
5425 *Oceanography*, **18(6)**, 851-867.

5426 Bluth, G. J. S., S. D. Doiron, C. C. Schnetzler, A. J. Krueger and L. S. Walter (1992), Global
5427 tracking of the SO₂ clouds from the June 1991 Mount Pinatubo eruptions, *Geophys. Res.*
5428 *Lett.*, 19, 151-154.

5429 Bluth, G. J. S., C. C. Schnetzler, A. J. Krueger and L. S. Walter (1993), The contribution of
5430 explosive volcanism to global atmospheric sulphur dioxide concentrations, *Nature*, 366, 327-
5431 329.

5432 Bruhl, C., J. Lelieveld, P. J. Crutzen, and H. Tost, (2012), The role of carbonyl sulphide as a source
5433 of stratospheric sulphate aerosol and its impact on climate, *Atmos. Chem. Phys.*, 12, 1239-
5434 1253, doi:10.5194/acp-12-1239-2012.

5435 Brühl, C., J. Lelieveld, H. Tost, M. Höpfner, and N. Glatthor (2015), Stratospheric sulphur and its
5436 implications for radiative forcing simulated by the chemistry climate model EMAC, *J.*
5437 *Geophys. Res. Atmos.*, 120, 2103–2118, doi:10.1002/2014JD022430.

5438 Budyko, M. I., 1969: The effect of solar radiation variations on the climate of the Earth. *Tellus*,
5439 doi:10.3402/tellusa.v21i5.10109.

5440 Burrows J. P., E. Hözle, A. P. H. Goede, H. Visser, and W. Fricke (1995), SCIAMACHY –
5441 Scanning Imaging Absorption Spectrometer for Atmospheric Chartography, *Acta*
5442 *Astronautica*, 35(7), 445 – 451.

5443

5444 Cadle, R. D., and E. R. Allen, 1970: Atmospheric Photochemistry. *Science (80-.)*, **167**, 243 LP-
5445 263. <http://science.sciencemag.org/content/167/3916/243.abstract>.

5446 Carn, S. A., A. J. Krueger, G. J. S. Bluth, S. J. Schaefer, N. A. Krotkov, I. M. Watson and S. Datta
5447 (2003), Volcanic eruption detection by the Total Ozone Mapping Spectrometer (TOMS)
5448 instruments: a 22-year record of sulfur dioxide and ash emissions. In: *Volcanic Degassing*
5449 (eds. C. Oppenheimer, D. M. Pyle, and J. Barclay), Geological Society, London, Special
5450 Publications, 213, 177-202.

5451 Carn, S. A., Clarisse, L., and Prata, A. J. (2016), Multi-decadal satellite measurements of global
5452 volcanic degassing, *J. Volcanol. Geotherm. Res.*, 311, 99 – 134.

5453 Caldeira, K., G. Bala, and L. Cao, 2013: The Science of Geoengineering. *Annu. Rev. Earth*
5454 *Planet. Sci.*, doi:10.1146/annurev-earth-042711-105548.

5455

5456

5457 Callendar, G. S. (1941). Infra-red absorption by carbon dioxide, with special reference to
5458 atmospheric radiation. *Quarterly Journal of the Royal Meteorological Society*, 67(291),
5459 263–275. <http://doi.org/10.1002/qj.49706729105>

5460 Callendar, G. S., 1938: The artificial production of carbon dioxide and its influence on
5461 temperature. *Quart. J. Roy. Meteor. Soc.*, doi: 10.1002/qj.49706427503
5462 (<https://dx.doi.org/10.1002/qj.49706427503>).

5463 Callis, L. B., M. Natarajan, and R. E. Boughner, 1983: On the relationship between the

5464 greenhouse effect, atmospheric photochemistry, and species distribution. *J. Geophys. Res.*
5465 *Ocean.*, **88**, 1401–1426, doi:doi:10.1029/JC088iC02p01401.
5466 <https://doi.org/10.1029/JC088iC02p01401>.

5467 Carbon Dioxide and Climate: A Scientific Assessment. (1979). Washington D.C., U.S.A.:
5468 National Academy of Sciences. <http://doi.org/10.17226/12181>

5469 Carslaw, K. S., Boucher, O., Spracklen, D., Mann, G., Rae, J. G., Woodward, S. and Kumala,
5470 M.: A review of natural aerosol interactions and feedbacks within the Earth System, *Atmos.*
5471 *Chem. Phys.*, **10**, 1701–1737, 2010.

5472 Carslaw, K. S., Lee, L., Reddington, C., Pringle, K., Rap, A., Forster, P., Mann, G., Spracklen,
5473 D., Woodhouse, M., Regayre, L. and Pierce, J.: Large contribution of natural aerosols to
5474 uncertainty in indirect forcing, *Nature*, **503**(doi:10.1038/nature12674), 67–71, 2013.

5475 Carslaw, K.S., Gordon, H., Hamilton, D.S. et al. 2017: Aerosols in the Pre-industrial
5476 Atmosphere, *Curr Clim Change Rep*, **3**, <https://doi.org/10.1007/s40641-017-0061-2>

5477 Carslaw, K. S., Lee, L. A., Reddington, C. L., Pringle, K. J., Rap, A., Forster, P. M., ... and
5478 Pierce, J. R. Large contribution of natural aerosols to uncertainty in indirect forcing. *Nature*,
5479 **503**(7474), 67, 2013.

5480 Charlson, R. J., Langner, J., Rodhe, H., Leovy, C. B., & Warren, S. G. (1991). Perturbation of
5481 the northern hemisphere radiative balance by backscattering from anthropogenic sulfate
5482 aerosols. *Tellus A: Dynamic Meteorology and Oceanography*, **43**(4), 152-163.

5483 Charlson, R. J., Schwartz, S. E., Hales, J. M., Cess, R. D., Coakley, J. J., Hansen, J. E., &
5484 Hofmann, D. J. (1992). Climate forcing by anthropogenic aerosols. *Science*, **255**(5043),
5485 423-430.

5486 Cess, R.D., 1976: [Climate Change: An Appraisal of Atmospheric Feedback Mechanisms Employing Zonal Climatology. *J. Atmos. Sci.*, **33**, 1831–1843,](https://doi.org/10.1175/1520-0469(1976)033<1831:CCAOA>2.0.CO;2)
5488 [https://doi.org/10.1175/1520-0469\(1976\)033<1831:CCAOA>2.0.CO;2](https://doi.org/10.1175/1520-0469(1976)033<1831:CCAOA>2.0.CO;2)

5489 Cess, R. D., Zhang, M.-H., Potter, G. L., Barker, H. W., Colman, R. A., Dazlich, D. A., ...
5490 Wetherald, R. T. (1993). Uncertainties in Carbon Dioxide Radiative Forcing in Atmospheric

5491 General Circulation Models. *Science*, 262(5137), 1252–1255.
5492 <http://doi.org/10.1126/science.262.5137.1252>

5493 Cess, R. D., and Coauthors, 1990: Intercomparison and interpretation of climate feedback
5494 processes in 19 atmospheric general circulation models. *J. Geophys. Res. Atmos.*, 95,
5495 16601–16615, doi:10.1029/JD095iD10p16601. <https://doi.org/10.1029/JD095iD10p16601>.

5496 —, and Coauthors, 1993: Uncertainties in Carbon Dioxide Radiative Forcing in Atmospheric
5497 General Circulation Models. *Science* (80- .), 262, 1252 LP-1255,
5498 doi:10.1126/science.262.5137.1252.
5499 <http://science.sciencemag.org/content/262/5137/1252.abstract>.

5500 Cess, R. D., et al. (1996), Cloud feedback in atmospheric general circulation models: An update,
5501 *J. Geophys. Res.*, 101, 12,791–12,794

5502 Cess, R.D., *et al.*, Uncertainties in carbon dioxide radiative forcing, *Science* 262, 1252 (1993).

5503 Chamberlain, J. W., H. M. Foley, G. J. MacDonald, and M. A. Ruderman, 1982: In Carbon
5504 dioxide review 1982, W. Clark, Ed., Oxford University Press, Clarendon, England, 255–
5505 277.

5506 Chameides, W., and J. C. G. Walker, 1973: A photochemical theory of tropospheric ozone. *J.*
5507 *Geophys. Res.*, **78**, 8751–8760, doi:10.1029/JC078i036p08751.
5508 <http://dx.doi.org/10.1029/JC078i036p08751>.

5509 Chameides, W. L., and R. J. Cicerone, 1978: Effects of nonmethane hydrocarbons in the
5510 atmosphere. *J. Geophys. Res. Ocean.*, **83**, 947–952, doi:doi:10.1029/JC083iC02p00947.
5511 <https://doi.org/10.1029/JC083iC02p00947>.

5512 Chapman, S., 1930: On ozone and atomic oxygen in the upper atmosphere. *Philos. Mag.*, **10**,
5513 369–383.

5514 Chanin, M.-L., and V. Ramaswamy, 1998: Chapter 5. Trends in Stratospheric
5515 Temperatures. *Scientific Assessment of Ozone Depletion: 1998*, D.L. Albritton, R.. Watson,
5516 P.J. Aucamp, and G. Megie, Eds.

5517 Charlson, R. J., J. Langner, H. Rodhe, C. B. Leovy, and S. G. Warren, 1991: Perturbation of the
5518 Northern-Hemisphere Radiative Balance by Backscattering from Anthropogenic Sulfate
5519 Aerosols. *Tellus Ser. a-Dynamic Meteorol. Oceanogr.*, 43, 152–163.

5520 Charlson, R. J., Langner, J., Rodhe, H., Leovy, C. B., & Warren, S. G. (1991). Perturbation of
5521 the northern hemisphere radiative balance by backscattering from anthropogenic sulfate
5522 aerosols. *Tellus A: Dynamic Meteorology and Oceanography*, 43(4), 152-163.

5523 Charlson, R. J., Schwartz, S. E., Hales, J. M., Cess, R. D., Coakley, J. J., Hansen, J. E., &
5524 Hofmann, D. J. (1992). Climate forcing by anthropogenic aerosols. *Science*, 255(5043),
5525 423-430.

5526 Chédin A, Husson N, Scott NA. Une banque de données pour l'étude des phénomènes de
5527 transfert radiatif dans les atmosphères planétaires: la banque GEISA. *Bull Inform Centre*
5528 *Données Stellaires* (France) 1982;22:121–121.

5529 Chen, C.-T., and V. Ramaswamy, 1996: Sensitivity of Simulated Global Climate to Perturbations
5530 in Low Cloud Microphysical Properties. Part II: Spatially Localized Perturbations. *J.*
5531 *Clim.*, 9, 2788–2801, doi:10.1175/1520-
5532 0442(1996)009<2788:SOSGCT>2.0.CO;2. [https://doi.org/10.1175/1520-0442\(1996\)009%3C2788:SOSGCT%3E2.0.CO](https://doi.org/10.1175/1520-0442(1996)009%3C2788:SOSGCT%3E2.0.CO).

5534 Chen, Y. C., Christensen, M. W., Diner, D. J., & Garay, M. J. (2015). Aerosol-cloud interactions
5535 in ship tracks using Terra MODIS/MISR. *Journal of Geophysical Research: Atmospheres*,
5536 120(7), 2819-2833.

5537 Chen, C.-C. and Gettelman, A.: Simulated 2050 aviation radiative forcing from contrails and
5538 aerosols, *Atmos. Chem. Phys.*, 16, 7317-7333, <https://doi.org/10.5194/acp-16-7317-2016>,
5539 2016.

5540 Chiang, J. C. H. & Bitz, C. M. Influence of high latitude ice cover on the marine Intertropical
5541 Convergence Zone. *Clim. Dyn.* 25, 477-496 (2005).

5542 Chiodo, G., L. M. Polvani, D. R. Marsh, A. Stenke, W. Ball, E. Rozanov, S. Muthers, and K.
5543 Tsigaridis, 2018: The Response of the Ozone Layer to Quadrupled CO₂ Concentrations. *J.*

5544 *Clim.*, **31**, 3893–3907, doi:10.1175/JCLI-D-17-0492.1. <https://doi.org/10.1175/JCLI-D-17-0492.1>.

5546 Chiou, E. W., L. W. Thomason, and W. P. Chu (2006), Variability of Stratospheric Water Vapor
5547 Inferred from SAGE II, HALOE, and Boulder (Colorado) Balloon Measurements, *J. Climate*,
5548 19, 4121-4133.

5549 Christoforou, P, and S. Hameed, 1997: Solar cycle and the Pacific 'centers of action', Geophys.
5550 Res. Lett., 24, 293-296.

5551 Chuang, C. C., J. E. Penner, K. E. Taylor, and J. J. Walton, 1993: Climate effects of
5552 anthropogenic sulfate: Simulations from a coupled chemistry/climate model. 7.
5553 http://inis.iaea.org/search/search.aspx?orig_q=RN:25046956.

5554 Chung, E.-S., and B. J. Soden, 2015: An Assessment of Direct Radiative Forcing, Radiative
5555 Adjustments, and Radiative Feedbacks in Coupled Ocean–Atmosphere Models. *J. Clim.*,
5556 28, 4152–4170, doi:10.1175/JCLI-D-14-00436.1. <https://doi.org/10.1175/JCLI-D-14-00436.1>.

5558 Chylek, P., & Wong, J. (1995). Effect of absorbing aerosols on global radiation budget.
5559 *Geophysical research letters*, 22(8), 929-931.

5560 Chylek, P., and J. Wong, 1995: Effect of absorbing aerosols on global radiation budget.
5561 Geophys. Res. Lett., 22, 929–931, doi:10.1029/95GL00800.
5562 <https://doi.org/10.1029/95GL00800>.

5563 Ciais, P., Gasser, T., Paris, J., Caldeira, K., Raupach, M., Canadell, J., Patwardhan, A.,
5564 Friedlingstein, P., Piao, S., Gitz, V., Raupach, M., Canadell, J., Patwardhan, A.,
5565 Friedlingstein, P., Piao, S. and Gitze, V.: Attributing the increase in atmospheric CO₂ to
5566 emitters and absorbers, *Nat. Clim. Chang.*, 3(doi:10.1038/nclimate1942), 926–930, 2013a.

5567 Ciais, P., Sabine, C., Bala, G., Bopp, L., Brovkin, V., Canadell, J., Chhabra, A., DeFries, R.,
5568 Galloway, J., Heimann, M., Jones, C., Quéré, C. Le, Myneni, R. B., Piao, S. and Thornton,
5569 P.: Carbon and Other Biogeochemical Cycles, *Clim. Chang.* 2013 - *Phys. Sci. Basis*, 465–
5570 570, doi:10.1017/CBO9781107415324.015, 2013b.

5571 Clark, W. C. (ed.), 1982: Carbon dioxide review 1982. Oxford University Press, Clarendon,
5572 England, United States, <https://www.osti.gov/servlets/purl/5963903>.

5573 Clette, F. and L. Lefèvre, 2016: The new sunspot number: Assembling all corrections, *Sol. Phys.*
5574 291, 2629–2651, <https://doi.org/10.1007/s11207-016-1014-y>

5575 Coakley, J. A., Bernstein, R. L., & Durkee, P. A. (1987). Effect of ship-stack effluents on cloud
5576 reflectivity. *Science*, 237(4818), 1020-1022.

5577 Coakley, J. Jr. (1981), Stratospheric Aerosols and the Tropospheric Energy Budget: Theory Versus
5578 Observations, *J. Geophys. Res.*, 86, 9761-9766.

5579 Coddington, O., J. L. Lean, P. Pilewskie, M. Snow, and D. Lindholm, 2106: A solar irradiance
5580 climate data record, *Bulletin American Meteor. Soc.*, BAMS.

5581 Cole-Dai, J. (2010), Volcanoes and climate, *WIREs Climate Change*, doi:10.1002/wcc.76.

5582 Collins, J. W., and Coauthors, 2017: AerChemMIP: Quantifying the effects of chemistry and
5583 aerosols in CMIP6. *Geosci. Model Dev.*, **10**, 585–607, doi:10.5194/gmd-10-585-2017.

5584 Collins, W. D., Feldman, D. R., Kuo, C., & Nguyen, N. H. (2018). Large regional shortwave
5585 forcing by anthropogenic methane informed by Jovian observations. *Science Advances*,
5586 4(9). <http://doi.org/10.1126/sciadv.aas9593>

5587 Collins, W. J., S. Sitch, and O. Boucher, 2010: How vegetation impacts affect climate metrics for
5588 ozone precursors. *J. Geophys. Res.*, **115**, D23308, doi:10.1029/2010jd014187.
5589 <http://dx.doi.org/10.1029/2010JD014187>.

5590 Collins, W. J., M. M. Fry, H. Yu, J. S. Fuglestvedt, D. T. Shindell, and J. J. West: Global and
5591 regional temperature-change potentials for near-term climate forcers, *Atmos. Chem.
5592 Phys.*, **13**, 2471-2485, <https://doi.org/10.5194/acp-13-2471-2013>.

5593 Collins, W. D., and Coauthors, 2006: Radiative forcing by well-mixed greenhouse gases:
5594 Estimates from climate models in the Intergovernmental Panel on Climate Change (IPCC)
5595 Fourth Assessment Report (AR4). *J. Geophys. Res.*, **111**, D14317.

5596 Collins, W. D., Ramaswamy, V., Schwarzkopf, M. D., Sun, Y., Portmann, R. W., Fu, Q., ...

5597 Zhong, W. Y. (2006). Radiative forcing by well-mixed greenhouse gases: Estimates from
5598 climate models in the Intergovernmental Panel on Climate Change (IPCC) Fourth
5599 Assessment Report (AR4). *Journal of Geophysical Research Atmospheres*, *111*(14), 1–15.
5600 <http://doi.org/10.1029/2005JD006713>

5601 Collins, W. J., Lamarque, J., Schulz, M., Boucher, O., Eyring, V., Hegglin, I., Maycock, A.,
5602 Myhre, G., Prather, M., Shindell, D. and Smith, S. J.: AerChemMIP : quantifying the effects
5603 of chemistry and aerosols in, , 585–607, doi:10.5194/gmd-10-585-2017, 2017.

5604 Colman, R. A., and S. B. Power (2010), Atmospheric radiative feedbacks associated with transient
5605 climate change and climate variability, *Clim. Dyn.*, *34*, 919–933, doi:10.1007/s00382-009-
5606 0541-8.

5607 Conover, John H. "Anomalous cloud lines." *Journal of the Atmospheric Sciences* *23*, no. 6
5608 (1966): 778-785.

5609 Cooke, W. F., & Wilson, J. J. (1996). A global black carbon aerosol model. *Journal of*
5610 *Geophysical Research: Atmospheres*, *101*(D14), 19395-19409.

5611 Cooke, W. F., Lioussse, C., Cachier, H., & Feichter, J. (1999). Construction of a 1×1 fossil fuel
5612 emission data set for carbonaceous aerosol and implementation and radiative impact in the
5613 ECHAM4 model. *Journal of Geophysical Research: Atmospheres*, *104*(D18), 22137-22162.

5614 Costantino, L., & Bréon, F. M. (2013). Aerosol indirect effect on warm clouds over South-East
5615 Atlantic, from co-located MODIS and CALIPSO observations. *Atmos. Chem. Phys.*, *13*(1),
5616 69-88.

5617 [Crook, J. A., L. S. Jackson ,S. M. Osprey, P. M. Forster](#) , 2015: A comparison of temperature
5618 and precipitation responses to different Earth radiation management geoengineering
5619 schemes, *J. Geophys. Res. Atmospheres*, <https://doi.org/10.1002/2015JD023269>

5620

5621 Crutzen, P. J., 1970: The influence of nitrogen oxides on the atmospheric ozone content. *Q. J. R.*
5622 *Meteorol. Soc.*, **96**, 320–325, doi:10.1002/qj.49709640815.
5623 <https://doi.org/10.1002/qj.49709640815>.

5624

5625 Crutzen, P. J., 1972a: SST's: A Threat to the Earth's Ozone Shield. *Ambio*, **1**, 41–51.
5626 <http://www.jstor.org/stable/4311946>.

5627 Crutzen, P. J., 1972b: *Gas-phase nitrogen and methane chemistry in the atmosphere*. Stockholm,
5628 20 pp.

5629 Crutzen, P. J., 1973: *A discussion of the chemistry of some minor constituents in the stratosphere
5630 and troposphere*. Stockholm,.

5631 Crutzen, P. J., 1979: The role of NO and NO₂ in the chemistry of the troposphere and
5632 stratosphere. *Annu. Rev. Earth Planet. Sci.*, **7**, 443–472.

5633 ——, and J. Lelieveld, 2001: Human Impacts on Atmospheric Chemistry. *Annu. Rev. Earth
5634 Planet. Sci.*, **29**, 17–45.

5635 Crutzen, P. J. (1976), The possible importance of CSO for the sulfate layer of the stratosphere,
5636 *Geophys. Res. Lett.*, **3**, 73–76, doi:10.1029/GL003i002p00073.

5637 Crutzen, P. (2006), Albedo Enhancement by Stratospheric Sulfur Injections: A Contribution to
5638 Resolve a Policy Dilemma? *Climatic Change*, **77**, 211–220.

5639 Crutzen, P. J., 2006: Albedo enhancement by stratospheric sulfur injections: A contribution to
5640 resolve a policy dilemma? *Clim. Change*, doi:10.1007/s10584-006-9101-y.

5641 Cubasch, U., R. Voss, G. C. Hegerl, J. Waszkewitz, and T. J. Crowley, 1997: Simulation of the
5642 influence of solar radiation variations on the global climate with an ocean-atmosphere
5643 general circulation model, *Climate Dynamics*, **13**, 757–767.

5644

5645 Damon, P., and J. Jirikowic, 1992: The Sun as a Low-Frequency Harmonic Oscillator.
5646 *Radiocarbon*, **34**(2), 199–205. doi:10.1017/S003382220001362X.

5647 Daniel, J. S., and S. Solomon, 1998: On the climate forcing of carbon monoxide. *J. Geophys.
5648 Res. Atmos.*, **103**, 13249–13260, doi:doi:10.1029/98JD00822.

5649 <https://doi.org/10.1029/98JD00822>.

5650 de Graaf, M., Tilstra, L. G., Wang, P., & Stammes, P. (2012). Retrieval of the aerosol direct
5651 radiative effect over clouds from spaceborne spectrometry. *Journal of Geophysical*
5652 *Research: Atmospheres*, 117(D7).

5653 de Graaf, M., N. Bellouin, L.G. Tilstra, J.M. Haywood, and P. Stammes, Aerosol direct radiative
5654 effect from episodic smoke emissions over the southeast Atlantic Ocean from 2006 to 2009,
5655 Geophy. Res. Letts, 41, 21, 7723–7730, DOI: 10.1002/2014GL061103, 2014.

5656 Delworth, T. L., V. Ramaswamy, and G. L. Stenchikov (2005), The impact of aerosols on
5657 simulated ocean temperature, heat content, and sea level in the 20th century. *Geophys Res*
5658 *Lett*, 32, L24709.

5659 Delworth, T. L., et al. (2006), GFDL's CM2 global coupled climate models. Part I: Formulation
5660 and simulation characteristics, *J. Clim.*, 19, 643–674, doi:10.1175/JCLI3629.1.

5661 DeLand, M. T., and R. P. Cebula, 1998: NOAA 11 Solar Backscatter Ultraviolet, model 2
5662 (SBUV/2) instrument solar spectral irradiance measurements in 1989–1994: 2. Results,
5663 validation, and comparisons, *J. Geophys. Res.*, 103(D13), 16251–16273,
5664 doi:10.1029/98JD01204.

5665 DeLand, M. T., and R. P. Cebula, 2008: Creation of a composite solar ultraviolet irradiance data
5666 set, *J. Geophys. Res.*, 113, A11103, doi:10.1029/2008JA013401.

5667 Delaygue, G. and E. Bard, 2011: An Antarctic view of Beryllium-10 and solar activity for the
5668 past millennium. *Clim. Dyn.* 36: 2201. <https://doi.org/10.1007/s00382-010-0795-1>

5669 Denman, K. L., and Coauthors, 2007: Couplings Between Changes in the Climate System and
5670 Biogeochemistry. *Climate Change 2007: The Physical Science Basis. Contribution of*
5671 *Working Group I to the Fourth Assessment Report of the Intergovernmental Panel on*
5672 *Climate Change*, D. Qin, M. Manning, Z. Chen, M. Marquis, K.B. Averyt, M. Tignor, and
5673 H.L. Miller, Eds., Cambridge University Press, Cambridge, United Kingdom and New
5674 York, NY, USA.

5675 Denman, K. L., Brasseur, G., Chidthaisong, A., Ciais, P., Cox, P. M., Dickinson, R. E.,

5676 Hauglustaine, D., Heinze, C., Holland, E., Jacob, D., Lohmann, U., Ramachandran, S., Dias,
5677 P. L. da S., Wofsy, S. C. and Zhang, X.: Couplings between changes in the climate system
5678 and biogeochemistry, in Climate Change 2007: The Physical Science Bases. Contribution of
5679 Working Group I to the Fourth Assessment Report of the Intergovernmental Panel on
5680 Climate Change, edited by S. Solomon D. Qin, M. Manning, Z. Chen, M. Marquis, K.B.
5681 Averyt, M. Tignor and H.L. Miller, Cambridge University Press, Cambridge, UK., 2007.

5682 Derwent, R. G. (1990), Trace gases and their relative contribution to the greenhouse effect, Rep,
5683 Atomic Energy Research Establishment Harwell Oxon UK. Report AERE- R13716.

5684 Deshler, T., M. E. Hervig, D. J. Hofmann, J. M. Rosen, and J. B. Liley (2003), Thirty years of in
5685 situ stratospheric aerosol size distribution measurements from Laramie, Wyoming (41°N),
5686 using balloon-borne instruments, J. Geophys. Res., 108(D5), 4167,
5687 doi:10.1029/2002JD002514

5688 Deshler, T., R. Anderson-Sprecher, H. Jager, J. Barnes, D. J. Hoffmann, B Clemesha, D. Simonich,
5689 M. Osborn, R. J. Grainger, S. Godin-Beekmann (2006), Trends in the nonvolcanic component
5690 of stratospheric aerosol over the period 1971-2004, J. Geophys Res., 111, D01201,
5691 doi:10.1029/2005JD006089.

5692 Deshler, T. (2008), A review of global stratospheric aerosol: Measurements, importance, life cycle,
5693 and local stratospheric aerosol, Atmospheric research, 90, 223-232.

5694 Dessler, A. E., M. R. Schoeberl, T. Wang, S.M. Davis, K. H. Rosenlof, and J.-P. Vernier (2014),
5695 Variations of stratospheric water vapor over the past three decades, J. Geophys. Res. Atmos.,
5696 119, 12,588–12,598, doi:10.1002/2014JD021712.

5697 Despres, V., Huffman, J., Burrows, S. M., Hoose, C., Safatov, A., Buryak, G., Frohlich-
5698 Nowoisky, J., Elbert, W., M. Andreae, Polsch, U. and Jaenicke, R.: Primary biological
5699 aerosol particles in the atmosphere: a review, Tellus B, 64(15598),
5700 doi:10.3402/tellusb.v64i0.15598, 2012.

5701 Deuzé, J.L., Bréon, F.M., Devaux, C., Goloub, P.H., Herman, M., Lafrance, B., Maignan, F.,
5702 Marchand, A., Nadal, F., Perry, G. and Tanré, D., 2001. Remote sensing of aerosols over

5703 land surfaces from POLDER-ADEOS-1 polarized measurements. *Journal of Geophysical*
5704 *Research: Atmospheres*, 106(D5), pp.4913-4926.

5705 Dhomse, S., K. Emmerson, G. Mann, N. Bellouin, K. Carslaw, M. Chipperfield, R. Hommel, N.
5706 Abraham, P. Telford, P. Braesicke, M. Dalvi, C. Johnson, F. O'Connor, O. Morgenstern, J.
5707 Pyle, T. Deshler, J. Zawodny, and L. Thomason (2014), Aerosol microphysical simulations
5708 of the Mt. Pinatubo eruption with the UM-UKCA composition-climate model, *Atmos. Chem.*
5709 *Phys.*, 14,11221-11246, doi:10.5194/ACP-14-11221-2014.

5710 Dickinson, R. E., and R. J. Cicerone, 1986: Future global warming from atmospheric trace gases.
5711 *Nature*, 319, 109–115, doi:10.1038/319109a0. <https://doi.org/10.1038/319109a0>.

5712 Dickinson, R.E., S.C. Liu, and T.M. Donahue, 1978: Effect of Chlorofluoromethane Infrared
5713 Radiation on Zonal Atmospheric Temperatures. *J. Atmos. Sci.*, 35, 2142–
5714 2152, [https://doi.org/10.1175/1520-0469\(1978\)035<2142:EOCIRO>2.0.CO;2](https://doi.org/10.1175/1520-0469(1978)035<2142:EOCIRO>2.0.CO;2)

5715 Dickinson, R.E., S.C. Liu, and T.M. Donahue, 1978: Effect of Chlorofluoromethane Infrared
5716 Radiation on Zonal Atmospheric Temperatures. *J. Atmos. Sci.*, 35, 2142–
5717 2152, [https://doi.org/10.1175/1520-0469\(1978\)035<2142:EOCIRO>2.0.CO;2](https://doi.org/10.1175/1520-0469(1978)035<2142:EOCIRO>2.0.CO;2)

5718 Dines, W. H., 1917: The heat balance of the atmosphere. *Quart. J. Roy. Meteor. Soc.*, vol. 43,
5719 issue 182, pp 151-158. <https://doi.org/10.1002/qj.49704318203>.

5720 Donner, L. J., and V. Ramanathan, 1980: Methane and nitrous oxide: their effects on the
5721 terrestrial climate. *Journal of the Atmospheric Sciences*. 37:119-124

5722 Donner, L. and V. Ramanathan, 1980: Methane and Nitrous Oxide: Their Effects on the
5723 Terrestrial Climate. *J. Atmos. Sci.*, 37, 119–124, [https://doi.org/10.1175/1520-0469\(1980\)037<0119:MANOTE>2.0.CO;2](https://doi.org/10.1175/1520-0469(1980)037<0119:MANOTE>2.0.CO;2)

5725 Doutriaux-Boucher, M., Webb, M., Gregory, J. and Boucher, O.: Carbon dioxide induced
5726 stomatal closure increases radiative forcing via a rapid reduction in low cloud, *Geophysical*
5727 *Research Letters*, -, 2009.

5728 Dorland, R., F. J. Dentener, and J. Lelieveld, 1997: Radiative forcing due to tropospheric ozone
5729 and sulfate aerosols. *J. Geophys. Res. Atmos.*, 102, 28079–28100,

5730 doi:doi:10.1029/97JD02499. <https://doi.org/10.1029/97JD02499>.

5731 Dogar, M., G. Stenchikov, S. Osipov, B Wyman, M. Zhao (2017), Sensitivity of the Regional
5732 Climate in the Middle East and North Africa to Volcanic Perturbations, *J. Geophys. Res.*
5733 *Atmos.*, 122, doi:10.1002/2017JD026783.

5734 Doughty, C. E., C. B. Field, and A. M. S. McMillan, 2011: Can crop albedo be increased through
5735 the modification of leaf trichomes, and could this cool regional climate? *Clim. Change*,
5736 doi:10.1007/s10584-010-9936-0.

5737 Douglass, D. H. and B. D. Clader, 2002: Climate sensitivity of the Earth to solar irradiance,
5738 *Geophys. Res. Lett.*, 29, 10.1029/2002GL015345.

5739 Drayson, S.R., (1976). Rapid computation of the Voigt profile, *Journal of Quantitative*
5740 *Spectroscopy and Radiative Transfer*, 16(7), 611—614. [https://doi.org/10.1016/0022-4073\(76\)90029-7](https://doi.org/10.1016/0022-4073(76)90029-7)

5741

5742 Dubovik, O., and M. King, A flexible inversion algorithm for retrieval of aerosol optical
5743 properties from Sun and sky radiance measurements, *J. Geophys. Res.*, 105, 20,673–20,696,
5744 2000.

5745 Duce, R. A., LaRoche, J., Altieri, K., Arrigo, K. R., Baker, A. R., Capone, D. G., Cornell, S.,
5746 Dentener, F., Galloway, J., Ganeshram, R. S., Geider, R. J., Jickells, T., Kuypers, M. M.,
5747 Langlois, R., Liss, P. S., Liu, S. M., Middelburg, J. J., Moore, C. M., Nickovic, S., Oschlies,
5748 A., Pedersen, T., Prospero, J., Schlitzer, R., Seitzinger, S., Sorensen, L. L., Uematsu, M.,
5749 Ulloa, O., Voss, M., Ward, B. and Zamora, L.: Impacts of Atmospheric Anthropogenic
5750 Nitrogen on the Open Ocean, *Science* (80-.), 320(5878), 893–897,
5751 doi:10.1126/science.1150369, 2008.

5752 Duda, D. P., Bedka, S. T., Minnis, P., Spangenberg, D., Khlopenkov, K., Chee, T., and Smith Jr.,
5753 W. L.: Northern Hemisphere contrail properties derived from Terra and Aqua MODIS data
5754 for 2006 and 2012, *Atmos. Chem. Phys.*, 19, 5313-5330, <https://doi.org/10.5194/acp-19-5313-2019>, 2019.

5755

5756 Dudok de Wit, T., Kopp, G., Fröhlich, C., and M. Schöll, 2017: Methodology to create a new
5757 total solar irradiance record: Making a composite out of multiple data records. *Geophys.*
5758 *Res. Lett.*, 44, 1196–1203, doi:10.1002/2016GL071866.

5759 Dutton, E. G., and J. R. Christy (1992), Solar radiative forcing at selected locations and evidence
5760 for global lower tropospheric cooling following the eruptions of El Chichón and Pinatubo,
5761 *Geophys. Res. Lett.*, 19, 2313-2316.

5762 Dykema, J. A., D. W. Keith, J. G. Anderson, and D. Weisenstein, 2014: Stratospheric controlled
5763 perturbation experiment: A small-scale experiment to improve understanding of the risks of
5764 solar geoengineering. *Philos. Trans. R. Soc. A Math. Phys. Eng. Sci.*,
5765 doi:10.1098/rsta.2014.0059.

5766

5767 Eddy, J. A., 1976: The Maunder Minimum, *Science, New Series*, 192, 4245, 1189-1202.

5768 Ekholm, N., 1901: On the variations of the climate of the geological and historical past and their
5769 causes. *Quart. J. Roy. Meteor. Soc.*, 27, 117, 1-62.

5770 Ellingson, R. G., & Fouquart, Y. (1991). The intercomparison of radiation codes in climate
5771 models: An overview. *Journal of Geophysical Research: Atmospheres*, 96(D5), 8925–8927.
5772 <http://doi.org/10.1029/90JD01618>

5773 English, J., O. Toon, and M. Mills (2013), Microphysical simulations of large volcanic eruptions:
5774 Pinatubo and Toba, *J. Geophys. Res. Atmos.*, 118, 1880-1895, doi:10.1002/JGRD.50196.

5775 Etminan, M., Myhre, G., Highwood, E. J., & Shine, K. P. (2016). Radiative forcing of carbon
5776 dioxide, methane, and nitrous oxide: A significant revision of the methane radiative forcing.
5777 *GEOPHYSICAL RESEARCH LETTERS*, 43(24), 12614–12623.
5778 <http://doi.org/10.1002/2016GL071930>

5779 Etminan, M., Myhre, G., Highwood, E. J. and Shine, K. P.: Radiative forcing of carbon dioxide,
5780 methane, and nitrous oxide: A significant revision of the methane radiative forcing,
5781 *Geophysical Research Letters*, 43(24), 12614-12623, 2016.

5782 Evan, A., Flamant, C., Gaetani, M. and Guichard, F.: The past, present and future of African
5783 dust, *Nature*, 531, 493–495, 2016.

5784 Evan, A. T. (2012), Atlantic hurricane activity following two major volcanic eruptions, *J.*
5785 *Geophys. Res.* 117, D06101.

5786 Eyring, V., and Coauthors, 2013: Long-term ozone changes and associated climate impacts in
5787 CMIP5 simulations. *J. Geophys. Res. Atmos.*, **118**, 5029–5060, doi:10.1002/jgrd.50316.
5788 <http://dx.doi.org/10.1002/jgrd.50316>.

5789 Eyring, V., S. Bony, G. A. Meehl, C. A. Senior, B. Stevens, R. J. Stouffer, and K. E. Taylor,
5790 2016: Overview of the Coupled Model Intercomparison Project Phase 6 (CMIP6)
5791 experimental design and organization. *Geosci. Model Dev.*, **9**, 1937–1958,
5792 doi:10.5194/gmd-9-1937-2016. <https://www.geosci-model-dev.net/9/1937/2016/>

5793

5794 Fabian, P., and P. G. Pruchniewicz, 1977: Meridional distribution of ozone in the troposphere
5795 and its seasonal variations. *J. Geophys. Res.*, **82**, 2063–2073,
5796 doi:doi:10.1029/JC082i015p02063. <https://doi.org/10.1029/JC082i015p02063>.

5797 Fahey, D.W. U. Schumann, S. Ackerman, P. Artaxo, O. Boucher, M. Danilin, B. Kärcher, P.
5798 Minnis, T. Nakajima, and O. B. Toon (1999). Aviation-Produced Aerosols and Cloudiness.
5799 In Aviation and the Global Atmosphere. A Special Report of IPCC Working Groups I and
5800 III J.E. Penner, D.H. Lister, D.J. Griggs, D.J. Dokken, M. McFarland (Eds). Cambridge
5801 University Press, Cambridge, UK, 65–120.

5802 Feddema, J., Oleson, K., Bonan, G., Mearns, L., Buja, L., Meehl, G. and Washington, W.: The
5803 importance of land-cover change in simulating future climates, *Science* (80-.), 310, 1674–
5804 1678, 2005.

5805 Feichter, J., U. Lohmann and I. Schult, 1997: The atmospheric sulfur cycle in ECHAM-4 and its
5806 impact on the shortwave radiation. *Climate Dynamics*, 13, 235–246.

5807 Fels, S. B., J. D. Mahlman, M. D. Schwarzkopf, and R. W. Sinclair, 1980: Stratospheric
5808 Sensitivity to Perturbations in Ozone and Carbon Dioxide: Radiative and Dynamical

5809 Response. *J. Atmos. Sci.*, **37**, 2265–2297, doi:10.1175/1520-
5810 0469(1980)037<2265:SSTPIO>2.0.CO;2. [https://doi.org/10.1175/1520-0469\(1980\)037%3C2265:SSTPIO%3E2.0.CO](https://doi.org/10.1175/1520-0469(1980)037%3C2265:SSTPIO%3E2.0.CO).

5812 Fels, S. B., Kiehl, J. T., Lacis, A. A., & Schwarzkopf, M. D. (1991). Infrared cooling rate
5813 calculations in operational general circulation models: Comparisons with benchmark
5814 computations. *J. Geophys. Res.*, **96**, 9105–9120. <http://doi.org/10.1029%2F91JD00516>.

5815 Field, C. B., Barros, V. R., Mach, K. J., Mastrandrea, M. D., Aalst, M. van, Adger, W. N., Arent,
5816 D. J., Barnett, J., Betts, R., Bilir, T. E., Birkmann, J., Carmin, J., Chadee, D. D., Challinor,
5817 A. J., Chatterjee, M., Cramer, W., Davidson, D. J., Estrada, Y. O., Gattuso, J.-P., Hijioka,
5818 Y., Hoegh-Guldberg, O., Huang, H.-Q., Insarov, G. E., Jones, R. N., Kovats, R. S., Lankao,
5819 P. R., Larsen, J. N., Losada, I. J., Marengo, J. A., McLean, R. F., Mearns, L. O., Mechler,
5820 R., Morton, J. F., Niang, I., Oki, T., Olwoch, J. M., Opondo, M., Poloczanska, E. S.,
5821 Pörtner, H.-O., Redsteer, M. H., Reisinger, A., Revi, A., Schmidt, D. N., Shaw, M. R.,
5822 Solecki, W., Stone, D. A., Stone, J. M. R., Strzepek, K. M., Suarez, A. G., Tschakert, P.,
5823 Valentini, R., Vicuña, S., Villamizar, A., Vincent, K. E., Warren, R., White, L. L.,
5824 Wilbanks, T. J., Wong, P. P. and Yohe, G. W.: Technical Summary, in Climate Change
5825 2014: Impacts, Adaptation, and Vulnerability. Part A: Global and Sectoral Aspects.
5826 Contribution of Working Group II to the Fifth Assessment Report of the Intergovernmental
5827 Panel on Climate Change, edited by C. B. Field, V. R. Barros, D. J. Dokken, K. J. Mach, M.
5828 D. Mastrandrea, T. E. Bilir, M. Chatterjee, K. L. Ebi, Y. O. Estrada, R. C. Genova, B.
5829 Girma, E. S. Kissel, A. N. Levy, S. MacCracken, P. R. Mastrandrea, and L. L. White, pp.
5830 35–94, Cambridge University Press, Cambridge, UK and New York, NY, USA., 2014.

5831 Fiocco, G., and G. Grams (1964), Observations of the aerosol layer at 20 km by optical radar, *J.*
5832 *Atmos. Sci.*, **21**, 323–324.

5833 Fiore, A. M., and Coauthors, 2012: Global air quality and climate. *Chem. Soc. Rev.*, **41**, 6663–
5834 6683. <http://dx.doi.org/10.1039/C2CS35095E>.

5835 Fiore, A. M., V. Naik, and E. M. Leibensperger, 2015: Air Quality and Climate Connections. *J.*
5836 *Air Waste Manage. Assoc.*, **65**, 645–685, doi:10.1080/10962247.2015.1040526.
5837 <http://www.tandfonline.com/doi/full/10.1080/10962247.2015.1040526>.

5838 Fisher, D., C. Hales, W-C. Wang, M. Ko, N. D. Sze, 1990: Model calculations of the relative
5839 effects of CFCs and their replacements on global warming. *Nature* 344(6266):513-516.
5840 DOI: [10.1038/344513a0](https://doi.org/10.1038/344513a0).

5841 Fisher, D. A., C. H. Hales, W. C. Wang, M. K. W. Ko, and N. D. Sze (1990), Model-calculations
5842 of the relative effects of CFCs and their replacements on global warming, *Nature*, 344(6266),
5843 513–516, doi:10.1038/344513a0.

5844 Fisher et al., 1990D.A. Fisher, C.H. Hales, W.C. Wang, M.K.W. Ko, N.D. SzeModel
5845 calculations of the relative effects of CFCs and their replacements on global warming
5846 *Nature*, 344 (1990), pp. 513-516

5847 Fisher, D., C.H. Hales, W.C. Wang, M.K.W. Ko, N.D. Sze, 1990: Model calculations of the
5848 relative effects of CFCs and their replacements on global warming *Nature*, 344 (1990),
5849 pp. 513-516.

5850 Fishman, J., and P. J. Crutzen, 1978: The origin of ozone in the troposphere. *Nature*, **274**, 855–
5851 858. <http://dx.doi.org/10.1038/274855a0>.

5852 Fishman, J., V. Ramanathan, P. J. Crutzen, and S. C. Liu, 1979a: Tropospheric ozone and
5853 climate. *Nature*, **282**, 818–820. <http://dx.doi.org/10.1038/282818a0>.

5854 Fishman, J., S. Solomon, and P. J. Crutzen, 1979b: Observational and theoretical evidence in
5855 support of a significant in-situ photochemical source of tropospheric ozone. *Tellus*, **31**, 432–
5856 446, doi:10.1111/j.2153-3490.1979.tb00922.x. <https://doi.org/10.1111/j.2153-3490.1979.tb00922.x>.

5858 Fläschner, D., Mauritsen, T. and Stevens, B.: Understanding the inter-model spread in global-
5859 mean hydrological sensitivity, *Journal of Climate*, **29**, 801-817, 2016.

5860 Fleming, J. R., 2007: The Callendar Effect, American Meteorological Society, Boston, MA.

5861 Fleming, J. R., 1998: Historical perspectives on climate change. Oxford University Press. ISBN
5862 978-0195078701.

5863 Folland, C. K., Palmer, T. N. & Parker, D. E. Sahel rainfall and worldwide sea temperatures, 1901-
5864 85. *Nature* **320**, 602-607 (1986).

5865 Forster, P., V. Ramaswamy, P. Artaxo, T. Berntsen, R. Betts, D.W. Fahey, J. Haywood, J. Lean,
5866 D.C. Lowe, G. Myhre, J. Nganga, R. Prinn, G. Raga, M. Schulz and R. Van Dorland, 2007:
5867 Changes in Atmospheric Constituents and in Radiative Forcing. In: *Climate Change 2007: The Physical Science Basis. Contribution of Working Group I to the Fourth Assessment Report of the Intergovernmental Panel on Climate Change* [Solomon, S., D. Qin, M. Manning, Z. Chen, M. Marquis, K.B. Averyt, M.Tignor and H.L. Miller (eds.)]. Cambridge University Press, Cambridge, United Kingdom and New York, NY, USA.

5868

5869

5870

5871

5872 Forster, P. M., Richardson, T., Maycock, A. C., Smith, C. J., Samset, B. H., Myhre, G.,
5873 Andrews, T., Pincus, R. and Schulz, M.: Recommendations for diagnosing effective
5874 radiative forcing from climate models for CMIP6, *Journal of Geophysical Research: Atmospheres*, 121(20), 12460-12475, 2016.

5875

5876 Forster, P., and Coauthors, 2007: Changes in Atmospheric Constituents and in Radiative
5877 Forcing. *Climate Change 2007: The Physical Science Basis. Contribution of Working Group I to the Fourth Assessment Report of the Intergovernmental Panel on Climate Change*, D. Qin, M. Manning, Z. Chen, M. Marquis, K.B. Averyt, M. Tignor, and H.L. Miller, Eds., Cambridge University Press, Cambridge, United Kingdom and New York, NY, USA.

5878

5879

5880

5881

5882 Forster, P. M., 2016: Inference of Climate Sensitivity from Analysis of Earth's Energy Budget.
5883 *Annu. Rev. Earth Planet. Sci.*, 44, 85–106, doi:doi:10.1146/annurev-earth-060614-105156.
5884 <http://www.annualreviews.org/doi/abs/10.1146/annurev-earth-060614-105156>.

5885 Forster, P., and Coauthors, 2007: Changes in Atmospheric Constituents and in Radiative
5886 Forcing. *Climate Change 2007: The Physical Science Basis. Contribution of Working Group I to the Fourth Assessment Report of the Intergovernmental Panel on Climate Change*, D. Qin, M. Manning, Z. Chen, M. Marquis, K.B. Averyt, M. Tignor, and H.L. Miller, Eds., Cambridge University Press, Cambridge, United Kingdom and New York, NY, USA.

5887

5888

5889

5890

5891 Forster, P. M., 1999: Radiative forcing due to stratospheric ozone changes 1979–1997, using
5892 updated trend estimates. *J. Geophys. Res. Atmos.*, **104**, 24395–24399,
5893 doi:doi:10.1029/1999JD900770. <https://doi.org/10.1029/1999JD900770>.

5894 Forster, P. M., and K. P. Shine, 1997: Radiative forcing and temperature trends from
5895 stratospheric ozone changes. *J. Geophys. Res. Atmos.*, **102**, 10841–10855,
5896 doi:doi:10.1029/96JD03510. <https://doi.org/10.1029/96JD03510>.

5897 Forster, P. M., and K. P. Shine, 1999: Stratospheric water vapour changes as a possible
5898 contributor to observed stratospheric cooling. *Geophys. Res. Lett.*, **26**, 3309–3312,
5899 doi:doi:10.1029/1999GL010487. <https://doi.org/10.1029/1999GL010487>.

5900 Foster, G., and S. Rahmstorf, 2011: Global temperature evolution 1979–2010, *Environ. Res.*
5901 *Lett.*, **6**, doi:10.1088/1748-9326/6/4/044022.

5902 Forster, P., Ramaswamy, V., Artaxo, P., Berntsen, T., Betts, R., Fahey, D. W., Haywood, J.,
5903 Lean, J., Lowe, D. C., Myhre, G., Nganga, J., Prinn, R., Raga, G. and Dorland, R. Van:
5904 Changes in Atmospheric Constituents and in Radiative Forcing, in *Climate Change 2007: The Physical Science Basis. Contribution of Working Group I to the Fourth Assessment Report of the Intergovernmental Panel on Climate Change*, edited by S. Solomon D. Qin, M. Manning, Z. Chen, M. Marquis, K.B. Averyt, M.Tignor and H.L. Miller, pp. 130–234, Cambridge University Press, Cambridge, United Kingdom and New York, NY, USA., 5908 2007.

5910 Forster, P., V. Ramaswamy, P. Artaxo, T. Berntsen, R. Betts, D.W. Fahey, J. Haywood, J. Lean, 5911 D.C. Lowe, G. Myhre, J. Nganga, R. Prinn, G. Raga, M. Schulz and R. Van Dorland (2007), 5912 Changes in Atmospheric Constituents and in Radiative Forcing. In: *Climate Change 2007: The Physical Science Basis. Contribution of Working Group I to the Fourth Assessment Report of the Intergovernmental Panel on Climate Change* [Solomon, S., D. Qin, M. Manning, Z. Chen, M. Marquis, K.B. Averyt, M.Tignor and H.L. Miller (eds.)]. Cambridge University 5915 Press, Cambridge, United Kingdom and New York, NY, USA.

5916 Forster, P., and Coauthors, 2007: Changes in Atmospheric Constituents and in Radiative
5918 Forcing. *Climate Change 2007: The Physical Science Basis. Contribution of Working*

5919 *Group I to the Fourth Assessment Report of the Intergovernmental Panel on Climate*
5920 *Change*, D. Qin, M. Manning, Z. Chen, M. Marquis, K.B. Averyt, M. Tignor, and H.L.
5921 Miller, Eds., Cambridge University Press, Cambridge, United Kingdom and New York,
5922 NY, USA.

5923 Forster, P. M., Richardson, T., Maycock, A. C., Smith, C. J., Samset, B. H., Myhre, G., Andrews,
5924 T., Pincus, R., and Schulz, M. (2016), Recommendations for diagnosing effective radiative
5925 forcing from climate models for CMIP6, *J. Geophys. Res. Atmos.*, 121, 12,460– 12,475,
5926 doi:[10.1002/2016JD025320](https://doi.org/10.1002/2016JD025320).

5927 Forster, P. M. *et al.* Evaluating adjusted forcing and model spread for historical and future
5928 scenarios in the CMIP5 generation of climate models. *J. Geophys. Res. Atmos.* **118**, 1139-
5929 1150 (2013).

5930 Forster, P.M. (2016) Inference of Climate Sensitivity from Analysis of Earth's Energy Budget
5931 Annual Review of Earth and Planetary Sciences 2016 44:1, 85-106

5932 Forsyth, P. Y., In the wake of Etna, 44 B.C., Classical Antiq., 7, 49-57, 1988.

5933 Foukal, P., 1981: Sunspots and changes in the global output of the sun. Proc. The Physics of
5934 Sunspots, 1981, Sunspot, NM, A83-18101 06-92), 391-423.

5935 Foukal, P. and J. Lean, 1988: Magnetic modulation of solar luminosity by photospheric activity,
5936 *Astrophys. J.*, 328, 347-357.

5937 Foukal, P. and J. Lean, 1990: An empirical model of total solar irradiance variations between
5938 1874-1988, *Science*, 247, 556-558.

5939 Foukal, P. V., Mack, P. E., and J. E. Vernazza, 1977: The effect of sunspots and faculae on the
5940 solar constant, *Astrophysical Journal*, Part 1, vol. 215, Aug. 1, 1977, p. 952-959.

5941 Foukal, P. North, G. and T. Wigley, 2004: A Stellar View on Solar Variations and Climate,
5942 *Science*, 306, 5693, pp. 68-69, DOI: 10.1126/science.1101694

5943 Fourier, J.B. 1824: M6moire sur les temp6ratures du globe terrestre et des espaces planetaires.
5944 *Mem. Acad. Sci. Inst. Fr.* 7, 569-604.

5945 Franklin, B., Meteorological imaginations and conjectures, 1784: Manchr. Lit. Philos. Soc. Mem.
5946 Proc., 2, 122. (Reprinted in Weatherwise, 35, 262, 1982.).

5947 Franklin, B., Meteorological imaginations and conjectures, Manchr. Lit. Philos. Soc. Mem. Proc.,
5948 2, 122, 1784. (Reprinted in Weatherwise, 35, 262, 1982.)

5949 Friedman, A., Y-Hwang, J. Chiang. and D. Frierson, 2013: Interhemispheric temperature
5950 asymmtery over the 20th Century and in future projections. *J. Climate* 26(15), 5419-5433

5951 Friedlingstein, P., Cox, P., Betts, R., Bopp, L., Bloh, W. von, Brovkin, V., P. Cadule, Doney, S.,
5952 Eby, M., I. Fung, G. Bala, J. John, C. Jones, F. Joos, T. Kato, M. Kawamiya, Knorr, W., K.
5953 Lindsay, H. D. Mathews, T. Raddatz, P. Rayner, Reick, C., E. Roeckner, Schnitzler, K.-G.,
5954 Schnurr, R., K. Strassmen, A. J. Weaver, C. Yoshikawa and Zeng, N.: Climate-carbon cycle
5955 feedback analysis, results from the C4MIP Model intercomparison, *J. Clim.*, 19, 3337–
5956 3353, 2006.

5957 Free, M. and J. Angell (2002), Effect of volcanoes on the vertical temperature profile in radiosonde
5958 data, *J. Geophys. Res.*, 107, No. D10, 10.1029/2001JD001128.

5959 Free, Melissa, and A. Robock (1998), Global warming in the context of the Little Ice Age. *J.*
5960 *Geophys. Res.*, **104**, 19,057-19,070.

5961 Friis-Christensen, E., and K Lassen, 1991: Length of the Solar Cycle: An Indicator of Solar
5962 Activity Closely Associated with Climate, *Science*, 254, pp. 698-700, DOI:
5963 10.1126/science.254.5032.698

5964 Fröhlich, C., 2013: Total Solar Irradiance: What Have We Learned from the Last Three Cycles
5965 and the Recent Minimum? *Space Sci Rev*, 176: 237. <https://doi.org/10.1007/s11214-011-9780-1>

5967 Fröhlich, C. and J. Lean, 2004: Solar radiative output and its variability: Evidence and
5968 Mechanisms, *Astron. Astrophys. Rev.*, 12 (4), 273-320, doi: 10.1007/s00159-004-0024-1.

5969 Fröhlich, C., Romero, J., Roth, H. et al., 1995: VIRGO: Experiment for helioseismology and
5970 solar irradiance monitoring, *Sol Phys* 162: 101. <https://doi.org/10.1007/BF00733428>

5971 Fry, M. M., et al., 2012: The influence of ozone precursor emissions from four world regions on
5972 tropospheric composition and radiative climate forcing, *J. Geophys. Res.*, **117**, D07306,
5973 doi:10.1029/2011JD017134.

5974 Fuglestvedt, J. S., I. S. A. Isaksen, and W. Wang, 1996: Estimates of indirect global warming
5975 potentials for CH₄, CO and NO_x. *Clim. Change*, **34**, 405–437.

5976 Fuglestvedt, J. S., T. K. Berntsen, I. S. A. Isaksen, H. Mao, X.-Z. Liang, and W.-C. Wang, 1999:
5977 Climatic forcing of nitrogen oxides through changes in tropospheric ozone and methane;
5978 global 3D model studies. *Atmos. Environ.*, **33**, 961–977, doi:10.1016/s1352-
5979 2310(98)00217-9. <http://www.sciencedirect.com/science/article/pii/S1352231098002179>.

5980 Fuglestvedt, J. S., K. P. Shine, T. Berntsen, J. Cook, D. S. Lee, A. Stenke, R. B. Skeie, G. J. M.
5981 Velders, and I. A. Waitz (2010), Transport impacts on atmosphere and climate: Metrics,
5982 *Atmos. Environ.*, **44**(37), 4648–4677, doi:10.1016/j.atmosenv.2009.04.044.

5983 Fueglistaler, S., A. E. Dessler, T. J. Dunkerton, I. Folkins, Q. Fu, and P. W. Mote (2009), Tropical
5984 tropopause layer, *Rev. Geophys.*, **47**, RG1004, doi:10.1029/2008RG000267.

5985 Fueglistaler, S., Liu, Y. S., Flannaghan, T. J., Haynes, P. H., Dee, D. P., Read et al. (2013), The
5986 relation between atmospheric humidity and temperature trends for stratospheric water, *J.*
5987 *Geophys. Res. Atmos.*, **118**, 105 –1074.

5988 Fyfe, J. C., K. von Salzen, J. N. S. Cole, N. P. Gillett, and J. P. Vernier (2013), Surface response
5989 to stratospheric aerosol changes in a coupled atmosphere-ocean model. *Geophysical Research*
5990 *Letters*, **40**, 584-588.

5991 Ganguly, D., Rasch, P. J., Wang, H. & Yoon, 2012: J. Fast and slow responses of the South
5992 Asian monsoon system to anthropogenic aerosols. *Geophys. Res. Lett.* **39**, L18804

5993 Gao, C., Robock, A., & Ammann, C. (2008). Volcanic forcing of climate over the past 1500
5994 years: An improved ice core-based index for climate models. *Journal of Geophysical*
5995 *Research: Atmospheres*, **113**(D23).

5996 Gao, C., A. Robock, and C. Ammann (2008), Volcanic forcing of climate over the past 1500 years:
5997 An improved ice core-based index for climate models, *J. Geophys. Res.*, 113, D23111,
5998 doi:10.1029/2008JD010239.

6000 Gasser, T., Peters, G. P., Fuglestvedt, J. S., Collins, W. J., Shindell, D. T., and Ciais, P.: Accounting
6001 for the climate–carbon feedback in emission metrics, *Earth Syst. Dynam.*, 8, 235–253,
https://doi.org/10.5194/esd-8-235-2017, 2017.

6002 Gasser, T. and Ciais, P.: A theoretical framework for the net land-to-atmosphere CO₂ flux and
6003 its implications in the definition of “emissions from land-use change,” *Earth Syst. Dyn.*, 4,
6004 171–186, doi:10.5194/esd-4-171–2013, 2013.

6005 Gassó, S. (2008). Satellite observations of the impact of weak volcanic activity on marine clouds.
6006 *Journal of Geophysical Research: Atmospheres*, 113(D14).

6007 Gauss, M., and Coauthors, 2006: Radiative forcing since preindustrial times due to ozone change
6008 in the troposphere and the lower stratosphere. *Atmos. Chem. Phys.*, 6, 575–599.

6009 Ghan, S. J.: Technical Note: Estimating aerosol effects on cloud radiative forcing, *Atmospheric
6010 Chemistry and Physics*, 13(19), 9971–9974, 2013.

6011 Ghan, S.J., Easter, R.C., Chapman, E.G., Abdul-Razzak, H., Zhang, Y., Leung, L.R., Laulainen,
6012 N.S., Saylor, R.D. and Zaveri, R.A., 2001. A physically based estimate of radiative forcing
6013 by anthropogenic sulfate aerosol. *Journal of Geophysical Research: Atmospheres*, 106(D6),
6014 pp.5279–5293.

6015 Ghan, S et al. Challenges in constraining anthropogenic aerosol effects on cloud radiative forcing
6016 using present-day spatiotemporal variability. *PNAS*, 113, 5804–5811, 2016.

6017 Gidden, M. J., Riahi, K., Smith, S. J., Fujimori, S., Luderer, G., Kriegler, E., van Vuuren, D. P.,
6018 van den Berg, M., Feng, L., Klein, D., Calvin, K., Doelman, J. C., Frank, S., Fricko, O.,
6019 Harmsen, M., Hasegawa, T., Havlik, P., Hilaire, J., Hoesly, R., Horing, J., Popp, A.,
6020 Stehfest, E. and Takahashi, K.: Global emissions pathways under different socioeconomic
6021 scenarios for use in CMIP6: a dataset of harmonized emissions trajectories through the end
6022 of the century, *Geosci. Model Dev. Discuss.*, (November), 1–42, doi:10.5194/gmd-2018-

6023 266, 2018.

6024 Ginoux, P., Prospero, J., Gill, T. E., Hsu, N. C. and Zhao, M.: Global scale attribution of
6025 anthropogenic and natural dust sources and their emission rates based on MODIS deep blue
6026 aerosol products, *Rev. Geophys.*, 50,(RG3005,), DOI:10.1029/2012RG000388, 2012.

6027 Gitz, V. and Ciais, P.: Amplifying effects of land-use change on future atmospheric CO₂ levels,
6028 *Global Biogeochem. Cycles*, 17(1), 1024; doi:10.1029/2002GB001963, 2003.

6029 Gomez Martin, J. C., J. S. Brooke, W. Feng, M. Hopfner, M. J. Mills, and J. M. C. Plane (2017),
6030 Impacts of meteoric sulfur in the Earth's atmosphere, *J. Geophys. Res. Atmos.*, 122,
6031 doi:10.1002/2017JD027218.

6032 Goody, R. M., and Y. L. Yung, 1985: *Atmospheric Radiation: Theoretical Basis*. Second edition.
6033 Oxford University Press, New York, 1989. 519 pp.

6034 Goody, R. M., & Yung, Y. L. (1995). *Atmospheric Radiation : Theoretical Basis*. Oxford
6035 University Press. Retrieved from [https://global.oup.com/academic/product/atmospheric-
6036 radiation-9780195102918#.W9NLN4c8GC4.mendeley](https://global.oup.com/academic/product/atmospheric-radiation-9780195102918#.W9NLN4c8GC4.mendeley)

6037 Govindasamy, B., and K. Caldeira (2000), Geoengineering Earth's radiation balance to mitigate
6038 CO₂-induced climate change. *Geophysical Research Letters*, 27, 2141-2144.

6039 Granier, C., K. P. Shine, J. S. Daniel, I. E. Hansen, S. Lal, and F. Stordal, 1999: Climate Effects
6040 of Ozone and Halocarbon Changes. *Scientific Assessment of Ozone Depletion: 1998*, D.L.
6041 Albritton, P.J. Aucamp, G. Mégie, and R.T. Watson, Eds.

6042 Granier, C., and Coauthors, 2011: Evolution of anthropogenic and biomass burning emissions of
6043 air pollutants at global and regional scales during the 1980–2010 period. *Clim. Change*,
6044 109, 163–190, doi:10.1007/s10584-011-0154-1. <http://dx.doi.org/10.1007/s10584-011-0154-1>.

6046 Graf, H.-F., J. Feichter and B. Langmann, 1997: Volcanic sulfur emissions: Estimates of source
6047 strength and its contribution to the global sulfate distribution. *J. Geophys. Res.*, 102,
6048 10727–10738.

6049 Graham, B., Guyon, P., Maenhaut, W., Taylor, P. E., Ebert, M., Matthias-Maser, S., Mayol-
6050 Bracero, O. L., Godoi, R. H. M., Artaxo, P., Meixner, F. X., Moura, M. A. L., Rocha, C. H.
6051 E., VanGrieken, R., Globsky, M. M., Flagan, R. C. and Andreae, M. O.: Composition and
6052 diurnal variability of the natural Amazonian aerosol, *J. Geophys. Res.*, 108(D24), 4765,
6053 doi:10.1029/2003JD004049, 2003.

6054 Grattan, J., Brayshaw, M., Sadler, J. (1998), Modelling the distal impacts of past volcanic gas
6055 emissions: evidence of Europewide environmental impacts from gases emitted during the
6056 eruption of Italian and Icelandic volcanoes in 1783. *Quaternaire* 9, 25– 35.

6057 Gray, L. J., et al., 2010: Solar influences on climate, *Rev. Geophys.*, 48, RG4001,
6058 doi:10.1029/2009RG000282.

6059 Gregory, J. M., and Coauthors, 2004: A new method for diagnosing radiative forcing and climate
6060 sensitivity. *Geophys. Res. Lett.*, 31, L03205, doi:10.1029/2003gl018747.

6061 ——, C. D. Jones, P. Cadule, and P. Friedlingstein, 2009: Quantifying Carbon Cycle Feedbacks.
6062 *J. Clim.*, 22, 5232–5250, doi:10.1175/2009JCLI2949.1.
6063 <https://doi.org/10.1175/2009JCLI2949.1>.

6064 Greene, M. T. (2000), High achiever, *Nature*, 407, pp 947.

6065 Gregory, J. M., Bi, D., Collier, M. A., Dix, M. R., Hirst, A. C., Hu, A., Huber, M., Knutti, R.,
6066 Marsland, S. J., Meinshausen, M., Rashid, H. A., Rotstayn, L. D., Schurer, A. and Church, J.
6067 A. (2013), Climate models without pre-industrial volcanic forcing underestimate historical
6068 ocean thermal expansion. *Geophysical Research Letters*, 40 (8). pp. 1600-1604. ISSN 0094-
6069 8276 doi: <https://doi.org/10.1002/grl.50339>

6070 Gruner, P., Kleinert, H., (1927), Die dammerung erscheinen, *Probl. Kosm. Phys.*, 10, 1-113.

6071 Gruber, S., Blahak, U., Haenel, F., Kottmeier, C., Leisner, T., Muskatel, H., Storelvmo, T. ,
6072 Vogel, B., 2019: A process study on thinning of Arctic winter cirrus clouds with high-
6073 resolved ICON-ART simulations. *J. Geophys. Res.*, **Under revi.**

6074 Guenther, A., Karl, T., Harley, P., Wiedinmyer, C., Palmer, P. I. and Geron, C.: Estimates of
6075 global terrestrial emissions using MEGAN (Model of Emissions of Gases and Aerosols

6076 from Nature), *Atmos. Chem. Phys.*, 6, 3181–3210, doi:10.5194/acp-6-3181-2006, 2006.

6077 Guo, S., G. J. S. Bluth, W. I. Rose, I. M. Watson, and A. J. Prata (2004a), Re-evaluation of SO₂
6078 release of the 15 June 1991 Pinatubo eruption using ultraviolet and infrared satellite sensors,
6079 *Geochem. Geophys. Geosyst.*, 5, Q04001, doi:10.1029/2003GC000654.

6080 Guo, S., W. I. Rose, G. J. S. Bluth, and I. M. Watson (2004b), Particles in the great Pinatubo
6081 volcanic cloud of June 1991: The role of ice, *Geochem. Geophys. Geosyst.*, 5, Q05003,
6082 doi:10.1029/2003GC000655.

6083

6084 Haagen-Smit, A. J., 1952: Chemistry and Physiology of Los Angeles Smog. *Ind. Eng. Chem.*, **44**,
6085 1342–1346.

6086 Haberreiter, M., M. Scholl, T. D. de Wit, M. Kretzschmar, S. Misios, K. Tourpali, and W.
6087 Schmutz, 2017: A new observational solar irradiance composite, *J Geophys Res-Space*,
6088 122(6), 5910-5930, doi: 10.1002/2016ja023492.

6089 Hameed, S., and R. D. Cess, 1983: Impact of a global warming on biospheric sources of methane
6090 and its climatic consequences. *Tellus B*, **35B**, 1–7, doi:doi:10.1111/j.1600-
6091 0889.1983.tb00001.x. <https://doi.org/10.1111/j.1600-0889.1983.tb00001.x>.

6092 Hameed, S., R. D. Cess, and J. S. Hogan, 1980: Response of the global climate to changes in
6093 atmospheric chemical composition due to fossil fuel burning. *J. Geophys. Res. Ocean.*, **85**,
6094 7537–7545, doi:doi:10.1029/JC085iC12p07537. <https://doi.org/10.1029/JC085iC12p07537>.

6095 Hamill, P., E. J. Jensen, P. B. Russell, J. J. Bauman (1997), The life cycle of stratospheric aerosol
6096 particles, *Bull. Amer. Meteorol. Soc.*, 7, 1395-1410.

6097 Hamilton, D. S., Hantson, S., Scott, C. E., Kaplan, J. O., Pringle, K. J., Nieradzik, L. P., Rap, A.,
6098 Folberth, G. A., Spracklen, D. V. and Carslaw, K. S.: Reassessment of pre-industrial fire
6099 emissions strongly affects anthropogenic aerosol forcing, *Nat. Commun.*, 9(1),
6100 doi:10.1038/s41467-018-05592-9, 2018.

6101 Hampson, J., 1965: Chemiluminescent emission observed in the stratosphere and mesosphere.

6102 *Les Problèmes Meteorologiques de la Stratosphère et de la Mesosphère*, Presses
6103 Universitaires de France, Paris, p. 393.

6104 Hartmann, D. L., Klein Tank, A., Alexander, L., Brönnimann, S., Charabi, Y., Dentener, F. J.,
6105 Easterling, D. R., Kaplan, A., Soden, B., Thorne, P., Wild, M. and Zhai, P. M.:
6106 Observations: Atmosphere and Surface, in Climate Change 2013: The Physical Science
6107 Basis. Contribution of Working Group I to the Fifth Assessment Report of the
6108 Intergovernmental Panel on Climate Change, pp. 159–218., 2013.

6109 Haug, G. H., D. Günther, L. C. Peterson, D. M. Sigman, K. A. Hughen, and B. Aeschlimann,
6110 2003: Climate and the collapse of Maya Civilization, *Science*, 299, 1731-1735

6111 Han, Q., Rossow, W. B., & Lacis, A. A. (1994). Near-global survey of effective droplet radii in
6112 liquid water clouds using ISCCP data. *Journal of Climate*, 7(4), 465-497.

6113 Hansen, J. E., Sato, M., Lacis, A., Ruedy, R., Tegen, I., & Matthews, E. (1998). Climate forcings
6114 in the industrial era. *Proceedings of the National Academy of Sciences*, 95(22), 12753-
6115 12758.

6116 Hansen, J., and Coauthors, 1997a: Forcings and chaos in interannual to decadal climate change.
6117 *J. Geophys. Res. Atmos.*, **102**, 25679–25720, doi:doi:10.1029/97JD01495.
6118 <https://doi.org/10.1029/97JD01495>.

6119 —, M. Sato, and R. Ruedy, 1997b: Radiative forcing and climate response. *J. Geophys. Res.*
6120 *Atmos.*, **102**, 6831–6864, doi:doi:10.1029/96JD03436. <https://doi.org/10.1029/96JD03436>.

6121 Hansen, J., 2002: Climate forcing in Goddard Institute for Space Studies SI2000 simulations. *J*
6122 *Geophys Res*, 107, 4347.

6123 Hansen, J. E., A. Lacis, and S. A. Lebedeff, 1982: In Carbon dioxide review 1982, W. Clark,
6124 Ed., Oxford University Press, Clarendon, England, 284–289.

6125 Hansen, J. E., and Andrew A. Lacis, 1990: Sun and dust versus greenhouse gases: an assessment
6126 of their relative roles in global climate change. *Nature* volume 346, pages 713–719.

6127 Hansen, J., A. Lacis, D. Rind, G. Russell, P. Stone, I. Fung, R. Ruedy, and J. Lerner, 1984:
6128 Climate sensitivity: Analysis of feedback mechanisms. In *Climate Processes and Climate*
6129 *Sensitivity*. J.E. Hansen and T. Takahashi, Eds., AGU Geophysical Monograph 29, Maurice
6130 Ewing Vol. 5. American Geophysical Union, pp. 130-163. 10.1029/GM029.

6131 Hansen, J., A. Lacis, R. Ruedy, M. Sato, and H. Wilson, 1993: How Sensitive Is the Worlds
6132 Climate. *Natl. Geogr. Res. Explor.*, **9**, 142–158.

6133 ——, M. Sato, R. Ruedy, A. Lacis, and V. Oinas, 2000: Global warming in the twenty-first
6134 century: An alternative scenario. *Proc. Natl. Acad. Sci. U. S. A.*, **97**, 9875–9880.

6135 Hansen, J., D. Johnson, A. Lacis, S. Lebedeff, P. Lee, D. Rind, and G. Russell, 1981: Climate
6136 Impact of Increasing Atmospheric Carbon Dioxide. *Science*, **213**, 957 LP-966,
6137 doi:10.1126/science.213.4511.957.
6138 <http://science.sciencemag.org/content/213/4511/957.abstract>.

6139 Hansen, J., D. Johnson, A. Lacis, S. Lebedeff, P. Lee, D. Rind, and G. Russell, 1981: Climate
6140 Impact of Increasing Atmospheric Carbon Dioxide. *Science*, **213**, 957 LP-966,
6141 doi:10.1126/science.213.4511.957. <http://science.sciencemag.org/content/213/4511/957>.

6142 ——, I. Fung, A. Lacis, D. Rind, S. Lebedeff, R. Ruedy, G. Russell, and P. Stone, 1988: Global
6143 climate changes as forecast by Goddard Institute for Space Studies three-dimensional
6144 model. *J. Geophys. Res. Atmos.*, **93**, 9341–9364, doi:10.1029/JD093iD08p09341.
6145 <https://doi.org/10.1029/JD093iD08p09341>.

6146 ——, A. Lacis, R. Ruedy, M. Sato, and H. Wilson, 1993: How Sensitive Is the Worlds Climate.
6147 *Natl. Geogr. Res. Explor.*, **9**, 142–158.

6148 ——, M. Sato, and R. Ruedy, 1997: Radiative forcing and climate response. *J. Geophys. Res.*,
6149 **102**, 6831–6864.

6150 ——, and Coauthors, 2005: Efficacy of climate forcings. *J. Geophys. Res.*, **110**, D18104,
6151 doi:10.1029/2005JD005776.

6152 Harshvardhan (1979), Perturbation of the Zonal Radiation Balance by a Stratospheric Aerosol
6153 Layer, *J. Atmos. Sci.*, **36**, 1274-1285.

6154 Hauglustaine, D. A., C. Granier, G. P. Brasseur, and G. Mégie, 1994: The importance of
6155 atmospheric chemistry in the calculation of radiative forcing on the climate system. *J.*
6156 *Geophys. Res. Atmos.*, 99, 1173–1186, doi:10.1029/93JD02987.
6157 <https://doi.org/10.1029/93JD02987>.

6158 Haywood, J.M., and Shine, K.P., 1995. The effect of anthropogenic sulfate and soot aerosol on
6159 the clear sky planetary radiation budget. *Geophys. Res. Letts.*, 22, 5, 603-606.

6160 Haywood, J.M. and Shine, K.P., 1997. Multi-spectral Calculations of the Direct Radiative
6161 Forcing of Tropospheric Sulfate and Soot Aerosols using a Column Model. *Quart. J. of the*
6162 *Roy. Meteorol. Soc.*, 123, 1907-1930.

6163 Haywood, J.M., Roberts, D.L., Slingo, A., Edwards, J.M. and Shine, K.P., 1997. General
6164 Circulation Model Calculations of the Direct Radiative Forcing by Anthropogenic Sulfate
6165 and Fossil-Fuel Soot Aerosol. *J. Clim.*, 10, 1562-1577.

6166 Haywood, J.M. and Ramaswamy, V., 1998. Global sensitivity studies of the direct radiative
6167 forcing of sulfate and black carbon aerosol. *J. Geophys. Res.*, 103, 6043-6058.

6168 Haywood, J.M., Ramaswamy, V., and Soden, B.J., 1999. Tropospheric aerosol climate forcing in
6169 clear-sky satellite observations over the oceans. *Science*, 283, 1299-1305.

6170 Haywood, J.M., Francis, P.N., Glew, M.D., Dubovik, O., and Holben, B.N, Comparison of
6171 aerosol size distributions, radiative properties, and optical depths determined by aircraft
6172 observations and Sun photometers during SAFARI-2000. *J. Geophys. Res.*, 108(D13),
6173 8471, doi:10.1029/2002JD002250, 2003.

6174 Haywood, J. M., M. D. Schwarzkopf, and V. Ramaswamy, 1998: Estimates of radiative forcing
6175 due to modeled increases in tropospheric ozone. *J. Geophys. Res. Atmos.*, **103**, 16999–
6176 17007, doi:doi:10.1029/98JD01348. <https://doi.org/10.1029/98JD01348>.

6177 Haywood, J. M., Jones, A., Bellouin, N. & Stephenson, D. Asymmetric forcing from stratospheric
6178 aerosols impacts Sahelian rainfall. *Nat. Clim. Change* **3**, 660-665 (2013).

6179 Haywood, J. M., A. Jones, N. Bellouin, and D. Stephenson (2013), Asymmetric forcing from
6180 stratospheric aerosols impacts Sahelian rainfall. *Nat Clim Change*, 3, 660-665.

6181 Haywood, J. M., A. Jones, and G. S. Jones, 2014: The impact of volcanic eruptions in the period
6182 2000–2013 on global mean temperature trends evaluated in the HadGEM2-ES climate model.
6183 *Atmospheric Science Letters*, 15, 92-96.

6184 Haywood, J. M., and K. P. Shine, 1995: The effect of anthropogenic sulfate and soot aerosol on
6185 the clear-sky planetary radiation budget. *Geophys. Res. Lett.*, 22, 603–606.

6186 Hauglustaine, D. A., and G. P. Brasseur, 2001: Evolution of tropospheric ozone under
6187 anthropogenic activities and associated radiative forcing of climate. *J. Geophys. Res.*, **106**,
6188 32337–32360.

6189 Hauglustaine, D. A., C. Granier, and G. P. Brasseur, 1995: Impact of increased methane
6190 emissions on the atmospheric composition and related radiative forcing on the climate
6191 system. *Atmospheric Ozone as a Climate Gas, NATO-ASI Series*, W.-C. Wang and I.
6192 Isaksen, Eds., Springer-Verlag, Berlin, Germany, 189–203.

6193 Heald, C. and Spracken, D.: Land use change impacts on air quality and climate, *Chem. Rev.*,
6194 225(10), 4476–4496; DOI: 10.1021/cr500446g, 2015.

6195 Hegerl, G.C., et al., 1996: Detecting greenhouse-gas-induced climate change with an optimal
6196 fingerprint method. *J. Clim.*, **9**, 2281–2306.

6197 Hegerl, G.C., et al., 1997: Multi-fingerprint detection and attribution of greenhouse-gas and
6198 aerosol-forced climate change. *Clim. Dyn.*, **13**, 613–634.

6199 Hegerl, G. C. *et al.* Challenges in quantifying changes in the global water cycle. *Bull. Am.
6200 Meteorol. Soc.* **96**, 1097-1115 (2015).

6201 Heckendorn, P., and Coauthors (2009), The impact of geoengineering aerosols on stratospheric
6202 temperature and ozone. *Environ Res Lett*, 4, 045108.

6203 Hegglin, M. I., and T. G. Shepherd, 2009: Large climate-induced changes in ultraviolet index
6204 and stratosphere-to-troposphere ozone flux. *Nat. Geosci.*, **2**, 687–691,
6205 doi:http://www.nature.com/ngeo/journal/v2/n10/supplinfo/ngeo604_S1.html.
6206 <http://dx.doi.org/10.1038/ngeo604>.

6207 Hergesell, M., 1919: Die Strahlung der Atmosphäre unter Zungrundlegung bon Lindeberger
6208 Temperatur: und Feuchtigkeits Messungen. *Die Arbeiten des Preusslichen Aero-*
6209 *nautischen Observatoriums bei Lindenberg*, Vol. 13, Braunschweig, Germany, Firedr.
6210 Vieweg and Sohn, 1-24.

6211 Herring, W. S., and T. R. Borden, Jr., 1965: Mean distributions of ozone density over
6212 North America, 1963-1964. Environmental Research Papers, No. 162. AFCRL 65-
6213 913, Air Force Cambridge Research Laboratories, Bedford, Mass., 19 pp.

6214 Hickey, J. R., Stowe, L. L., Jacobowitz, H., Pellegrino, P., Maschhoff, R. H., House, F., and T.
6215 H. Vonder Haar, 1980: Initial Solar Irradiance Determinations from Nimbus 7 Cavity
6216 Radiometer Measurements, *Science*, 208, 281-283, DOI: 10.1126/science.208.4441.281

6217 Hill, S. A., Ming, Y. & Held, 2015: I. M. Mechanisms of forced tropical meridional energy flux
6218 change. *J. Clim.* **28**, 1725–1742

6219 Hill, S., and Y. Ming, 2012: Nonlinear climate response to regional brightening of tropical
6220 marine stratocumulus. *Geophys. Res. Lett.*, doi:10.1029/2012GL052064.

6221 Hodnebrog Ø, Etminan M, Fuglestvedt JS, Marston G, Myhre G, Nielsen CJ, Shine KP,
6222 Wallington TJ 2013: Global Warming Potentials and Radiative Efficiencies of Halocarbons
6223 and Related Compounds: A Comprehensive Review *Reviews of Geophysics* 51:300-378
6224 10.1002/rog.20013.

6225 Hoesly, R. M., and Coauthors, 2017: Historical (1750–2014) anthropogenic emissions of reactive
6226 gases and aerosols from the Community Emission Data System (CEDS). *Geosci. Model*
6227 *Dev. Discuss.*, **2017**, 1–41, doi:10.5194/gmd-2017-43. <http://www.geosci-model-dev-discuss.net/gmd-2017-43/>.

6229 Hofmann, D. J., J. M. Rosen, T. J. Pepin, and R. G. Pinnick (1975), Stratospheric aerosol
6230 measurements I: Time variations at northern midlatitudes, *J. Atmos. Sci.*, 32, 1446–1456.

6231 Holben, Brent N., T. F[†] Eck, I[†] Slutsker, D. Tanre, J. P. Buis, A. Setzer, E. Vermote et al.
6232 "AERONET—A federated instrument network and data archive for aerosol
6233 characterization." *Remote sensing of environment* 66, no. 1 (1998): 1-16.

6234 Holton, J.R., P. H. Haynes, M. E.. McIntyre, A. R. Douglass, R. B. Rood, L. Pfister (1995),
6235 Stratosphere-troposphere exchange, *Rev. Geophys.*, 33, 403-439.

6236 Hood, L. L., S. Misios, D. M. Mitchell, E. Rozanov, L. J. Gray, K. Tourpali, K. Matthes, H.
6237 Schmidt, G. Chiodo, R. Thiéblemont, D. Shindell, and A. Krivolutsky, 2015: Solar signals
6238 in CMIP-5 simulations: the ozone response, *Quarterly Journal Roy. Meteor. Soc.*, 141, I692,
6239 2670-2689, Part A DOI10.1002/qj.2553.

6240 Höpfner, M., Glatthor, N., Grabowski, U., Kellmann, S., Kiefer, M., Linden et al. (2013), Sulfur
6241 dioxide (SO₂) as observed by MIPAS/Envisat: temporal development and spatial distribution
6242 at 15–45 km altitude, *Atmos. Chem. Phys.*, 13, 10405 – 10423, doi:10.5194/acp-13-10405-
6243 2013.

6244 Höpfner, M., Boone, C. D., Funke, B., Glatthor, N., Grabowski, U., Günther et al. (2015), Sulfur
6245 dioxide (SO₂) from MIPAS in the upper troposphere and lower stratosphere 2002 – 2012,
6246 *Atmos. Chem. Phys.*, 15, 7017 – 7037, doi:10.5194/acp-15-7017-2015.

6247 Hough, A. M., and R. G. Derwent, 1990: Changes in the global concentration of tropospheric
6248 ozone due to human activities. *Nature*, **344**, 645–648.

6249 Houghton, J. T., 1963: Absorption in the stratosphere by some water vapor lines in the ν_2
6250 band. *Quart. J. Roy. Meteor. Soc.*, **89**, 332-338.

6251 Houghton, R.: Interactions between land-use change and climate-carbon cycle feedbacks, *Curr.*
6252 *Clim. Chang. Reports*, 4(2), 115–127, 2018.

6253 Howard, J. N., D. L. Burch and D. Williams, 1955: Near-infrared transmission through
6254 synthetic atmosphere. *Geophysics Research Papers*, No. 40, Air Force Cambridge
6255 Research Center, AFCRC-TR-55-213, 214 pp.

6256 Hoyt, D. V., and K. H. Schatten, 1997: The Role of the Sun in Climate Change, Oxford
6257 University Press.

6258 Hoyt, D. V., 1979. The Smithsonian Astrophysical Observatory solar constant program. *Revs.*
6259 *Geophys. and Space Physics*, 17, 427-458.

6260 Hoyt, D. V., and K. H. Schatten, 1997: The Role of the Sun in Climate Change, Oxford
6261 University Press.

6262 Hudson, H.S., Silva, S., Woodard, M. et al., 1982: The effects of sunspots on solar irradiance,
6263 Solar Physics 76: 211. <https://doi.org/10.1007/BF00170984>

6264 Hulbert, E. O. (1931). The temperature of the lower atmosphere of the earth. *Physical Review*,
6265 38(10), 1876–1890. <http://doi.org/10.1103/PhysRev.38.1876>

6266 Humphreys, W. J. (1913), Volcanic dust and other factors in the production of climatic changes,
6267 and their possible relation to ice gases, J. Franklin Inst., Aug. 131-172.

6268 Humphreys, W. J. (1940), Physics of the Air, McGraw-Hill, New York, 676 pp.

6269 Huneeus, N., Schulz, M., Balkanski, Y., Griesfeller, J., Prospero, M. J., Kinne, S., ... & Diehl, T.
6270 (2011). Global dust model intercomparison in AeroCom phase I. *Atmospheric Chemistry
6271 and Physics*, 11, 7781-7816.

6272 Husar, R. B., Prospero, J. M., & Stowe, L. L. (1997). Characterization of tropospheric aerosols
6273 over the oceans with the NOAA advanced very high resolution radiometer optical thickness
6274 operational product. *Journal of Geophysical Research: Atmospheres*, 102(D14), 16889-
6275 16909.

6276 Husson, N. B. Bonnet, N.A. Scott, & A. Chédin. (1992). Management and study of
6277 spectroscopic information: the GEISA program. *J. Quant. Spectrosc. Rad. Trans.*, 48, 509-
6278 518. [https://doi.org/10.1016/0022-4073\(92\)90116-L](https://doi.org/10.1016/0022-4073(92)90116-L)

6279 Hsu, N. C., Tsay, S. C., King, M. D., & Herman, J. R. (2006). Deep blue retrievals of Asian
6280 aerosol properties during ACE-Asia. *IEEE Transactions on Geoscience and Remote
6281 Sensing*, 44(11), 3180-3195.

6282 Hwang, Y.-T., Frierson, D. M. W. & Kang, S. M. Anthropogenic sulfate aerosol and the southward
6283 shift of tropical precipitation in the late 20th century. *Geophys. Res. Lett.* **40**, 2845-2850
6284 (2013).

6285

6286 Iacobellis, S. F., Frouin, R., & Somerville, R. C. (1999). Direct climate forcing by biomass-
6287 burning aerosols: Impact of correlations between controlling variables. *Journal of*
6288 *Geophysical Research: Atmospheres*, 104(D10), 12031-12045.

6289 I.E. Gordon, L.S. Rothman, C. Hill, R.V. Kochanov, Y. Tan, P.F. Bernath, M. Birk, V. Boudon,
6290 A. Campargue, K.V. Chance, B.J. Drouin, J.-M. Flaud, R.R. Gamache, J.T. Hedges, D.
6291 Jacquemart, V.I. Perevalov, A. Perrin, K.P. Shine, M.-A.H. Smith, J. Tennyson, G.C. Toon,
6292 H. Tran, V.G. Tyuterev, A. Barbe, A.G. Császár, V.M. Devi, T. Furtenbacher, J.J. Harrison,
6293 J.-M. Hartmann, A. Jolly, T.J. Johnson, T. Karman, I. Kleiner, A.A. Kyuberis, J. Loos,
6294 O.M. Lyulin, S.T. Massie, S.N. Mikhailyko, N. Moazzen-Ahmadi, H.S.P. Müller, O.V.
6295 Naumenko, A.V. Nikitin, O.L. Polyansky, M. Rey, M. Rotger, S.W. Sharpe, K. Sung, E.
6296 Starikova, S.A. Tashkun, J. Vander Auwera, G. Wagner, J. Wilzewski, P. Wcisło, S. Yu,
6297 E.J. Zak, The HITRAN2016 molecular spectroscopic database, *Journal of Quantitative*
6298 *Spectroscopy and Radiative Transfer*, Volume 203, 2017, Pages 3-69, ISSN 0022-4073,
6299 <https://doi.org/10.1016/j.jqsrt.2017.06.038>.

6300 Iles, C. E., G. C. Hegerl, A. P. Schurer, and X. Zhang (2013), The effect of volcanic eruptions on
6301 global precipitation, *J. Geophys. Res.*, 118, 8770-8786, doi:10.1002/JGRD.50678.

6302 IPCC, Annex II: Climate System Scenario Tables . *Climate Change 2013: The Physical Science*
6303 *Basis. Contribution of Working Group I to the Fifth Assessment Report of the*
6304 *Intergovernmental Panel on Climate Change*, T.F. Stocker D. Qin, G.-K. Plattner, M.
6305 Tignor, S.K. Allen, J. Boschung, A. Nauels, Y. Xia, V. Bex and P.M. Midgley, Ed.,
6306 Cambridge University Press, Cambridge, United Kingdom and New York, NY, USA,
6307 1395–1446.

6308 Isaksen, I. S. A., and Ø. Hov, 1987: Calculation of trends in the tropospheric concentration of
6309 O₃, OH, CO, CH₄ and NO_x. *Tellus B*, 39B, 271–285, doi:doi:10.1111/j.1600-
6310 0889.1987.tb00099.x. <https://doi.org/10.1111/j.1600-0889.1987.tb00099.x>.

6311 Isaksen, I. S. A., J. S. Fuglestvedt, Y.-P. Lee, C. Johnson, R. Atkinson, J. Lelieveld, H.
6312 Sidebottom, and A. M. Thompson, 1991: Tropospheric Processes: Observations and
6313 interpretation. *Scientific Assessment of Ozone Depletion: 1991*, D.L. Albritton, R.T.
6314 Watson, S. Solomon, R.F. Hampson, and F. Ormond, Eds.

6315 ——, V. Ramaswamy, H. Rodhe, and T. M. L. Wigley, 1992: Radiative Forcing of Climate.
6316 *Climate Change 1992: The Supplementary Report to the IPCC Scientific Assessment*, J.T.
6317 Houghton, B.A. Callander, and S.K. Varney, Eds., Cambridge University Press, Cambridge,
6318 U.K., New York, NY, USA, Victoria, Australia.

6319 Isaksen, I. S. A., and Coauthors, 2009: Atmospheric composition change: Climate-Chemistry
6320 interactions. *Atmos. Environ.*, **43**, 5138–5192, doi:10.1016/j.atmosenv.2009.08.003.
6321 <http://www.sciencedirect.com/science/article/pii/S1352231009006943>.

6322 Isaksen, I., V. Ramaswamy, H. Rodhe, and T. M. L. Wigley, 1992: Radiative forcing of climate.
6323 Climate Change 1992: The Supplementary Report to the IPCC Scientific Assessment, 47–
6324 67.

6325 Iversen, T., A. Kirkevåg, J. E. Kristjansson, and Ø. Seland, 2000: Climate effects of sulfate and
6326 black carbon estimated in a global climate model. In *Air Pollution Modeling and its
6327 Application XIV*, S.-E. Gryning and F.A. Schiermeier, Eds. Kluwer/Plenum Publishers, New
6328 York, 335–342.

6329

6330 Jacquinet-Husson, N., R. Armante, N.A. Scott, A. Chédin, L. Crépeau, C. Boutammine, A.
6331 Bouhdaoui, C. Crevoisier, V. Capelle, C. Bonne, N. Poulet-Crovisier, A. Barbe, D. Chris
6332 Benner, V. Boudon, L.R. Brown, J. Buldyreva, A. Campargue, L.H. Coudert, V.M. Devi,
6333 M.J. Down, B.J. Drouin, A. Fayt, C. Fittschen, J.-M. Flaud, R.R. Gamache, J.J. Harrison, C.
6334 Hill, Ø. Hodnebrog, S.-M. Hu, D. Jacquemart, A. Jolly, E. Jiménez, N.N. Lavrentieva, A.-
6335 W. Liu, L. Lodi, O.M. Lyulin, S.T. Massie, S. Mikhailenko, H.S.P. Müller, O.V.
6336 Naumenko, A. Nikitin, C.J. Nielsen, J. Orphal, V.I. Perevalov, A. Perrin, E. Polovtseva, A.
6337 Predoi-Cross, M. Rotger, A.A. Ruth, S.S. Yu, K. Sung, S.A. Tashkun, J. Tennyson, Vl.G.
6338 Tyuterev, J. Vander Auwera, B.A. Voronin, & A. Makie. (2016). The 2015 edition of the
6339 GEISA spectroscopic database, *Journal of Molecular Spectroscopy*, 327, 31–72.
6340 <https://doi.org/10.1016/j.jms.2016.06.007>.

6341 Jacob, D. J., and D. A. Winner, 2009: Effect of climate change on air quality. *Atmos. Environ.*,
6342 **43**, 51–63, doi:10.1016/j.atmosenv.2008.09.051.

6343 <http://www.sciencedirect.com/science/article/B6VH3-4TNWH49-4/2/30b98e804a7d8cab841c22038bc0c264>.

6345 Jacobson, M. Z. (2001). Global direct radiative forcing due to multicomponent anthropogenic
6346 and natural aerosols. *Journal of Geophysical Research: Atmospheres*, 106(D2), 1551-1568.

6347 Jacobson, M. Z., and J. E. Ten Hoeve, 2012: Effects of urban surfaces and white roofs on global
6348 and regional climate. *J. Clim.*, doi:10.1175/JCLI-D-11-00032.1.

6349 Jethva, H., Torres, O., Remer, L. A., & Bhartia, P. K. (2013). A color ratio method for
6350 simultaneous retrieval of aerosol and cloud optical thickness of above-cloud absorbing
6351 aerosols from passive sensors: Application to MODIS measurements. *IEEE Transactions on*
6352 *Geoscience and Remote Sensing*, 51(7), 3862-3870.

6353 Jickells, T. D., An, Z. S., Andersen, K. K., Baker, A. R., Bergametti, C., Brooks, N., Cao, J. J.,
6354 Boyd, P. W., Duce, R. A., Hunter, K. A., Kawahata, H., Kubilay, N., LaRoche, J., Liss, P.
6355 S., Mahowald, N., Prospero, J. M., Ridgwell, A. J., Tegen, I. and Torres, R.: Global iron
6356 connections between desert dust, ocean biogeochemistry, and climate, *Science* (80-.),
6357 308(5718), doi:10.1126/science.1105959, 2005.

6358 Jimenez, JL, et al. Evolution of organic aerosols in the atmosphere. *Science* 326, 1525-1529,
6359 2009,

6360 Johnson, B. T., Shine, K. P., & Forster, P. M. (2004). The semi-direct aerosol effect: Impact of
6361 absorbing aerosols on marine stratocumulus. *Quarterly Journal of the Royal Meteorological*
6362 *Society*, 130(599), 1407-1422.

6363 Jones, A., Roberts, D. L. and Slingo, A. 1994. A climate model study of the indirect radiative
6364 forcing by anthropogenic sulfate aerosols. *Nature* 370, 450–453.

6365 Jones, A., Roberts, D. L., Woodage, M. J., and Johnson, C. E., 2001. Indirect sulfate aerosol
6366 forcing in a climate model with an interactive sulfur cycle, *J. Geophys. Res.*, **106**, 20293-
6367 20310, doi:10.1029/2000JD000089

6368 Jones, A., D. L. Roberts, and A. Slingo, 1994: A climate model study of indirect radiative
6369 forcing by anthropogenic sulfate aerosols. *Nature*, 370, 450–453.

6370 A. Jones, J. Haywood, O. Boucher, B. Kravitz, and A. Robock, 2010: Geoengineering by
6371 stratospheric SO₂ injection: results from the Met Office HadGEM2 climate model and
6372 comparison with the Goddard Institute for Space Studies ModelE; *Atmos. Chem. Phys.*, **10**,
6373 5999–6006, [doi:10.5194/acp-10-5999-2010](https://doi.org/10.5194/acp-10-5999-2010)

6374

6375 Jones, A. C., J. M. Haywood, and A. Jones, 2016: Climatic impacts of stratospheric
6376 geoengineering with sulfate, black carbon and titania injection. *Atmos. Chem. Phys.*, **16**,
6377 2843–2862, doi:10.5194/acp-16-2843-2016. [https://www.atmos-chem-
6378 phys.net/16/2843/2016/](https://www.atmos-chem-phys.net/16/2843/2016/) (Accessed December 20, 2018).

6379 [Jones, Alexandra L.](#), D Feldman, [Stuart Freidenreich](#), [David J Paynter](#), [V Ramaswamy](#), W D
6380 Collins, and R Pincus, 2017: **A New Paradigm for Diagnosing Contributions to Model**
6381 **Aerosol Forcing Error**. *Geophysical Research Letters*, **44**(23),
6382 DOI:[10.1002/2017GL075933](https://doi.org/10.1002/2017GL075933)

6383 Johnson, C., J. Henshaw, and G. McInnes, 1992: Impact of aircraft and surface emissions of
6384 nitrogen oxides on tropospheric ozone and global warming. *Nature*, **355**, 69.
6385 <https://doi.org/10.1038/355069a0>.

6386 Johnson, C. E., and R. G. Derwent, 1996: Relative radiative forcing consequences of global
6387 emissions of hydrocarbons, carbon monoxide and NO_x from human activities estimated
6388 with a zonally-averaged two-dimensional model. *Clim. Change*, **34**, 439–462.

6389 Johnston, H., 1971: Reduction of Stratospheric Ozone by Nitrogen Oxide Catalysts from
6390 Supersonic Transport Exhaust. *Science (80-.)*, **173**, 517–522.
6391 <http://www.jstor.org/stable/1732244>.

6392 Junge, C. E., 1962: Global ozone budget and exchange between stratosphere and troposphere.
6393 *Tellus*, **14**, 363–377, doi:doi:10.1111/j.2153-3490.1962.tb01349.x.
6394 <https://doi.org/10.1111/j.2153-3490.1962.tb01349.x>.

6395 Jungclaus, J. H., Bard, E., Baroni, M., Braconnot, P., Cao, J., Chini, L. P., et al., 2017: The
6396 PMIP4 contribution to CMIP6 - Part 3: the Last Millennium, scientific objective and

6397 experimental design for the PMIP4 past1000 simulations. *Geoscientific Model*
6398 *Development*, 10, 4005-4033. doi:10.5194/gmd-2016-278.

6399

6400 Kaplan, L. D. (1952). On the Pressure Dependence of Radiative Heat Transfer in the
6401 Atmosphere. *Journal of Meteorology*. [http://doi.org/10.1175/1520-0469\(1952\)009<0001:OTPDOR>2.0.CO;2](http://doi.org/10.1175/1520-0469(1952)009<0001:OTPDOR>2.0.CO;2)

6402

6403 Kang, S., I. Held, D. Frierson, and M. Zhao, 2008: The response of the ITCZ to extratropical
6404 thermal forcing: Idealized slab ocean experiments with a GCM. *J. Climate*, 21(14), 3521-
6405 3532.

6406 Kaplan, L. D., 1960: The influence of carbon dioxide variations on the atmospheric heat
6407 balance. *Tellus*, **12**, 204-208.

6408 Kärcher, Bernd (2018) *Formation and Radiative Forcing of Contrail Cirrus*. *Nature*
6409 *Communications*, pp. 1-17. Nature Publishing Group. DOI: [10.1038/s41467-018-04068-0](https://doi.org/10.1038/s41467-018-04068-0)
6410 ISSN 2041-1723.

6411 Kaufman, Y. J., Tanre, D. and Boucher, O.: A satellite view of aerosols in the climate system,
6412 *Nature*, 419(6903), 215-223, 2002.

6413 Keeling, C. D., 1960: The concentration and isotopic abundances of carbon dioxide in the
6414 atmosphere. *Tellus*, 12, 2, 200-203.

6415 Keith, D. W., and H. Dowlatabadi, 1992: a serious look at geoengineering. *Eos, Trans. Am.*
6416 *Geophys. Union*, doi:10.1029/91EO00231.

6417

6418 Kiehl, J. T., T. L. Schneider, R. W. Portmann, and S. Solomon, 1999: Climate forcing due to
6419 tropospheric and stratospheric ozone. *J. Geophys. Res.*, **104**, 31239–31254.

6420 Kiehl, J.T. and B.A. Boville, 1988: The Radiative-Dynamical Response of a Stratospheric-
6421 Tropospheric General Circulation Model to Changes in Ozone. *J. Atmos. Sci.*, 45, 1798–
6422 1817, [https://doi.org/10.1175/1520-0469\(1988\)045<1798:TRDROA>2.0.CO;2](https://doi.org/10.1175/1520-0469(1988)045<1798:TRDROA>2.0.CO;2)

6423 Kiehl, J. T., and B. P. Briegleb, 1993: The relative roles of sulfate aerosols and greenhouse gases
6424 in climate forcing. *Science* (80-.), 260, 311–314, doi:10.1126/science.260.5106.311.
6425 <http://science.scienmag.org/content/260/5106/311.abstract>

6426 Kiehl, J. T., and B. P. Briegleb, 1993: The relative roles of sulfate aerosols and greenhouse gases
6427 in climate forcing. *Science* (80-.), 260, 311–314, doi:10.1126/science.260.5106.311.
6428 <http://science.scienmag.org/content/260/5106/311.abstract>.

6429 Kiehl, J. T., & Briegleb, B. P. (1993). The relative roles of sulfate aerosols and greenhouse gases
6430 in climate forcing. *Science*, 260(5106), 311-314.

6431 Kiehl, J. T., and H. Rodhe, Modeling geographical and seasonal forcing due to aerosols, in
6432 Proceedings of the Dahlem Workshop on Aerosol Forcing of Climate, edited by R. J.
6433 Chaffson and J. Heintzenberg, pp. 281-296, John Wiley, New York, 1995.

6434 Kirchner, I., G. Stenchikov, H. Graf, A. Robock, J. Antuña, 1999: Climate Model Simulation of
6435 Winter Warming and Summer Cooling Following the 1991 Mount Pinatubo Volcanic
6436 Eruption, *J. Geophys. Res.*, 104, 19,039-19,055.

6437 Kirtman, B., and Coauthors, 2013: Near-term Climate Change: Projections and Predictability.
6438 *Climate Change 2013: The Physical Science Basis. Contribution of Working Group I to the*
6439 *Fifth Assessment Report of the Intergovernmental Panel on Climate Change*, T.F. Stocker et
6440 al., Eds., Cambridge University Press, Cambridge, United Kingdom and New York, NY,
6441 USA.

6442 Kirschke, S., Bousquet, P., Ciais, P., Saunois, M., Canadell, J., Dlugokencky, E., Bergamashi, P.,
6443 Berman, D., Blake, D., Bruhwiler, L., Cameron-Smith, P., Castaldi, S., Chevalier, F., Feng,
6444 L., Fraser, A., Heimann, M., Hodson, E., Houweling, S., Josse, B., Fraser, P., Krummel, P.,
6445 Lamarque, J. F., Langenfelds, R., LeQuere, C., Naik, V., O'Doherty, S., Palmer, P., Pison,
6446 I., Plummer, D., Poulter, B., Prinn, R., Rigby, M., Ringeval, B., Santini, M., Schmidt, M.,
6447 Shindel, D., Simpson, I., Spahni, R., Steele, L., Strode, S., Sudo, K., Szopa, S., G.R., van
6448 der W., Voulgarakis, A., van Weele, M., Weiss, R., Williams, J. and Zeng, G.: Three
6449 decades of global methane sources and sinks, *Nature-geoscience*, 6, 813–823, 2013.

6450 Krasnopolksy, M. V., M.S. Fox-Rabinovitz, and D.V. Chalikov, 2005, New Approach to
6451 Calculation of Atmospheric Model Physics: Accurate and Fast Neural Network Emulation
6452 of Longwave Radiation in a Climate Model *Monthly Weather Review*, **133**., 1370-1383

6453 Kravitz, B., A. Robock, P. M. Forster, J. M. Haywood, M. G. Lawrence, and H. Schmidt, 2013:
6454 An overview of the Geoengineering Model Intercomparison Project (GeoMIP). *J. Geophys.*
6455 *Res. Atmos.*, doi:10.1002/2013JD020569.

6456 Kravitz, B., and Coauthors (2013), Climate model response from the Geoengineering Model
6457 Intercomparison Project (GeoMIP). *Journal of Geophysical Research-Atmospheres*, **118**,
6458 8320-8332.

6459 Kremser, S., Thomason, L. W., von Hobe, M., Hermann, M., Deshler, T., Timmreck et al.:
6460 Stratospheric aerosol – Observations, processes, and impact on climate, *Rev. Geophys.*, **54**,
6461 278 – 335, doi:10.1002/2015RG000511, 2016.

6462 Krivova, N.A. and S. K. Solanki, 2008: Models of solar irradiance variations: Current status, *J*
6463 *Astrophys Astron*, **29**: 151. <https://doi.org/10.1007/s12036-008-0018-x>

6464 Krivova, N. A., Vieira, L. E. A., and S. K. Solanki, 2010: Reconstruction of solar spectral
6465 irradiance since the Maunder minimum. *J. Geophys. Res.*, **115**, A12112,
6466 doi:10.1029/2010JA015431.

6467 Krueger, A. J., S. J. Schaefer, N. A. Krotkov, G. Bluth, and S. Barker (2000), Ultraviolet remote
6468 sensing of volcanic emissions. Remote sensing of active volcanism. *Geophys Monograph*,
6469 **116**, 25-43.

6470 Ko, M. K. W., and Coauthors, 1995: Model simulations of stratospheric ozone. *Scientific*
6471 *Assessment of Ozone Depletion: 1994*, D.L. Albritton, R.T. Watson, and P.J. Aucamp, Eds.

6472 Kopp, G. and G. Lawrence, 2005: The Total Irradiance Monitor (TIM): Instrument Design, *Sol*
6473 *Phys*, **230**: 91. <https://doi.org/10.1007/s11207-005-7446-4>

6474 Kopp, G., and J. L. Lean, 2011: A new low value of Total Solar Irradiance: evidence and climate
6475 significance, *Geophys. Res. Lett.*, **38**, L01706, doi:10.1029/2010GL045777.

6476 Kopp, G., N. Krivova, Chi-Ju Wu, and J. Lean, 2016: The impact of the revised sunspot record
6477 on solar irradiance reconstructions, *Solar Phys.*, DOI 10.1007/s11207-016-0853-x

6478 Kvalevåg, M. M., and G. Myhre, 2013: The effect of carbon-nitrogen coupling on the reduced
6479 land carbon sink caused by tropospheric ozone. *Geophys. Res. Lett.*, **40**, 3227–3231,
6480 doi:doi:10.1002/grl.50572. <https://doi.org/10.1002/grl.50572>.

6481 Kristjánsson, J. E., H. Muri, and H. Schmidt, 2015: The hydrological cycle response to cirrus
6482 cloud thinning. *Geophys. Res. Lett.*, doi:10.1002/2015GL066795.

6483 Kinne, S., Schulz, M., Textor, C., Guibert, S., Balkanski, Y., Bauer, S., Berntsen, E., Berglen,
6484 T.F., Boucher, O., Chin, M. and Collins, W., 2006. An AeroCom initial assessment—optical
6485 properties in aerosol component modules of global models. *Atmospheric Chemistry and*
6486 *Physics*, **6**, pp.1815-1834.

6487 Koffi, B., Schulz, M., Bréon, F.M., Griesfeller, J., Winker, D., Balkanski, Y., Bauer, S.,
6488 Berntsen, T., Chin, M., Collins, W.D. and Dentener, F., 2012. Application of the CALIOP
6489 layer product to evaluate the vertical distribution of aerosols estimated by global models:
6490 AeroCom phase I results. *Journal of Geophysical Research: Atmospheres*, **117**(D10).

6491 Kloster, S., Mahowald, N. M., Randerson, J. T., Thornton, P. E., Hoffman, F. M., Levis, S.,
6492 Lawrence, P. J., Feddema, J. J., Oleson, K. W. and Lawrence, D. M.: Fire dynamics during
6493 the 20th century simulated by the Community Land Model, *Biogeosciences*, **7**(6),
6494 doi:10.5194/bg-7-1877-2010, 2010.

6495 Kondratiev, K. Y., and H. I. Niilisk, 1960: On the question of carbon dioxide heat radiation
6496 in the atmosphere. *Geofis. Pura Appl.*, **46**, 216-230.

6497 Koschmeider H. 1924. Therie der horizontalen sichtweite. *Beitr. Phys. Freien Atmos.* **12**: 33–35.
6498 Langner, J. and H. Rodhe, *J. Atmos. Chem.* **13**, 225 (1991)

6499 Kotchenruther, R.A. and Hobbs, P.V., 1998. Humidification factors of aerosols from biomass
6500 burning in Brazil. *Journal of Geophysical Research: Atmospheres*, **103**(D24), pp.32081-
6501 32089.

6502 Kotchenruther, R.A., Hobbs, P.V. and Hegg, D.A., 1999. Humidification factors for atmospheric
6503 aerosols off the mid-Atlantic coast of the United States. *Journal of Geophysical Research: Atmospheres*, 104(D2), pp.2239-2251.

6505 Kohfeld, K. E. and Harrison, S. P.: DIRTMAP: The geological record of dust, *Earth Sci. Rev.*,
6506 54, 81–114, 2001.

6507

6508 Lacis, A., 1985: Chlorofluorocarbons and stratospheric ozone. *Global Environmental Problems*,
6509 S.F. Singer, Ed., Paragon House, New York.

6510 Lacis, A. A., D. J. Wuebbles, and J. A. Logan, 1990: Radiative forcing of climate by changes in
6511 the vertical distribution of ozone. *J. Geophys. Res. Atmos.*, 95, 9971–9981,
6512 doi:doi:10.1029/JD095iD07p09971. <https://doi.org/10.1029/JD095iD07p09971>.

6513 Lacis., A., J. Hansen, M. Sato (1992), *Geophys. Res. lett.*, 19, No. 15, 1607-1610.

6514 Lacis, A. A., D. J. Wuebbles, and J. A. Logan, 1990: Radiative forcing of climate by changes in
6515 the vertical distribution of ozone. *J. Geophys. Res. Atmos.*, 95, 9971–9981,
6516 doi:10.1029/JD095iD07p09971. <http://dx.doi.org/10.1029/JD095iD07p09971>

6517 Lambert, A., R. G. Grainger, J. J. Remedios, C. D. Rodgers, M. Corney, and F. W. Taylor (1993),
6518 Measurements of the evolution of the Mt. Pinatubo aerosol cloud by ISAMS, *Geophys. Res. Lett.*, 20(12), 1287–1290, doi:10.1029/93GL00827.

6520 Lamarque, J. F., and Coauthors, 2010: Historical (1850–2000) gridded anthropogenic and
6521 biomass burning emissions of reactive gases and aerosols: methodology and application.
6522 *Atmos. Chem. Phys.*, 10, 7017–7039, doi:10.5194/acp-10-7017-2010. <http://www.atmos-chem-phys.net/10/7017/2010/>.

6524 —, and Coauthors, 2013: The Atmospheric Chemistry and Climate Model Intercomparison
6525 Project (ACCMIP): overview and description of models, simulations and climate
6526 diagnostics. *Geosci. Model Dev.*, 6, 179–206, doi:10.5194/gmd-6-179-2013.
6527 <http://www.geosci-model-dev.net/6/179/2013/>.

6528 Lamarque, J.-F., Bond, T. C., Eyring, V., Granier, C., Heil, A., Klimont, Z., Lee, D., Liousse, C.,
6529 Mieville, A., Owen, B., Schultz, M. G., Shindell, D., Smith, S. J., Stehfest, E., Van
6530 Aardenne, J., Cooper, O. R., Kainuma, M., Mahowald, N., McConnell, J. R., Naik, V.,
6531 Riahi, K. and Van Vuuren, D. P.: Historical (1850-2000) gridded anthropogenic and
6532 biomass burning emissions of reactive gases and aerosols: Methodology and application,
6533 *Atmos. Chem. Phys.*, 10(15), doi:10.5194/acp-10-7017-2010, 2010.

6534 Lamarque, J. F., Kyle, P. P., Meinshausen, M., Riahi, K., Smith, S. J., van Vuuren, D. P.,
6535 Conley, A. J. and Vitt, F.: Global and regional evolution of short-lived radiatively-active
6536 gases and aerosols in the Representative Concentration Pathways, *Clim. Change*, 109(1),
6537 191–212, doi:10.1007/s10584-011-0155-0, 2011.

6538 Langley, S.P. 1884. Researches on solar heat and its absorption by the Earth's atmosphere. A
6539 report of the Mount Whitney Expedition. Professional Papers of the Signal Service, No. 15,
6540 Government Printing office, Washington, DC.

6541 Lawrence, D. M., Hurt, G. C., Arneth, A., Brovkin, V., Calvin, K. V., Jones, A. D., Jones, C. D.,
6542 Lawrence, P. J., Noblet-Ducoudré, N. De, Pongratz, J., Seneviratne, S. I. and Shevliakova,
6543 E.: The Land Use Model Intercomparison Project (LUMIP) contribution to CMIP6:
6544 Rationale and experimental design, *Geosci. Model Dev.*, 9(9), 2973–2998,
6545 doi:10.5194/gmd-9-2973-2016, 2016.

6546 Lashof, D. A., and D. R. Ahuja (1990), Relative contributions of greenhouse gas emissions to
6547 global warming, *Nature*, 344(6266), 529–531, doi:10.1038/344529a0.

6548 Lashof, D. A., 1989: The dynamic greenhouse: Feedback processes that may influence future
6549 concentrations of atmospheric trace gases and climatic change. *Clim. Change*, **14**, 213–242.
6550 <https://doi.org/10.1007/BF00134964>.

6551 Latham, J., 1990: Control of global warming? [10]. *Nature*, doi:10.1038/347339b0.

6552 Lean, J., 2017: Sun Climate Connections, Oxford Research Encyclopedias, Climate Science,
6553 DOI: 10.1093/acrefore/9780190228620.013.9.

6554 Lean, J., 2018a: Estimating solar irradiance since 850, *Earth and Space Science*, doi:
6555 10.1002/2017EA000357

6556 Lean, J., 2018b: Observation-Based Detection and Attribution of Twenty-first Century Climate
6557 Change, *WIREs Climate Change*, 9, doi: 10.1002/wcc.511

6558 Lean, J. and D. Rind, 2008: How natural and anthropogenic Influences alter Global and regional
6559 surface temperatures: 1889 to 2006, *Geophys. Res. Lett.*, 35, L18701,
6560 doi:10.1029/2008GL034864.

6561 Lean, J. L., and M. T. DeLand, 2012: How Does the Sun's Spectrum Vary? *J. Clim.*, 25, 2556-
6562 2560.

6563 Lean, J., Skumanich, A., and O. R. White, 1992: Estimating the Sun's Radiative Output During
6564 the Maunder Minimum, *Geophysical Research Letters*, 19,1591-1495.

6565 Lean, J., J. Beer and R. Bradley, 1995: Reconstruction of solar irradiance since 1610:
6566 Implications for climate change, *Geophys. Res. Lett.*, 22, 3195-3198.

6567 Lean, J. L., G.J. Rottman, H.L. Kyle, T.N. Woods, J.R. Hickey, and L.C. Puga, 1997: Detection
6568 and parameterization of variations in solar mid and near ultraviolet radiation (200 to 400
6569 nm), *J. Geophys. Res.*, 102, 29939-29956.

6570 Lean, J., Wang, Y.-M., and N. R. Sheeley, Jr., 2002: The effect of increasing solar activity on the
6571 Sun's total and open magnetic flux during multiple cycles; Implications for solar forcing of
6572 climate, *Geophys. Res. Lett.*, 29, doi:10.1029/2002GL015880.

6573 Lean, J. L., G. Rottman, J. Harder and G Kopp, 2005: SORCE contributions to new
6574 understanding of global change and solar variability, *Solar Phys.*, 230:27-53.

6575 LeGrande, A., K. Tsigaridis, S. Bauer (2016), Role of atmospheric chemistry in the climate
6576 impacts of stratospheric volcanic injections, *Nature Geosci.*, doi:10.1038/NGEO2771.

6577 Lejeune, Q., Davin, E. L., Gudmundsson, L., Winckler, J. and Seneviratne, S. I.: Historical
6578 deforestation locally increased the intensity of hot days in northern mid-latitudes, *Nat. Clim.
6579 Chang.*, 8(5), 386–390, doi:10.1038/s41558-018-0131-z, 2018.

6580 Lelieveld, J., and P. J. Crutzen, 1992: Indirect chemical effects of methane on climate warming.
6581 *Nature*, **355**, 339. <https://doi.org/10.1038/355339a0>.

6582 Lelieveld, J. O. S., P. J. Crutzen, and F. J. Dentener, 1998: Changing concentration, lifetime and
6583 climate forcing of atmospheric methane. *Tellus B*, **50**, 128–150, doi:doi:10.1034/j.1600-
6584 0889.1998.t01-1-00002.x. <https://doi.org/10.1034/j.1600-0889.1998.t01-1-00002.x>.

6585 Levy, H., 1971: Normal Atmosphere: Large Radical and Formaldehyde Concentrations
6586 Predicted. *Science (80-.)*, **173**, 141–143.

6587 Lesins, G., Chylek, P., & Lohmann, U. (2002). A study of internal and external mixing scenarios
6588 and its effect on aerosol optical properties and direct radiative forcing. *Journal of*
6589 *Geophysical Research: Atmospheres*, **107**(D10), AAC-5.

6590 Lilensten, J., T. Dudok de Wit, and K. Matthes (eds), 2015: Earth's climate response to a
6591 changing Sun, EDP Science, doi: 10.1051/9782759817337.

6592 Liou, K-N., 2002: An Introduction to Atmospheric Radiation. Academic Press, San Diego, CA,
6593 583pp.

6594 Lippmann, M., & Albert, R. E. (1969). The effect of particle size on the regional deposition of
6595 inhaled aerosols in the human respiratory tract. *American Industrial Hygiene Association*
6596 *Journal*, **30**(3), 257-275.

6597 Liu, S. C., 1977: Possible effects on tropospheric O₃ and OH due to NO_x emissions. *Geophys.*
6598 *Res. Lett.*, **4**, 325–328, doi:doi:10.1029/GL004i008p00325.
6599 <https://doi.org/10.1029/GL004i008p00325>.

6600 Liu, S. C., D. Kley, M. McFarland, J. D. Mahlman, and H. Levy, 1980: On the origin of
6601 tropospheric ozone. *J. Geophys. Res. Ocean.*, **85**, 7546–7552,
6602 doi:doi:10.1029/JC085iC12p07546. <https://doi.org/10.1029/JC085iC12p07546>.

6603 —, M. Trainer, F. C. Fehsenfeld, D. D. Parrish, E. J. Williams, D. W. Fahey, G. Hübler, and P.
6604 C. Murphy, 1987: Ozone production in the rural troposphere and the implications for
6605 regional and global ozone distributions. *J. Geophys. Res. Atmos.*, **92**, 4191–4207,
6606 doi:doi:10.1029/JD092iD04p04191. <https://doi.org/10.1029/JD092iD04p04191>.

6607 Lockwood, M., R G Harrison, T Woollings and S K Solanki, 2010: Are cold winters in Europe
6608 associated with low solar activity? *Environ. Res. Lett.* 5 (2010) 024001.

6609 Löffler, M., S. Brinkop, P. Jockel (2016), Impact of major volcanic eruptions on stratospheric
6610 water vapour, *Atmos. Chem. Phys.*, 16, 6547–6562, 2016, [www.atmos-chem-
6611 phys.net/16/6547/2016/](http://www.atmos-chem-phys.net/16/6547/2016/), doi:10.5194/acp-16-6547-2016.

6612 Lohmann, U., Rotstayn, L., Storelvmo, T., Jones, A., Menon, S., Quaas, J., Ekman, A. M. L.,
6613 Koch, D. and Ruedy, R.: Total aerosol effect: radiative forcing or radiative flux
6614 perturbation?, *Atmospheric Chemistry and Physics*, 10(7), 3235-3246, 2010.

6615 London, J., 1962: Mesospheric dynamics, Part III. Final Report, Contract No. AF19
6616 (604)-5492, Department of Meteorology and Oceanography, New York University,
6617 99 pp.

6618 Lovelock, J. E., Maggs, R. J., & Wade, R. J. (1973). Halogenated Hydrocarbons in and over the
6619 Atlantic. *Nature*, 241, 194. Retrieved from <https://doi.org/10.1038/241194a0>

6620 Loeb, N. G., & Kato, S. (2002). Top-of-atmosphere direct radiative effect of aerosols over the
6621 tropical oceans from the Clouds and the Earth's Radiant Energy System (CERES) satellite
6622 instrument. *Journal of Climate*, 15(12), 1474-1484.

6623 Loeb, N. G., & Manalo-Smith, N. (2005). Top-of-atmosphere direct radiative effect of aerosols
6624 over global oceans from merged CERES and MODIS observations. *Journal of Climate*,
6625 18(17), 3506-3526.

6626 Lohmann, U., J. Feichter, J. Penner, and R. Leaitch, Indirect effect of sulfate and carbonaceous
6627 aerosols: A mechanistic treatment, *J. Geophys. Res.*, 105, 12,193–12,206, 2000.

6628 Lohmann, U., Rotstayn, L., Storelvmo, T., Jones, A., Menon, S., Quaas, J., ... & Ruedy, R.
6629 (2010). Total aerosol effect: radiative forcing or radiative flux perturbation?. *Atmospheric
6630 Chemistry and Physics*, 10(7), 3235-3246.

6631 Le Quéré, C., Andrew, R. M., Canadell, J. G., Sitch, S., Ivar Korsbakken, J., Peters, G. P.,
6632 Manning, A. C., Boden, T. A., Tans, P. P., Houghton, R. A., Keeling, R. F., Alin, S.,
6633 Andrews, O. D., Anthoni, P., Barbero, L., Bopp, L., Chevallier, F., Chini, L. P., Ciais, P.,

6634 Currie, K., Delire, C., Doney, S. C., Friedlingstein, P., Gkritzalis, T., Harris, I., Hauck, J.,
6635 Haverd, V., Hoppema, M., Klein Goldewijk, K., Jain, A. K., Kato, E., Körtzinger, A.,
6636 Landschützer, P., Lefèvre, N., Lenton, A., Lienert, S., Lombardozzi, D., Melton, J. R.,
6637 Metzl, N., Millero, F., Monteiro, P. M. S., Munro, D. R., Nabel, J. E. M. S., Nakaoka, S. I.,
6638 O'Brien, K., Olsen, A., Omar, A. M., Ono, T., Pierrot, D., Poulter, B., Rödenbeck, C.,
6639 Salisbury, J., Schuster, U., Schwinger, J., Séférian, R., Skjelvan, I., Stocker, B. D., Sutton,
6640 A. J., Takahashi, T., Tian, H., Tilbrook, B., Van Der Laan-Luijkx, I. T., Van Der Werf, G.
6641 R., Viovy, N., Walker, A. P., Wiltshire, A. J. and Zaehle, S.: Global Carbon Budget 2016,
6642 Earth Syst. Sci. Data, 8(2), 605–649, doi:10.5194/essd-8-605-2016, 2016.

6643 Le Quere, C., Andres, R. J., Boden, T., Conway, T., Houghton, R. A., House, J. I., Marland, G.,
6644 Peters, G. P., van der Werf, G. R., Ahlstrom, A., Andrew, R. M., Bopp, L., Canadell, J. G.,
6645 Ciais, P., Doney, S. C., Enright, C., Friedlingstein, P., Huntingford, C., Jain, A. K.,
6646 Jourdain, C., Kato, E., Keeling, R. F., Klein Goldewijk, K., Levis, S., Levy, P., Lomas, M.,
6647 Poulter, B., Raupach, M. R., Schwinger, J., Sitch, S., Stocker, B. D., Viovy, N., Zaehle, S.
6648 and Zeng, N.: The global carbon budget 1959–2011, Earth Syst. Sci. Data, 5, 165–185,
6649 doi:10.5194/essd-5-165–2013, 2013.

6650 Logan, J. A., 1985: Tropospheric ozone: Seasonal behavior, trends, and anthropogenic influence.
6651 *J. Geophys. Res. Atmos.*, **90**, 10463–10482, doi:10.1029/JD090iD06p10463.
6652 <http://dx.doi.org/10.1029/JD090iD06p10463>.

6653 Logan, J. A., M. J. Prather, S. C. Wofsy, and M. B. McElroy, 1978: Atmospheric chemistry:
6654 response to human influence. *Philos. Trans. R. Soc. London A Math. Phys. Eng. Sci.*, **290**,
6655 187–234, doi:10.1098/rsta.1978.0082.
6656 <http://rsta.royalsocietypublishing.org/content/290/1367/187>.

6657 Logan, J. A., M. J. Prather, S. C. Wofsy, and M. B. McElroy, 1981: Tropospheric chemistry: A
6658 global perspective. *J. Geophys. Res.*, **86**, 7210–7254, doi:10.1029/JC086iC08p07210.
6659 <http://dx.doi.org/10.1029/JC086iC08p07210>.

6660 Luther, F. M., 1982: In Carbon dioxide review 1982, W. Clark, Ed., Oxford University Press,
6661 Clarendon, England, 290–295.

6662

6663 Machta, L., and T. Carpenter, 1971: Trends in high cloudiness at Denver and Salt Lake
6664 City. *Man's Impact on the Climate* (W. H. Matthews, W. W. Kellogg and G. D.
6665 Robinson, Eds.), MIT Press, pp. 410–415.

6666 Machta, L., and T. Carpenter, 1971: Trends in high cloudiness at Denver and Salt Lake City.
6667 *Man's Impact on the Climate* (W. H. Matthews, W. W. Kellogg and G. D. Robinson, Eds.),
6668 MIT Press, pp. 410–415.

6669 MacKay, R. M., M. K. W. Ko, R.-L. Shia, Y. Yang, S. Zhou, and G. Molnar, 1997: An
6670 Estimation of the Climatic Effects of Stratospheric Ozone Losses during the 1980s. *J. Clim.*,
6671 **10**, 774–788, doi:10.1175/1520-0442(1997)010<0774:AEOTCE>2.0.CO;2.
6672 [https://doi.org/10.1175/1520-0442\(1997\)010%3C0774:AEOTCE%3E2.0.CO](https://doi.org/10.1175/1520-0442(1997)010%3C0774:AEOTCE%3E2.0.CO).

6673 MacMartin, D. G., D. W. Keith, B. Kravitz, and K. Caldeira, 2013: Management of trade-offs in
6674 geoengineering through optimal choice of non-uniform radiative forcing. *Nat. Clim. Chang.*,
6675 doi:10.1038/nclimate1722.

6676 Mahowald, N.: Aerosol indirect effect on biogeochemical cycles and climate, *Science* (80-.),,
6677 334(6057), doi:10.1126/science.1207374, 2011.

6678 Mahowald, N., Ward, D. S., Kloster, S., Flanner, M. G., Heald, C. L., Heavens, N. G., Hess, P.
6679 G., Lamarque, J.-F. and Chuang, P. Y.: Aerosol impacts on climate and biogeochemistry.,
6680 2011.

6681 Mahowald, N. M., Scanza, R., Brahney, J., Goodale, C. L., Hess, P. G., Moore, J. K. and Neff,
6682 J.: Aerosol Deposition Impacts on Land and Ocean Carbon Cycles, *Curr. Clim. Chang.*
6683 Reports, 3(1), 16–31, doi:10.1007/s40641-017-0056-z, 2017a.

6684 Mahowald, N. M., Ward, D. S., Doney, S. C., Hess, P. G. and Randerson, J. T.: Are the impacts
6685 of land use on warming underestimated in climate policy?, *Environ. Res. Lett.*, 12(9),
6686 doi:10.1088/1748-9326/aa836d, 2017b.

6687 Mahowald, N. M., Randerson, J. T., Lindsay, K., Munoz, E., Doney, S. C., Lawrence, P.,
6688 Schlunegger, S., Ward, D. S., Lawrence, D. and Hoffman, F. M.: Interactions between land

6689 use change and carbon cycle feedbacks, *Global Biogeochem. Cycles*, 31(1), 96–113,
6690 doi:10.1002/2016GB005374, 2017c.

6691 Mahowald, N. M. M., Kloster, S., Engelstaedter, S., Moore, J. K. K., Mukhopadhyay, S.,
6692 McConnell, J. R. R., Albani, S., Doney, S. C. C., Bhattacharya, A., Curran, M. A. J. A. J.,
6693 Flanner, M. G. G., Hoffman, F. M. M., Lawrence, D. M. M., Lindsay, K., Mayewski, P. A.
6694 A., Neff, J., Rothenberg, D., Thomas, E., Thornton, P. E. E. and Zender, C. S. S.: Observed
6695 20th century desert dust variability: impact on climate and biogeochemistry, *Atmos. Chem.*
6696 *Phys.*, 10(22), 10875–10893, doi:10.5194/acp-10-10875-2010, 2010.

6697 Mahowald, N. N. M.: Anthropocene changes in desert area: sensitivity to climate model
6698 predictions, *Geophys. Res. Lett.*, 34(L18817), doi:10.1029/2007GL030472,
6699 doi:10.1029/2007GL030472, 2007.

6700 Malinina, E., Rozanov, A., Rozanov, V., Liebing, P., Bovensmann, H., and Burrows, J. P. (2018),
6701 Aerosol particle size distribution in the stratosphere retrieved from SCIAMACHY limb
6702 measurements, *Atmos. Meas. Tech.*, 11, 2085–2100, <https://doi.org/10.5194/amt-11-2085-2018>.

6704 Mann, M. E., M. A. Cane, S. E. Zebiak, and A. Clement, 2005: Volcanic and solar forcing of the
6705 tropical Pacific over the past 1000 Years, *J. Clim.*, 18, 447–456.

6706 Mann, M. E., Z. Zhang, S. Rutherford, R. S. Bradley, M. K. Hughes, D. Shindell, C. Ammann,
6707 G. Faluvegi, and F. Ni, 2009: Global Signatures and Dynamical Origins of the Little Ice
6708 Age and Medieval Climate Anomaly, *Science*, 326, 5957, 1256–1260, DOI:
6709 10.1126/science.1177303.

6710 Manabe, S., & Wetherald, R. T. (1967). Thermal Equilibrium of the Atmosphere with a Given
6711 Distribution of Relative Humidity. *Journal of the Atmospheric Sciences*, 24(3), 241–259.
6712 [http://doi.org/10.1175/1520-0469\(1967\)024<0241:TEOTAW>2.0.CO;2](http://doi.org/10.1175/1520-0469(1967)024<0241:TEOTAW>2.0.CO;2)

6713 Manabe, S., & Wetherald, R. T. (1975). The Effects of Doubling the CO₂ Concentration on the
6714 climate of a General Circulation Model. *Journal of the Atmospheric Sciences*, 32(1), 3–15.
6715 [http://doi.org/10.1175/1520-0469\(1975\)032<0003:TEODTC>2.0.CO;2](http://doi.org/10.1175/1520-0469(1975)032<0003:TEODTC>2.0.CO;2)

6716 Manabe, S., and R. T. Wetherald, 1967: Thermal Equilibrium of the Atmosphere with a Given
6717 Distribution of Relative Humidity. *J. Atmos. Sci.*, **24**, 241–259, doi:10.1175/1520-
6718 0469(1967)024<0241:TEOTAW>2.0.CO;2. [https://doi.org/10.1175/1520-0469\(1967\)024%3C0241:TEOTAW%3E2.0.CO.](https://doi.org/10.1175/1520-0469(1967)024%3C0241:TEOTAW%3E2.0.CO.)

6720 Manabe, S., and R. T. Wetherald, 1967: Thermal Equilibrium of the Atmosphere with a Given
6721 Distribution of Relative Humidity. *J. Atmos. Sci.*, **24**, 241–259, doi:10.1175/1520-
6722 0469(1967)024<0241:teotaw>2.0.co;2. <http://journals.ametsoc.org/doi/abs/10.1175/1520-0469%281967%29024%3C0241%3ATEOTAW%3E2.0.CO%3B2>.

6724 Manabe, S., and F. Moller, 1961: On the radiative equilibrium and heat balance of the
6725 atmosphere. *Mon. Wea. Rev.*, **89**, 503-532.

6726 ----, and R. F. Strickler, 1964: Thermal equilibrium of the atmosphere with a convective
6727 adjustment. *J. Atmos. Sci.*, **21**, 361-385.

6728 ----, and R. Wetherald, 1967: Thermal equilibrium of the atmosphere with a given distribution of
6729 relative humidity. *J. Atmos. Sci.*, **24(3)**, 241-259.

6730 ----, and R. Wetherald, 1975: The effects of doubling CO₂ concentration on the climate of
6731 general circulation model. *J. Atmos. Sci.*, **32(1)**, 3-15.

6732 ----, and R. J. Stouffer, 1980: Sensitivity of a global climate model to an increase of
6733 CO₂ concentration in the atmosphere. *J. Geophys. Res.*, **85(C10)**, 5529-5554.

6734 Marlon, J., Bartlein, P., Carcaillet, C., Gavin, D., Harrison, S., Higuera, P., Joos, F., Power, M.
6735 and Prentice, I. C.: Climate and human influences on global biomass burning over the past
6736 two millennia, *Nature-Geosciences*, **1**, 697–701, 2008.

6737 Marlon, J. R., Bartlein, P. J., Gavin, D. G., Long, C. J., Anderson, R. S., Briles, C. E., Brown, K.
6738 J., Colombaroli, D., Hallett, D. J., Power, M. J., Scharf, E. A. and Walsh, M. K.: Long-term
6739 perspective on wildfires in the western USA, *Proc. Natl. Acad. Sci.*, **109(9)**, E535–E543,
6740 doi:10.1073/pnas.1112839109, 2012.

6741 Martin, J. H., Gordon, M. and Fitzwater, S. E.: The case for iron, *Limnol. Oceanogr.*, **36(8)**,
6742 1793–1802, doi:10.4319/lo.1991.36.8.1793, 1991.

6743 Martin, P. E., & Barker, E. F. (1932). The Infrared Absorption Spectrum of Carbon Dioxide.

6744 *Phys. Rev.*, 41(3), 291–303. <http://doi.org/10.1103/PhysRev.41.291>

6745 Martin, G. M., D. W. Johnson, and An Spice. "The measurement and parameterization of
6746 effective radius of droplets in warm stratocumulus clouds." *Journal of the Atmospheric*
6747 *Sciences* 51, no. 13 (1994): 1823-1842.

6748

6749 Marsh, D. R., J.-F. Lamarque, A. J. Conley, and L. M. Polvani, 2016: Stratospheric ozone
6750 chemistry feedbacks are not critical for the determination of climate sensitivity in
6751 CESM1(WACCM). *Geophys. Res. Lett.*, 43, 3928–3934, doi:doi:10.1002/2016GL068344.
6752 <https://doi.org/10.1002/2016GL068344>.

6753 Marvel, K., Schmidt, G. A., Miller, R. L. and Nazarenko, L. S.: Implications for climate
6754 sensitivity from the response to individual forcings, *Nature Climate Change*, 6, 386, 2015.

6755 Mastenbrook, H. J., 1963: Frost-point hygrometer measurement in the stratosphere and the
6756 problem of moisture contamination. *Humidity and Moisture*, Vol. 2, New York,
6757 Reinhold Publishing Co., 480-485.

6758 Matthes, K., Funke, B., Andersson, M., Barnard, L., Beer, J., et al., 2017: Solar forcing for
6759 CMIP6 (v3.2). *Geoscientific Model Development*, Katlenburg-Lindau Vol. 10, Iss. 6: 2247-
6760 2302.

6761 Mathews, E. and Fung, I.: Methane emission from natural wetlands: Global distribution, area and
6762 environmental characteristics of sources, *Global Biogeochem. Cycles*, 1(1), 61–86, 1987.

6763 Matthews, H. D., Graham, T. L., Keverian, S., Lamontagne, C., Seto, D. and Smith, T. J.:
6764 National contributions to observed global warming, *Environ. Res. Lett.*, 9(1),
6765 doi:10.1088/1748-9326/9/1/014010, 2014.

6766 Mauceri, S., Pilewskie, P., Richard, E. et al., 2018: Revision of the Sun's Spectral Irradiance as
6767 Measured by SORCE SIM, *Sol Phys* 293: 161. <https://doi.org/10.1007/s11207-018-1379-1>.

6768 Maycock AC, Joshi MM, Shine KP, Scaife AA 2013: The circulation response to idealized
6769 changes in water vapor. *J Climate* 26:545-561 DOI: 10.1175/JCLI-D-12-00155.1

6770 Moore, C. M. M., Mills, M. M. M., Arrigo, K. R. R., Berman-Frank, I., Bopp, L., Boyd, P. W.
6771 W., Galbraith, E. D. D., Geider, R. J. J., Guieu, C., Jaccard, S. L. L., Jickells, T. D. D., La
6772 Roche, J., Lenton, T. M. M., Mahowald, N. M. M., Marañón, E., Marinov, I., Moore, J. K.
6773 K., Nakatsuka, T., Oschlies, A., Saito, M. A. A., Thingstad, T. F. F., Tsuda, A. and Ulloa,
6774 O.: Processes and patterns of oceanic nutrient limitation, *Nat. Geosci.*, 6(9), 701–710,
6775 doi:10.1038/ngeo1765, 2013.

6776 McCracken, K. G., J. Beer, F. Steinhilber, and J. Abreu, 2013: The Heliosphere in Time, Space
6777 *Sci. Rev.*, 176, 59-71 DOI 10.1007/s11214-011-9851-3.

6778 McClatchey, R. A., Benedict, W. S., Clough, S. A., Burch, D. E., Calfee, R. F., Fox, K., ...
6779 Garing, J. S. (1973). *AFCRL Atmospheric Absorption Line Parameters Compilation*.
6780 Bedford, MA.

6781 McConnell, J. C., M. B. McElroy, and S. C. Wofsy, 1971: Natural Sources of Atmospheric CO.
6782 *Nature*, 233, 187. <http://dx.doi.org/10.1038/233187a0>.

6783 McCormick, M.P. (1987), SAGE II: An overview. *Adv. Space Res.*, 7, 219–226.

6784 McCormick, R. A., & Ludwig, J. H. (1967). Climate modification by atmospheric aerosols.
6785 *Science*, 156(3780), 1358-1359.

6786 McCoy, D. T., & Hartmann, D. L. (2015). Observations of a substantial cloud-aerosol indirect
6787 effect during the 2014–2015 Bárðarbunga-Veiðivötn fissure eruption in Iceland.
6788 *Geophysical Research Letters*, 42(23), 10-409.

6789 McElroy, M. B., S. C. Wofsy, J. E. Penner, and J. C. McConnell, 1974: Atmospheric Ozone:
6790 Possible Impact of Stratospheric Aviation. *J. Atmos. Sci.*, 31, 287–304, doi:10.1175/1520-
6791 0469(1974)031<0287:AOPIOS>2.0.CO;2. [https://doi.org/10.1175/1520-0469\(1974\)031%3C0287:AOPIOS%3E2.0.CO](https://doi.org/10.1175/1520-0469(1974)031%3C0287:AOPIOS%3E2.0.CO).

6793 —, —, and Y. L. Yung, 1977: The nitrogen cycle: perturbations due to man and their
6794 impact on atmospheric N₂O and O₃. *Philos. Trans. R. Soc. London B Biol. Sci.*, 277, 159–

6795 181, doi:10.1098/rstb.1977.0009.
6796 <http://rstb.royalsocietypublishing.org/content/277/954/159>.

6797 McGregor, S., and A. Timmermann (2011), The effect of explosive tropical volcanism on ENSO,
6798 *J. Clim.*, 24(8), 2178–2191.

6799 Meehl, G. A., and Coauthors, 2007: Global Climate Projections. *Climate Change 2007: The*
6800 *Physical Science Basis. Contribution of Working Group I to the Fourth Assessment Report*
6801 *of the Intergovernmental Panel on Climate Change*, D. Qin, M. Manning, Z. Chen, M.
6802 Marquis, K.B. Averyt, M. Tignor, and H.L. Miller, Eds., Cambridge University Press,
6803 Cambridge, United Kingdom and New York, NY, USA.

6804 Meehl, G. A., J. M. Arblaster, K. Matthes, F. Sassi, and H. van Loon, 2009: Amplifying the
6805 Pacific Climate System Response to a Small 11-Year Solar Cycle Forcing, *Science*, 325,
6806 1114-1118, DOI: 10.1126/science.1172872.

6807 Meehl, G. A. *et al.* Relative increase of record high maximum temperatures compared to record
6808 low minimum temperatures in the US. *Geophys. Res. Lett.* **36**, L23701 (2009).

6809 Meehl, G. A., J. M. Arblaster, J. T. Fasullo, A. Hu, and K. E. Trenberth (2011), Model-based
6810 evidence of deep-ocean heat uptake during surface-temperature hiatus periods. *Nature Clim*
6811 *Change*, 1, 360-364.

6812 Meftah, M., L. Damé, D. Bolsée, A. Hauchecorne, N. Pereira, D. Sluse, G. Cessateur, A. Irbah1,
6813 J. Bureau, M. Weber3, K. Bramstedt, T. Hilbig3, R. Thiéblemont, M. Marchand, F.
6814 Lefèvre1, A. Sarkissian and S. Bekki, (2018): SOLAR-ISS: A new reference spectrum
6815 based on SOLAR/SOLSPEC observations, *A&A* 611, A1 [https://doi.org/10.1051/0004-
6816 6361/201731316](https://doi.org/10.1051/0004-6361/201731316)

6817 Meyer, K., Platnick, S., & Zhang, Z. (2015). Simultaneously inferring above-cloud absorbing
6818 aerosol optical thickness and underlying liquid phase cloud optical and microphysical
6819 properties using MODIS. *Journal of Geophysical Research: Atmospheres*, 120(11), 5524-
6820 5547.

6821 Michaels, P. J., and P. C. Knappenberger, 2000: Natural Signals in the MSU lower tropospheric
6822 temperature Record, *Geophys. Res. Lett.*, 27, 2,905-2,908.

6823 Mickley, L. J., P. P. Murti, D. J. Jacob, J. A. Logan, D. M. Koch, and D. Rind, 1999: Radiative
6824 forcing from tropospheric ozone calculated with a unified chemistry-climate model. *J.*
6825 *Geophys. Res. Atmos.*, **104**, 30153–30172, doi:doi:10.1029/1999JD900439.
6826 <https://doi.org/10.1029/1999JD900439>.

6827 Mie, G., 1908: Beiträge zur Optik trüber Medien, speziell kolloidaler Metallösungen. *Annalen*
6828 *der Physik*. **330**(3): 377–445.

6829 Migeotte, M. V. (1948). Spectroscopic Evidence of Methane in the Earth's Atmosphere. *Phys.*
6830 *Rev.*, 73(5), 519–520. <http://doi.org/10.1103/PhysRev.73.519.2>

6831 Ming, Y., Ramaswamy, V. and Persad, G.: Two opposing effects of absorbing aerosols on
6832 global-mean precipitation, *Geophysical Research Letters*, 37, L13701, 2010.

6833 Minnis, P., E. F. Harrison, L. L. Stowe, G. G. Gibson, F. M. Denn, D. R. Doelling, and W. L.
6834 Smith, 1993: Radiative Climate Forcing by the Mount Pinatubo Eruption. *Science* (80-.),
6835 259, 1411 LP-1415, doi:10.1126/science.259.5100.1411.
6836 <http://science.sciencemag.org/content/259/5100/1411.abstract>.

6837 Minnis, P., Young, D.F., Garber, D.P., Nguyen, L., Smith, W.L. and Palikonda, R., 1998.
6838 Transformation of contrails into cirrus during SUCCESS. *Geophysical Research Letters*,
6839 25(8), pp.1157-1160.

6840 Minnis, P., Schumann, U., Doelling, D.R., Gierens, K.M. and Fahey, D.W., 1999. Global
6841 distribution of contrail radiative forcing. *Geophysical Research Letters*, 26(13), pp.1853-
6842 1856.

6843 Mills, M., A. Schmidt, R. Easter, S. Solomon, D. Kinnison, S. Ghan, R. Neely III, D. Marsh, A.
6844 Conley, C. Bardeen, and A. Gettelman (2016), Global volcanic aerosol properties derived
6845 from emissions, 1990-2014, using CESM1(WACCM), *J. Geophys. Res., Atmos.*, 121,
6846 doi:10.1002/2015JD024290.

6847 Min, S. K. *et al.* Human contribution to more-intense precipitation extremes. *Nature* **470**, 378–381
6848 (2011).

6849 Ming, Y. & Ramaswamy, V. A model investigation of aerosol-induced changes in tropical
6850 circulation. *J. Clim.* **24**, 5125–5133 (2011).

6851 Minnis, P., E. F. Harrison, L. L. Stowe, G. G. Gibson, F. M. Denn, D. R. Doelling, and W. L.
6852 Smith Jr. (1993), Radiative climate forcing by the Mt. Pinatubo eruption. *Science*, 259, 1411–
6853 1415.

6854 Misios, S., D. M. Mitchell, L. J. Gray, K. Tourpali, K. Matthes, L. Hood, H. Schmidt, G. Chiodo,
6855 R. Thiéblemont, E. Rozanov, and A. Krivolutsky, 2015: Solar signals in CMIP-5
6856 simulations: effects of atmosphere-ocean coupling, *Q.J.R. Meteorol. Soc.*.. doi:
6857 10.1002/qj.2695.

6858 Mishchenko, M. I., Geogdzhayev, I. V., Cairns, B., Rossow, W. B., & Lacis, A. A. (1999).
6859 Aerosol retrievals over the ocean by use of channels 1 and 2 AVHRR data: sensitivity
6860 analysis and preliminary results. *Applied Optics*, 38(36), 7325–7341.

6861 Mitchell, J. F., Johns, T. C., Gregory, J. M., & Tett, S. F. B. (1995). Climate response to
6862 increasing levels of greenhouse gases and sulfate aerosols. *Nature*, 376(6540), 501.

6863 Mitchell, D. L., and W. Finnegan, 2009: Modification of cirrus clouds to reduce global warming.
6864 *Environ. Res. Lett.*, doi:10.1088/1748-9326/4/4/045102.

6865 Mitchell, D. M., S. Misios, L. J. Gray, K. Tourpali, K. Matthes, L. Hood, H. Schmidt, G. Chiodo,
6866 R. Thiéblemont, E. Rozanov, D. Shindell, and A. Krivolutsky, 2015: Solar signals in CMIP-
6867 5 simulations: the stratospheric pathway. *Q.J.R. Meteorol. Soc.*, 141: 2390–2403. doi:
6868 10.1002/qj.2530.

6869 Mitchell, J F., [S. Manabe](#), T Tokioka, and V Meleshko, 1990: Equilibrium climate
6870 change In *Climate Change: The IPCC Scientific Assessment*, Cambridge, UK, Cambridge
6871 University Press, 131–172.

6872 Mlynczak, M. G., Daniels, T. S., Kratz, D. P., Feldman, D. R., Collins, W. D., Mlawer, E. J., ...
6873 Mast, J. C. (2016). The spectroscopic foundation of radiative forcing of climate by carbon

6874 dioxide. *Geophysical Research Letters*, 43(10), 5318–5325.

6875 <http://doi.org/10.1002/2016GL068837>

6876 Molina, M. J., and F. S. Rowland, 1974: Stratospheric Sink for Chlorofluoromethanes: Chlorine
6877 Atom Catalyzed Destruction of Ozone. *Nature*, 810–812.

6878 Möller, F., 1963: On the influence of changes in the CO₂ concentration in air on the
6879 radiation balance of the earth's surface and on the climate. *J. Geophys. Res.*, **68**, 3877–
6880 3886.

6881 Monks, P. S., and Coauthors, 2015: Tropospheric ozone and its precursors from the urban to the
6882 global scale from air quality to short-lived climate forcer. *Atmos. Chem. Phys.*, **15**, 8889–
6883 8973, doi:10.5194/acp-15-8889-2015. <https://www.atmos-chem-phys.net/15/8889/2015/>.

6884 Montzka, S. A., M. Krol, E. Dlugokencky, B. Hall, P. Jöckel, and J. Lelieveld, 2011: Small
6885 Interannual Variability of Global Atmospheric Hydroxyl. *Science (80-.)*, **331**, 67–69.
6886 <http://www.sciencemag.org/content/331/6013/67.abstract>.

6887 Murray, L. T., L. J. Mickley, J. O. Kaplan, E. D. Sofen, M. Pfeiffer, and B. Alexander, 2014:
6888 Factors controlling variability in the oxidative capacity of the troposphere since the Last
6889 Glacial Maximum. *Atmos. Chem. Phys.*, **14**, 3589–3622, doi:Doi 10.5194/Acp-14-3589-
6890 2014.

6891 Murgatroyd, R. J., 1960: Some recent measurements by aircraft of humidity up to
6892 50,000 ft. in the tropics and their relation- ship to meridional circulation: *Proc.*
6893 *Symp. Atmos. Ozone*, Oxford, 20-25 July 1959, IUGG Monogr. No. 3, Paris, p. 30.

6894 Myhre, G., Highwood, E. J., Shine, K. P., & Stordal, F. (1998). New estimates of radiative
6895 forcing due to well mixed greenhouse gases. *Geophysical Research Letters*, 25(14), 2715–
6896 2718. <http://doi.org/10.1029/98GL01908>

6897 Myhre, G., Shindell, D., Breon, G.-M., Collins, W., Fuglestvedt, J., Huang, J., Koch, D.,
6898 Lamarque, J. F., Lee, D., Mendoza, B., Nakajima, T., Robock, A., Stephens, G., Takemura,
6899 T. and Zhang, H.: Anthropogenic and Nature Radiative Forcing, in Climate Change 2013:
6900 The Physical Science Basis. Contribution of Working Group I to the Fifth Assessment

6901 Report of the Intergovernmental Panel on Climate Change, edited by T. Stocker, D. Qin, G.
6902 K. Plattner, M. Tignor, S. Allen, J. Boschung, A. Nauels, Y. Xia, V. Bex, and P. Midgley,
6903 pp. 659–740, Cambridge University Press, Cambridge, UK., 2013.

6904 Myhre, G., and Coauthors, 2013: Anthropogenic and Natural Radiative Forcing. *Climate Change*
6905 *2013: The Physical Science Basis. Contribution of Working Group I to the Fifth Assessment*
6906 *Report of the Intergovernmental Panel on Climate Change*, T.F. Stocker et al., Eds.,
6907 Cambridge University Press, Cambridge, U.K. and New York, NY, USA, 659–740.

6908 Myhre, G., and Coauthors, 2013: Anthropogenic and Natural Radiative Forcing. *Climate Change*
6909 *2013: The Physical Science Basis. Contribution of Working Group I to the Fifth Assessment*
6910 *Report of the Intergovernmental Panel on Climate Change*, T.F. Stocker et al., Eds.,
6911 Cambridge University Press, Cambridge, U.K. and New York, NY, USA, 659–740.

6912 Myhre, G., Shindell, D., Bréon, F.-M., Collins, W., Fuglestvedt, J., Huang, J., Koch, D.,
6913 Lamarque, J.-F., Lee, D., Mendoza, B., Nakajima, T., Robock, A., Stephens, G., Takemura,
6914 T. and Zhang, H., Anthropogenic and Natural Radiative Forcing. In: Climate Change 2013:
6915 The Physical Science Basis. Contribution of Working Group I to the Fifth Assessment
6916 Report of the Intergovernmental Panel on Climate Change. T. F. Stocker, D. Qin, G.-K.
6917 Plattner, M. Tignor, S. K. Allen et al. (Editors), Cambridge University Press, Cambridge,
6918 United Kingdom and New York, NY, USA, pp. 659-740, 2013.

6919 Myhre, G., E. J. Highwood, K. P. Shine, and F. Stordal, 1998: New estimates of radiative forcing
6920 due to well mixed greenhouse gases. *Geophys. Res. Lett.*, 25.

6921 —, and Coauthors, 2018: Quantifying the Importance of Rapid Adjustments for Global
6922 Precipitation Changes. *Geophys. Res. Lett.*, 45, 11,399-11,405, doi:10.1029/2018gl079474.

6923 Myhre, G. *et al.* Anthropogenic and Natural Radiative Forcing. In: *Climate Change 2013: The*
6924 *Physical Science Basis. Contribution of Working Group I to the Fifth Assessment Report of*
6925 *the Intergovernmental Panel on Climate Change* (eds Stocker TF, et al.) (Cambridge Univ.
6926 Press, 2013).

6927 Myhre, G., D. Shindell, F.-M. Bréon, W. Collins, J. Fuglestvedt, J. Huang, D. Koch, J.-F.
6928 Lamarque, D. Lee, B. Mendoza, T. Nakajima, A. Robock, G. Stephens, T. Takemura and H.

6929 Zhang (2013), Anthropogenic and Natural Radiative Forcing. In: Climate Change (2013), The
6930 Physical Science Basis. Contribution of Working Group I to the Fifth Assessment Report of
6931 the Intergovernmental Panel on Climate Change [Stocker, T.F., D. Qin, G.-K. Plattner, M.
6932 Tignor, S.K. Allen, J. Boschung, A. Nauels, Y. Xia, V. Bex and P.M. Midgley (eds.)].
6933 Cambridge University Press, Cambridge, United Kingdom and New York, NY, USA

6934 Myhre, G., O. Boucher, F.-M. Bréon, P. Forster, and D. Shindell, 2015: Declining uncertainty in
6935 transient climate response as CO₂ forcing dominates future climate change. *Nat. Geosci.*, **8**, doi:10.1038/ngeo2371.

6937 Myhre, D. Shindell, F.-M. Bréon, W. Collins, J. Fuglestvedt, J. Huang, D. Koch, J.-F. Lamarque,
6938 D. Lee, B. Mendoza, T. Nakajima, A. Robock, G. Stephens, T. Takemura and H. Zhang, G.,
6939 Anthropogenic and Natural Radiative Forcing. *Climate Change 2013: The Physical Science
6940 Basis. Contribution of Working Group I to the Fifth Assessment Report of the
6941 Intergovernmental Panel on Climate Change*, T.F. Stocker D. Qin, G.-K. Plattner, M.
6942 Tignor, S.K. Allen, J. Boschung, A. Nauels, Y. Xia, V. Bex and P.M. Midgley, Ed.,
6943 Cambridge University Press, Cambridge, United Kingdom and New York, NY, USA, 659–
6944 740.

6945 Myhre, G., and F. Stordal (1997), Role of spatial and temporal variations in the computation of
6946 radiative forcing and GWP, *J. Geophys. Res.*, **102**(D10), 11181–11200,
6947 doi:10.1029/97JD00148.

6948 Myhre, G., Shindell, D., Bréon, F.-M., Collins, W., Fuglestvedt, J., Huang, J., Koch, D.,
6949 Lamarque, J.-F., Lee, D., Mendoza, B., Nakajima, T., Robock, A., Stephens, G., Takemura,
6950 T. and Zhang, H., Anthropogenic and Natural Radiative Forcing. In: Climate Change 2013:
6951 The Physical Science Basis. Contribution of Working Group I to the Fifth Assessment
6952 Report of the Intergovernmental Panel on Climate Change. T. F. Stocker, D. Qin, G.-K.
6953 Plattner, M. Tignor, S. K. Allen et al. (Editors), Cambridge University Press, Cambridge,
6954 United Kingdom and New York, NY, USA, pp. 659-740, 2013.

6955 Myhre, G., F. Stordal, K. Restad and I.S.A. Isaksen, 1998: Estimation of the direct radiative
6956 forcing due to sulfate and soot aerosols. *Tellus*, **50B**, 463–477.

6957 van Marle, M. J. E., and Coauthors, 2017: Historic global biomass burning emissions for CMIP6
6958 (BB4CMIP) based on merging satellite observations with proxies and fire models (1750-
6959 2015). *Geosci. Model Dev.*, **10**, 3329–3357, doi:10.5194/gmd-10-3329-2017.
6960 <https://doi.org/10.5194/gmd-10-3329-2017>.

6961 Van Marle, M. J. E., Kloster, S., Magi, B. I., Marlon, J. R., Daniau, A. L., Field, R. D., Arneth,
6962 A., Forrest, M., Hantson, S., Kehrwald, N. M., Knorr, W., Lasslop, G., Li, F., Mangeon, S.,
6963 Yue, C., Kaiser, J. W. and Van Der Werf, G. R.: Historic global biomass burning emissions
6964 for CMIP6 (BB4CMIP) based on merging satellite observations with proxies and fire
6965 models (1750-2015), *Geosci. Model Dev.*, **10**(9), 3329–3357, doi:10.5194/gmd-10-3329-
6966 2017, 2017.

6967

6968 Nadelhoffer, K. J., Emmett, B. A., Gundersen, P., Kjønaas, O. J., Koopmans, C. J., Schleppi, P.,
6969 Tietema, A. and Wright, R. F.: Nitrogen deposition makes a minor contribution to carbon
6970 sequestration in temperate forests, *Nature*, 398(March 11, 1999), 145–148 [online]
6971 Available from: <http://www.nature.com>, 1999.

6972 Naik, V., and Coauthors, 2013: Preindustrial to present-day changes in tropospheric hydroxyl
6973 radical and methane lifetime from the Atmospheric Chemistry and Climate Model
6974 Intercomparison Project (ACCMIP). *Atmos. Chem. Phys.*, **13**, 5277–5298, doi:10.5194/acp-
6975 13-5277-2013.

6976 National Research Council 1979. *Carbon Dioxide and Climate: A Scientific Assessment*.
6977 Washington, DC: The National Academies Press, . <https://doi.org/10.17226/12181>.

6978 National Research Council, 1982. *Carbon dioxide and Climate: A Second Assessment*.
6979 Washington, DC: The National Academies Press, 96 pages.
6980 <https://doi.org/10.17226/18524>

6981 National Research Council, 1996: A plan for a research program on Aerosol Radiative Forcing
6982 and Climate Change. Washington, DC: The National Academies Press, 161pp.

6983 National Research Council, 2005: Radiative Forcing of Climate Change: Expanding the Concept
6984 and Addressing Uncertainties. The National Academies Press, Washington, DC, 208pp.
6985 <https://www.nap.edu/catalog/11175/radiative-forcing-of-climate-change-expanding-the->
6986 [concept-and-addressing](#).

6987 National Research Council, 2005: *Radiative Forcing of Climate Change: Expanding the Concept*
6988 *and Addressing Uncertainties*. The National Academies Press, 224 pp.

6989 National Research Council, 2005: Radiative Forcing of Climate Change: Expanding the Concept
6990 and Addressing Uncertainties. The National Academies Press, Washington, DC,
6991 <https://www.nap.edu/catalog/11175/radiative-forcing-of-climate-change-expanding-the->
6992 [concept-and-addressing](#)

6993 Neff, U., S. J. Burns, A. Mangini, M. Mudelsee, D. Fleitmann, and A. Matter, 2001: Strong
6994 coherence between solar variability and the monsoon in Oman between 9 and 6 kyr ago,
6995 *Nature*, 411, 290-293.

6996 Niemeier, U., C. Timmreck, H. F. Graf, S. Kinne, S. Rast, and S. Self (2009), Initial fate of fine
6997 ash and sulfur from large volcanic eruptions. *Atmos Chem Phys*, 9, 9043-9057.

6998 Niemeier, U. and S. Tilmes (2017), Sulfur injections for a cooler planet, *Science* 357, no. 6348,
6999 246-248.

7000 U. Niemeier and C. Timmreck (2015), What is the limit of climate engineering by stratospheric
7001 injection of SO₂?, *Atmos. Chem. Phys.*, 15, 9129–9141, 2015
7002 <https://doi.org/10.5194/acp-15-9129-2015>

7003

7004 Nowack, P. J., N. Luke Abraham, A. C. Maycock, P. Braesicke, J. M. Gregory, M. M. Joshi, A.
7005 Osprey, and J. A. Pyle, 2015: A large ozone-circulation feedback and its implications for
7006 global warming assessments. *Nat. Clim. Chang.*, 5, 41–45, doi:10.1038/nclimate2451.
7007 <http://dx.doi.org/10.1038/nclimate2451>.

7008 Novello, V. F., Vuille, M, Cruz, F. W., Stríkis, N. M., de Paula, M. S., Edwards, R. L., Cheng,
7009 H., Karmann, I., Jaqueto, P. F., Trindade, R. I. F., Hartmann, G. A., Moquet, Jean S., 2016:

7010 Centennial-scale solar forcing of the South American Monsoon System recorded in
7011 stalagmites, *Scientific Reports*, 6, Article number: 24762

7012

7013 Ocean Studies Board, 2015: Climate Intervention: Reflecting Sunlight to Cool the Earth. *Natl.*
7014 *Acad. Press*, doi:10.17226/18988.

7015 Ohba, M., H. Shiogama, T. Yokohata, and M. Watanabe (2013), Impact of strong tropical volcanic
7016 eruptions on ENSO simulated in a coupled GCM, *J. Clim.*, 26(14), 5169–5182.

7017 Oman, L., A. Robock, G. Stenchikov, G. A. Schmidt, and R. Ruedy (2005), Climatic response to
7018 high latitude volcanic eruptions. *J Geophys Res*, 110, D13103.

7019 Oman, L., A. Robock, G. Stenchikov, T. Thordarson, D. Koch, D. Shindell, and C. Gao (2006a),
7020 Modeling the distribution of the volcanic aerosol cloud from the 1783-1784 Laki eruption. *J*
7021 *Geophys Res*, 111, D12209.

7022 Oman, L., A. Robock, G. L. Stenchikov, and T. Thordarson (2006b), High-latitude eruptions cast
7023 shadow over the African monsoon and the flow of the Nile. *Geophys Res Lett*, 33, L18711.

7024 Olson, J., and Coauthors, 1997: Results from the Intergovernmental Panel on Climatic Change
7025 Photochemical Model Intercomparison (PhotoComp). *J. Geophys. Res. Atmos.*, **102**, 5979–
7026 5991, doi:doi:10.1029/96JD03380. <https://doi.org/10.1029/96JD03380>.

7027 Owens, A. J., C. H. Hales, D. L. Filkin, C. Miller, and M. McFarland, 1985: Multiple scenario
7028 ozone change calculations: The subtractive perturbation approach. *Atmospheric Ozone*, C.S.
7029 Zerefos and A. Ghazi, Eds., D. Reidel, Dordrecht, 82–86.

7030

7031 Paudel, R., Mahowald, N. M., Hess, P. G. M., Meng, L. and Riley, W. J.: Attribution of changes
7032 in global wetland methane emissions from pre-industrial to present using CLM4.5-BGC,
7033 *Environ. Res. Lett.*, 11(3), doi:10.1088/1748-9326/11/3/034020, 2016.

7034 Paulot, F., D. Paynter, P. Ginoux, V. Naik, and L. W. Horowitz, 2018: Changes in the aerosol
7035 direct radiative forcing from 2001 to 2015: observational constraints and regional
7036 mechanisms. *Atmos. Chem. Phys.*, **18**, 13265–13281, doi:10.5194/acp-18-13265-2018.

7037 Pausata, F. S., L. Chafik, R. Caballero, and D. S. Battisti (2015), Impacts of high-latitude volcanic
7038 eruptions on ENSO and AMOC, *Proc. Natl. Acad. Sci. U.S.A.*, **112**(45), 13,784–13,788.

7039 Pechony, O. and Shindell, D. T.: Driving forces of global wildfires over the past millennium and
7040 the forthcoming century, *Proc. Natl. Acad. Sci.*, **107**(45), 19167–19170,
7041 doi:10.1073/pnas.1003669107, 2010

7042 Peers, F., Waquet, F., Cornet, C., Dubuisson, P., Ducos, F., Goloub, P., ... & Thieuleux, F.
7043 (2015). Absorption of aerosols above clouds from POLDER/PARASOL measurements and
7044 estimation of their direct radiative effect. *Atmospheric Chemistry and Physics*, **15**(8), 4179-
7045 4196.

7046 Penner, J. E., Dickinson, R. E., & O'Neill, C. A. (1992). Effects of aerosol from biomass burning
7047 on the global radiation budget. *Science*, **256**(5062), 1432-1434. Stanhill, G., & Moreshet, S.
7048 (1992). Global radiation climate changes: The world network. *Climatic Change*, **21**(1), 57-
7049 75.

7050 Penner, J. E., Chuang, C. C., & Grant, K. (1998). Climate forcing by carbonaceous and sulfate
7051 aerosols. *Climate Dynamics*, **14**(12), 839-851.

7052 Penner et al., IPCC, 2001.

7053 Penner, J. E., R. E. Dickinson, and C. A. O'Neill, 1992: Effects of aerosol from biomass burning
7054 on the global radiation budget. *Science* (80- .), **256**, 1432–1434,
7055 doi:10.1126/science.256.5062.1432.
7056 <http://science.sciencemag.org/content/256/5062/1432.abstract>.

7057 Penner, J. E. and J. S. Chang, 1978: Possible variations in atmospheric ozone related to the
7058 eleven-year solar cycle, *Geophys. Res. Lett.*, **5**, 817.

7059 Penner, J. E., Dickinson, R. E., & O'Neill, C. A. (1992). Effects of aerosol from biomass burning
7060 on the global radiation budget. *Science*, **256**(5062), 1432-1434.

7061 Penner, J. E., R. E. Dickinson, and C. A. O'Neill, 1992: Effects of aerosol from biomass burning
7062 on the global radiation budget. *Science* (80-.), 256, 1432–1434,
7063 doi:10.1126/science.256.5062.1432.
7064 <http://science.scienmag.org/content/256/5062/1432.abstract>.

7065 Perlitz, J., and H.-F. Graf (2001), Troposphere-stratosphere dynamic coupling under strong and
7066 weak polar vortex conditions. *Geophys. Res. Lett.*, 28, 271–274.

7067 Perner, D., D. H. Ehhalt, H. W. Pätz, U. Platt, E. P. Röth, and A. Volz, 1976: OH - Radicals in
7068 the lower troposphere. *Geophys. Res. Lett.*, 3, 466–468, doi:doi:10.1029/GL003i008p00466.
7069 <https://doi.org/10.1029/GL003i008p00466>.

7070 Persad, G., [D J Paynter](#), [Y Ming](#), and [V Ramaswamy](#), 2017: Competing Atmospheric and Surface-
7071 Driven Impacts of Absorbing Aerosols on the East Asian Summertime Climate. *Journal of*
7072 *Climate*, 30(22), DOI:[10.1175/JCLI-D-16-0860.1](https://doi.org/10.1175/JCLI-D-16-0860.1).

7073 Peters, L. K., and Coauthors, 1995: The current state and future direction of Eulerian models in
7074 simulating the tropospheric chemistry and transport of trace species: a review. *Atmos.*
7075 *Environ.*, 29, 189–222, doi:[http://dx.doi.org/10.1016/1352-2310\(94\)00235-D](http://dx.doi.org/10.1016/1352-2310(94)00235-D).
7076 <http://www.sciencedirect.com/science/article/pii/135223109400235D>.

7077 Pierrehumbert, R. T. (2011). Infrared radiation and planetary temperature. *Physics Today*, 64(1),
7078 33–38. <http://doi.org/10.1063/1.3653855>

7079 Pilewski, P., G. Kopp, E. Richard, O. Coddington, S. Mauceri, T. Sparn, and T. Woods, 2018:
7080 TSIS-1 and continuity of the total and spectral solar irradiance climate data record,
7081 European Geosciences Union General Assembly 2018, Vienna, Austria, April 9-13.

7082

7083 Pinto, J. P., R. P. Turco, and O. B. Toon (1989), Self-limiting physical and chemical effects in
7084 volcanic eruption clouds, *J. Geophys. Res.*, 94(D8), 11,165–11,174,
7085 doi:10.1029/JD094iD08p11165.

7086 Pinnock, S., M. D. Hurley, K. P. Shine, T. J. Wallington, and T. J. Smyth (1995), Radiative
7087 forcing of climate by hydrochlorofluorocarbons and hydrofluorocarbons, *J. Geophys. Res.*,
7088 100(D11), 23227–23238, doi:[10.1029/95JD02323](https://doi.org/10.1029/95JD02323).

7089 Pincus, R., Forster, P. M., & Stevens, B. (2016). The Radiative Forcing Model Intercomparison
7090 Project (RFMIP): experimental protocol for CMIP6. *GEOSCIENTIFIC MODEL
7091 DEVELOPMENT*, 9(9), 3447–3460. <http://doi.org/10.5194/gmd-9-3447-2016>

7092 Pincus, R., Forster, P. M., & Stevens, B. (2016): The Radiative Forcing Model Intercomparison
7093 Project (RFMIP): experimental protocol for CMIP6. *GEOSCIENTIFIC MODEL
7094 DEVELOPMENT*, 9(9), 3447–3460. <http://doi.org/10.5194/gmd-9-3447-2016>

7095 Pinnock, S., M. D. Hurley, K. P. Shine, T. J. Wallington, and T. J. Smyth (1995), Radiative
7096 forcing of climate by hydrochlorofluorocarbons and hydrofluorocarbons, *J. Geophys. Res.*,
7097 100(D11), 23227–23238, doi:[10.1029/95JD02323](https://doi.org/10.1029/95JD02323)

7098 Pitari, G., and Coauthors (2014), Stratospheric ozone response to sulfate geoengineering: Results
7099 from the Geoengineering Model Intercomparison Project (GeoMIP). *Journal of Geophysical
7100 Research-Atmospheres*, 119, 2629–2653.

7101 Pitari, G., Schumann, U., Stordal, F., Zerefos, C., 2005. Aviation radiative forcing in 2000: an
7102 update of IPCC (1999). *Meteorol. Zeit* 114, 555–561.

7103 Plass, G. N. (1956a). Effect of Carbon Dioxide Variations on Climate. *American Journal of
7104 Physics*, 24(5), 376–387. <http://doi.org/10.1119/1.1934233>

7105 Plass, G. N. (1956b). Infrared Radiation in the Atmosphere. *American Journal of Physics*, 24(5),
7106 303–321. <http://doi.org/10.1119/1.1934220>

7107 Plass, G. N. (1956). The influence of the 15μ carbon-dioxide band on the atmospheric infra-red
7108 cooling rate. *Quarterly Journal of the Royal Meteorological Society*, 82(353), 310–324.
7109 <http://doi.org/10.1002/qj.49708235307>

7110 Plass, G. N. (1956). The Carbon Dioxide Theory of Climatic Change. *Tellus*, 8(2), 140–154.
7111 <http://doi.org/10.1111/j.2153-3490.1956.tb01206.x>

7112 Plass, G. N., 1956: The influence of the 15-micron carbon dioxide band on the atmospheric
7113 infrared cooling rate. *Quart. J. Roy. Meteor. Soc.*, **82**, 310-324.

7114 Platnick, S., 2018: The Earth Observer, vol. 30, Issue 2, pp1-3.

7115

7116

7117 Polson, D., M. Bollasina, G, C, Hegerl, and L. J. Wilcox, 2014: Decreased monsoon precipitation
7118 in the Northern Hemisphere due to anthropogenic aerosols, *Geophys. Res. Lett.*, **41**, 6023-
7119 6029. <https://doi.org/10.1002/2014GL060811>

7120

7121 Polvani, L, A. Banerjee, A. Schmidt, Northern Hemisphere continental winter warming following
7122 the 1991 Mt. Pinatubo eruption: reconciling models and observations (2019), *Atmos. Chem.*
7123 *Phys.*, **19**, 6351-6366, 2019, <https://doi.org/10.5194/acp-19-6351-2019>

7124 Ponater, M., Pechtl, S., Sausen, R., Schumann, U., and Hüttig, G. (2006) Potential of the
7125 cryoplane technology to reduce aircraft climate impact: a state-of-the-art assessment.
7126 *Atmos. Environ.*, **40**, 6928–6944.

7127 Portmann, R. W., S. Solomon, J. Fishman, J. R. Olson, J. T. Kiehl, and B. Briegleb, 1997:
7128 Radiative forcing of the Earth's climate system due to tropical tropospheric ozone
7129 production. *J. Geophys. Res.*, **102**, 9409–9418.

7130 Prather, M. J., 1994: Lifetimes and eigenstates in atmospheric chemistry. *Geophys. Res. Lett.*, **21**,
7131 801–804, doi:doi:10.1029/94GL00840. <https://doi.org/10.1029/94GL00840>.

7132 Prather, M., R. Sausen, A. S. Grossman, J. M. Haywood, D. Rind, and B. H. Subbaraya, 1999:
7133 Potential Climate Change from Aviation. *IPCC Special Report on Aviation and the Global*
7134 *Atmosphere*, 185–215.

7135 Prather, M. J., R. G. Derwent, D. Ehhalt, P. J. Fraser, E. Sanhueza, and X. Zhou, 1995: Other
7136 Trace Gases and Atmospheric Chemistry. *Climate Change 1994: Radiative Forcing of*
7137 *Climate Change and An Evalaution of the IPCC IS92 Emision Scenarios*, J.T. Houghton,

7138 L.G. Meira Filho, J. Bruce, H. Lee, B.A. Callendar, E. Haites, N. Harris, and K. Maskell,
7139 Eds., Cambridge, U.K., New York, NY, USA, Melbourne, Australia.

7140 Prather, M. J., and Coauthors, 2001: Atmospheric Chemistry and Greenhouse Gases. *Climate*
7141 *Change 2001: The Physical Science Basis. Contribution of Working Group I to the Third*
7142 *Assessment Report of the Intergovernmental Panel on Climate Change*, Y. Ding, D.J.
7143 Griggs, M. Noguer, P.J. van der Linden, X. Dai, K. Maskell, and C.A. Johnson, Eds.,
7144 Cambridge University Press, Cambridge, United Kingdom and New York, NY, USA.

7145 —, and Coauthors, 2018: How well can global chemistry models calculate the reactivity of
7146 short-lived greenhouse gases in the remote troposphere, knowing the chemical composition.
7147 *Atmos. Meas. Tech.*, **11**, 2653–2668, doi:10.5194/amt-11-2653-2018. <https://www.atmos-meas-tech.net/11/2653/2018/>.

7149 Predybaylo, E., G. L. Stenchikov, A. T. Wittenberg, and F. Zeng (2017), Impacts of a Pinatubo-
7150 Size Volcanic Eruption on ENSO, *J. Geophys. Res. Atmos.*, **122**, 925–947,
7151 doi:10.1002/2016JD025796.

7152 Previdi, M.: Radiative feedbacks on global precipitation, *Environmental Research Letters*, **5**(2),
7153 025211, 2010.

7154 Prinn, R. G., and Coauthors, 2001: Evidence for Substantial Variations of Atmospheric Hydroxyl
7155 Radicals in the Past Two Decades. *Science (80-.)*, **292**, 1882 LP-1888,
7156 doi:10.1126/science.1058673.
7157 <http://science.sciencemag.org/content/292/5523/1882.abstract>.

7158 Proctor, J., S. Hsiang, J. Burney, M. Burke, and W. Schlenker, 2018: Estimating global
7159 agricultural effects of geoengineering using volcanic eruptions. *Nature*,
7160 doi:10.1038/s41586-018-0417-3.

7161 Pueschel, R. F. (1996), Stratospheric Aerosols: Formation, Properties, Effects, *J. Aerosol Sci.*,
7162 **27**, No. 3, 383-402.

7163

7164 Quaas, J., Ming, Y., Menon, S., Takemura, T., Wang, M., Penner, J. E., ... & Sayer, A. M.
7165 (2009). Aerosol indirect effects—general circulation model intercomparison and evaluation
7166 with satellite data. *Atmospheric Chemistry and Physics*, 9(22), 8697–8717.

7167

7168 Ramanathan, V. (1975). Greenhouse Effect Due to Chlorofluorocarbons: Climatic
7169 Implications. *Science*, 190(4209), 50 LP-52 <http://doi.org/10.1126/science.190.4209.50>.

7170 Ramanathan, V., Lian, M. S., & Cess, R. D. (1979). Increased atmospheric CO₂: Zonal and
7171 seasonal estimates of the effect on the radiation energy balance and surface
7172 temperature. *Journal of Geophysical Research: Oceans*, 84(C8), 4949–4958.
7173 <http://doi.org/10.1029/JC084iC08p04949>

7174 _____, and A. Vogelmann, 1997: Greenhouse effect, atmospheric solar absorption, and the
7175 Earth's Radiation Budget: From the Arrhenius-Langley era to the 1990s. *Ambio*, 26, 1,
7176 pp38–46.

7177 Ramanathan, V., Crutzen, P. J., Kiehl, J. T. and Rosenfeld, D.: Atmosphere - Aerosols, climate,
7178 and the hydrological cycle, *Science*, 294(5549), 2119–2124, 2001.

7179 Ramanathan, V. (1975). Greenhouse Effect Due to Chlorofluorocarbons: Climatic Implications.
7180 *Science*, 190(4209), 50 LP-52. <http://doi.org/10.1126/science.190.4209.50>

7181 Ramanathan, V. (1980). Climatic Effects of Anthropogenic Trace Gases. In W. Bach, J.
7182 Pankrath, & J. Williams (Eds.), *Interactions of Energy and Climate: Proceedings of an*
7183 *International Workshop held in Münster, Germany, March 3–6, 1980* (pp. 269–280).
7184 Dordrecht, Holland: D. Reidel Publishing Company. <http://doi.org/10.1007/978-94-009-9111-8>

7186 Ramanathan, V., Callis, L. B., & Boughner, R. E. (1976). Sensitivity of Surface Temperature and
7187 Atmospheric Temperature to Perturbations in the Stratospheric Concentration of Ozone and
7188 Nitrogen Dioxide. *Journal of the Atmospheric Sciences*, 33(6), 1092–1112.
7189 <http://doi.org/10.1175/1520-0469> (1976)033<1092:SOSTAA>2.0.CO;2

7190 Ramanathan, V., Cicerone, R. J., Singh, H. B., & Kiehl, J. T. (1985). Trace gas trends and their

7191 potential role in climate change. *Journal of Geophysical Research: Atmospheres*, 90(D3),
7192 5547–5566. <http://doi.org/10.1029/JD090iD03p05547>

7193 Ramanathan, V., Lian, M. S., & Cess, R. D. (1979). Increased atmospheric CO₂: Zonal and
7194 seasonal estimates of the effect on the radiation energy balance and surface temperature.
7195 *Journal of Geophysical Research: Oceans*, 84(C8), 4949–4958.
7196 <http://doi.org/10.1029/JC084iC08p04949>

7197 Ramanathan, V., L. Callis, R. Cess, J. Hansen, I. Isaksen, W. Kuhn, A. Lacis, F. Luther, J.
7198 Mahlman, R. Reck, & M. Schlesinger(1987), Climate-chemical interactions and effects of
7199 changing atmospheric trace gases, *Rev. Geophys.*, 25(7), 1441–1482,
7200 doi:[10.1029/RG025i007p01441](https://doi.org/10.1029/RG025i007p01441).

7201 Ramanathan, V., and R. E. Dickinson, 1979: The Role of Stratospheric Ozone in the Zonal and
7202 Seasonal Radiative Energy Balance of the Earth-Troposphere System. *J. Atmos. Sci.*, 36,
7203 1084–1104, doi:10.1175/1520-0469(1979)036<1084:TROSOI>2.0.CO;2.
7204 <https://journals.ametsoc.org/doi/abs/10.1175/1520-0469%281979%29036%3C1084%3ATROSOI%3E2.0.CO%3B2>.

7205 —, M. S. Lian, and R. D. Cess, 1979: Increased atmospheric CO₂: Zonal and seasonal
7206 estimates of the effect on the radiation energy balance and surface temperature. *J. Geophys.*
7207 *Res. Ocean.*, 84, 4949–4958, doi:10.1029/JC084iC08p04949.
7208 <https://doi.org/10.1029/JC084iC08p04949>.

7209 —, R. J. Cicerone, H. B. Singh, and J. T. Kiehl, 1985: Trace gas trends and their potential role
7210 in climate change. *J. Geophys. Res. Atmos.*, 90, 5547–5566,
7211 doi:10.1029/JD090iD03p05547. <https://doi.org/10.1029/JD090iD03p05547>.

7212 —, and Coauthors, 1987: Climate-chemical interactions and effects of changing atmospheric
7213 trace gases. *Rev. Geophys.*, 25, 1441–1482, doi:10.1029/RG025i007p01441.
7214 <https://doi.org/10.1029/RG025i007p01441>.

7215 Ramanathan, V., 1975: Greenhouse Effect Due to Chlorofluorocarbons: Climatic Implications.
7216 *Science* (80-.), 190, 50 LP-52, doi:10.1126/science.190.4209.50.
7217 <http://science.sciencemag.org/content/190/4209/50.abstract>.

7219 ——, 1981: The Role of Ocean-Atmosphere Interactions in the CO₂ Climate Problem. *J. Atmos.*
7220 *Sci.*, 38, 918–930, doi:10.1175/1520-0469(1981)038<0918:TROOAI>2.0.CO;2.
7221 [https://doi.org/10.1175/1520-0469\(1981\)038%3C0918:TROOAI%3E2.0.CO](https://doi.org/10.1175/1520-0469(1981)038%3C0918:TROOAI%3E2.0.CO).

7222 Ramanathan, V., 1982: In Carbon dioxide review 1982, W. Clark, Ed., Oxford University Press,
7223 Clarendon, England, 278–283.

7224 Ramanathan, V., 1981: The Role of Ocean-Atmosphere Interactions in the CO₂-Climate
7225 Problems. *J. Atmos. Sci.*, 38: 918-930.

7226 Ramanathan, V., C. Chung, D. Kim, T. Bettge, L. Buja, J. T. Kiehl, W. M. Washington, Q. Fu,
7227 D. R. Sikka, and M. Wild, 2005: [Atmospheric Brown Clouds: Impacts on South Asian
7228 Climate and Hydrological Cycle. PNAS](#), Vol. 102, No. 15, 5326-5333.

7229 Ramanathan, V., and R. E. Dickinson, 1979: The Role of Stratospheric Ozone in the Zonal and
7230 Seasonal Radiative Energy Balance of the Earth-Troposphere System. *J. Atmos. Sci.*, **36**,
7231 1084–1104, doi:10.1175/1520-0469(1979)036<1084:TROSOI>2.0.CO;2.
7232 <https://journals.ametsoc.org/doi/abs/10.1175/1520-0469%281979%29036%3C1084%3ATROSOI%3E2.0.CO%3B2>.

7233 ——, L. B. Callis, and R. E. Boughner, 1976: Sensitivity of Surface Temperature and
7234 Atmospheric Temperature to Perturbations in the Stratospheric Concentration of Ozone and
7235 Nitrogen Dioxide. *J. Atmos. Sci.*, **33**, 1092–1112, doi:10.1175/1520-
7236 0469(1976)033<1092:SOSTAA>2.0.CO;2. [https://doi.org/10.1175/1520-0469\(1976\)033%3C1092:SOSTAA%3E2.0.CO](https://doi.org/10.1175/1520-0469(1976)033%3C1092:SOSTAA%3E2.0.CO).

7237 Ramanathan, V., and Coauthors, 1985: Trace gas effects on climate. *World Meteorological
7238 Organization Global Ozone Research and Monitoring Project Report NO. 16 Atmospheric
Ozone 1985 - Assessment of our Understanding of the Processes Controlling its Present
Distribution and Change.*

7239 Ramanathan, V., and Coauthors, 1987: Climate-chemical interactions and effects of changing
7240 atmospheric trace gases. *Rev. Geophys.*, **25**, 1441–1482,
7241 doi:doi:10.1029/RG025i007p01441. <https://doi.org/10.1029/RG025i007p01441>.

7242

7243 [Ramaswamy, V, M D Schwarzkopf](#), W J Randel, B D Santer, [B J Soden](#), and G Stenchikov,
7244 2006: Anthropogenic and natural influences in the evolution of lower stratospheric cooling.
7245 *Science*, **311**(5764), DOI:[10.1126/science.1122587](https://doi.org/10.1126/science.1122587)

7249 [Ramaswamy, V.](#), J W Hurrell, G A Meehl, A Phillips, B D Santer, [M Daniel Schwarzkopf](#), D J
7250 Seidel, S C Sherwood, and P W Thorne, 2006: Why do temperatures vary vertically (from
7251 the surface to the stratosphere) and what do we understand about why they might vary and
7252 change over time? In *Temperature Trends in the Lower Atmosphere: Steps for*
7253 *Understanding and Reconciling Differences*, Karl, T R, S J Hassol, C D Miller, W L
7254 Murray, eds., Washington, DC, A Report by the Climate Change Science
7255 Program/Subcommittee on Global Change Research, 15-28.

7256 Ramaswamy, V., and Coauthors, 2001: Radiative Forcing of Climate Change. *Climate Change*
7257 *2001: Working Group I: The Scientific Basis*, F. Joos and J. Srinivasan, Eds.

7258 Ramaswamy, V., Boucher, O., Haigh, J., Hauglustaine, D., Haywood, J.M., Myhre, G.,
7259 Nakajima, T., Shi, G.Y., and Solomon, S., Radiative Forcing of Climate Change. Climate
7260 Change: The Scientific Basis. Contribution of Working Group I to the Third Assessment
7261 Report of the Intergovernmental Panel on Climate Change [Houghton, J.T., Y. Ding, D.J.
7262 Griggs, M. Noguer, P.J. van der Linden, X. Dai, K. Maskell, and C.A. Johnson (eds.)].
7263 Cambridge University Press, Cambridge, United Kingdom and New York, NY, USA, 349-
7264 416, 881pp, 2001.

7265 [Ramaswamy, V.](#), and C-T Chen, 1997: Linear additivity of climate response for combined albedo
7266 and greenhouse perturbations. *Geophysical Research Letters*, **24**(5), 567-570.

7267 [Ramaswamy, V.](#), [M D Schwarzkopf](#), and W J Randel, 1996: Fingerprint of ozone depletion in the
7268 spatial and temporal pattern of recent lower-stratospheric cooling. *Nature*, **382**, 616-618.

7269 Ramaswamy, V., M. D. Schwarzkopf, and K. P. Shine, 1992: Radiative forcing of climate from
7270 halocarbon-induced global stratospheric ozone loss. *Nature*, **355**, 810-812,
7271 doi:10.1038/355810a0. <https://doi.org/10.1038/355810a0>.

7272 Ramaswamy, V., K. Shine, C. Leovy, W.-C. Wang, H. Rodhe, and D. Wuebbles, 1991:
7273 Radiative forcing of climate. *Scientific Assessment of Ozone Depletion: 1991*, D.L.
7274 Albritton, R.T. Watson, S. Solomon, R.F. Hampson, and F. Ormond, Eds.

7275 Ramaswamy, V., Boucher, O., Haigh, J., Hauglustaine, D., Haywood, J.M., Myhre, G.,
7276 Nakajima, T., Shi, G.Y., and Solomon, S., Radiative Forcing of Climate Change. Climate
7277 Change: The Scientific Basis. Contribution of Working Group I to the Third Assessment

7278 Report of the Intergovernmental Panel on Climate Change [Houghton, J.T., Y. Ding, D.J.
7279 Griggs, M. Noguer, P.J. van der Linden, X. Dai, K. Maskell, and C.A. Johnson (eds.)].
7280 Cambridge University Press, Cambridge, United Kingdom and New York, NY, USA, 349-
7281 416, 881pp, 2001.

7282 Ramaswamy, V., et al., (2006), Anthropogenic and natural influences in the evolution of lower
7283 stratospheric cooling. *Science*, 311, 1138–1141

7284 Ramaswamy, V., M. D. Schwarzkopf, and K. P. Shine, 1992: Radiative forcing of climate from
7285 halocarbon-induced global stratospheric ozone loss. *Nature*, 355, 810–812,
7286 doi:10.1038/355810a0. <https://doi.org/10.1038/355810a0>.

7287 ——, and Coauthors, 2001: Radiative Forcing of Climate Change. *Climate Change 2001: The*
7288 *Scientific Basis. Contribution of Working Group I to the Third Assessment Report of the*
7289 *Intergovernmental Panel on Climate Change*, Y. Ding, D.J. Griggs, M. Noguer, P.J. Van der
7290 Linden, X. Dai, K. Maskell, and C.A. Johnson, Eds., Cambridge University Press,
7291 Cambridge, United Kingdom and New York, NY, USA.

7292 Ramaswamy, V & Boucher, Olivier & Haigh, Joanna & Hauglustaine, D & Haywood, J &
7293 Myhre, Gunnar & Nakajima, T & Y Shi, G & Solomon, S. (2001). Radiative Forcing of
7294 Climate Change. In: *Climate Change 2001: The Scientific Basis. Contribution of Working*
7295 *Group I to the Third Assessment Report of the Intergovernmental Panel on Climate*
7296 *Change* [Houghton, J.T., Y. Ding, D.J. Griggs, M. Noguer, P.J. van der Linden, X. Dai, K.
7297 Maskell, and C.A. Johnson (eds.)]. Cambridge University Press, Cambridge, United
7298 Kingdom and New York, NY, USA, 881pp.

7299 Ramachandran, S., V. Ramaswamy, G.L. Stenchikov, and A. Robock (2000), Radiative impact of
7300 the Mt. Pinatubo volcanic eruption: Lower stratospheric response. *J. Geophys. Res.*,
7301 105(D19), 24409–24429.

7302 Randall, C. E., R. M. Bevilacqua, J. D. Lumpe, and K. W. Hoppel, (2001), Validation of POAM
7303 III aerosols: Comparison to SAGE II and HALOE. *J Geophys Res*, 106, 27,525-527,536.

7304 Randall, C. E., R. M. Bevilacqua, J. D. Lumpe, K. W. Hoppel, D. W. Rusch, and E. P. Shettle
7305 (2000), Comparison of polar ozone and aerosol measurement (POAM) II and Stratospheric

7306 Aerosol and Gas Experiment (SAGE) II aerosol measurements from 1994 to 1996. *J Geophys*
7307 *Res*, 105, 3929-3942.

7308 Randel, W., F. Wu, S. Oltmans, K. Rosenlof, G. Nedoluha (2004), Interannual Changes of
7309 Stratospheric Water vapor and Correlations with Tropical Tropopause Temperatures, *J.*
7310 *Atmos. Res.*, 61, 2133-2148.

7311 Rap, A., Forster, P.M., Haywood, J.M., Jones, A., and Boucher, O. (2010) Estimating the climate
7312 impact of linear contrails using the UK Met Office climate model. *Geophys. Res. Lett.*, 37,
7313 L20703.

7314 [Rasch, P.J.](#), [Simone Tilmes](#) , [Richard P Turco](#), [Alan Robock](#), [Luke Oman](#), [Chih-Chieh \(Jack\)](#)
7315 [Chen](#), [Georgiy L Stenchikov](#) and [Rolando R Garcia](#), 2008: An overview of geoengineering
7316 of climate using stratospheric sulphate aerosols, *Philosophical Transactions of the Royal*
7317 *Society –A- Mathematical, Physical and Engineering Sciences*
7318 <https://doi.org/10.1098/rsta.2008.0131>

7319

7320 Rayleigh, Lord (Strutt, Hon. J. W.), 1871: On the light from the sky, its polarization and
7321 colour. *The London, Edinburgh, and Dublin Philosophical Magazine and Journal of*
7322 *Science*. **41** (271): 107–120. [doi:10.1080/14786447108640452](https://doi.org/10.1080/14786447108640452).

7323 Rayleigh, Lord, 1881: On the electromagnetic theory of light. *The London, Edinburgh, and*
7324 *Dublin Philosophical Magazine and Journal of Science*. **12** (73): 81-
7325 101. [doi:10.1080/14786448108627074](https://doi.org/10.1080/14786448108627074).

7326 Richardson, T. B., and Coauthors, 2019: Efficacy of climate forcings in PDRMIP models.
7327 Submitted.

7328 Robock, A. (2000), Volcanic eruptions and climate, *Rev. Geophys.*, 38(2), 191–219,
7329 doi:10.1029/1998RG000054.

7330 Robock, A., Jerch, K. and Bunzl, M., 2008. 20 reasons why geoengineering may be a bad idea.
7331 *Bulletin of the Atomic Scientists*, 64(2), pp.14-59.

7332 Robock, A., Luke Oman, Georgiy L. Stenchikov, 2008: Regional climate responses to
7333 geoengineering with tropical and Arctic SO₂ injections; *Journal of Geophysical Research*
7334 *Atmospheres*. <https://doi.org/10.1029/2008JD010050>

7335

7336 Roe, G. H., N. Feldl, K. C. Armour, Y.-T. Hwang, and D. M. W. Frierson (2015), The remote
7337 impacts of climate feedbacks on regional climate predictability, *Nat. Geosci.*, 8, 135–139,
7338 doi:10.1038/ngeo2346.

7339 Rose, B. E. J., K. C. Armour, D. S. Battisti, N. Feldl, and D. D. B. Koll (2014), The dependence
7340 of transient climate sensitivity and radiative feedbacks on the spatial pattern of ocean heat
7341 uptake, *Geophys. Res. Lett.*, 41, 1071–1078, doi:10.1002/2013GL058955.

7342 Rotstayn, L. D. & Lohmann, U. Tropical rainfall trends and the indirect aerosol effect. *J. Clim.* **15**,
7343 2103–2116 (2002).

7344 Rotstayn, L. D., and J. E. Penner, 2001: Indirect Aerosol Forcing, Quasi Forcing, and Climate
7345 Response. *J. Clim.*, 14, 2960–2975, doi:10.1175/1520-
7346 0442(2001)014<2960:IAFQFA>2.0.CO;2. [https://doi.org/10.1175/1520-0442\(2001\)014%3C2960:IAFQFA%3E2.0.CO](https://doi.org/10.1175/1520-0442(2001)014%3C2960:IAFQFA%3E2.0.CO).

7348 Rotstayn, L., Indirect forcing by anthropogenic aerosols: A general circulation model calculation
7349 of the effective-radius and cloud lifetime effects, *J. Geophys. Res.*, 104, 9369–9380, 1999.

7350 Regener, V. H., 1938: Messung des Ozongehalts der Luft in Bodennähe. *Met. Zeitschr.*, **55**, 459–
7351 462.

7352 Renner, E. D., and G. E. Becker, 1970: Production of nitric oxide and nitrous oxide during
7353 denitrification by *Corynebacterium nephridii*. *J. Bacteriol.*, **101**, 821–826.
7354 <https://www.ncbi.nlm.nih.gov/pubmed/5438050>.

7355 Rigby, M., and Coauthors, 2017: Role of atmospheric oxidation in recent methane growth. *Proc.*
7356 *Natl. Acad. Sci. U. S. A.*, **114**, 5373–5377, doi:10.1073/pnas.1616426114.

7357 Robinson, E., and R. C. Robbins, 1970: Gaseous Atmospheric Pollutants from Urban and

7358 Natural Sources BT - Global Effects of Environmental Pollution: A Symposium Organized
7359 by the American Association for the Advancement of Science Held in Dallas, Texas,
7360 December 1968. S.F. Singer, Ed., Springer Netherlands, Dordrecht, 50–64
7361 https://doi.org/10.1007/978-94-010-3290-2_7.

7362 Roelofs, G.-J., J. Lelieveld, and R. Dorland, 1997: A three-dimensional chemistry/general
7363 circulation model simulation of anthropogenically derived ozone in the troposphere and its
7364 radiative climate forcing. *J. Geophys. Res. Atmos.*, **102**, 23389–23401,
7365 doi:doi:10.1029/97JD02210. <https://doi.org/10.1029/97JD02210>.

7366 Rohrer, F., and Coauthors, 2014: Maximum efficiency in the hydroxyl-radical-based self-
7367 cleansing of the troposphere. *Nat. Geosci.*, **7**, 559–563, doi:10.1038/ngeo2199.

7368 Royal Society, 2009: Geoengineering the climate. Science, governance, and uncertainty. Report
7369 10/09, Royal Society, London, UK, 82 pp.

7370 Ringeval, B., de Noblet-ducoudre, N., Ciais, P., Bousquet, P., Prigeent, C., Papa, F. and Rossow,
7371 W.: An attempt to quantify the impact of changes in wetland extent on methane emissions
7372 on the seasonal and interannual time scales, *Global Biogeochem. Cycles*, 24(GB2003),
7373 doi:10.1029/2008gb003354, 2010.

7374 Roger A. Pielke, S.: Land Use and Climate Change, *Science* (80-..), **310**, 1624–1625,
7375 doi:10.1126/science.1120529, 2005.

7376 Read, W. G., L. Froidevaux, and J. W. Waters (1993), Microwave limb sounder measurement of
7377 stratospheric SO₂ from the Mount Pinatubo volcano, *Geophys. Res. Lett.*, **20**, 1299–1302,
7378 doi:10.1029/93GL00831.

7379 Robock, A. (2000), Volcanic eruptions and climate, *Rev. Geophys.*, **38**(2), 191–219,
7380 doi:10.1029/1998RG000054.

7381 Robock, A., C. M. Ammann, L. Oman, D. Shindell, S. Levis, and G. Stenchikov (2009), Did the
7382 Toba volcanic eruption of 74 ka B.P. produce widespread glaciation? *Journal of Geophysical*
7383 *Research-Atmospheres*, **114**, D10107.

7384 Robock, A., M. Bunzl, B. Kravitz, and G. L. Stenchikov (2010), A Test for Geoengineering?
7385 *Science*, 327, 530-531.

7386 Russell, P. B., J. M. Livingston, E. G. Dutton, R. F. Pueschel, J. A. Reagan, T. E. DeFoor, M. A.
7387 Box, D. Allen, P. Pilewskie, B. M. Herman, S. A. Kinne and D. J. Hofmann (1993), Pinatubo
7388 and pre-Pinatubo optical-depth spectra: Mauna Loa measurements, comparisons, inferred
7389 particle size distributions, radiative effects, and relationship to lidar data, *J. Geophys. Res.*,
7390 98, 22969-22985.

7391 Richard, E., D. Harber, J. Rutkowski, K. O'Malia, M. Triplett, G. Drake, J. Harder, P. Pilewskie,
7392 S. Brown, A. Smith, and K. Lykke, 2011: Future Long-term Measurements of Solar
7393 Spectral Irradiance by the TSIS Spectral Irradiance Monitor: Improvements in Measurement
7394 Accuracy and Stability. *Proceedings 11th International Conference on New Developments*
7395 and Applications in Optical Radiometry

7396 Maui, HI, S. Park and E. Ikonen, Eds., paper INV004.

7397 Rind, D., J. Lean, and R. Healy, 1999: Simulated time-dependent climate response to solar
7398 radiative forcing since 1600, *J. Geophys. Res.*, 104(D2), 1973–1990,
7399 doi:10.1029/1998JD200020.

7400 Rind, D., J. Lean, J. Lerner, P. Lonergan, C. McLinden and A. Leboissitier, 2008: Exploring the
7401 Stratospheric/Tropospheric Response to Solar Forcing, *J. Geophys. Res.*, 113, D24103,
7402 doi:10.1029/2008JD010114.

7403 Roth, R., and F. Joos, 2013: A reconstruction of radiocarbon production and total solar irradiance
7404 from the Holocene ^{14}C and CO₂ records: implications of data and model uncertainties.
7405 *Clim. Past*, 9, 1879–1909, doi:10.5194/cp-9-1879-2013

7406 Rottman, G., 2006: Measurements of total and spectral solar irradiance, *Space Sci. Rev.*, 125, 39–
7407 51, DOI: 10.1007/s11214-006-9045-6.

7408 Rottman, G., Harder, J., and J. Fontenla, 2005: The Spectral Irradiance Monitor (SIM): Early
7409 Observations, *Solar Physics*, 230: 205. <https://doi.org/10.1007/s11207-005-1530-7>

7410

7411 Samset, B. H., and Coauthors, 2016: Fast and slow precipitation responses to individual climate
7412 forcers: A PDRMIP multimodel study. *Geophys. Res. Lett.*, 43,
7413 doi:10.1002/2016GL068064.

7414 Santer, B.D., et al., 1995: Towards the detection and attribution of an anthropogenic effect on
7415 climate. *Clim. Dyn.*, **12**, 77–100.

7416 Santer, B.D., et al., 1996: A search for human influences on the thermal structure of the
7417 atmosphere. *Nature*, **382**, 39–46.

7418 Santer, B.D., T.M.L. Wigley, T.P. Barnett, and E. Anyamba, 1996b: Detection of climate change,
7419 and attribution of causes. In: *Climate Change 1995: The Science of Climate
7420 Change* [Houghton, J.T., et al. (eds.)]. Cambridge University Press, Cambridge, United
7421 Kingdom and New York, NY, USA, pp. 407–443.

7422 Sausen, R., Isaksen, I., Grewe, V., Hauglustaine, D., Lee, D.S., Myhre, G., Kö hler, M.O., Pitari,
7423 G., Schumann, U., Stordal, F., Zerefos, C., 2005. Aviation radiative forcing in 2000: an
7424 update of IPCC (1999). *Meteorol. Zeit* **114**, 555–561.

7425 Schimel, D., and Coauthors, 1996: Radiative Forcing of Climate Change. *Climate Change 1995:
7426 The science of climate change*, J.T. Houghton, L.G. Meira Filho, B.A. Callandar, N. Harris,
7427 A. Kattenberg, and K. Maskell, Eds., Cambridge University Press, Cambridge, U.K., New
7428 York, NY, USA, Melbourne, Australia.

7429 Schimel, D. D., and Coauthors, 1996: Radiative forcing of climate change. (eds.). Contribution
7430 of Working Group I to the Second Assessment Report of the Intergovernmental Panel on
7431 Climate Change. Cambridge University Press, Cambridge, U.K. 572 pp. Climate Change
7432 1995—The Science of Climate Change, J.T. Houghton, L.G. Meira Filho, B.A. Callander,
7433 N. Harris, A. Kattenberg, and K. Maskell, Eds., Cambridge University Press, Cambridge,
7434 U.K., 65–131.

7435 Schimel, D., and Coauthors, 1996: Radiative Forcing of Climate Change. *Climate Change 1995:
7436 The science of climate change*, J.T. Houghton, L.G. Meira Filho, B.A. Callandar, N. Harris,
7437 A. Kattenberg, and K. Maskell, Eds., Cambridge University Press, Cambridge, U.K., New
7438 York, NY, USA, Melbourne, Australia.

7439 Schmidt, A et al., Satellite detection, long-range transport, & air quality impacts of volcanic
7440 sulfur dioxide from the 2014–2015 flood lava eruption at Bárðarbunga (Iceland). *JGR*,
7441 9739-9757, 2015.

7442 Schulz, M., Textor, C., Kinne, S., Balkanski, Y., Bauer, S., Berntsen, T., ... & Isaksen, I. S. A.
7443 (2006). Radiative forcing by aerosols as derived from the AeroCom present-day and pre-
7444 industrial simulations. *Atmospheric Chemistry and Physics*, 6(12), 5225-5246.

7445 Schwarz, J. P., J. R. Spackman, R. S. Gao, L. A. Watts, P. Stier, M. Schulz, S. M. Davis, S. C.
7446 Wofsy, and D. W. Fahey (2010), Global-scale black carbon profiles observed in the remote
7447 atmosphere and compared to models, *Geophys. Res. Lett.*, 37, L18812,
7448 doi:10.1029/2010GL044372.

7449 Stier, P., Feichter, J., Kinne, S., Kloster, S., Vignati, E., Wilson, J., Ganzeveld, L., Tegen, I.,
7450 Werner, M., Balkanski, Y., Schulz, M., Boucher, O., Minikin, A., and Petzold, A.: The
7451 aerosol climate model ECHAM5-HAM, *Atmos. Chem. Phys.*, 5, 1125–1156, 2005,
7452 <http://www.atmos-chem-phys.net/5/1125/2005/>.

7453 Shindell, D. T., Faluvegi, G., Rotstayn, L. & Milly, G. Spatial patterns of radiative forcing and
7454 surface temperature response. *J. Geophys. Res. Atmos.* **120**, 5385-5403 (2015).

7455 Shindell, D. T., Faluvegi, G., Rotstayn, L. & Milly, G. Spatial patterns of radiative forcing and
7456 surface temperature response. *J. Geophys. Res. Atmos.* **120**, 5385-5403 (2015).

7457 Schumann, U., Baumann, R., Baumgardner, D., Bedka, S. T., Duda, D. P., Freudenthaler, V.,
7458 Gayet, J.-F., Heymsfield, A. J., Minnis, P., Quante, M., Raschke, E., Schlager, H., Vázquez-
7459 Navarro, M., Voigt, C., and Wang, Z.: Properties of individual contrails: a compilation of
7460 observations and some comparisons, *Atmos. Chem. Phys.*, 17, 403-438,
7461 <https://doi.org/10.5194/acp-17-403-2017>, 2017.

7462 Schumann, U. and Mayer, B.: Sensitivity of surface temperature to radiative forcing by contrail
7463 cirrus in a radiative-mixing model, *Atmos. Chem. Phys.*, 17, 13833-13848,
7464 <https://doi.org/10.5194/acp-17-13833-2017>, 2017.

7465 Schneider, S. H., and R. E. Dickinson, 1974: Climate modeling. *Rev. Geophys.*, 12, 447–493,
7466 doi:10.1029/RG012i003p00447. <https://doi.org/10.1029/RG012i003p00447>.

7467 Scott, N.A., & Chedin, A. (1981) A Fast Line-by-Line Method for Atmospheric Absorption
7468 Computations: The Automatized Atmospheric Absorption Atlas. *Journal of Applied*
7469 *Meteorology*, 20(7), 802—812, [https://doi.org/10.1175/1520-0450\(1981\)020<0802:AFLBLM>2.0.CO;2](https://doi.org/10.1175/1520-0450(1981)020<0802:AFLBLM>2.0.CO;2).

7471 Von Schneidemesser, E., and Coauthors, 2015: Chemistry and the Linkages between Air Quality
7472 and Climate Change. *Chem. Rev.*, **115**, 3856–3897, doi:10.1021/acs.chemrev.5b00089.

7473 Schwarzkopf, M. D., and V. Ramaswamy, 1993: Radiative forcing due to ozone in the 1980s:
7474 Dependence on altitude of ozone change. *Geophys. Res. Lett.*, **20**, 205–208,
7475 doi:doi:10.1029/93GL00209. <https://doi.org/10.1029/93GL00209>.

7476 Singh, H. B., 1977: Atmospheric halocarbons: Evidence in favor of reduced average hydroxyl
7477 radical concentration in the troposphere. *Geophys. Res. Lett.*, **4**, 101–104,
7478 doi:doi:10.1029/GL004i003p00101. <https://doi.org/10.1029/GL004i003p00101>.

7479 Sitch, S., P. M. Cox, W. J. Collins, and C. Huntingford, 2007: Indirect radiative forcing of
7480 climate change through ozone effects on the land-carbon sink. *Nature*, **448**, 791-U4, doi:Doi
7481 10.1038/Nature06059.

7482 Seinfeld JH¹, Bretherton C², Carslaw KS³, Coe H⁴, DeMott PJ⁵, Dunlea EJ⁶, Feingold G⁷, Ghan
7483 S⁸, Guenther AB⁹, Kahn R¹⁰, Kraucunas I⁸, Kreidenweis SM⁵, Molina MJ¹¹, Nenes
7484 A¹², Penner JE¹³, Prather KA¹¹, Ramanathan V¹⁴, Ramaswamy V¹⁵, Rasch
7485 PJ⁸, Ravishankara AR⁵, Rosenfeld D¹⁶, Stephens G¹⁷, Wood R². 2016: Improving our
7486 fundamental understanding of the role of aerosol-cloud interactions in the climate system.
7487 Proc Natl Acad Sci, 113(21):5781-90. doi: 10.1073/pnas.1514043113.

7488 Senior, C. A., and J. F. B. Mitchell (2000), The time dependence of climate sensitivity, *Geophys.*
7489 *Res. Lett.*, 27, 2685–2688.

7490 Sherwood, S. C., Bony, S., Boucher, O., Bretherton, C., Forster, P. M., Gregory, J. M. and
7491 Stevens, B.: Adjustments in the Forcing-Feedback Framework for Understanding Climate
7492 Change, *Bulletin of the American Meteorological Society*, 96(2), 217-228, 2015.

7493 Shindell, D. T.: Inhomogeneous forcing and transient climate sensitivity, *Nature Climate
7494 Change*, 4(4), 274-277, 2014.

7495 Shindell, D., and Coauthors, 2013: Attribution of historical ozone forcing to anthropogenic
7496 emissions. *Nat. Clim. Chang.*, 3, 567. <https://doi.org/10.1038/nclimate1835>.

7497 Shindell, D. T., G. Faluvegi, N. Bell, and G. A. Schmidt, 2005: An emissions-based view of
7498 climate forcing by methane and tropospheric ozone. *Geophys. Res. Lett.*, 32, L04803,
7499 doi:10.1029/2004gl021900. <http://dx.doi.org/10.1029/2004GL021900>.

7500 Shindell, D. T., G. Faluvegi, N. Unger, E. Aguilar, G. A. Schmidt, D. M. Koch, S. E. Bauer, and
7501 R. L. Miller, 2006: Simulations of preindustrial, present-day, and 2100 conditions in the
7502 NASA GISS composition and climate model G-PUCCINI. *Atmos. Chem. Phys.*, 6, 4427–
7503 4459, doi:10.5194/acp-6-4427-2006. <http://www.atmos-chem-phys.net/6/4427/2006/>.

7504 Shindell, D. T., G. Faluvegi, D. M. Koch, G. A. Schmidt, N. Unger, and S. E. Bauer, 2009:
7505 Improved Attribution of Climate Forcing to Emissions. *Science (80-.)*, 326, 716–718,
7506 doi:10.1126/science.1174760. <http://www.sciencemag.org/content/326/5953/716.abstract>.

7507 Shindell, D., Kylenstierna, J., Vignati, E., van Dingenen, R., Amann, M., Klimont, Z.,
7508 Anenberg, S., Muller, N., Janssens-Maenhout, G., Raes, F., Schwartz, J., Faluvegi, G.,
7509 Pozzoli, L., Kupiainen, K., Hoglund-Isaksson, L., Emberson, L., Streets, D., Ramanathan,
7510 V., Hicks, K., Oanh, N., Milly, G., Williams, M., Demkine, V. and Fowler, D.:
7511 Simultaneously mitigating near-term climate change and improving human health and food
7512 security, *Science (80-.)*, 335, 185–189, 2012.

7513 Shindell, D. T., Lamarque, J.-F., Schulz, M., Flanner, M., Jiao, C., Chin, M., Young, P. J., Lee,
7514 Y. H., Rotstayn, L., Mahowald, N., Milly, G., Faluvegi, G., Balkanski, Y., Collins, W. J.,
7515 Conley, A. J., Dalsoren, S., Easter, R., Ghan, S., Horowitz, L., Liu, X., Myhre, G.,
7516 Nagashima, T., Naik, V., Rumbold, S. T., Skeie, R., Sudo, K., Szopa, S., Takemura, T.,
7517 Voulgarakis, A., Yoon, J.-H. and Lo, F.: Radiative forcing in the ACCMIP historical and

7518 future climate simulations, *Atmos. Chem. Phys.*, 13(6), doi:10.5194/acp-13-2939-2013,
7519 2013.

7520 Shindell, D. T., Borgford-Parnell, N., Brauer, M., Haines, A., Kuylenstierna, J., Leonard, S. A.,
7521 Ramanthan, V., Ravishankara, A. R., Amman, M. and Srivastava, L.: A climate policy
7522 pathway for near- and long-term benefits, *Science* (80-.), 356(6337), 493–494, 2017.

7523 Shine, K. P., Y. Fouquart, V. Ramaswamy, S. Solomon, and J. Srinivasan., 1995: Radiative
7524 forcing. *Climate Change 1994. Radiative Forcing of Climate Change and an Evaluation of*
7525 the IPCC IS92 Emission Scenarios, J.T. Houghton, L.G.M. Filho, J. Bruce, H. Lee, B.A.
7526 Callander, E. Haites, N. Harris, and K. Maskell, Eds., Cambridge University Press,
7527 Cambridge, U.K., 163–203.

7528 Shine, K. P., Derwent, R. G., Wuebbles, D. J., & J-J. Morcrette. (1990). Radiative Forcing of
7529 Climate. In J. T. Houghton, G. J. Jenkins, & J. J. Ephraums (Eds.), *Climate Change: The*
7530 *IPCC Scientific Assessment (1990)* (p. 410). Cambridge, Great Britain, New York, NY,
7531 USA and Melbourne, Australia: Cambridge University Press.

7532 Shine, K. P., Cook, J., Highwood, E. J. and Joshi, M. M.: An alternative to radiative forcing for
7533 estimating the relative importance of climate change mechanisms, *Geophysical Research*
7534 *Letters*, 30(20), 2047, 2003.

7535 Shine, K. P., R. G. Derwent, D. J. Wuebbles, and J.-J. Morcrette, 1990: Radiative forcing of
7536 Climate. *Radiative forcing of Climate*, J.T. Houghton, G.J. Jenkins, and J.J. Ephraums,
7537 Eds., 41–68.

7538 ——, Y. Fouquart, V. Ramaswamy, S. Solomon, and J. Srinivasan., 1995: Radiative forcing.
7539 *Climate Change 1994—Radiative Forcing of Climate Change and an Evaluation of the*
7540 the IPCC IS92 Emission Scenarios, J.T. Houghton, L.G.M. Filho, J. Bruce, H. Lee, B.A.
7541 Callander, E. Haites, N. Harris, and K. Maskell, Eds., Cambridge University Press,
7542 Cambridge, U.K., 163–203.

7543 Shine, K. P., Derwent, R. G., Wuebbles, D. J., & J-J. Morcrette. (1990). Radiative Forcing of
7544 Climate. In J. T. Houghton, G. J. Jenkins, & J. J. Ephraums (Eds.), *Climate Change: The*
7545 *IPCC Scientific Assessment (1990)* (p. 410). Cambridge, Great Britain, New York, NY,

7546 USA and Melbourne, Australia: Cambridge University Press.

7547 Shine, K. P., R. G. Derwent, D. J. Wuebbles, and J.-J. Morcrette, 1990: Radiative Forcing of
7548 Climate. *Climate Change: The IPCC Scientific Assessment (1990)*, J.T. Houghton, G.J.
7549 Jenkins, and J.J. Ephraums, Eds., Cambridge University Press, Cambridge, U.K. and New
7550 York, NY, USA.

7551 Shine, K. P., and Coauthors, 1995a: Radiative forcing due to changes in ozone: a comparison of
7552 different codes BT - Atmospheric Ozone as a Climate Gas. W.-C. Wang and I.S.A. Isaksen,
7553 Eds., Berlin, Heidelberg, Springer Berlin Heidelberg, 373–396.

7554 Shine, K. P., Y. Fouquart, V. Ramaswamy, S. Solomon, and J. Srinivasan, 1995b: Radiative
7555 Forcing. *Climate Change 1994: Radiative Forcing of Climate Change and An Evalaution of*
7556 *the IPCC IS92 Emision Scenarios*, J.T. Houghton, L.G. Meira Filho, J. Bruce, L. Hoesung,
7557 B.A. Callandar, E. Haites, N. Harris, and K. Maskell, Eds., Cambridge, U.K., New York,
7558 NY, USA, Melbourne, Australia.

7559 Shine, K. P., K. Labitzke, V. Ramaswamy, P. C. Simon, S. Solomon, and W.-C. Wang, 1995c:
7560 Radiative forcing and temperature trends. *Scientific Assessment of Ozone Depletion: 1994*,
7561 D.L. Albritton, R.T. Watson, and P.J. Aucamp, Eds., World Meteorological Organization
7562 (WMO), Geneva, Switzerland.

7563 Shine, K. P., Derwent, R. G., Wuebbles, D. J., & J-J. Morcrette. (1990). Radiative Forcing of
7564 Climate. In J. T. Houghton, G. J. Jenkins, & J. J. Ephraums (Eds.), Climate Change: The
7565 IPCC Scientific Assessment (1990) (p. 410). Cambridge, Great Britain, New York, NY,
7566 USA and Melbourne, Australia: Cambridge University Press.

7567 Shine, K. P.: 1991, 'On the cause of the relative greenhouse strength of gases such as the
7568 halocarbons', *Journal of the Atmospheric Science* 48, 1513–1518.

7569 Shine, K. P., and P. M. d. F. Forster, 1999: The effect of human activity on radiative forcing of
7570 climate change: a review of recent developments. *Glob. Planet. Change*, **20**, 205–225,
7571 doi:[https://doi.org/10.1016/S0921-8181\(99\)00017-X](https://doi.org/10.1016/S0921-8181(99)00017-X).
7572 <http://www.sciencedirect.com/science/article/pii/S092181819900017X>.

7573 Smith, C. J., and Coauthors, 2018: Understanding Rapid Adjustments to Diverse Forcing Agents.
7574 *Geophys. Res. Lett.*, 45, 12,12-23,31, doi:10.1029/2018GL079826.
7575 <https://doi.org/10.1029/2018GL079826>.

7576 Smith, H. J. P., Dube, D. J., Gardner, M. E., Clough, S. A., Kneizys, F. X., & L.S. Rothman.
7577 (1978). *FASCODE -- Fast Atmosphere Signature Code (Spectral Transmittance and*
7578 *Radiance)*. Hanscom AFB, MA.

7579 Smith, C. J., Kramer, R. J., Myhre, G., Forster, P., Soden, B., Andrews, T., Boucher, O.,
7580 Faluvegi, G., Fläschner, D., Hodnebrog, Ø., Kasoar, M., Kharin, V., Kirkevåg, A.,
7581 Lamarque, J. F., Mülmenstädt, J., Olivié, D., Richardson, T., Samset, B. H., Shindell, D.,
7582 Stier, P., Takemura, T., Voulgarakis, A. and Watson-Parris, D.: Understanding rapid
7583 adjustments to diverse forcing agents, *Geophysical Research Letters*, 45, 12023-
7584 12031, <https://doi.org/10.1029/2018GL079826>, 2018.

7585 Snow, M., Eparvier, F., Harder, J., Jones, A., McClintock, W., Richard, E., and T. Woods, 2018:
7586 Ultraviolet Solar Spectral Irradiance Variation on Solar Cycle Timescales. *Proceedings of*
7587 *the International Astronomical Union*, 13(S340), 203-208.
7588 doi:10.1017/S1743921318001278

7589 Steinhilber, F, Abreu, J. A., Beer, J., Brunner, I., Christl, M., Fischer, H., Heikkila, U., Kubik, P.
7590 W., Mann, M., McCracken, K. G., Miller, H., Miyahara, H., Oerter, H., and Wilhelms, F.,
7591 2012: 9,400 years of cosmic radiation and solar activity from ice cores and tree rings.
7592 *Proceedings of the National Academy of Sciences*, 109, i16, 5967-5971 DOI
7593 10.1073/pnas.1118965109

7594 Stevens, M. J., and G. R. North, 1996: Detection of the climate response to the solar cycle, *J.*
7595 *Atmos. Sci.*, 53, 2594-2608.

7596 Slingo, A., 1990: Sensitivity of the Earth's radiation budget to changes in low clouds.
7597 *Nature*, 343, 49. <https://doi.org/10.1038/343049a0>.

7598 Stenchikov, G., T. L. Delworth, V. Ramaswamy, R. J. Stouffer, A. Wittenberg, and F. Zeng,
7599 2009: Volcanic signals in oceans. *J. Geophys. Res. Atmos.*, doi:10.1029/2008JD011673.

7600 Storelvmo, T., J. E. Kristjansson, H. Muri, M. Pfeffer, D. Barahona, and A. Nenes, 2013: Cirrus
7601 cloud seeding has potential to cool climate. *Geophys. Res. Lett.*,
7602 doi:10.1029/2012GL054201.

7603 Soden, B. J., Held, I. M., Colman, R., Shell, K. M., Kiehl, J. T. and Shields, C. A.: Quantifying
7604 Climate Feedbacks Using Radiative Kernels, *Journal of Climate*, 21(14), 3504-3520, 2008.

7605 Soden, B. J., Collins, W. D., & Feldman, D. R. (2018). Reducing uncertainties in climate models.
7606 *Science*, 361(6400), 326–327. <http://doi.org/10.1126/science.aau1864>

7607 Soden, B. J., W. D. Collins, and D. R. Feldman, 2018: Reducing uncertainties in climate models.
7608 *Science*, 361, 326–327, doi:10.1126/science.aau1864.

7609 Soden, B. J., Collins, W. D. and Feldman, D. R.: Reducing uncertainties in climate models,
7610 *Science*, 361(6400), 326-327, 2018.

7611 Solomon, S., 1999: Stratospheric ozone depletion: A review of concepts and history. *Rev.*
7612 *Geophys.*, **37**, 275–316.

7613 Stephens, G. L., 2005: Cloud Feedbacks in the Climate System: A Critical Review. *J. Clim.*, 18,
7614 237–273, doi:10.1175/JCLI-3243.1. <https://doi.org/10.1175/JCLI-3243.1>.

7615 Stevenson, D. S., C. E. Johnson, W. J. Collins, R. G. Derwent, K. P. Shine, and J. M. Edwards,
7616 1998: Evolution of tropospheric ozone radiative forcing. *Geophys. Res. Lett.*, **25**, 3819–
7617 3822, doi:doi:10.1029/1998GL900037. <https://doi.org/10.1029/1998GL900037>.

7618 —, and Coauthors, 2013: Tropospheric ozone changes, radiative forcing and attribution to
7619 emissions in the Atmospheric Chemistry and Climate Model Intercomparison Project
7620 (ACCMIP). *Atmos. Chem. Phys.*, **13**, 3063–3085, doi:10.5194/acp-13-3063-2013.
7621 <http://www.atmos-chem-phys.net/13/3063/2013/>.

7622 Stolarski, R., V. Fioletov, L. Bishop, S. Godin, R. D. Bojkov, V. Kirchhoff, M.-L. Chanin, and J.
7623 Zawodny, 1991: Ozone and temperature trends. *Scientific Assessment of Ozone Depletion:*
7624 *1991*, D.L. Albritton, R.T. Watson, S. Solomon, R.F. Hampson, and F. Ormond, Eds.

7625 Stone, D., L. K. Whalley, and D. E. Heard, 2012: Tropospheric OH and HO₂ radicals: field

7626 measurements and model comparisons. *Chem. Soc. Rev.*, **41**, 6348–6404,
7627 doi:10.1039/c2cs35140d.

7628 Stordal, F., R. G. Derwent, I. S. A. Isaksen, D. J. Jacob, M. Kanakidou, J. A. Logan, and M. J.
7629 Prather, 1995: Model Simulations of global tropospheric ozone. *Scientific Assessment of*
7630 *Ozone Depletion: 1994*, D.L. Albritton, R.T. Watson, and P.J. Aucamp, Eds., World
7631 Meteorological Organization (WMO), Geneva, Switzerland.

7632 Stouffer, R. J., S. Manabe, and K. Bryan, 1989): Interhemispheric asymmetry in climate
7633 response to a gradual increase of atmospheric CO₂. *Nature*, **342**, 660-662.

7634 Stephens, G. L., 2005: Cloud feedbacks in the climate system: A critical review. *J. Climate*, **18**,
7635 237–273, doi:10.1175/JCLI-3243.1

7636 Sterner EO and DJA Johansson (2017). The effect of climate–carbon cycle feedbacks on emission
7637 metrics *Environ. Res. Lett.* **12** 034019 10.1088/1748-9326/aa61dc

7638 Stott, P.A., et al., 2000: External control of 20th century temperature by natural and anthropogenic
7639 forcings. *Science*, **290**, 2133–2137.

7640 Stott, P. A., Stone, D. A. & Allen, M. R. Human contribution to the European heatwave of
7641 2003. *Nature* **432**, 610–614 (2004).

7642 Stouffer, R.J., S. Manabe, and K.Y. Vinnikov, 1994: Model assessment of the role of natural
7643 variability in recent global warming. *Nature*, **367**, 634–636.

7644 <http://science.sciencemag.org/content/195/4279/673.abstract>.

7645 Sitch, S., Friedlingstein, P., Gruber, N., Jones, S., Murray-Tortarolo, G., Ahlstrom, A., Doney,
7646 S., Graven, H., Heinze, C., Huntingford, C., Levis, S., Levy, P., Lomas, M., Poulter, B.,
7647 Viovy, N., Zaehle, S., Zeng, N., Piao, S., LeQuere, C., Smith, B., Zhu, Z. and Myneni, R.:
7648 Recent trends and drivers of regional sources and sinks of carbon dioxide, *Biogeosciences*,
7649 **12**, 653–2015, 2015.

7650 Santer, B. D., and Coauthors (2014), Volcanic contribution to decadal changes in tropospheric
7651 temperature. *Nature Geoscience*, **7**, 185-189.

7652 Sato, M., J. E. Hansen, M. P. McCormick, and J. B. Pollack (1993), Stratospheric aerosol optical
7653 depths, 1850–1990, *J. Geophys. Res.*, 98(D12), 22,987–22,994, doi:10.1029/93JD02553.

7654 Schmidt, G., et al. (2011), Climate forcing reconstructions for use in PMIP simulations of the last
7655 millennium (v1.0). *Geosci. Model Dev.*, 4, 33–45.

7656 Schneider, D. P., C. M. Ammann, B. L. Otto-Bliesner, and D. S. Kaufman (2009), Climate
7657 response to large, high-latitude and low-latitude volcanic eruptions in the Community
7658 Climate System Model. *J. Geophys. Res. Atmos.*, 114, D15101.

7659 Scope, J. P. (1862), Volcanoes: The character of their phenomena, their share in the structure and
7660 composition of the surface of the globe and their relation to its internal forces, 2nd ed.,
7661 London: Longman, Green, Longmans, and Roberts.

7662 Sekiya, T., K. Sudo, and T. Nagai (2016), Evolution of stratospheric sulfate aerosol from the 1991
7663 Pinatubo eruption: Roles of aerosol microphysical processes, *J. Geophys. Res. Atmos.*, 121,
7664 doi:10.1002/2015JD024313.

7665 Sheng, J.-X., D. K. Weisentstein, B.-P. Luo, E. Rozanov, A. Stenke, J. Anet, H. Bingemer, and T.
7666 Peter (2015), Global atmospheric sulfur budget under volcanically quiescent conditions:
7667 Aerosol-chemistry-climate model predictions and validation, *J. Geophys. Res. Atmos.*, 120,
7668 256–276, doi:10.1002/2014JD021985.

7669 Shindell, D.T., G.A. Schmidt, R.L. Miller, and M. Mann (2003), Volcanic and solar forcing of
7670 climate change during the preindustrial era. *J. Clim.*, 16, 4094–4107.

7671 Shindell, D.T., G.A. Schmidt, M. Mann, and G. Faluvegi (2004), Dynamic winter climate response
7672 to large tropical volcanic eruptions since 1600. *J. Geophys. Res.*, 109, D05104,
7673 doi:10.1029/2003JD004151.

7674 Simkin, T., L. Siebert, L. McClelland, D. Bridge, C. G. Newhall, J. H. Latter (1981), *Volcanoes
7675 of the World*, New York, Hutchinson Ross.

7676 Simkin, T. (1993), Terrestrial volcanism in space and time, *Annu. Rev. Earth. Planet. Sci.*, 21,
7677 427–452.

7678 Soden, B. J., R. T. Wetherald, G. L. Stenchikov, and A. Robock (2002), Global cooling following
7679 the eruption of Mt. Pinatubo: A test of climate feedback of water vapor. *Science*, 296, 727-
7680 730.

7681 Solomon, S., J. S. Daniel, R. R. Neely, J. P. Vernier, E. G. Dutton, and L. W. Thomason (2011),
7682 The Persistently Variable "Background" Stratospheric Aerosol Layer and Global Climate
7683 Change. *Science*, 333, 866-870.

7684 Stenchikov, G., R. Dickerson, K. Pickering, W. Ellis, B. Doddridge, S. Kondragunta, O. Poulida,
7685 J. Scala, W.-K. Tao (1996), Stratosphere-Troposphere Exchange in a Mid-Latitude Mesoscale
7686 Convective Complex: Part 2, Numerical Simulations, *J. Geophys. Res.*, **101**, 6837-6851.

7687 Stenchikov, G.L., et al. (1998), Radiative forcing from the 1991 Mount Pinatubo volcanic eruption.
7688 *J. Geophys. Res.*, 103(D12), 13837–13857.

7689 Stenchikov, G.L., et al. (2002), Arctic Oscillation response to the 1991 Mount Pinatubo eruption:
7690 effects of volcanic aerosols and ozone depletion. *J. Geophys. Res.*, 107(D24), 4803,
7691 doi:10.1029/2002JD002090.

7692 Stenchikov, G., et al. (2004), Arctic Oscillation response to the 1991 Pinatubo eruption in the
7693 SKYHI GCM with a realistic quasi-biennial oscillation. *J. Geophys. Res.*, 109, D03112,
7694 doi:10.1029/2003JD003699.

7695 Stenchikov, G., et al. (2006), Arctic Oscillation response to volcanic eruptions in the IPCC AR4
7696 climate models. *J. Geophys. Res.*, 111, D07107, doi:10.1029/2005JD006286.

7697 Stenchikov, G., T. L. Delworth, V. Ramaswamy, R. J. Stouffer, A. Wittenberg, and F. Zeng (2009),
7698 Volcanic signals in oceans, *J. Geophys. Res.*, D16104, 114, doi:10.1029/2008JD011673.

7699 Stenchikov, G. (2016), The role of volcanic activity in climate and global change, In the book
7700 Climate Change, Observed Impact on Planet Earth, 2nd Edition, Trevor Letcher, Ed., ISBN:
7701 978-0-444-63524-2, pp. 419-448.

7702 Stothers, R. (1996), Major optical depth perturbations to the stratosphere from volcanic eruptions:
7703 Pyrheliometric period, 1881-1960, *J. Geophys. Res.*, 101, No. D2, 3901-3920.

7704 Stothers, R. (1997), Stratospheric aerosol clouds due to very large volcanic eruptions of the early
7705 twentieth century: Effective particle size and conversion from pyrheliometric to visual optical
7706 depth, *J. Geophys. Res.*, 102, No. D5, 6143-6151.

7707 Stothers, R., 2001a: Major optical depth perturbations to the stratosphere from volcanic eruptions:
7708 Stellar extinction period, 1961-1978. *J. Geophys. Res.*, 106(D3), 2993–3003.

7709 Stothers, R., 2001b: A chronology of annual mean radii of stratospheric aerosol from volcanic
7710 eruptions during the twentieth century as derived from ground-based spectral extinction
7711 measurements. *J. Geophys. Res.*, 106(D23), 32043–32049.

7712

7713 Tarasick, D, Galbally, I, Cooper, OR, Ancellet, G, Leblanc, T, Wallington, TJ, Ziemke, J,
7714 Liu, X, Steinbacher, M, Stähelin, J, Vigouroux, C, Hannigan, J, García, O, Foret, G,
7715 Zanis, P, Weatherhead, E, Petropavlovskikh, I, Worden, H, Osman, M, Liu, J, Lin, M,
7716 Schultz, M, Granados-Muñoz, M, Thompson, AM, Oltmans, SJ, Cuesta, J, Dufour, G,
7717 Thouret, V, Hassler, B and Trickl, T., 2018. Tropospheric Ozone Assessment Report
7718 (TOAR): Tropospheric ozone observations—How well do we know tropospheric ozone
7719 changes? *Elem. Sci. Anth.* . in-review, 2019.

7720 Taylor, K. E., and J. E. Penner, 1994: Response of the climate system to atmospheric aerosols
7721 and greenhouse gases. *Nature*, 369, 734–737, doi:10.1038/369734a0.
7722 <https://doi.org/10.1038/369734a0>.

7723 Tebaldi, C., and R. Knutti, 2007: The use of the multi-model ensemble in probabilistic climate
7724 projections. *Philos. Trans. R. Soc. A Math. Phys. Eng. Sci.*, **365**, 2053–2075,
7725 doi:10.1098/rsta.2007.2076. <https://doi.org/10.1098/rsta.2007.2076>.

7726 Tegen, I., Lacis, A. A., & Fung, I. (1996). The influence on climate forcing of mineral aerosols
7727 from disturbed soils. *Nature*, 380(6573), 419.

7728 Telegadas, K., and J. London, 1954: A physical model of Northern Hemisphere troposphere
7729 for winter and summer. Scientific Report No. 1, Contract AF19 (122)-165; Research
7730 Div. College of Engineering, New York University, 55. pp.

7731 Tett, S.F.B., et al. (2002), Estimation of natural and anthropogenic contributions to twentieth
7732 century temperature change. *J. Geophys. Res.*, 107(D16), 4306, doi:10.1029/2000JD000028.

7733 Textor, C., Schulz, M., Guibert, S., Kinne, S., Balkanski, Y., Bauer, S., ... & Dentener, F. (2007).
7734 The effect of harmonized emissions on aerosol properties in global models—an AeroCom
7735 experiment. *Atmospheric Chemistry and Physics*, 7(17), 4489-4501.

7736 The royal society, 2009: *Royal Society Geoengineering the climate: science, governance and*
7737 *uncertainty*.

7738 Thompson, A. M., and R. J. Cicerone, 1986: Possible perturbations to atmospheric CO, CH₄,
7739 and OH. *J. Geophys. Res. Atmos.*, **91**, 10853–10864, doi:doi:10.1029/JD091iD10p10853.
7740 <https://doi.org/10.1029/JD091iD10p10853>.

7741 ——, R. W. Stewart, M. A. Owens, and J. A. Herwehe, 1989: Sensitivity of tropospheric
7742 oxidants to global chemical and climate change. *Atmos. Environ.*, **23**, 519–532,
7743 doi:[https://doi.org/10.1016/0004-6981\(89\)90001-2](https://doi.org/10.1016/0004-6981(89)90001-2).
7744 <http://www.sciencedirect.com/science/article/pii/0004698189900012>.

7745 Thornton, P. E., Doney, S. C., Lindsay, K., Moore, J. K. K., Mahowald, N., Randerson, J. T.,
7746 Fung, I., Lamarque, J.-F. F., Feddema, J. J., Lee, Y.-H. Y.-H., Peter E. Thornton K.
7747 Lindsay, J. K. Moore, N. Mahowald, J. T. Randerson, I. Fung, J.-F. Lamarque, J. Feddema,
7748 Y.-H. Lee, S. D., Thornton, P. E., Doney, S. C., Lindsay, K., Moore, J. K. K., Mahowald,
7749 N., Randerson, J. T., Fung, I., Lamarque, J.-F. F., Feddema, J. J. and Lee, Y.-H. Y.-H.:
7750 Carbon-nitrogen interactions regular climate-carbon cycle feedbacks: results from an
7751 atmosphere-ocean general circulation model, *Biogeosciences*, 6(10), 2009–2099, 2009.

7752 Tian, D., Dong, W., Gong, D., Guo, Y. & Yang, 2016: S. Fast responses of climate system to
7753 carbon dioxide, aerosols and sulfate aerosols without the mediation of SST in the CMIP5. *Int.*
7754 *J. Climatol.* **37**, 1156–1166.

7755 Toll, V., Christensen, M., Gassó, S., & Bellouin, N. (2017). Volcano and Ship Tracks Indicate
7756 Excessive Aerosol-Induced Cloud Water Increases in a Climate Model. *Geophysical*
7757 *research letters*, 44(24).

7758 Turner, A. J., C. Frankenberg, P. O. Wennberg, and D. J. Jacob, 2017: Ambiguity in the causes
7759 for decadal trends in atmospheric methane and hydroxyl. *Proc. Natl. Acad. Sci.*,
7760 <http://www.pnas.org/content/early/2017/04/18/1616020114.abstract>.

7761 —, —, and E. A. Kort, 2019: Interpreting contemporary trends in atmospheric methane.
7762 *Proc. Natl. Acad. Sci.*, **116**, 2805 LP-2813, doi:10.1073/pnas.1814297116.
7763 <http://www.pnas.org/content/116/8/2805.abstract>.

7764 Twomey, S. A.: The Nuclei of Natural Cloud Formation. Part II: The Supersaturation in Natural
7765 Clouds and the Variation of Cloud Droplet Concentrations, *Geofis. Pure Appl.*, **43**, 227–
7766 242, 1959.

7767 Twomey, S. A.: The influence of pollution on the shortwave albedo of clouds, *J. Atmos. Sci.*, **34**,
7768 1149–1152, 1977.

7769 Twomey, S. The influence of pollution on the shortwave albedo of clouds. *J. Atmos. Sci.* **34**, 1149–
7770 1152 (1977).

7771 Tyndall, J., 1861: On the Absorption and Radiation of Heat by Gases and Vapours, and on
7772 the Physical Connexion of Radiation, Absorption, and Conduction", *Philosophical
7773 Transactions of the Royal Society of London*, Volume 151, pages 1–36.

7774 Thomason, L. W., and G. Taha (2003), SAGE III aerosol extinction measurements: Initial results.
7775 *Geophys Res Lett*, **30**, 1631.

7776 Thomason, L., and Th. Peter (Eds.) (2006), Assessment of Stratospheric Aerosol Properties
7777 (ASAP), WCRP-124, WMO/TD- No. 1295, SPARC Report No. 4, February 2006.

7778 Thomason, L. W., Ernest, N., Millán, L., Rieger, L., Bourassa, A., Vernier, J.-P. et al. (2018), A
7779 global space-based stratospheric aerosol climatology: 1979–2016, *Earth Syst. Sci. Data*, **10**,
7780 469-492, <https://doi.org/10.5194/essd-10-469-2018>.

7781 Tilmes, S., R. R. Garcia, D. E. Kinnison, A. Gettelman, and P. J. Rasch (2009), Impact of
7782 geoengineered aerosols on the troposphere and stratosphere. *Journal of Geophysical
7783 Research-Atmospheres*, **114**, D12305.

7784 Tilmes, S., and Coauthors, 2013: The hydrological impact of geoengineering in the
7785 Geoengineering Model Intercomparison Project (GeoMIP). *Journal of Geophysical*
7786 *Research-Atmospheres*, 118, 11036-11058.

7787 Timmreck, C., H.-F. Graf, and I. Kirchner (1999), A one and half year interactive MA/ECHAM4
7788 simulation of Mount Pinatubo Aerosol. *Journal of Geophysical Research-Atmospheres*, 104,
7789 9337-9359.

7790 Timmreck, C., H.-F. Graf, S. J. Lorenz, U. Niemeier, D. Zanchettin, D. Matei, J. H. Jungclaus, and
7791 T. J. Crowley (2010), Aerosol size confines climate response to volcanic super eruptions,
7792 *Geophys. Res. Lett.*, 37, L24705, doi:10.1029/2010GL045464.

7793 Timmreck, C. (2012), Modeling the climatic effects of large explosive volcanic eruptions. *Wiley*
7794 *Interdisciplinary Reviews-Climate Change*, 3, 545-564.

7795 Toohey, M., K. Krüger, M. Bittner, C. Timmreck, and Schmidt, H. (2014), The Impact of Volcanic
7796 Aerosol on the Northern Hemisphere Stratospheric Polar Vortex: Mechanisms and Sensitivity
7797 to Forcing Structure, *Atmos. Chem. Phys.*, 14(23), 13063 – 13079, doi:10.5194/acp-14-
7798 13063-2014.

7799 Toon, O. B., and J. B. Pollack (1976), A global average model of atmospheric aerosols for radiative
7800 transfer calculations, *J. Appl. Meteorol.*, 15, 225-246.

7801 Trenberth, K., and A. Dai, 2007: Effect of Mount Pinatubo volcanic eruption on the hydrological
7802 cycle as analaog of geoengineering. *Geophys Res Lett*, **34**, L15702.

7803 Trepte, C. R., M. H. Hitchman (1992), Tropical stratospheric circulation deduced from satellite
7804 aerosol data, *Nature*, 355, 626-628.

7805 Turco, R. P., R. C. Witten and O. B. Toon (1982), Stratospheric Aerosols: Observation and Theory,
7806 *Reviewes of Geophysics and Space Physics*, 20, No. 2, 233-279.

7807

7808 Unger, N., T. C. Bond, J. S. Wang, D. M. Koch, S. Menon, D. T. Shindell, and S. Bauer, 2010:
7809 Attribution of climate forcing to economic sectors. *Proc. Natl. Acad. Sci.*, 107 (8) 3382-
7810 3387. <https://doi.org/10.1073/pnas.0906548107>

7811 Unger, N.: Human land-use driven reduction of forest volatiles cools global climate, *Nat. Clim.
7812 Chang.*, doi:10.1038/nclimate2347, 2014.

7813 Unger, N., Bond, T., Wang, J. S., Koch, D. M., Menon, S., Shindell, D. and Bauer, S.:
7814 Attribution of climate forcing to economic sectors, *Proc. Natl. Acad. Sci. USA*, 107(8),
7815 3382–3387, 2010.

7816 Unruh, Y.C., S. K. Solanki, and M. Fligge, 2000: Modelling solar irradiance variations:
7817 Comparison with observations, including line-ratio variations. *Space Sci. Rev.*, 94, 1-2,
7818 145-152, doi:10.1023/A:1026758904332.

7819

7820 van Dorland, R., Dentener, F. J., & Lelieveld, J. (1997). Radiative forcing due to tropospheric
7821 ozone and sulfate aerosols. *Journal of Geophysical Research: Atmospheres*, 102(D23),
7822 28079-28100.

7823 Van de Hulst, H. C., 1957: Light scattering by small particles. By H. C. **van de Hulst**. New York
7824 (John Wiley and Sons), London (Chapman and Hall). 470pp

7825 von Savigny, C., Ernst, F., Rozanov, A., Hommel, R., Eichmann, K.-U., Rozanov, V., Burrows, J.
7826 P., and Thomason, L. W. (2015), Improved stratospheric aerosol extinction profiles from
7827 SCIAMACHY: validation and sample results, *Atmos. Meas. Tech.*, 8, 5223 – 5235.

7828 Vecchi G. A., et al., Weakening of tropical Pacific atmospheric circulation due to anthropogenic
7829 forcing, *Nature*, **441**. 73 - 76 (2006).

7830 Vernier, J. P., et al. (2009), Tropical stratospheric aerosol layer from CALIPSO lidar observations,
7831 *J. Geophys. Res.*, 114, D00H10, doi:10.1029/2009JD011946.

7832 Vernier, J.-P., L. W. Thomason, J.-P. Pommereau, A. Bourassa, J. Pelon, A. Garnier,
7833 A. Hauchecorne, L. Blanot, C. trepte, Doug Degenstein, and F. Vagrás (2011), Major

7834 influence of tropical volcanic eruptions on the stratospheric aerosol layer during the last
7835 decade, *Geophys. Res. Lett.*, 38, L12807, doi:10.1029/2011GL047563.

7836 Verschuren, D., K. R. Laird, and B. F. Cumming, 2000: Rainfall and drought in equatorial east
7837 Africa during the past 1,100 years, *Nature*, 403, 410-414 doi:10.1038/35000179

7838 Voigt, C., U. Schumann, A. Minikin, A. Abdelmonem, A. Afchine, S. Borrmann, M. Boettcher,
7839 B. Buchholz, L. Bugliaro, A. Costa, J. Curtius, M. Dollner, A. Dörnbrack, V. Dreiling, V.
7840 Ebert, A. Ehrlich, A. Fix, L. Forster, F. Frank, D. Fütterer, A. Giez, K. Graf, J. Groß, S.
7841 Groß, K. Heimerl, B. Heinold, T. Hüneke, E. Järvinen, T. Jurkat, S. Kaufmann, M.
7842 Kenntner, M. Klingebiel, T. Klimach, R. Kohl, M. Krämer, T.C. Krisna, A. Luebke, B.
7843 Mayer, S. Mertes, S. Molleker, A. Petzold, K. Pfeilsticker, M. Port, M. Rapp, P. Reutter, C.
7844 Rolf, D. Rose, D. Sauer, A. Schäfler, R. Schlage, M. Schnaiter, J. Schneider, N. Spelten, P.
7845 Spichtinger, P. Stock, A. Walser, R. Weigel, B. Weinzierl, M. Wendisch, F. Werner, H.
7846 Wernli, M. Wirth, A. Zahn, H. Ziereis, and M. Zöger, 2017: [ML-CIRRUS: The Airborne](#)
7847 [Experiment on Natural Cirrus and Contrail Cirrus with the High-Altitude Long-Range](#)
7848 [Research Aircraft HALO. *Bull. Amer. Meteor. Soc.*, 98](#), 271–288,
7849 <https://doi.org/10.1175/BAMS-D-15-00213.1>

7850 Voulgarakis, A., and Coauthors, 2013: Analysis of present day and future OH and methane
7851 lifetime in the ACCMIP simulations. *Atmos. Chem. Phys.*, **13**, 2563–2587, doi:10.5194/acp-
7852 13-2563-2013.

7853

7854 Ward, D. S. S. and Mahowald, N. M.: Contributions of developed and developing countries to
7855 global climate forcing, *Environ. Res. Lett.*, 9(074008), doi:10.1088/1748-9326/9/7/074008,
7856 doi:10.1088/1748-9326/9/7/074008, 2014.

7857 Ward, D. S. S. and Mahowald, N. M.: Local sources of global climate forcing from different
7858 categories of land use activities, *Earth Syst. Dyn.*, 6(1), 175–2015, doi:10.5194/esd-6-175-
7859 2015, 2015.

7860 Ward, D. S. S., Mahowald, N. M. M. and Kloster, S.: Potential climate forcing of land use and
7861 land cover change, *Atmos. Chem. Phys.*, 14(23), 12701–12724, doi:10.5194/acp-14-12701-

7862 2014, 2014.

7863 Wang, C. Anthropogenic aerosols and the distribution of past large-scale precipitation change.
7864 *Geophys. Res. Lett.* **42**, 10,876-10,884 (2015).

7865 Wang, W. C., Yung, Y. L., Lacis, A. A., Mo, T., & Hansen, J. E. (1976). Greenhouse Effects due
7866 to Man-Made Perturbations of Trace Gases. *Science*, *194*(4266), 685 LP-690.
7867 <http://doi.org/10.1126/science.194.4266.685>.

7868 Wang, W.-C., Y.-C. Zhuang, and R. D. Bojkov, 1993: Climate implications of observed changes
7869 in ozone vertical distributions at middle and high latitudes of the northern hemisphere.
7870 *Geophys. Res. Lett.*, *20*, 1567–1570, doi:10.1029/93GL01318.
7871 <https://doi.org/10.1029/93GL01318>.

7872 Wang, W. C., Yung, Y. L., Lacis, A. A., Mo, T., & Hansen, J. E. (1976). Greenhouse Effects due
7873 to Man-Made Perturbations of Trace Gases. *Science*, *194*(4266), 685 LP-690.
7874 <http://doi.org/10.1126/science.194.4266.685>

7875 Wang, C. C., and L. I. Davis, 1974: Measurement of Hydroxyl Concentrations in Air Using a
7876 Tunable uv Laser Beam. *Phys. Rev. Lett.*, *32*, 349–352, doi:10.1103/PhysRevLett.32.349.
7877 <https://link.aps.org/doi/10.1103/PhysRevLett.32.349>.

7878 —, —, C. H. Wu, S. Japar, H. Niki, and B. Weinstock, 1975: Hydroxyl Radical
7879 Concentrations Measured in Ambient Air. *Science* (80-.), *189*, 797–800.
7880 <http://www.jstor.org/stable/1740212>.

7881 Wang, W.-C., and N. D. Sze, 1980: Coupled effects of atmospheric N₂O and O₃ on the Earth's
7882 climate. *Nature*, *286*, 589. <http://dx.doi.org/10.1038/286589a0>.

7883 Wang, H., P. J. Rasch, and G. Feingold, 2011: Manipulating marine stratocumulus cloud amount
7884 and albedo: A process-modelling study of aerosol-cloud-precipitation interactions in
7885 response to injection of cloud condensation nuclei. *Atmos. Chem. Phys.*, doi:10.5194/acp-
7886 11-4237-2011.

7887 Wang, Y.-M., J. L. Lean, and N. R. Sheeley, Jr., 2005: Modeling the Sun's magnetic field and
7888 irradiance since 1713, *Astrophys. J.*, *625*, 522–538.

7889 ——, D. J. Wuebbles, W. M. Washington, R. G. Isaacs, and G. Molnar, 1986: Trace gases and
7890 other potential perturbations to global climate. *Rev. Geophys.*, **24**, 110–140,
7891 doi:doi:10.1029/RG024i001p00110. <https://doi.org/10.1029/RG024i001p00110>.

7892 Wagner, J. Wilzewski, P. Wcisło, S. Yu, E.J. Zak, The HITRAN2016 molecular spectroscopic
7893 database, *Journal of Quantitative Spectroscopy and Radiative Transfer*, Volume 203, 2017,
7894 Pages 3-69, ISSN 0022-4073, <https://doi.org/10.1016/j.jqsrt.2017.06.038>

7895 Wallington, T. J., J. H. Seinfeld, and J. R. Barker, 2018: 100 Years of progress in gas-phase
7896 atmospheric chemistry research. *Meteorol. Monogr.*, doi:10.1175/AMSMONOGRAPHSD-
7897 18-0008.1. <https://doi.org/10.1175/AMSMONOGRAPHSD-18-0008.1>.

7898 Washington, W., and G. Meehl, 1989: Climate sensitivity due to increased CO₂: experiments
7899 with a coupled atmosphere and ocean general circulation model. *Clim. Dyn.*, **4**, [1](#), 1–38.

7900 Watson, R. J., H. Rodhe, H. Oeschger, and U. Siegenthaler, 1990: Greenhouse gases and
7901 aerosols. *Climate Change: The IPCC Scientific Assessment (1990)*, J.T. Houghton, G.J.
7902 Jenkins, and J.J. Ephraums, Eds., Cambridge, U.K. and New York, NY, USA.

7903 Weart, S. R. (1997). Global Warming, Cold War, and the Evolution of Research Plans.
7904 *Historical Studies in the Physical and Biological Sciences*, **27**(2), 319–356.
7905 <http://doi.org/10.2307/27757782>.

7906 Weisenstein, D. K., D. W. Keith, and J. A. Dykema, 2015: Solar geoengineering using solid
7907 aerosol in the stratosphere. *Atmos. Chem. Phys.*, **15**, 11835–11859, doi:10.5194/acp-15-
7908 11835-2015. <https://www.atmos-chem-phys.net/15/11835/2015/> (Accessed December 20,
7909 2018).

7910 Wei, T., Yang, S., Moore, J. C., Shi, P., Cui, X., Duan, Q., Xu, B., Dai, Y., Yuan, W., Wei, X.,
7911 Yang, Z., Wen, T., Teng, F., Gao, Y., Chou, J., Yan, X., Wei, Z., Guo, Y., Jiang, Y., Gao,
7912 X., Wang, K., Zheng, X., Ren, F., Lv, S., Yu, Y., Liu, B., Luo, Y., Li, W., Ji, D., Feng, J.,
7913 Wu, Q., Cheng, H., He, J., Fu, C., Ye, D., Xu, G. and Dong, W.: Developed and developing
7914 world responsibilities for historical climate change and CO₂ mitigation, *Proc. Natl. Acad.
7915 Sci.*, **109**(32), 12911–12915, doi:10.1073/pnas.1203282109, 2012.

7916 W. H. Matthews, W. W. Kellogg and G. D. Robinson, 1971, *Man's Impact on the Climate* MIT
7917 Press.

7918 Wigley, T. M. L., 1987: Relative contributions of different trace gases to the greenhouse effect.
7919 *Clim. Monit.*, 16, 14–29.

7920 Wigley, T. M. L., 1989: Possible climate change due to SO₂-derived cloud condensation nuclei.
7921 *Nature*, 339, 365–367, doi:10.1038/339365a0. <https://doi.org/10.1038/339365a0>.

7922 Winton, M., K. Takahashi, and I. M. Held (2010), Importance of ocean heat uptake efficacy to
7923 transient climate change, *J. Clim.*, 23, 2333–2344, doi:10.1175/2009jcli3139.1.

7924 WMO, 1982: Report of the meeting of experts on potential climatic effects of ozone and other
7925 minor trace gases. WMO Global Ozone Research and Monitoring Project Report No 14.

7926 WMO, 1986: *Atmospheric Ozone 1985*. Global Ozone Research and Monitoring Project Report
7927 No. 16. World Meteorological Organization, Geneva. Volume III.

7928 WMO, 1986: Global ozone research and monitoring project. Atmospheric Ozone. WMO,
7929 Geneva, Switzerland.

7930 World Meteorological Organization Global Ozone Research and Monitoring Project Report NO.
7931 16 Atmospheric Ozone 1985 - Assessment of our Understanding of the Processes
7932 Controlling its Present Distribution and Change.

7933 —, J. C. McConnell, and M. B. McElroy, 1972: Atmospheric CH₄, CO, and CO₂. *J. Geophys.*
7934 *Res.*, 77, 4477–4493, doi:doi:10.1029/JC077i024p04477.
7935 <https://doi.org/10.1029/JC077i024p04477>.

7936 Wuebbles, D. J., F. M. Luther, and J. E. Penner, 1983: Effect of coupled anthropogenic
7937 perturbations on stratospheric ozone. *J. Geophys. Res. Ocean.*, 88, 1444–1456,
7938 doi:doi:10.1029/JC088iC02p01444. <https://doi.org/10.1029/JC088iC02p01444>.

7939 Wetherald, R. T., and S. Manabe, 1975: The Effects of Changing the Solar Constant on the
7940 Climate of a General Circulation Model, *J. Atmos. Sciences*, 32, 2044–2059,
7941 [https://doi.org/10.1175/1520-0469\(1975\)032<2044:TEOCTS>2.0.CO;2](https://doi.org/10.1175/1520-0469(1975)032<2044:TEOCTS>2.0.CO;2)

7942 White, O. R., Skumanich, A., Lean, J., Livingston, W. C., and Keil, S. L., 1992: The Sun in a
7943 Non-cycling State, *Publications of the Astronomical Society of the Pacific*, 104, 1139-1143.

7944 White, W. B., J. Lean, D.R. Cayan, and M.D. Dettinger, 1997: Response of global upper ocean
7945 temperature to changing solar irradiance, *J. Geophys. Res.*, 102, 3255-3266.

7946 Wigley, T. M. L. and S. C. B. Raper, 1990: Climatic change due to solar irradiance changes,
7947 *Geophys. Res. Lett.* 17, 12, 2169-2172, 10.1029/GL017i012p02169.

7948 Wigley, T. M. L. (2006), A combined mitigation/geoengineering approach to climate stabilization.
7949 *Science*, 314, 452-454.

7950 Willson, R. C., 1979: Active cavity radiometer type IV, *Applied Optics*, 18, 179-188,
7951 <https://doi.org/10.1364/AO.18.000179>

7952 Willson, R.C., 2014: ACRIM3 and the total solar irradiance database, *Astrophys Space Sci* 352:
7953 341. <https://doi.org/10.1007/s10509-014-1961-4>

7954 Willson, R. C., Gulkis, S., Janssen, M., Hudson, H. S., and Chapman. G. A., 1981: Observations
7955 of Solar Irradiance Variability, *Science* 211, 4483, 700-702, DOI:
7956 10.1126/science.211.4483.700

7957 Woods, T. N., W. K. Tobiska, G. J. Rottman, and J. R. Worden, 2000: Improved solar Lyman α
7958 irradiance modeling from 1947 through 1999 based on UARS observations, *J. Geophys.*
7959 *Res.*, 105(A12), 27195-27215, doi:10.1029/2000JA000051.

7960

7961 Xie, S.-P., Lu, B. & Xiang, 2013: B. Similar spatial patterns of climate responses to aerosol and
7962 greenhouse gas changes. *Nat. Geosci.* **6**, 828–832.

7963

7964 Yamamoto, G., and T. Sasamori, 1958: Calculation of the absorption of the 15 μ carbon
7965 dioxide band. *Sci. Rept. Tohoku Univ. Fifth Ser.*, **10**, No. 2, 37-57.

7966 Young, P. J., and Coauthors, 2013: Pre-industrial to end 21st century projections of tropospheric

7967 ozone from the Atmospheric Chemistry and Climate Model Intercomparison Project
7968 (ACCMIP). *Atmos. Chem. Phys.*, **13**, 2063–2090, doi:10.5194/acp-13-2063-2013.
7969 <http://www.atmos-chem-phys.net/13/2063/2013/> (Accessed July 16, 2018).

7970 Young, P. Y., and Coauthors, 2018: Tropospheric Ozone Assessment Report: Assessment of
7971 global-scale model performance for global and regional ozone distributions, variability, and
7972 trends. *Elem Sci Anth.*, **6**, doi:<http://doi.org/10.1525/elementa.265>.

7973 Yorks, J. E., Palm, S. P. McGill, M. J. Hlavka, D. L. Hart, W. D., Selmer, P. A., and Nowottnick
7974 (2015), E. P.: CATS Algorithm Theoretical Basis Document, 1st ed., NASA, 2015.

7975

7976 Zennaro, P., Kehrwald, N., McConnell, J. R., Schüpbach, S., Maselli, O. J., Marlon, J.,
7977 Valelonga, P., Leuenberger, D., Zangrando, R., Spolaor, A., Borrotti, M., Barbaro, E.,
7978 Gambaro, A. and Barbante, C.: Fire in ice: Two millennia of boreal forest fire history from
7979 the Greenland NEEM ice core, *Clim. Past*, **10**(5), 1905–1924, doi:10.5194/cp-10-1905-
7980 2014, 2014.

7981 Zhang, J., Christopher, S. A., Remer, L. A., & Kaufman, Y. J. (2005). Shortwave aerosol
7982 radiative forcing over cloud-free oceans from Terra: 2. Seasonal and global distributions.
7983 *Journal of Geophysical Research: Atmospheres*, **110**(D10).

7984 Zhang, Y., 2008: Online-coupled meteorology and chemistry models: history, current status, and
7985 outlook. *Atmos. Chem. Phys.*, **8**, 2895–2932, doi:10.5194/acp-8-2895-2008.
7986 <https://www.atmos-chem-phys.net/8/2895/2008/>.

7987 Zhang X, et al. (2007) Detection of human influence on twentieth-century precipitation trends.
7988 *Nature* **448**:461–465.

7989 Zimmermann, P H., Feichter, J., Rath, H. K., Crutzen, P. J., and Weiss, W. (1989), A global
7990 three- dimensional source receptor model investigation using KrX5, *Atmos. Environ.* **23**, 25–
7991 35.

7992 1984: *Global Tropospheric Chemistry: A Plan for Action*. 194 pp.

7993 1985: *World Meteorological Organization Global Ozone Research and Monitoring Project*
7994 *Report NO. 16 Atmospheric Ozone 1985 - Assement of our Understanding of the Processes*
7995 *Controlling its Present Distribution and Change.*

7996 Zanchettin, Davide, Myriam Khodri, Claudia Timmreck, Matthew Toohey, Anja Schmidt, Edwin
7997 P. Gerber, Gabriele Hegerl, Alan Robock, Francesco S. R. Pausata, William T. Ball, Susanne
7998 E. Bauer, Slimane Bekki, Sandip S. Dhomse, Allegra N. LeGrande, Graham W. Mann,
7999 Lauren Marshall, Michael Mills, Marion Marchand, Ulrike Niemeier, Virginie Poulain,
8000 Eugene Rozanov, Angelo Rubino, Andrea Stenke, Kostas Tsigaridis, and Fiona Tummon
8001 (2016), The Model Intercomparison Project on the climatic response to Volcanic forcing
8002 (VolMIP): experimental design and forcing input data for CMIP6, *Geosci. Model Dev.*, 9,
8003 2701-2719, <https://doi.org/10.5194/gmd-9-2701-2016>.

8004 Zeilinga de Boer, J., D. T. Sanders (2002), *Volcanoes and Human History*, Princeton University
8005 Press, Princeton, NJ.

8006 Zielinski, G. (2000), Use of paleo-records in determining variability within the volcanism-climate
8007 system, *Quarterly Science reviews*, 19, 417-438.

8008